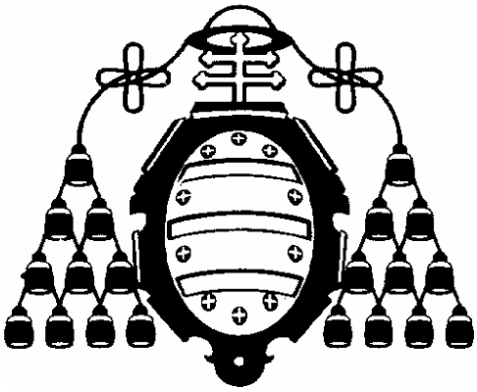

UNIVERSIDAD DE OVIEDO

ESCUELA POLITÉCNICA DE INGENIERÍA DE GIJÓN

MASTER EN TECNOLOGÍAS DE LA INFORMACIÓN Y COMUNICACIONES EN REDES MÓVILES

HYBRID LOCALIZATION ALGORITHM FOR LTE COMBINING SATELLITE AND TERRESTRIAL MEASUREMENTS

ALGORITMO HÍBRIDO DE LOCALIZACIÓN PARA LTE COMBINANDO MEDIDAS TERRESTRES Y DE SATÉLITES

ADRIÁN CARDALDA GARCÍA

JUNIO 2015

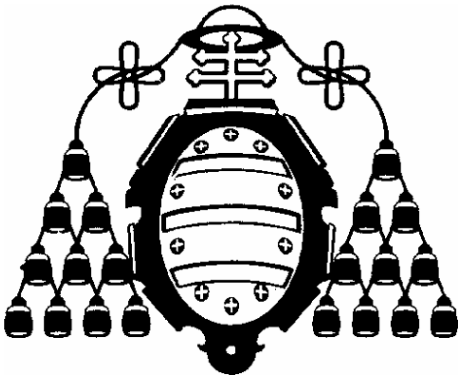

UNIVERSIDAD DE OVIEDO

ESCUELA POLITÉCNICA DE INGENIERÍA DE GIJÓN

MASTER EN TECNOLOGÍAS DE LA INFORMACIÓN Y COMUNICACIONES EN REDES MÓVILES

HYBRID LOCALIZATION ALGORITHM FOR LTE COMBINING SATELLITE AND TERRESTRIAL MEASUREMENTS

ALGORITMO HÍBRIDO DE LOCALIZACIÓN PARA LTE COMBINANDO MEDIDAS TERRESTRES Y DE SATÉLITES

ADRIÁN CARDALDA GARCÍA

JUNIO 2015

TUTOR: MANUEL ARREBOLA BAENA

Table of contents

List of figures

List of tables

Acronyms and Abbreviations

2DRMS	Twice the DRMS
3GPP	Third Generation Partnership Project
A-GNSS	Assisted GNSS
BDS	BeiDou
BeiDou	Chinese GNSS
Bluetooth	Wireless technology standard for WPAN
BS	Base Station
CEP	Circular Error Probability
cLBS	Commercial Location Based Services
DAS	Distributed Antenna Systems
DOP	Dilution Of Precision
DRMS	Deviation Root Mean Square or Distance Root Mean Square
E112	Enhanced 112, Location-enhanced emergency call service of the European Union
E911	Enhanced 911, Location-enhanced emergency call service of the United States

ECEF	Earth-centered, Earth-fixed
eCID	Enhanced Cell ID
EGNOS	European Geostationary Navigation Overlay Service
eNB	Evolved Node B or E-UTRAN Node B
ENU	East, North, Up
E-UTRA	Evolved UMTS Terrestrial Radio Access
FCC	Federal Communications Commission. An association from the US for the regulation of communications
FDE	Fault Detection and Exclusion
GALILEO	GNSS of the European Union
GDOP	Geometrical Dilution Of Precision
GLONASS	Russian GNSS
GNSS	Global Navigation Satellite System
GPS	Global Positioning System
GPRS	General Packet Radio Service
GSM	Global System for Mobile communications
HDOP	Horizontal Dilution Of Precision
LBS	Location Based Services
LoS	Line of Sight
LPP	Location Positioning Protocol
LSE	Least Squares Estimation

LTE	Long Term Evolution
MRA	Measurement Rejection Approach
MRSE	Mean Radial Spherical Error
PDOP	Position Dilution Of Precision
PRS	Positioning Reference Signal
PSAP	Public Safety Accessing Point
OTDOA	Observed Time Difference Of Arrival
R95	One of the standards for reporting GNSS accuracy
RAIM	Receiver Autonomous Integrity Monitoring
RAN	Radicalization Awareness Network
RSSI	Received Signal Strength Indicator
RSTD	Reference Symbol Time Delay
RTT	Round Trip Time
SBAS	Satellite Based Augmentation System
SEP	Spherical Error Probability
SIM	Subscriber Identity Module
TDOA	Time Difference Of Arrival
TDOP	Time Dilution Of Precision
TOA	Time Of Arrival
TTFF	Time-to-first-fix

UMTS	Universal Mobile Telecommunications System
VDOP	Vertical Dilution Of Precision
VoLTE	Voice Over LTE
WGS84	World Geodetic System 84
WiFi	Commonly used name for WLAN
WLAN	Wireless Local Area Network
WPAN	Wireless Personal Area Network

Capítulo 0

Resumen

0.1 Introducción

La telefonía móvil ha evolucionado considerablemente durante la última década. En la Unión Europea, el número de teléfonos móviles por habitante se ha duplicado de 2004 a 2012, llegando a haber más líneas de teléfono móvil que habitantes [1]. No solo se ha incrementado el número de usuarios, sino que con la aparición de los llamados teléfonos inteligentes o *smartphones*, los usos de estos terminales van mucho más allá de hacer llamadas.

Algunas (la mayor parte) de estas aplicaciones están destinadas al ocio. No obstante, también hay otras utilidades destinadas a monitorizar la salud, aplicaciones de navegación o incluso de seguridad. En esta línea, el 3GPP (Third Generation Partnership Project) ha introducido los llamados Location Based Services (LBS) para LTE. LBS son las siglas que engloban todos los servicios y tecnologías destinadas a determinar la posición de un terminal móvil. Una de las utilidades de estos servicios, tal vez la más importante, es que el terminal sea capaz de enviar su propia posición a los servicios de emergencia durante una llamada al 112 o 911. Atendiendo a las estadísticas en la Unión Europea, más de la mitad de las llamadas de emergencia se originan desde un teléfono móvil y en casi el 60 % de las ocasiones el usuario es incapaz de precisar su localización [2]. Por este motivo, la UE ha aprobado en la resolución E112 (de Enhanced 112) en 2003 una normativa para requerir que los operadores de red han de proporcionar a los servicios de emergencia toda la información disponible acerca de la localización de la persona efectuando la llamada.

En Estados Unidos, el organismo conocido como Comisión Federal de Comunicaciones (FCC por sus siglas en inglés), que engloba algunos de los principales operadores estadounidenses así como fabricantes de teléfonos móviles y el gobierno, va un paso más allá, imponiendo una serie de requisitos de precisión y disponibilidad que han de ser cumplidas en las llamadas al 911 en territorio estadounidense. El último acuerdo, de 2014 [3, 4], define como meta que en el 80 % de las llamadas al 911 se pueda proporcionar una posición con una exactitud superior a 50 metros, independientemente de que la llamada sea en interiores o exteriores. Este objetivo ha de cumplirse en el plazo de 72 meses. Además, define una serie de metas intermedias, empezando por ser capaz de proporcionar posiciones en dos dimensiones o en exteriores, que han de ser cumplidas en un futuro aún más cercano.

Para alcanzar dichas metas, será necesario utilizar todas y cada una de las tecnologías de localización disponibles hasta el momento, e investigar nuevas posibilidades. Actualmente, el 3GPP define tres tecnologías de localización para LTE: GNSS, OTDOA y ECID.

- GNSS (Sistema de Navegación Global por Satélite) es probablemente el sistema de localización más conocido. Se basa en el uso de satélites para calcular la posición del teléfono móvil. Éste ha de medir y transmitir una estimación de la distancia hasta el satélite llamada pseudo-rango. Para ello, el móvil calcula el TOA (tiempo de llegada) de la señal del satélite.
- OTDOA (Observed Time Difference Of Arrival) es un sistema de multilateración en el que el móvil ha de medir la diferencia entre los tiempos de llegada de señales procedentes de dos estaciones base. Las estaciones base transmiten una señal de localización llamada PRS (Positioning Reference Symbol) como parte de la señal LTE. La medida que realiza el móvil de la diferencia de tiempos entre PRS de dos celdas LTE se llama RSTD (Reference Symbol Time Delay).
- ECID (Enhanced Cell ID) es el último de los mecanismos de posicionamiento introducidos hasta ahora en LTE por el 3GPP. Está basado en la medida del RTT (round trip timing o tiempo de vuelo de ida y vuelta) de una señal entre la estación base y el móvil. Hasta E-UTRA Release 11, ECID solo es posible con la estación LTE de servicio, y no con las estaciones vecinas.

Estas tres tecnologías son muy diferentes entre sí. GNSS y ECID son métodos de trilateración, mientras que OTDOA está basado en la multilateración. Las particula-

ridades de cada uno de estos métodos se describen más en detalle en la Sección 2.1 de este documento. Como pueden combinarse para obtener un sistema de localización preciso será el principal objetivo de este Trabajo Fin de Master.

0.1.1 Objetivos

Este trabajo tiene dos objetivos principales:

- Proponer una solución para la localización de terminales móviles en LTE que cumplen los requisitos de exactitud solicitados por los principales operadores de red y servicios de emergencia. Se tomará como base el informe del FCC [3, 4] de Febrero de 2014.
- Analizar la aplicabilidad de las tecnologías existentes para localización en interiores. Estudiar otras posibilidades y proponer un modelo teórico.

Para alcanzar dichos objetivos, hay una serie de metas secundarias que también han de completarse:

- Plantear un algoritmo capaz de estimar posiciones utilizando varias medidas heterogéneas provenientes de múltiples tecnologías diferentes.
- Utilizar dicho algoritmo para analizar por separado el funcionamiento de OTDOA y ECID para localización.
- Validar el algoritmo propuesto de forma teórica y experimental.
- Estudiar el impacto de la Dilución de Precisión (DOP) en el resultado de la localización. Plantear una definición de DOP para LBS Híbrido.
- Identificar un conjunto de escenarios para simular las situaciones donde añadir medidas de OTDOA y ECID pueda mejorar el funcionamiento de A-GNSS.
- Estudiar las particularidades de la localización indoor y evaluar otras posibles soluciones como WLAN o Femtoceldas.

0.2 Desarrollo teórico

El algoritmo propuesto será una extensión del algoritmo WLS (Mínimos Cuadrados Ponderados) estandarizado por el 3GPP en el RAN# 4 para localización A-GNSS en el TS 36.171 [5]. Por lo tanto, el primer paso será describir brevemente dicho algoritmo, y a continuación plantear las modificaciones necesarias para incluir el resto de tecnologías. En esta sección solo se especificarán los pasos más importantes. Se puede encontrar información más detallada en los Capítulos 2 y 3 de este TFM.

0.2.1 GNSS

La localización mediante A-GNSS está basada en la medida de la distancia entre el dispositivo móvil y varios satélites. Cada una de dichas medidas tiene idealmente la forma:

$$\rho_{true} = \overline{TxRx} = \sqrt{(x_{tx} - x_{rx})^2 + (y_{tx} - y_{rx})^2 + (z_{tx} - z_{rx})^2}, \tag{1}$$

donde ρ_{true} representa un *rango*. Sin embargo, la medida real estará contaminada con los sesgos del receptor móvil y del transmisor de cada satélite. Esta medida contaminada se conoce como *pseudo-rango*:

$$\rho = \rho_{true} + c \cdot \tau_{rx} - c \cdot \tau_{tx} + \nu, \tag{2}$$

donde ν representa el resto de errores presentes en la medida, que se suele considerar como una componente de ruido blanco gaussiano. El sesgo del reloj de los satélites se puede calcular a través de las efemérides que transmite la red LTE y por tanto su efecto puede mitigarse. El error del receptor móvil sin embargo no se puede despreciar y es una de las variables a calcular como resultado del algoritmo.

El pseudo-rango se linealiza aplicando series de Taylor alrededor de un punto $P_0 = \{x_0, y_0, z_0, \tau_0\}$, con lo que se obtiene:

$$\begin{aligned} \rho(x, y, z, \tau) \approx \rho(x_0, y_0, z_0, \tau_0) + \nu + (x - x_0) \left.\frac{\partial \rho}{\partial x}\right|_{P=P_0} + (y - y_0) \left.\frac{\partial \rho}{\partial y}\right|_{P=P_0} + \dots \\ + (z - z_0) \left.\frac{\partial \rho}{\partial z}\right|_{P=P_0} + (\tau - \tau_0) \left.\frac{\partial \rho}{\partial \tau}\right|_{P=P_0} = \rho_0 + \nu + \dots \\ + \Delta x \left.\frac{\partial \rho}{\partial x}\right|_{P=P_0} + \Delta y \left.\frac{\partial \rho}{\partial y}\right|_{P=P_0} + \Delta z \left.\frac{\partial \rho}{\partial z}\right|_{P=P_0} + \Delta \tau \left.\frac{\partial \rho}{\partial \tau}\right|_{P=P_0} \end{aligned} \tag{3}$$

Midiendo los pseudo-rangos a n satélites se obtiene un sistema de n ecuaciones y cuatro incógnitas, que se puede resolver aplicando mínimos cuadrados:

$$\Delta\hat{\rho} = A \cdot \Delta\hat{X} + \hat{\nu}. \tag{4}$$

A es lo que se conoce como matriz del sistema o matriz de diseño [6] y toma la siguiente forma:

$$A = \begin{bmatrix} \frac{\partial\rho^1}{\partial x}\Big|_{P=P_0} & \frac{\partial\rho^1}{\partial y}\Big|_{P=P_0} & \frac{\partial\rho^1}{\partial z}\Big|_{P=P_0} & \frac{\partial\rho^1}{\partial \tau}\Big|_{P=P_0} \\ \frac{\partial\rho^2}{\partial x}\Big|_{P=P_0} & \frac{\partial\rho^2}{\partial y}\Big|_{P=P_0} & \frac{\partial\rho^2}{\partial z}\Big|_{P=P_0} & \frac{\partial\rho^2}{\partial \tau}\Big|_{P=P_0} \\ \vdots & \vdots & \vdots & \vdots \\ \frac{\partial\rho^n}{\partial x}\Big|_{P=P_0} & \frac{\partial\rho^n}{\partial y}\Big|_{P=P_0} & \frac{\partial\rho^n}{\partial z}\Big|_{P=P_0} & \frac{\partial\rho^n}{\partial \tau}\Big|_{P=P_0} \end{bmatrix} \tag{5}$$

Las derivadas parciales en A se calculan:

$$\frac{\partial\rho^j}{\partial x}\Big|_{P=P_0} = -\frac{1}{2} \cdot \frac{2 \cdot (x_{s_j} - x_0)}{\rho^j|_{P=P_0}} = \frac{(x_0 - x_{s_j})}{\rho^j(P_0)} \tag{6}$$

$$\frac{\partial\rho^j}{\partial y}\Big|_{P=P_0} = \frac{(y_0 - y_{s_j})}{\rho^j(P_0)} \tag{7}$$

$$\frac{\partial\rho^j}{\partial z}\Big|_{P=P_0} = \frac{(z_0 - z_{s_j})}{\rho^j(P_0)} \tag{8}$$

$$\frac{\partial\rho^j}{\partial \tau}\Big|_{P=P_0} = c, \tag{9}$$

donde ρ^j representa el pseudo-rango j correspondiente al satélite j y x_j, y_j y z_j son las coordenadas del satélite j en ECEF.

Además de los pseudo-rangos, es posible extraer de la información transmitida por el teléfono móvil la estimación del mismo acerca de la exactitud de cada medida. El mensaje contiene un valor *codePhaseRMSError*, definido en TS 36.355 [7], que contiene el error RMS. Este valor se usa para construir una matriz diagonal de pesos, W, cuyos coeficientes en la diagonal principal toman el valor $w_i = \frac{1}{RMS_i}$. La matriz de pesos se utiliza para ponderar las medidas recibidas, de forma que las medidas más precisas tengan más importancia en la solución final del algoritmo.

La ecuación a resolver aplicando WLS es:

$$\hat{X} = (A' \cdot W \cdot A)^{-1} \cdot A' \cdot W \cdot \Delta\hat{\rho}. \tag{10}$$

0.2.2 OTDOA

OTDOA es un sistema hiperbólico que se basa en la diferencia en el tiempo de llegada de dos señales. Esta diferencia de tiempos permite localizar al receptor sobre una curva llamada hipérbola, que sigue la ecuación:

$$\overline{PBS_2} - \overline{PBS_1} = K. \tag{11}$$

La medida que realiza el móvil para OTDOA se llama RSTD (Reference Symbol Time Delay):

$$K = (RSTD_{n,true} - \tau_{Tx,n} + \tau_{Tx,ref}) \cdot v_p + e_{RSTD}. \tag{12}$$

Reemplazando la medida en la ecuación de la hipérbola y sustiyendo $\overline{PBS_i}$ por la distancia entre el receptor, P, y la estación base i, el rango OTDOA se puede definir como:

$$\begin{aligned} \rho_{otdoa} = RSTD_{n,true} \cdot c - \tau_{Tx,n} \cdot c + \tau_{Tx,ref} \cdot c + e_{RSTD} = RSTD_{n,true} \cdot c + \nu_{RSTD} = \\ = \sqrt{(x-x_n)^2 + (y-y_n)^2 + (z-z_n)^2} - \sqrt{(x-x_{ref})^2 + (y-y_{ref})^2 + (z-z_{ref})^2}. \end{aligned} \tag{13}$$

En este caso OTDOA es un *rango*, y no pseudo-rango, ya que el sesgo del reloj del receptor no influye en la calidad de la medida, que afecta por igual a las señales de ambas estaciones bases y se cancela. Por tanto, una de las variables a calcular en el caso de GNSS, τ, no es necesaria para OTDOA, habiendo un total de tres incógnitas.

Tras linealizar el rango OTDOA usando series de Taylor, se obtiene lo siguiente:

$$\begin{aligned} \rho_T(x,y,z) \approx \rho_T(x_0,y_0,z_0) + \nu + (x-x_0)\left.\frac{\partial \rho_T}{\partial x}\right|_{P=P_0} + (y-y_0)\left.\frac{\partial \rho_T}{\partial y}\right|_{P=P_0} + \dots \\ + (z-z_0)\left.\frac{\partial \rho_T}{\partial z}\right|_{P=P_0} = \rho_{T,0} + \nu + \Delta x \left.\frac{\partial \rho_T}{\partial x}\right|_{P_0} + \Delta y \left.\frac{\partial \rho_T}{\partial y}\right|_{P_0} + \Delta z \left.\frac{\partial \rho_T}{\partial z}\right|_{P_0}. \end{aligned} \tag{14}$$

Definiendo el sistema de ecuaciones igual que para GNSS en Eq. (4), la matriz del sistema OTDOA tendrá como coeficientes:

$$\left.\frac{\partial \rho_T^j}{\partial x}\right|_{P=P_0} = \frac{1}{2}\cdot\frac{2\cdot(x_{ref}-x_0)}{d_{ref}|_{P=P_0}} - \frac{1}{2}\cdot\frac{2\cdot(x_{bs_j}-x_0)}{d_{bs_j}|_{P=P_0}} = \\ = \frac{(x_{ref}-x_0)}{d_{ref}(P_0)} - \frac{(x_{bs_j}-x_0)}{d_{bs_j}(P_0)} \tag{15}$$

$$\left.\frac{\partial \rho_T^j}{\partial y}\right|_{P=P_0} = \frac{(y_{ref}-y_0)}{d_{ref}(P_0)} - \frac{(y_{bs_j}-y_0)}{d_{bs_j}(P_0)} \tag{16}$$

$$\left.\frac{\partial \rho_T^j}{\partial z}\right|_{P=P_0} = \frac{(z_{ref}-z_0)}{d_{ref}(P_0)} - \frac{(z_{bs_j}-z_0)}{d_{bs_j}(P_0)} \tag{17}$$

$$\left.\frac{\partial \rho_T^j}{\partial \tau}\right|_{P=P_0} = 0. \tag{18}$$

Uno de los parámetros que envía el móvil para OTDOA es la estimación de la precisión de la medida (ver Sección 2.3.4). Este valor puede utilizarse para calcular los coeficientes de la matriz de pesos del algoritmo WLS, como se ha hecho para GNSS.

0.2.3 ECID

ECID mide, como GNSS, el tiempo de llegada de una señal del transmisor (en este caso una estación LTE) hasta el móvil. Sin embargo, también mide el tiempo en dirección opuesta, desde el móvil hasta la estación, y la información que se transmite es el tiempo de vuelo de bajada y subida. Esto tiene dos efectos importantes: elimina la dependencia de la medida en el sesgo temporal del receptor del móvil, y también del sesgo en el transmisor de la estación base. Por tanto, como OTDOA, para posicionamiento con ECID hay que calcular tres incógnitas.

Un rango ECID se define así:

$$\rho_E = RTT\cdot v_p + \nu_{RTT} = \overline{BsUe} = \sqrt{(x_{bs}-x_{ue})^2+(y_{bs}-y_{ue})^2+(z_{bs}-z_{ue})^2}, \tag{19}$$

y si se lineariza mediante series de Taylor, el resultado sigue la expresión:

$$\rho_E(x,y,z) \approx \rho_{E,0} + \nu + \Delta x\left.\frac{\partial \rho_E}{\partial x}\right|_{P=P_0} + \Delta y\left.\frac{\partial \rho_E}{\partial y}\right|_{P=P_0} + \Delta z\left.\frac{\partial \rho_E}{\partial z}\right|_{P=P_0}. \tag{20}$$

Los coeficientes de la matriz del sistema para ECID tienen la siguiente forma:

$$\left.\frac{\partial \rho_E^j}{\partial x}\right|_{P=P_0} = \frac{(x_0 - x_{s_j})}{d_{bs_j}(P_0)} \tag{21}$$

$$\left.\frac{\partial \rho_E^j}{\partial y}\right|_{P=P_0} = \frac{(y_0 - y_{s_j})}{d_{bs_j}(P_0)} \tag{22}$$

$$\left.\frac{\partial \rho_E^j}{\partial z}\right|_{P=P_0} = \frac{(z_0 - z_{s_j})}{d_{bs_j}(P_0)} \tag{23}$$

$$\left.\frac{\partial \rho_E^j}{\partial \tau}\right|_{P=P_0} = 0. \tag{24}$$

El posicionamiento con ECID presenta dos inconvenientes fundamentales. La primera es que el protocolo LPP solo define medidas ECID para la estación base a la que el móvil está conectado y no para las celdas vecinas. Este problema se resuelve como parte de E-UTRA Rel 11, donde se han definido medidas para todas las estaciones LTE. El segundo problema es que el mensaje estándar de ECID no incluye ningún parámetro para indicar la calidad de la medida, y no es posible definir una matriz de pesos. La solución es asignar a todas las medidas ECID un peso uniforme.

0.2.4 Localización Híbrida

El algoritmo híbrido para localización consiste en combinar todas las medidas disponibles en un solo sistema de ecuaciones. La ecuación a resolver es la del sistema WLS (Eq. (10)). La única particularidad es que los coeficientes de la matriz de sistema, A, serán diferentes para cada ecuación (es decir, para cada fila de la matriz A), dependiendo de si la medida es de GNSS, OTDOA o ECID. Los coeficientes de la matriz de pesos W también se adaptarán al tipo de medida.

0.2.5 Dilución de Precisión

La Dilución de Precisión (DOP, por sus siglas en inglés) es un término que se usa en sistemas de radiolocalización para referirse a la influencia de la geometría del sistema en la exactitud de la posición calculada [6, 8, 9].

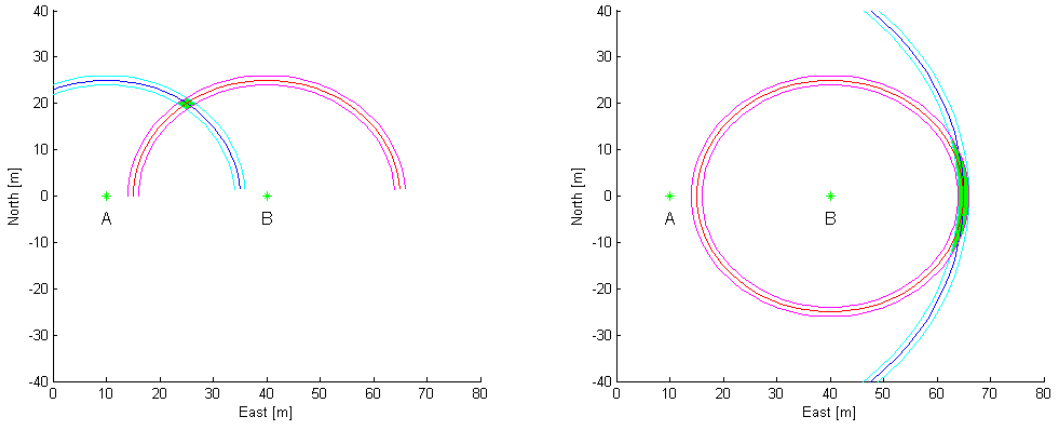

Figura 1: Dilución de Precisión

Para entender este concepto, Fig. 1 representa un sistema de dos transmisores, A y B, y un receptor cuya posición es a priori desconocida. El receptor esta midiendo el tiempo de llegada de señales provenientes de los dos transmisores, en color azul para el transmisor A, y el rojo para B. Las líneas en magenta y cian representan la incertidumbre asociada a cada medida, debido a los errores de la medición. El dispositivo receptor estará ubicado en algún punto dentro del área comprendida entre las líneas cian y magenta. En la imagen de la izquierda, se puede observar que este área es relativamente pequeña. Es lo que se conoce como una *buena geometría* para la localización, y presentará valores de DOP bajos. En la derecha, el sistema de transmisores es el mismo, pero el receptor está en otra posición diferente. El área donde el receptor puede encontrarse es mucho más grande que el otro caso. Esta es una *mala geometría*, y el DOP será alto.

Para calcular el DOP, hay que introducir antes una nueva matriz, Q, la matriz de cofactores, que se puede calcular a partir de la matriz de sistema, A:

$$Q = (A'A)^{-1} = \begin{bmatrix} \sigma_x^2 & \sigma_{xy} & \sigma_{xz} & \sigma_{x\tau} \\ \sigma_{xy} & \sigma_y^2 & \sigma_{yz} & \sigma_{y\tau} \\ \sigma_{xz} & \sigma_{yz} & \sigma_z^2 & \sigma_{z\tau} \\ \sigma_{x\tau} & \sigma_{y\tau} & \sigma_{z\tau} & \sigma_\tau^2 \end{bmatrix}. \tag{25}$$

Los valores de DOP se calculan con los términos de la diagonal principal de Q. Hay varias definiciones de DOP, en función de las dimensiones de interés:

$$DOP \equiv GDOP \equiv \sqrt{\sigma_x^2 + \sigma_y^2 + \sigma_z^2 + \sigma_\tau^2} \tag{26}$$

$$PDOP \equiv \sqrt{\sigma_x^2 + \sigma_y^2 + \sigma_z^2} \tag{27}$$

$$HDOP \equiv \sqrt{\sigma_x^2 + \sigma_y^2} \tag{28}$$

$$VDOP \equiv \sigma_z \tag{29}$$

$$TDOP \equiv \sigma_\tau \tag{30}$$

Analizando el DOP se puede explicar, por ejemplo, por qué OTDOA y ECID no presentan generalmente buenos resultados en tres dimensiones: la altitud de las estaciones base es normalmente similar, por lo que el PDOP es muy alto. Sin embargo, el HDOP es generalmente bueno, lo que explica por qué se obtienen buenas posiciones bidimensionales.

0.2.6 Fuentes de error

Hay varias fuentes de error que pueden perturbar las medidas de GNSS, OTDOA y ECID. Las más importantes han sido descritas y analizadas para este TFM en los Capítulos 2 y 3. En concreto, será de especial interés para este trabajo el análisis de los errores que pueden afectar a las medidas OTDOA y ECID. Uno de los más importantes es el error de sincronización entre estaciones base, que va a afectar severamente la calidad de las medidas RSTD (ver Sección 3.1.3.A).

0.3 Simulaciones y resultados

Durante los Capítulos 4 y 5 de este TFM, se han obtenido resultados tanto con Matlab como en el laboratorio, utilizando sistemas de test certificados de la familia TS8980 de Rohde & Schwarz y teléfonos móviles comerciales.

0.3.1 OTDOA

Las primeras simulaciones van destinadas a probar la validez del algoritmo propuesto para localización únicamente con señales OTDOA. En la Sección 4.1, se han propuesto cuatro escenarios con diferentes valores de HDOP y GDOP.

A partir del estudio del GDOP (Fig. 3.2), se ha comprobado que, en la mayor parte de ocasiones, la constelación de estaciones base no proporciona suficiente diversidad de altura para obtener posiciones tridimensionales. Solamente uno de los escenarios (OTDOA Escenario 1) ha sido capaz de proporcionar buenas estimaciones de la coordenada Z. Los otros escenarios, con altitudes de las estaciones base más realistas, no han funcionado bien para 3D.

A. Análisis del error en las medidas RSTD

El cálculo de la posición del móvil se basa en las medidas RSTD, que estarán contaminadas por ruido y contendrán errores. De acuerdo con las especificaciones del 3GPP, el máximo error permitido para la medida RSTD oscila entre ± 5 y ± 10 T_s, dependiendo del ancho de banda de la señal PRS y de si las estaciones base se solapan en frecuencia. La influencia de los errores en las medidas RSTD en el resultado del algoritmo se puede observar en Fig. 2.

También se ha analizado la influencia del error de sincronización entre las estaciones base, observando que es un parámetro crítico para el buen funcionamiento del posicionamiento OTDOA. Los errores en las coordenadas absolutas de las antenas también influyen en la posición calculada. Sin embargo, la relación entre el error en la posición calculada y el error en las coordenadas de la antena depende de la posición relativa entre el móvil y la constelación de estaciones base y es imposible de predecir a priori. No obstante, a partir de los resultados de las simulaciones se puede concluir que si la posición de las antenas se conoce con una precisión de ± 5 metros, el error inducido en el cálculo final puede despreciarse.

B. Rendimiento del algoritmo con posiciones aleatorias

Durante todas las simulaciones anteriores, el dispositivo móvil se encontraba siempre en una posición fija. En esta simulación, se han tomado 1000 medidas con el móvil en

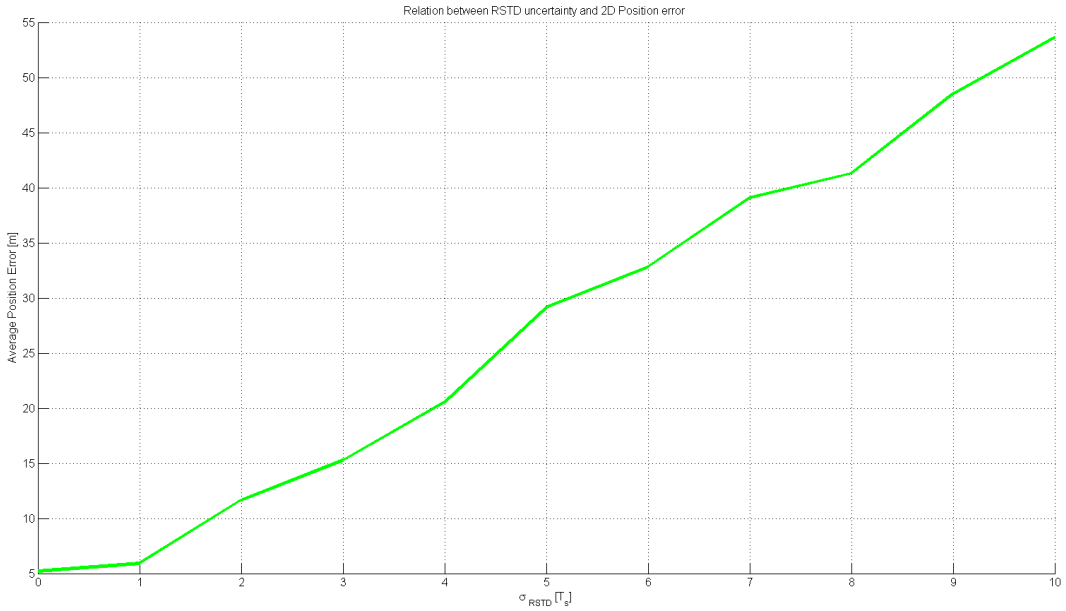

Figura 2: Error en la posición calculada (2D) en función de la varianza del error en la medida RSTD.

posiciones aleatorias dentro del área formada por la constelación de estaciones base. Además, se ha alternado el error de sincronización entre estaciones base de -100 a +100 nanosegundos, y la varianza de las medidas RSTD de 0 a 10 T_s. Los resultados se recogen desde Tab. 4.11 a Tab. 4.14 para el escenario en dos dimensiones. En general, se concluye que el algoritmo de localización OTDOA puede cumplir los requisitos del FCC (en 80 % de las iteraciones la posición calculada ha de tener un error inferior a 50 metros) para dos dimensiones, si las estaciones base están sincronizadas a 10 nanosegundos y la varianza del error en la medida RSTD es menor o igual a 5 T_s.

C. Analísis de la geometría de la constelación

Finalmente se ha analizado la influencia de la geometría de las estaciones base en los resultados del algoritmo. Para ello, se han simulado una serie de constelaciones, cuya distribución de DOP se muestra en Fig. 3

Los resultados obtenidos para todas las constelaciones bajo estudio pueden consultarse en la Sección 4.1.7. De todas las constelaciones analizadas, las que mejor rendimiento han presentado son el pentágono regular, el hexágono y la constelación de 7 estaciones formando un panal. Para todas ellas, no obstante, los requisitos del FCC solo se cumplen si la sincronización entre estaciones base es de 10 nanosegundos o mejor.

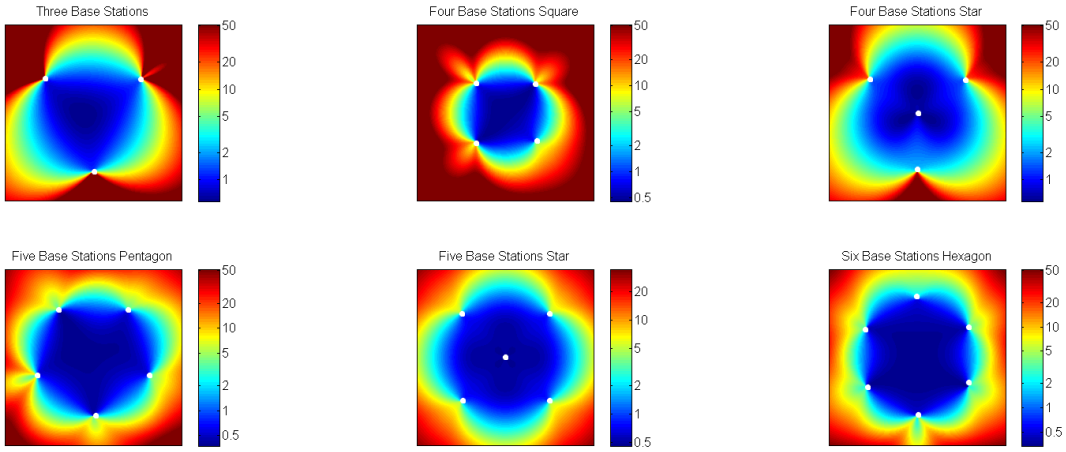

Figura 3: Diferentes constelaciones y su distribución de DOP.

D. Resultados en el sistema de test

En la parte de resultados se ha comparado el funcionamiento de dos móviles, uno comercial y un prototipo, en varios escenarios para OTDOA (Secciones 5.2.2 y 5.2.3). Para el primer test, se ha supuesto que las estaciones base están perfectamente sincronizadas. En Fig. 4, se puede ver un diagrama polar del error en la posición calculada para los dos móviles en dos escenarios, uno con buen DOP y otro con mal DOP, viéndose claramente que el rendimiento es mucho mejor si el DOP es bueno.

En Tab. 1, se recoge el porcentaje de iteraciones con éxito (error en la posición calculada inferior a 50 metros) para los dos escenarios, variando el error de sincronización entre estaciones base.

BS$_{sync}$ [ns]	**Proto 1**		**SG Light**	
	Good DOP	Bad DOP	Good DOP	Bad DOP
10	100	90	100	58
10	100	96	100	68
25	100	49	100	37
50	100	11	100	17
100	100	0	98	0

Tabla 1: Porcentaje de éxito para posicionamiento OTDOA.

En los resultados se ha visto que el prototipo funcionaba ligeramente mejor que el móvil comercial, pero ambos eran capaces de obtener resultados que cumplen los requisitos de la FCC siempre y cuando el DOP sea aceptable.

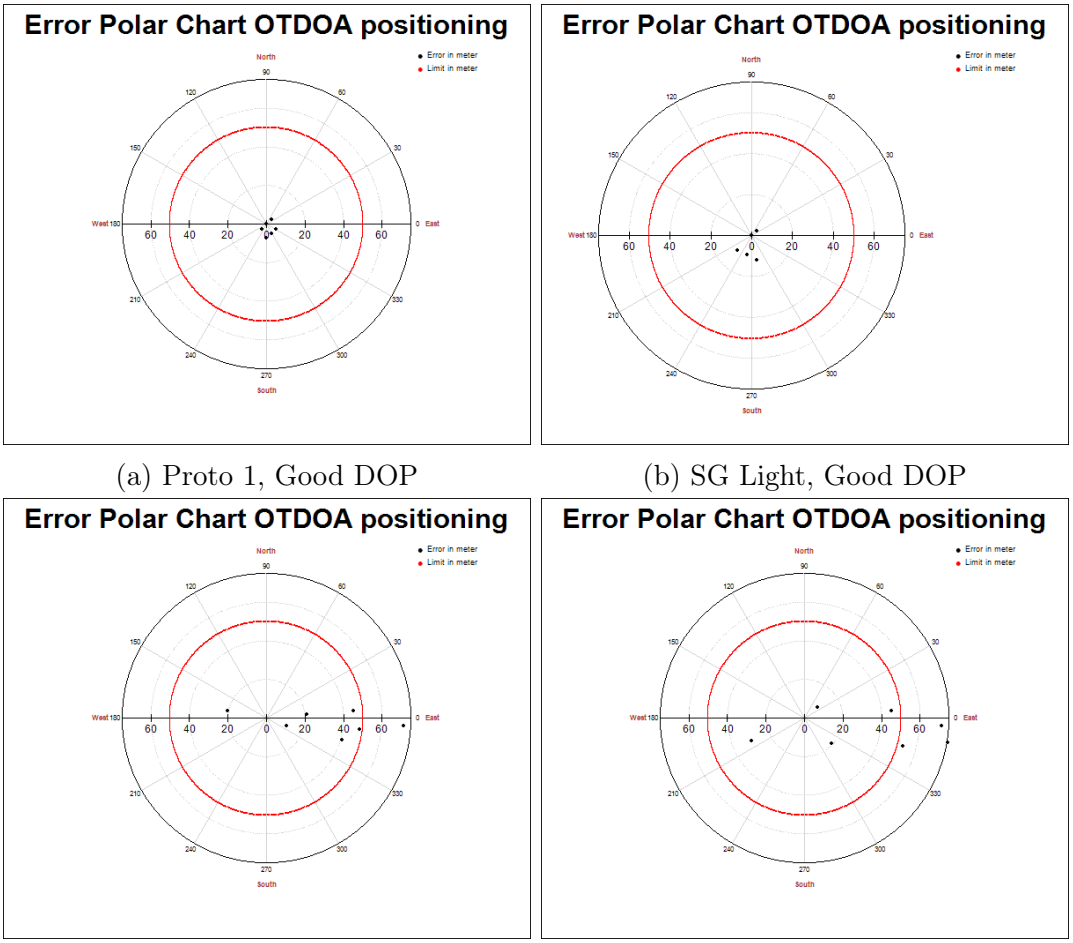

(a) Proto 1, Good DOP (b) SG Light, Good DOP

(c) Proto 1, Bad DOP (d) SG Light, Bad DOP

Figura 4: Resultados de posicionamiento OTDOA sin error de sincronización entre estaciones base.

E. Reflexión sobre los resultados

Los resultados vistos en simulación parecen a primera vista contradecirse con respecto a los resultados obtenidos en el sistema real con respecto al error de sincronización entre estaciones base. En simulaciones se ha llegado a la conclusión de que por encima de 10 nanosegundos de error de sincronización los resultados empeoraban considerablemente, mientras que en el sistema de test, para el escenario con buen DOP, los resultados no empeoran tanto. Sin embargo, si que lo hacen para el escenario con mal DOP. En la simulación, la posición del móvil era aleatoria, lo que quiere decir que en unas iteraciones tenía buen DOP y en otras malo, mientras que el sistema real, debido a limitaciones del mismo, solo se han simulado dos posiciones. El error de sincronización entre estaciones base afecta más en escenarios con mal DOP, al igual que todos los errores, como se ha visto durante el desarrollo teórico: $E_{pos} \propto DOP \cdot E_{medida}$.

0.3.2 OTDOA y ECID

Para las mismas constelaciones que se han utilizado con OTDOA, se incluye una medida ECID con la estación base (Sección 4.2), ya que hasta E-UTRA Rel. 11 no es posible realizar medidas RTT a las celdas vecinas. En Fig. 5, se muestra la nueva distribución de DOP para las constelaciones tras incluir esta medida ECID. Se puede ver que el DOP ha mejorado con respecto al caso anterior, por lo que cabe esperar también mejores resultados.

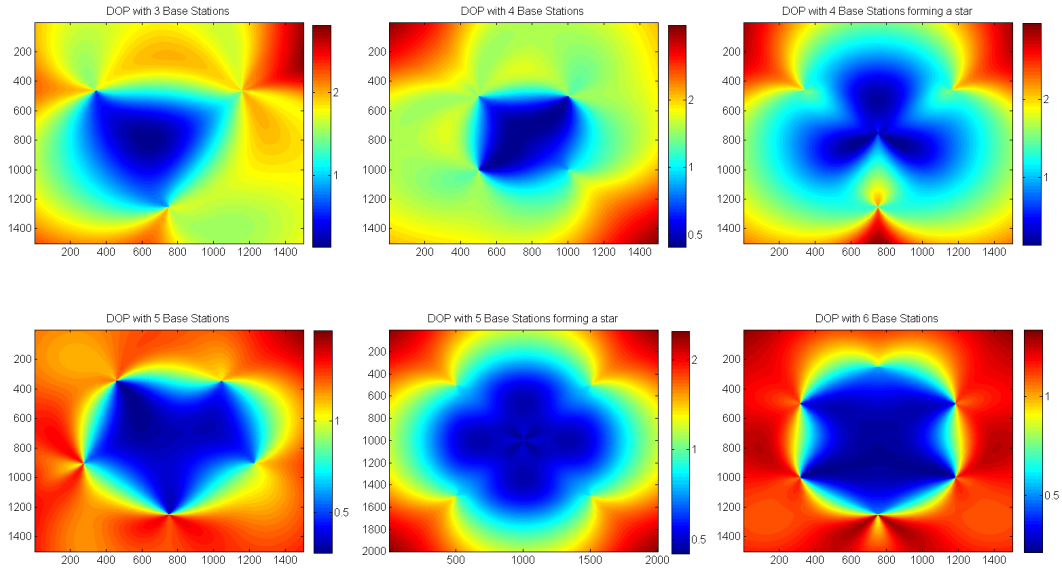

Figura 5: Diferentes constelaciones y su distribución de DOP para OTDOA + ECID.

Se repite la simulación, con las mismas mil posiciones aleatorias de la sección anterior. Se puede observar una ligera mejoría de los resultados, si bien todavía están limitados por las mismas restricciones de sincronización entre celdas LTE del caso anterior.

A. OTDA y ECID en interiores

En la Sección 4.3, se ha analizado la viabilidad del algoritmo para localización en interiores. Para ello, se ha propuesto un modelo que despliega pico y femtoceldas en el interior del edificio. Se propone una medida ECID con la estación base y medidas OTDOA para todo el resto de estaciones LTE, incluyendo pico y femtoceldas. Incluso así, los resultados obtenidos no alcanzan a cumplir los objetivos del FCC, pues la

precisión necesaria solamente se consigue en algo más del 50 % de las ocasiones y si la sincronización de las femtoceldas es perfecta.

0.3.3 Posicionamiento Híbrido

Como último paso, solo queda incluir las medidas GNSS. Para ello, se simularán varios escenarios con diferentes combinaciones de satélites y medidas terrestres.

A. Cuatro o más satélites con buen DOP

Si hay cuatro o más satélites disponibles y el DOP de la constelación es bueno, el algoritmo es capaz de calcular posiciones precisas sin utilizar medidas de OTDOA y ECID. De hecho, como se puede observar en Tab. 4.29, añadir estas medidas puede ser contraproducente, ya que la sincronización entre estaciones base u otras fuentes de error puede empeorar los resultados.

B. Cuatro o más Satélites con mal DOP

Si hay cuatro o más satélites, pero el DOP de la constelación es malo, si que hay beneficio en añadir medidas terrestres. En Tab. 2 se muestran los resultados de todas las combinaciones posibles de tecnologías.

LBS type	**BS$_{sync}$ [ns]**	**Errors [m]**			**[%]E$_P$ <**		
		$\langle E \rangle$	Max$_E$	Min$_E$	<50 m	<100 m	<500 m
GNSS	-	49.93	128.87	2.65	61.0	89.6	100
GNSS + OTDOA	0	13.71	39.63	0.44	100	100	100
	10	36.02	69.57	10.45	91.1	100	100
	25	89.59	126.35	60.61	0	80.2	100
	50	181.57	217.07	146.89	0	0	100
GNSS + ECID	-	19.51	61.08	0.74	98.5	100	100
Hybrid	0	13.16	33.95	0.70	100	100	100
	10	33.06	68.71	8.42	95.0	100	100
	25	80.91	129.95	56.18	0	95.5	100
	50	161.31	208.80	130.86	0	0	100

Tabla 2: Rendimiento del algoritmo con cuatro satélites y mal DOP.

Si la sincronización de las estaciones base es buena, la solución óptima es combinar GNSS con OTDOA y ECID (si hay medidas disponibles). En caso contrario, GNSS + ECID ofrece mejores resultados.

También se han analizado los resultados del algoritmo de localización híbrido, comparando el escenario con cuatro satélites pero mal DOP y el mismo escenario añadiendo OTDOA con dos teléfonos reales. Los resultados, como se puede ver en la Fig. 6, mejoran considerablemente al añadir OTDOA.

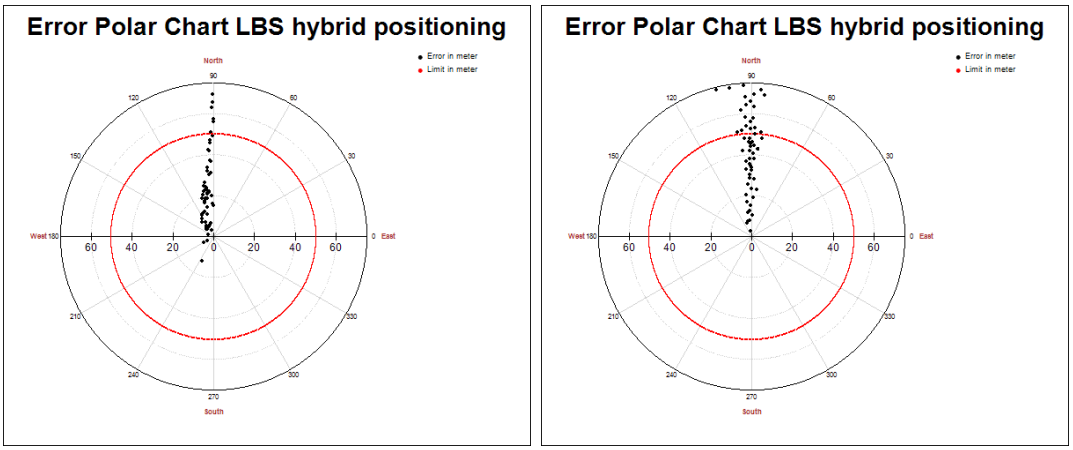

(a) Proto 2, GNSS

(b) SG Light, GNSS

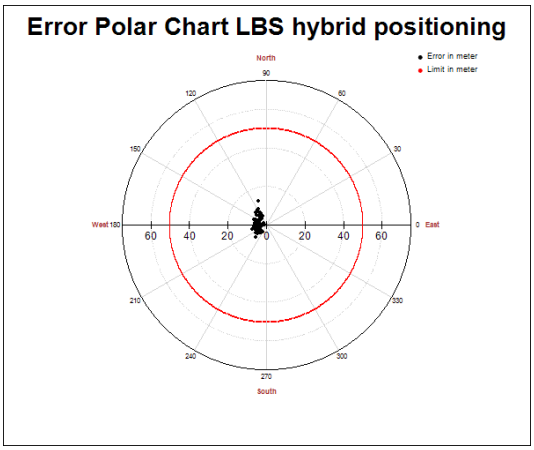

(c) Proto 2, Hybrid

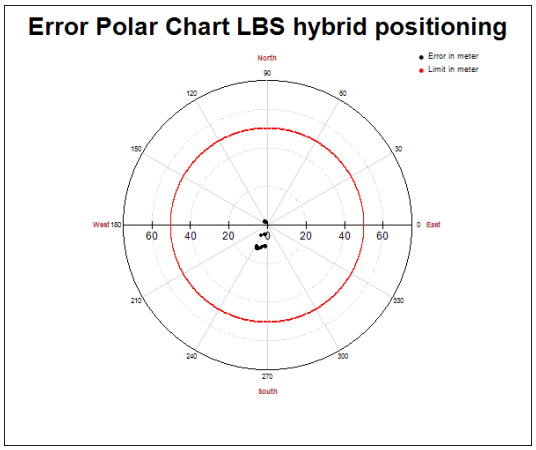

(d) SG Light, Hybrid

Figura 6: Comparación entre GNSS y Localización Híbrida.

En esta figura, se ha supuesto una sincronización perfecta entre las estaciones LTE. En Tab. 3, se presenta el porcentaje de iteraciones con éxito (error menor a 50 metros) para diferentes valores de error de sincronización, para el móvil comercial y el prototipo 2.

$\mathbf{BS}_{sync}$ [ns]	Proto 2	SG Light
0	100	100
10	100	100
25	100	100
50	100	100
100	95	56

Tabla 3: Porcentaje de iteraciones con éxito para localización Híbrida con errores de sincronización.

C. Solo dos satélites visibles

Otro caso de interés es aquel donde no hay suficientes satélites visibles. En este caso, algunas combinaciones no serán posibles, ya que GNSS o GNSS + ECID no reúnen suficientes medidas para calcular la posición del móvil. Los resultados para las diferentes tecnologías se muestran en Tab. 4, donde se puede ver que el algoritmo Híbrido es la mejor opción en este caso.

LBS type	$\mathbf{BS}_{sync}$ [ns]	**Errors [m]**			**[%]E$_P$ <**		
		$\langle E \rangle$	Max_E	Min_E	<50 m	<100 m	<500 m
GNSS	-	∞	∞	∞	0.0	0.0	0.0
GNSS + OTDOA	0	17.74	60.05	0.81	99.6	100	100
	10	43.04	91.42	10.95	69.5	100	100
	25	106.83	149.81	70.67	0	33.4	100
	50	216.34	263.72	171.77	0	0	100
GNSS + ECID	-	∞	∞	∞	0.0	0.0	0.0
Hybrid	0	16.83	64.43	0.81	99.8	100	100
	10	39.01	81.29	11.12	80.1	100	100
	25	93.37	143.45	59.72	0	69.8	100
	50	179.72	237.55	139.31	0	0	100

Tabla 4: Rendimiento del algoritmo con solo dos satélites visibles.

En cuanto a los resultados en el sistema real, aquí es donde mejor pueden apreciarse las diferencias entre el móvil comercial y el prototipo, siendo esté último el que mejor rendimiento ofrece. Fig. 7 muestra la gráfica polar del error en la posición calculada sin error de sincronización entre las estaciones base, y Tab. 5 muestra el porcentaje de éxito para los diversos casos estudiados.

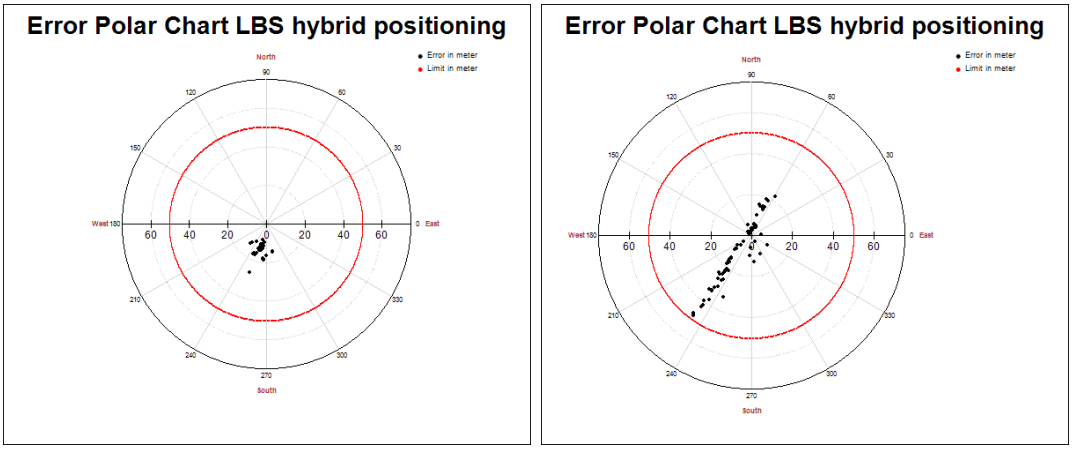

(a) Proto 2, $BS_{sync} = 0$ [ns] (b) SG Light, $BS_{sync} = 0$ [ns]

Figura 7: Posicionamiento Híbrido con dos satélites.

BS_{sync} [ns]	Proto 2	SG Light
0	100	100
25	100	92
50	100	77

Tabla 5: Porcentaje de iteraciones con éxito para localización Híbrida con dos satélites.

D. Escenario con propagación multicamino

Además de los errores de sincronización, en el mundo real las señales de LTE y de satélite estarán afectadas por otro tipo de fuentes de error. En Tab. 6, se muestran los resultados si tanto la señal del satélite como la de OTDOA están contaminadas con componentes multicamino. Para el caso sin error de sincronización entre estaciones de LTE, se muestra el diagrama polar del error en Fig. 8. En el caso de OTDOA, se ha simulado un perfil ETU30, especificado por el 3GPP (véase Tab. 5.6). La señal GNSS tiene una componente adicional con un retraso de 300 nanosegundos y -7 dB con respecto a la componente directa.

BS_{sync} [ns]	Proto 2	SG Light
0	100	97
10	100	90
25	100	81
50	100	67

Tabla 6: Porcentaje de iteraciones con éxito para localización Híbrida con propagación multicamino.

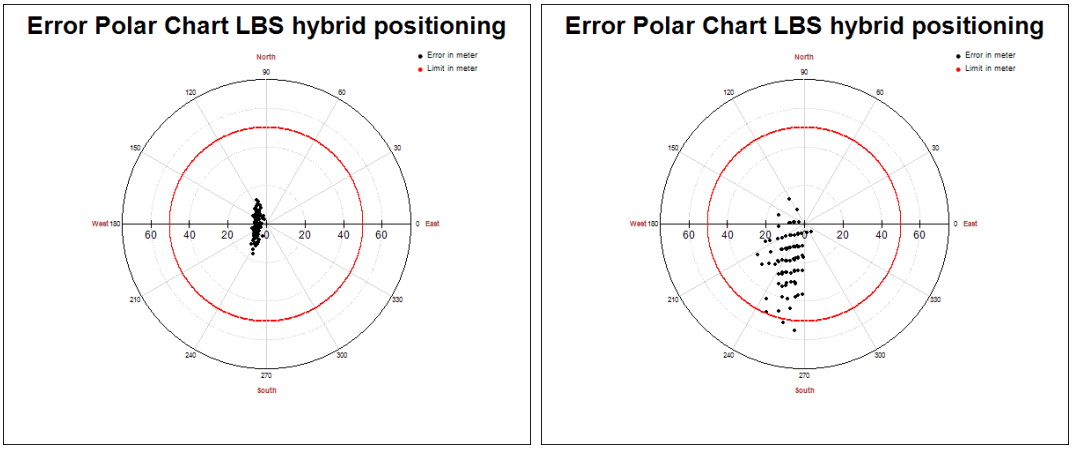

(a) Proto 2, $\mathrm{BS}_{sync} = 0$ [ns] (b) SG Light, $\mathrm{BS}_{sync} = 0$ [ns]

Figura 8: Localización Híbrida con propagación multicamino.

0.3.4 Localización en interiores

Para localización en interiores no se han obtenido hasta ahora los resultados que requiere la FCC. Se ha visto que sin GNSS, ECID y OTDOA por sí solos no son capaces de obtener la exactitud y disponibilidad necesarias, salvo que se desplieguen femtoceldas y éstas estén perfectamente sincronizadas.

En la improbable situación de que haya algún satélite visible, el algoritmo funciona correctamente (ver Sección 4.4.4), pero esto no ocurrirá en la mayoría de los casos.

La principal restricción para el funcionamiento de OTDOA y ECID con femtoceldas es la sincronización entre las mismas. Esto no sería un problema para ECID, ya que las medidas RTT no requieren sincronización entre las diferentes estaciones base. Por tanto, a partir de E-UTRA Rel. 11, será posible aplicar el algoritmo planteado con pico y femtoceldas, incluso aunque éstas no estén sincronizadas. Dichas celdas han de utilizarse solo para ECID.

Esta propuesta se ha simulado en la Sección 4.5, mejorando notablemente los resultados obtenidos hasta ahora, y cumpliendo los requisitos del FCC. Sin embargo, para ello hace falta instalar las femtoceldas en todos los edificios en los que necesite localización en interiores, con los costes de despliegue y mantenimiento que ello conlleva.

0.4 Conclusiones

En este TFM, se ha presentado un algoritmo para localización de dispositivos móviles en LTE, que combina medidas de satélites, OTDOA y ECID. Su funcionamiento ha sido analizado a través de simulaciones con matlab así como con teléfonos móviles reales y una plataforma de test certificada para 4G. Se han estudiado escenarios en exteriores y en interiores. El principal objetivo de este algoritmo era alcanzar los requisitos de precisión y disponibilidad exigidos por los principales operadores de red y los servicios de emergencia como parte de las regulaciones para el E911. Adicionalmente, se han introducido conceptos como Dilusión de Precisión (DOP) y su influencia en la exactitud de las posiciones calculadas. También se han presentado las posibles fuentes de error que afectan a OTDOA y ECID. De este trababjo se han extraído las siguientes conclusiones:

- Si hay suficientes satélites disponibles (cuatro o más) y la geometría de la constelación de satélites es favorable, el algoritmo es capaz de calcular posiciones que satisfacen las condiciones de la FCC usando solo GNSS.
- Si hay menos de cuatro satélites disponibles, o el DOP de la constelación no es bueno, GNSS puede ser combinado con OTDOA y ECID para obtener la exactitud necesaria.
- Utilizar OTDOA y ECID sin GNSS solo es válido para calcular posiciones bidimensionales. La altitud es difícil de calcular debido a la poca diversidad de alturas que presentan normalmente las estaciones base, que proporciona un valor de GDOP bastante malo.
- En algunos escenarios, se puede inferir el valor de la altitud. Un ejemplo es asumir que el dispositivo móvil se encuentra sobre la superficie de la Tierra.
- El valor de DOP para sistemas TDoA y ToA coincide.
- El análisis del DOP de una constelación de estaciones base ha de ser una parte central de la planificación de redes LTE que sean aptas para posicionamiento OTDOA y ECID. En este TFM se han propuesto y analizado varias geometrías de constelaciones.
- La sincronización entre estaciones base es crucial para OTDOA. El error de sincronización ha de mantenerse por lo menos por debajo de 50 nanosegundos para

obtener resultados de posicionamiento aceptables. Si OTDOA es la única tecnología utilizada, este error de sincronización debería ser incluso más bajo, sin superar los 10 ns.

- ECID es una alternativa más acertada si la sincronización de las celdas LTE no puede garantizarse. Las medidas de RTT a las celdas vecinas serán posibles a partir de E-UTRA Rel. 11
- La combinación de GNSS, OTDOA y ECID en interiores no es suficiente, ya que el número de satélites visibles será reducido, y en interiores la altitud es una variable bastante importante en la posición calculada. Se debe utilizar algún mecanismo adicional. En este trabajo se ha propuesto el despliegue de femto o picoceldas dentro de ciertos edificios como medida para alcanzar los requisitos de la FCC. Estas celdas han de estar muy bien sincronizadas o han de emplearse solo para medidas de ECID.
- El algoritmo planteado puede ser expandido con mucha facilidad para incluir otras tecnologías adicionales.

En resumen, el algoritmo planteado en este TFM alcanzará las metas requeridas por la FCC en la mayoría de los escenarios, si se tienen en cuenta las restricciones de sincronización entre celdas y de geometría de las constelaciones propuestas. Sin embargo, hay una serie de casos particulares que se deben analizar por separado:

En entornos urbanos muy densos, túneles u otros sitios donde no haya línea de visión con ningún satélite, OTDOA y ECID solo pueden utilizarse para calcular posiciones bidimensionales. Será necesario utilizar la superficie de la tierra como altitud.

En interiores, si no se han desplegado femtoceldas, es posible que el algoritmo propuesto no alcance los requisitos de exactitud para E911. Este tipo de escenarios ha de ser estudiado con más detalle y soluciones adicionales serán necesarias para aquellos edificios donde instalar celdas LTE no sea una opción viable.

0.5 Trabajos Futuros

Durante este TFM se han encontrado una serie de temas que merece la pena investigar con más detalle en el futuro.

0.5.1 Análisis exhaustivo del canal OTDOA

Este TFM ha utilizado para calcular sus resultados un modelo de propagación definido por el 3GPP, el perfil ETU30. Este modelo ha sido diseñado a partir de medidas de canal de ciudades muy concurridas como Nueva York o Tokio. Sin embargo, dado que es un modelo, realiza algunas simplificaciones y suposiciones que no se corresponden al 100 % con la realidad. Además, este modelo solo es válido para condiciones similares a aquellas en las que las medidas han sido tomadas, pero puede no ser válido para áreas semiurbanas, ciudades menos concurridas o el campo. OTDOA es una tecnología que se ve severamente afectada por errores en la medida de los tiempos de recepción o vuelo de las señales. Por tanto, una caracterización detallada del canal para OTDOA, especialmente de la propagación multicamino, será beneficioso para entender mejor las limitaciones y las posibles fuentes de error que afecten a la localización.

Para plantear este modelo, se requieren más medidas de campo en escenarios representativos. A partir de dichas medidas, se pueden definir una serie de perfiles de propagación nuevos para estudiar el mayor rango de escenarios posible.

0.5.2 WiFi, Bluetooth y otras tecnologías

Otra posibilidad para solucionar el problema de la localización en interiores sin necesidad de desplegar una red de femtoceldas pasa por utilizar los recursos existentes para realizar las medidas. Estos recursos comprenden puntos de acceso WiFi, dispositivos Bluetooth, etc. Las extensiones del protpcolo LPP (LPPe) definen una serie de interfaces para posibilitar la realización de estas medidas y que sean transmitidas a la red LTE.

Los siguientes pasos para mejorar el algoritmo propuesto están relacionados con la inclusión de estas tecnologías:

- Analizar la exactitud y precisión de las medidas de potencia de señal WiFi (RSSI) y decidir si incluir estas medidas al algoritmo mejorará los resultados o no. Las medidas de potencia son por lo general mucho menos precisas que las medidas temporales debido a la drástica pérdida de la potencia de la señal al atravesar obstáculos como paredes.

- Extender el algoritmo para incluir medidas de WLAN RTT (tiempo de vuelo de ida y vuelta). Estas medidas siguen el mismo concepto teórico que ECID, por lo que a priori los buenos resultados obtenidos con ECID y femtoceldas deberían extenderse a los puntos de acceso WiFi.
- Investigar otras posibilidades adicionales, como Bluetooth.

Chapter 1

Introduction

Communication technology has greatly evolved during the last century, especially during the last few decades. Since the invention of the telephone in 1871 by Antonio Meucci, this device has increasingly gained importance in our daily lives. Nowadays, the mobile phone has become almost an extension of the human body: in Europe, the number of mobile phone subscriptions (i.e. number of registered SIM cards) per 1000 inhabitants was an average of 1298 for the EU-28[1] in 2012 [1], meaning that there are more mobile phone subscriptions than people.

In Fig. 1.1, published by Eurostat in 2014, a per country comparison for the EU-28 and other non-member states in Europe can be seen. Within the EU-28, Latvia is the country with the most mobile phones per inhabitant (1,898 registered sim cards per person), only surpassed by the non-member Albania, with a total of 1,936, almost two mobile phone subscription per citizen. Spain stays a bit below the average, with *only* 1220 subscriptions per 1000 inhabitants. These astonishing figures are even more remarkable if we compare the trend over the last few years: between 2004 and 2012, the average number of mobile phone subscriptions have increased around a 50 %. The highest rates are seen in east European countries where, for instance, Albania has quadrupled the registered SIM cards since 2004. In contrast, other countries like Luxembourg show a quite stable mobile phone penetration rate, and the number of mobile phone subscriptions has remained almost unchanged during the last few years.

[1]The 28 states members of the European Union.

	2004	2006	2008	2010	2011	2012
EU-28	870		1 060	1 225 (b)	1 267	1 298
Belgium	810	890	1 050	1 112 (b)	1 144 (b)	1 181
Bulgaria	620	1 070	1 370	1 359 (b)	1 474	1 601
Czech Republic	1 060	1 240	1 330	1 276 (b)	1 290	1 251
Denmark	960	1 070	1 200	1 415 (b)	1 473	1 516
Germany	900	1 040	1 310	1 170 (b)	1 211	1 242
Estonia	930	1 170	1 210	1 205 (b)	1 350	1 499
Ireland	940	1 120	1 220	1 124 (b)	1 134	1 197
Greece	840	1 250	1 690	1 172 (b)	1 121	1 200
Spain	910	1 050	1 100	1 185 (b)	1 249	1 220
France	720	820	910	936 (b)	1 001	1 060 (b)
Croatia	659	970	1 100	1 479 (b)	1 192	
Italy	1 080	1 370	1 520	1 584 (b)	1 615	1 642
Cyprus	900	1 130	1 290	1 243 (b)	1 296	1 312
Latvia	660	950	980	1 580 (b)	1 701	1 898
Lithuania	890	1 390	1 490	1 558 (b)	1 614	1 649
Luxembourg	1 430	1 520	1 460	1 432 (b)	1 428	1 458 (b)
Hungary	860	990	1 220	1 084 (b)	1 102	1 107 (b)
Malta	770	860	940	1 062 (b)	1 267	1 319
Netherlands	910	1 130	1 230	1 165 (b)	1 251	1 233
Austria	980	920	870	1 430 (b)	1 506	1 571
Poland	600	960	1 160	1 144 (b)	1 194 (b)	1 311
Portugal	930	1 160	1 410	1 526 (b)	1 573	1 577
Romania	470	810	1 140	1 188 (b)	1 168	1 129
Slovenia	930	910	1 020	1 032 (b)	1 055	1 069
Slovakia	790	910	1 020	1 140 (b)	1 119	1 153
Finland	960	1 080	1 300	1 508 (b)	1 633	1 694
Sweden	980	1 060	1 190	1 307 (b)	1 380	1 444
United Kingdom	1 000	1 160	1 260	1 331 (b)	1 352	1 371
Iceland	998	950	1 070	1 181	1 212	1 249
Liechtenstein	750	820	970	:	:	:
Norway	990	1 050	1 110	:	:	:
Switzerland	850	1 000	1 170	:	:	:
Montenegro	779	1 127	1 093	2 260	1 870	1 595
FYR of Macedonia	492	695	883	1 098	1 105	1 085
Albania	415	636	1 002	1 558	1 801	1 936
Serbia	579	895	1 148	1 357	1 404 (b)	1 266
Turkey	491	726	878	851	886	906

Figure 1.1: Number of mobile phone subscriptions per 1000 people. Source: [1].

The relevance of mobile phones in the present world is out of question. That is the reason why more and more research is focused on exploring and maximizing the possibilities of these devices.

Current mobile phones are not just devices to call and be called. Current mobile phones are complete entertainment stations with access to the internet, powerful processors and high quality cameras. They can be used to run an almost infinite number of applications, play videos, listen to music, etc. Nevertheless, mobile devices are more than mere entertainment centres. They are equipped with sensors like accelerometers and gyroscopes which can be used for monitoring the human body and gather information for health applications; they contain GNSS receivers to provide the users accurate location and directions; they can record video or take pictures better than some digital cameras. The full potential of mobile phones is still to be reached, and every day new applications and technologies are developed and released. Studying one of these new technologies is the purpose of this Thesis.

1.1 Motivation

One of these applications is the emergency call that puts the users in direct contact with the police, the ambulance or the firemen in case of emergency. Knowing the exact location of the person who is in need of assistance is a key element to the improvement of emergency services. It would reduce the amount of time required to reach to this person and potentially save lives. However, when a person calls the emergency services, he might not know accurately his location. For instance, if a group of hikers gets lost in the mountains and requires the emergency services to find them, they will not be able to precise where they are. Another example, if your car stops working in the highway and you need to call for a tow, you might not know the exact kilometre point where you are. In fact, the EU has estimated that more than half of the calls to emergency services are done with a mobile device and in almost 60% of them the caller is unable to provide its current position accurately [2]. According to [10], there were 336 million wireless subscriber devices by the end of 2013. In the United States, 44 % of the households had wireless-only connection (i.e. 44% of the houses do not have a land-line telephone). That is the reason behind the resolution of the EU in 2003 to require network operators to provide emergency services with any information available about the location of the caller. This resolution was called the Enhanced 112 (**E112**) as a reference to the European emergency call service number, 112. That is also the reason why the Third Generation Partnership Project (**3GPP**) specifications for the Long Term Evolution (**LTE**) standard have included the so called Location Based Services (**LBS**) to group of all services used to determine the mobile device position.

Below, all currently defined LBS technologies in the 3GPP standard for LTE will be shortly introduced:

- Global Navigation Satellite System (**GNSS**) is the most known and used of all LBS, which uses satellites to compute the position of the GNSS receiver embedded in the mobile phone. The estimation of the distance between the GNSS receiver and each of the satellites is called a *pseudo-range*. Calculating the pseudo-range to three satellites will result in a system with three equations and three unknowns (the receive coordinates latitude, longitude and altitude or, more generically x, y and z). An additional satellite is required for the time correction [11], given in total a system with four unknowns (x, y, z and t) and four equations. This technique is called trilateration.

Current GNSS systems are Global Positioning System (**GPS**) from the US, GLONASS from Russia, GALILEO from the EU and the Chinese BeiDou. In the adequate conditions, i.e. if the GNSS receiver has a direct line of sight (**LoS**) to at least four satellites, the accuracy reached with GNSS is beyond questioning. In particular, for GPS, the US government claims to obtain an accuracy of 7.8 metres for the pseudo-range measurement under worst case conditions and a total of 3.5 metre horizontal accuracy in the final position [2]. However, these conditions are not always met. High density urban areas, tunnels, forests or indoor locations are critical for GNSS, as there might be not enough visible satellites. In Fig. 1.2, the total number of available GPS satellites in a typical city centre is depicted.

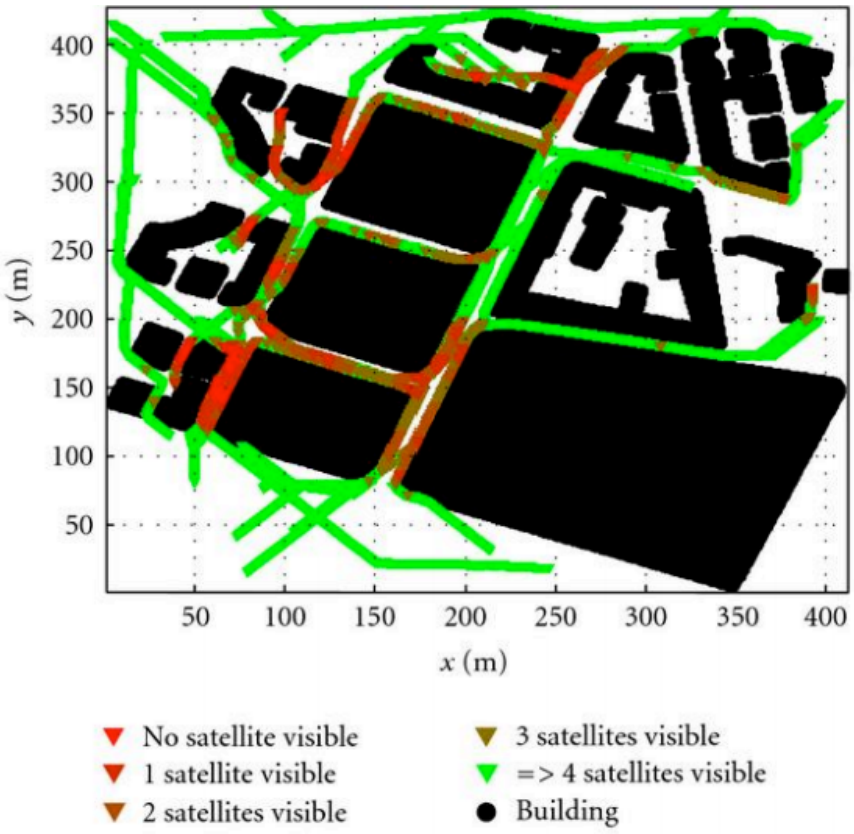

Figure 1.2: Number of visible GPS satellites in a city centre. Source: [12].

As it can be appreciated, there are several points across the city centre where not enough satellites are visible. This problem can be partially overcome with Assisted GNSS (**A-GNSS**), where the cellular network assists the GNSS receiver with assistance data containing the Almanac and/or Ephemeris data for the visible satellites. By doing so, the GNSS receiver in the mobile phone can know

[2]Checked in `http://www.gps.gov/systems/gps/performance/accuracy/` on February 8th, 2015.

which satellites should be in view, its location and expected Doppler shift. This information helps narrowing the search region and reduces the acquisition times from minutes to seconds. However, even A-GNSS is bound to have at least four visible satellites. Given that almost 50% of the location requests are made within an indoor environment [2], it is likely that in a high percentage of location sessions not enough satellites will be in line of sight. Moreover, it should not be overlooked that each of the different GNSS systems belongs to a certain government. The availability of the GNSS signal for each system cannot be ensured. For all these reasons, additional methods are required to compensate the shortcomings of GNSS.

These other methods, as compared to satellite navigation, are called terrestrial positioning or network positioning technologies and they comprise Observed Time Difference Of Arrival (**OTDOA**) and Enhanced Cell ID (**eCID or E-CID**).

- OTDOA is a hyperbolic location system in which the mobile device tries to measure the time difference between signals received from different base stations. This technique is called *multilateration*. It was firstly introduced as a positioning feature for Evolved UMTS Terrestrial Radio Access (**E-UTRA**) Release 9 in the 3GPP RAN#42 meeting [13] in 2008. The necessary changes were introduced to the required RAN1 specifications (TS-36211 to TS-36214) during 2009. From the mathematical point of view, OTDOA could be seen as a descendant of LORAN-C navigation system[3], used for maritime navigation in the second half of the 20$^{\text{th}}$ century.
- E-CID is another positioning technique introduced in E-UTRA release 9. The mobile device is requested to measure and report the serving Cell ID, the timing advance (difference between its transmit and receive time) and the IDs, estimated power and timing of the detected neighbour cells. Therefore, it can be classified as a Time of Arrival (**TOA**) technique.

All three technologies form the Location Based Services defined so far for LTE. All of them use time measurements, although GNSS and eCID are ToA methods (hence they define spheres of location) while OTDOA is a TDoA method and it defines a hyperbolic hyperboloid of location. These particularity will arise difficulties when combining all measurements together, and it will be one of the key points of this Thesis.

[3] `http://en.wikipedia.org/wiki/Loran-C`

LBS can be used for entertainment purposes (many existing applications use the location of the users as an input to interact with elements in their area) or for navigation (to give the users directions to their desired destination), but in this thesis the focus will be on LBS as a functionality to improve the E911 and E112 services. The accuracy requirements for the E911 location information in the US are defined by the Federal Communication Commission (**FCC**) in agreement with all the major US network operators[4].

The latest agreement, from 2014 [3, 4], defines a series of requirements and goals to be met by all mobile phone manufacturers and network operators in the US during a period of several months. The main goal is to improve the accuracy of the location provided to the Public Safety Accessing Point (**PSAP**) for wireless calls for both indoor and outdoor environments to 50 metres. This target needs to be achieved for a certain percentage of all calls and this percentage is increased over time until a final goal of 80% of all Voice Over LTE (**VoLTE**) calls in 72 months [3]. To do so, a number of *heightened location accuracy technologies* need to be used and combined. The short-term goals include the deployment and improvement of the recently developed location technologies A-GNSS, OTDOA and ECID, first for horizontal (2-D) positioning and afterwards for including as well height information.

On the mid-term, the focus will be on improving the existing solutions and introducing **dispatchable location solutions** (especially for indoors), defined by the FCC as *the verified or corroborated street address of the calling party plus additional information such as floor, suite, apartment or similar information that may be needed to adequately identify the location of the calling party* [10]. In order to provide these solutions, existing in-building technologies (Wireless Location Area Network (**WLAN**), Bluetooth, etc.) and new infrastructures must be employed. These new infrastructures still need to be defined, but some potential candidates are beacons, Distributed Antenna Systems (**DAS**), Commercial LBS (**cLBS**) solutions and/or deployment of pico- and femto-cells either in the unlicensed frequency spectrum[5] or as part of the LTE network (see [14] for more information about taking advantage of the unlicensed spectrum for improving LTE).

The long-term goals include the full deployment of VoLTE and the improvement of the solutions until a position within 50 metres accuracy can be provided for 80% of all emergency calls.

[4]See `http://www.fcc.gov/`

[5]Part of the frequency spectrum who is available for everyone to use.

1.2 Problem Statement

In the previous section, several LBS technologies have been introduced and briefly defined. The requirements of the authorities and network operators regarding accurate positioning in general as well as specifically for emergency called services have also been presented. However, how the LBS technologies can be combined and used to meet the requirements is not yet explained.

The methods introduced can be classified according to different criteria:

- From the mathematical point of view, there are TDoA (OTDOA) and ToA (A-GNSS and eCID) methods. A positioning system with TDoA measurements uses a multilateration method, while ToA measurements are combined by trilateration.
- From the geometrical point of view, we have spheres (A-GNSS, eCID) and hyperbolic hyperboloids (OTDOA).
- From the technological point of view, there are satellite navigation (A-GNSS) and terrestrial positioning techniques (OTDOA and eCID).

How can this heterogeneous group of technologies be combined together? The answer to that question is not trivial. There are methods for calculating positions separately for each of the technologies [15–17], but there is very little literature on how to get a unique position combining any set of two or three of them. This will be called as Hybrid LBS and it will be the first topic of this Thesis.

A second point of concern is the feasibility of OTDOA and/or eCID as standalone methods for LBS positioning. Although OTDOA and eCID have already been studied in several publications, how will they perform in the real field? Which factors can affect their accuracy?

Existing literature suggests that the accuracy which can be reached with network-based positioning methods is less than the accuracy of GNSS services if enough satellites are available [18]. Current trend seems to indicate that the order of priority for a location fix should be A-GNSS, then OTDOA and finally eCID. Nevertheless, some questions remain unanswered: is it possible to improve the accuracy of GNSS by including terrestrial positioning measurements even if enough satellites are available? How do the relative locations between the satellites (i.e. the geometry of the constellation)

affect the results? How does the geometry of the base stations affect the results? When should measurements be ignored or discarded? The answer to all these questions will come partly from the geometrical analysis of the system (by calculating the Dilution of Position (**DOP**)) and partly from the experimentation with different scenarios.

Finally, a special situation that needs to be addressed separately is *indoor positioning*. Typically, in an indoor scenario not enough satellites will be available, and even if they are, all of them will come from the same region of the sky, what means that the geometrical distribution of the satellites will not be optimal for the trilateration. How can an accurate position indoors be computed? The latest topic of this Thesis will be to take a close look at the indoor scenario and analyse further possibilities to achieve accurate indoor positioning.

1.3 Objectives

The goal of this Master Thesis is to answer all the questions exposed in the previous section. For that, the following objectives should be achieved:

- Propose a solution for accurate location estimation that meets the requirements of accuracy demanded by network operators and emergency services authorities for the outdoors scenario.
- Analyse the feasibility of the existing technologies for the indoor scenario. Study further possibilities and propose a theoretical model for indoor positioning.

For reaching those objectives, the following steps or side goals should also be fulfilled:

- Propose an algorithm to calculate a position estimation by using a number of heterogeneous measurements from different technologies.
- Use this algorithm to study the feasibility of OTDOA and eCID technologies for standalone positioning.
- Validate the proposed algorithm theoretically and experimentally.

- Analyse the impact of the Dilution of Precision in the positioning results. Propose a definition of the DOP for Hybrid LBS scenarios.
- Identify a set of representative scenarios to simulate the conditions where OTDOA and eCID measurements should be combined with A-GNSS to improve the performance.
- Propose a mechanism to determine when measurements are not contributing to the improvement of the solution and should be rejected or discarded.
- Study the particularities of indoor scenarios.
- Evaluate other possibilities for indoors, e.g. WLAN or femtocells.

Chapter 2

Theoretical Background

In this chapter, the theory behind the three LBS technologies mentioned before (A-GNSS, OTDOA and eCID) will be analysed. This analysis will be the first step towards finding a location algorithm able to combine multiple measurements from different systems.

2.1 Position calculation methods

Before defining each of the technologies that will be considered during this Thesis, it is worth to dedicate a few lines to analyse and compare the different mathematical methods to compute a position, commonly used in localization and navigation systems. These are called *triangulation*, *trilateration* and *multilateration*.

2.1.1 Triangulation

Triangulation is the technique to determine the position of an object by measuring angles to this object from known points. It is a very ancient method, already used by the Greek philosopher Thales to estimate the height of the pyramids in Egypt.

It can be mathematically explained by Fig. 2.1. The distance to a point C needs to be calculated (x in the figure). For that, the positions of two known points A and B will be used, and the angles α and β will be measured.

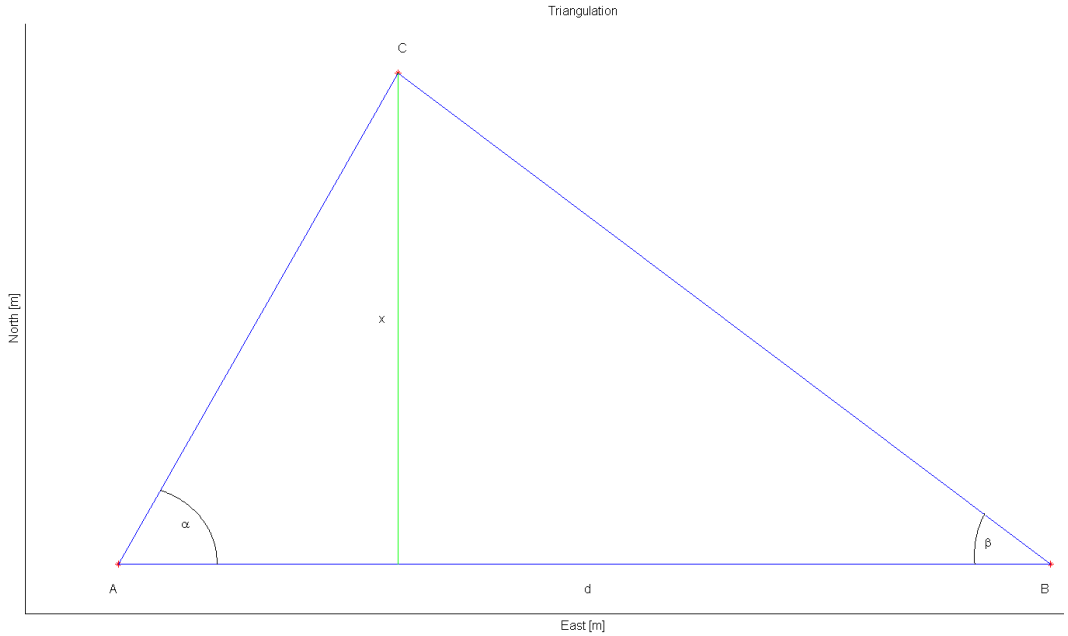

Figure 2.1: Triangulation

By applying the trigonometric identities, the following equation can be obtained:

$$d = \frac{x}{\tan\alpha} + \frac{x}{\tan\beta}. \tag{2.1}$$

As $\tan\phi = \frac{\sin\phi}{\cos\phi}$, Eq. (2.1) can be transformed into

$$d = x\left(\frac{\cos\alpha}{\sin\alpha} + \frac{\cos\beta}{\sin\beta}\right), \tag{2.2}$$

which can be rewritten used the identity $\sin(\phi+\psi) = sin\phi\cos\psi + \cos\phi\sin\psi$:

$$d = x \cdot \frac{\sin(\alpha+\beta)}{\sin\alpha\sin\beta}. \tag{2.3}$$

Finally, the x can be calculated as follows:

$$x = d \cdot \frac{\sin\alpha\sin\beta}{\sin(\alpha+\beta)}. \tag{2.4}$$

Triangulation is used for positioning methods where the Angle of Arrival (**AoA**) of the radio signal can be measured. For that purpose, arrays of antennas placed side by side are used. If the distance between the antennas is small, the incident front of the signal can be considered as straight, and by measuring the phase difference between

the signals received by the antennas, the angle of arrival of the signal can be calculated with fair accuracy. Another method to measure the AoA is to use a directional antenna to determine which direction produces the strongest received signal.

2.1.2 Trilateration

Trilateration is often confused with triangulation, although the base principle is completely different. Trilateration requires to measure the absolute distance between the receiver and the transmitter. The most common methods for measuring distance are to calculate the ToA of the signal (as in satellite navigation) or using a Received Signal Strength Indicator (**RSSI**) to estimate the power of the received signal and compare it with the transmission power.

The locus of points with constant distance to a known point is a circumference in 2-D models and a sphere in three-dimensional models. This can be seen in Fig. 2.2.

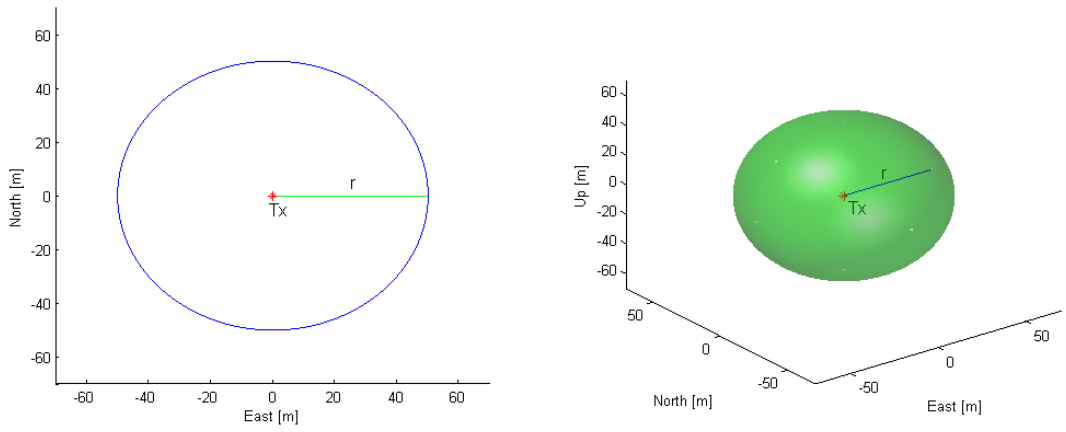

Figure 2.2: Circumference and sphere

The equation of the circumference is:

$$(x-a)^2 + (y-b)^2 = K, \tag{2.5}$$

where a and b are the coordinates of the centre of the circumference, i.e. the transmitter and K is a constant value which represents the radius of the circumference squared. If instead the positioning system is working in 3-D, the equation of the sphere is:

$$(x-a)^2 + (y-b)^2 + (z-c)^2 = K. \tag{2.6}$$

K will be here the radius of the sphere squared. This constant value K can be related to the time measurement as follows:

$$K = r^2 = (m_T \cdot v_p)^2 + e_{m_T}^2, \tag{2.7}$$

where m_T represents the time measurement and v_p stands for the speed of propagation. e_{m_T} is the error associated to the measurement.

If the position of the transmitter is known, the distance to the receiver is enough to estimate a circumference along which the receiver must be located. Measuring the distance to multiple transmitters allows the receiver to estimate multiple circumferences, determining its position by finding the intersection point between them. In Fig. 2.3, it can be seen that to uniquely identify the position of the receiver, at least three measurements are required.

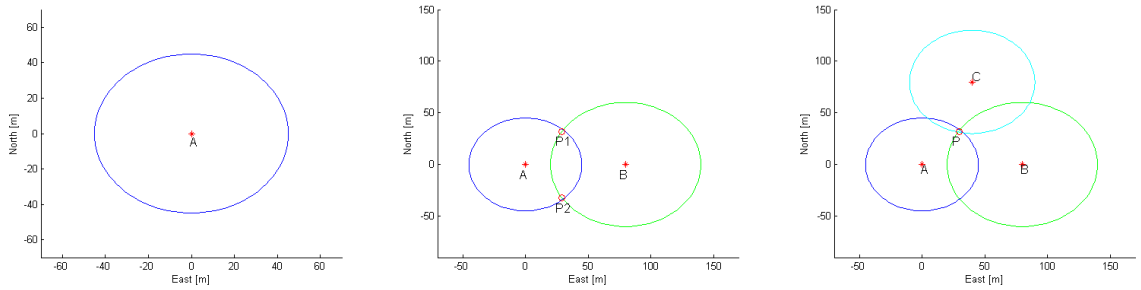

Figure 2.3: Trilateration

2.1.3 Multilateration

Multilateration is a position computation technique based on the difference in the distances to two base stations at known locations. This is done by measuring the TDoA between two signals at the receiver. The advantage over trilateration is that here the receiver does not need to know at what time instant the signal was transmitted. Hence, it does not require to be synchronized with the network of transmitters.

Geometrically, the locus of points for which the ratio of the distances to two fixed points is constant is called a *hyperbola*, if the location is done in a two-dimensional space. The generalization of the hyperbola for the 3-D case is a *hyperbolic hyperboloid*, often called just hyperboloid. The two fixed points (the pair of eNBs) are called *focus* of the hyperbola. The standard equation defining the hyperbola is:

$$\frac{x^2}{a^2} - \frac{y^2}{b^2} = 1. \tag{2.8}$$

An example of a hyperbola is depicted in Fig. 2.4. P represents the location of the receiver, which a priori could be anywhere in the surface of the hyperbola/hyperboloid. BS_1 and BS_2 are the transmitters or base stations, here focus of the hyperbola. The parameters a and b of the hyperbola have been chosen as $a = b = \sqrt{10}$ for this example. The dashed red lines are the *asymptotes* of the hyperbola, i.e. the lines to which the hyperbola branches tend when $x, y \to \infty$. The distance between the centre of the hyperbola (O) and each of the focus is $\sqrt{a^2 + b^2}$. Finally, the *eccentricity* of a hyperbola is defined as $\epsilon = \frac{\sqrt{a^2+b^2}}{a^2}$.

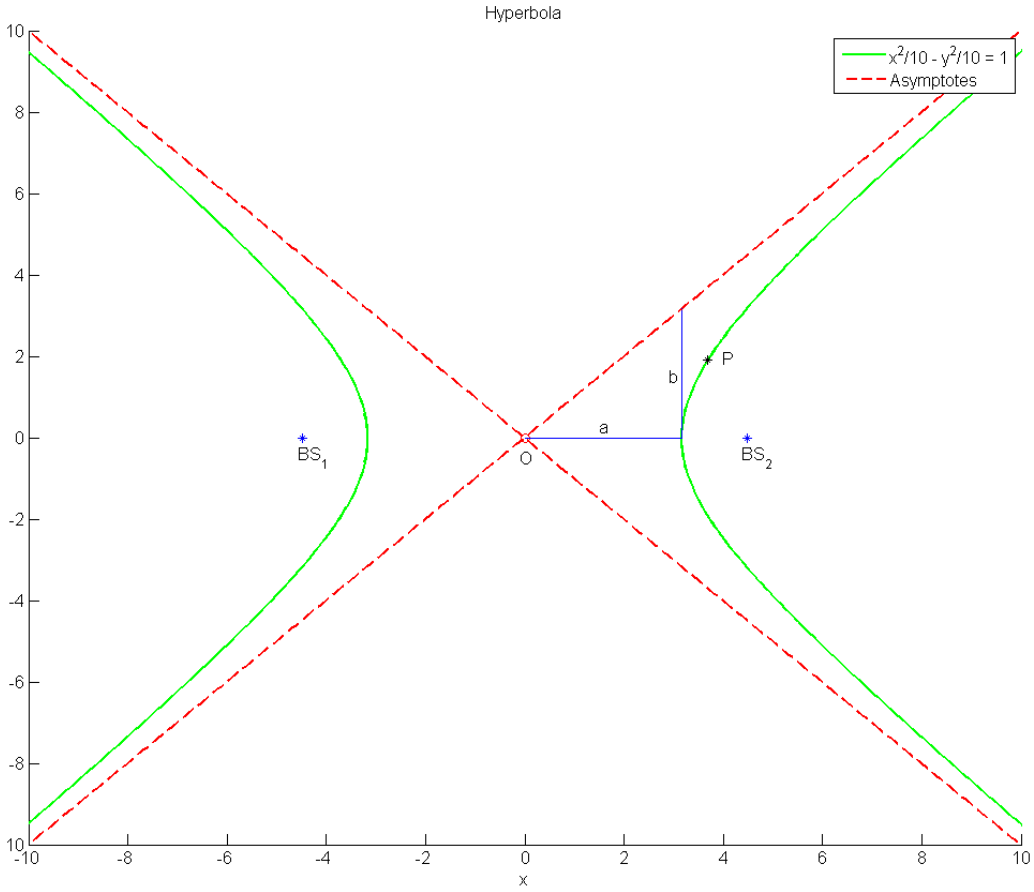

Figure 2.4: Example of a hyperbola with $a = b = \sqrt{10}$.

Analogously, the hyperboloid is defined by the following equation:

$$\frac{x^2}{a^2} + \frac{y^2}{b^2} - \frac{z^2}{c^2} = \pm 1. \tag{2.9}$$

If the right side of the equation has the + sign, the hyperboloid has *one-sheet*. For localization, the hyperboloid of two sheets is normally used, and hence the equation is defined with the minus sign on the right side. This type of hyperboloid is represented in Fig. 2.5.

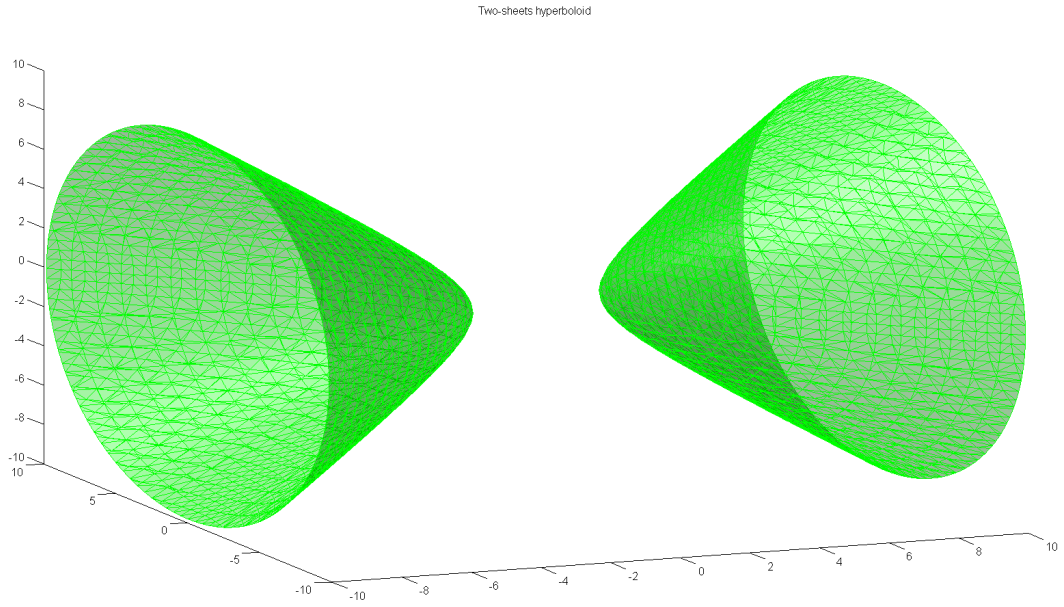

Figure 2.5: Example of a two-sheets hyperboloid.

A. Principles of hyperboloid localization

The mathematical derivation will be done assuming three-dimensional location to maintain generality. A Cartesian coordinate system with X, Y and Z coordinates is defined, where X and Y represent the horizontal plane and Z stands for the vertical coordinate. If the 2-D equations are required, the Z-coordinate terms should be neglected. Graphically, it can be appreciated that Fig. 2.4 is a horizontal cut of Fig. 2.5 at Z = 0. The position of the receiver will be denoted as $P = \{x, y, z\}$ and the position of a base station i is given by $BS_i = \{x_i, y_i, z_i\}$. In Eq. (2.10), the basic property of the hyperboloid is introduced mathematically:

$$\overline{PBS_2} - \overline{PBS_1} = K, \tag{2.10}$$

where K represents a constant value and $\overline{PBS_i}$ is the distance between the receiver located in P and the Base Station i. To simplify the notation, this will be denoted as

d_i:

$$d_2 - d_1 = K, \tag{2.11}$$

where $d_i = \sqrt{(x - x_i)^2 + (y - y_i)^2 + (z - z_i)^2}$. The constant value K is multiple of the *time delay* (TD), which is the value that the receiver should measure and report. If v_p stands for the *propagation speed*, then K can be defined as follows:

$$K = TD \cdot v_p + e_{TD}, \tag{2.12}$$

where e_{TD} represents the error associated to the time delay measurement. In Fig. 2.6, the influence of the variation of TD on the hyperbola can be seen. The value of Time Delay is calculated relative to the distance D between both Base Stations and the propagation speed.

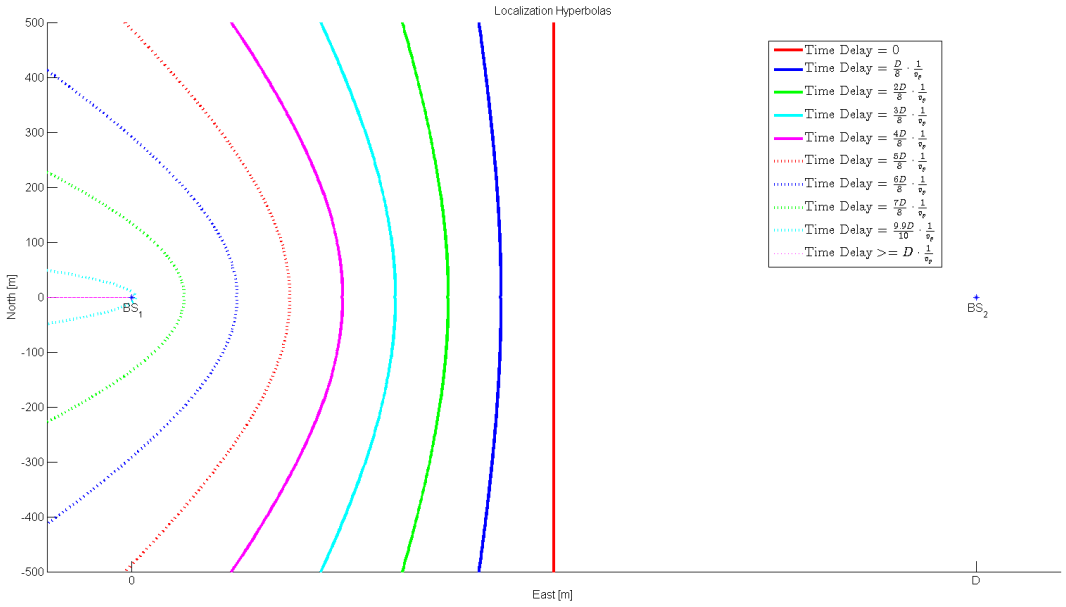

Figure 2.6: Localization hyperbola in function of the time delay measurement.

For $TD = 0$ and $TD >= D$, the result is not a hyperbola. These are the two degenerate cases for which the mathematical calculation of the hyperbola diverges to a straight line.

From Fig. 2.6, it can be seen how one time delay measurement is enough to approximate the position of the receiver to a curve. For a 2-D location, at least two time delay measurements are required. However, two hyperbolas can potentially cut in more

than one point. In order to have a 100% certainty in all cases, three measurements are required (see Fig. 2.7).

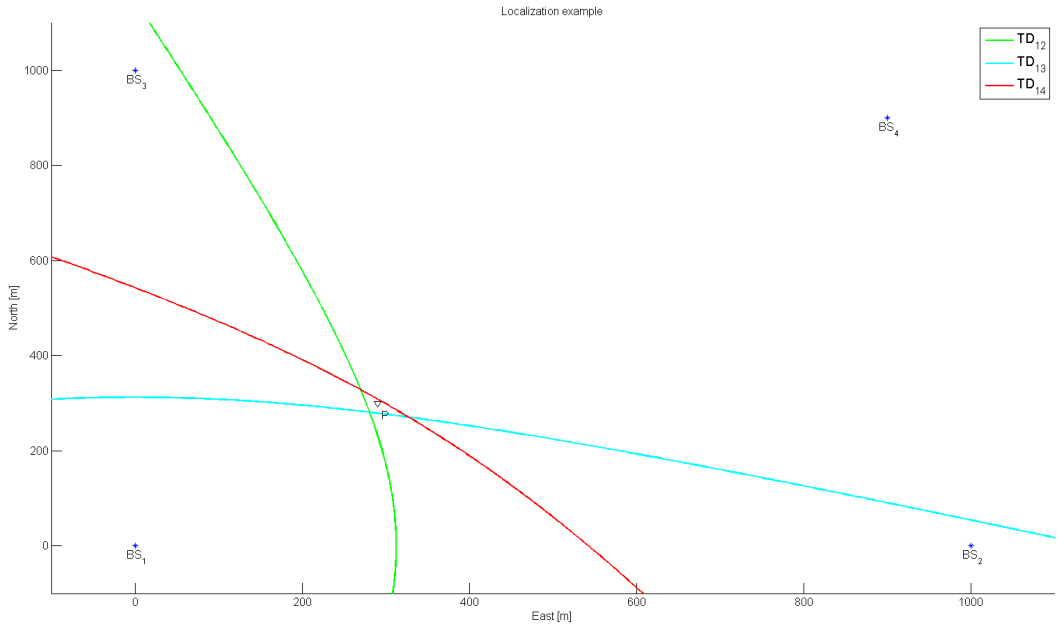

Figure 2.7: Example of 2-D hyperbolic location or multilateration

2.2 GNSS

Global Navigation Satellite Systems are system of satellites providing geo-spatial positioning with global coverage around the world. The position of a device is calculated by an embedded GNSS receiver which measures the time signals received from each satellite. Via a *trilateration* method (see Section 2.1.2), the GNSS receiver is able to compute its position combining line-of-sight measurements from three or more satellites.

Nowadays, there are two fully operational GNSSs: the United States Global Positioning System (**GPS**) and the Russian GLONASS. In addition to that, China is working on the extension of its regional Satellite Navigation System (BeiDou) into the global Compass and the European Union is involved in the initial deployment phase of their Galileo positioning system [19, 20].

There are also some regional satellite systems under development, like the Indian Regional Navigational Satellite System (**IRNSS**), the Japanese Quasi-Zenit Satellite

System (**QZSS**) or the French Doppler Orbitography and Radiopositioning Integrated by Satellite (**DORIS**).

All these GNSSs have (or will have) a constellation formed by between 20 and 30 active satellites in the medium Earth orbit (**MEO**) spread between several orbital planes of more than 50° and around 12 hours or orbital period [9, 20].

2.2.1 Brief history of GNSS

Satellite navigation can be considered as a successor of the hyperbolic localization and navigation systems popularized after the World War II (see Section 2.3.1). The first satellite navigation system was deployed in the 1960s by the United States military forces [21]. It was called *Transit*, and it took advantage of the *Doppler* effect to calculate the position of the receiver. One of the main disadvantages of this system is that the satellites were equipped with a quartz oscillator to keep the accuracy of the clock. The quartz oscillator is not as accurate as the atomic clocks deployed in newer satellites from other navigation systems and the synchronization between satellites could not be maintained to the degree of accuracy that GNSS has nowadays. Transit remained operational until 1996, when it ceased navigation service due to being made obsolete by modern systems like GPS.

The so-called modern satellite systems started with GPS, first deployed in 1978 but not globally available until 1994. Its main current competitor, GLONASS, was completely functional in 1995. The satellites in these systems transmit a broadcast signal containing orbital data sufficient to derive the satellite position and a *precise* time signal. This time signal is possible due to the high precision atomic clocks embedded in the satellites.

In the late 1990s and the 2000s, the research to further enhance the accuracy of GNSS has lead to the development of GNSS augmentation techniques for improving the accuracy, reliability and availability of satellite navigation through the integration of external information into the calculation process. These are called Satellite Based Augmentation Systems (**SBAS**) and comprehend a huge number of technologies, both global and regional, to increase GNSS attributes using a large variety of methods. A few examples are the Wide Area Augmentation System (**WAAS**), operated by the United States Federal Aviation Administration; the European Geostationary Naviga-

tion Overlay Service (**EGNOS**), or the Wide Area GPS Enhancement (**WAGE**), used by US military applications [20].

Further improvements in the receiver's side include the reduction of errors by, for instance, the implementation of Kalman filters to combine the constantly changing data into a unique estimated position, speed and time.

2.2.2 A-GNSS

GNSS is the main positioning technology defined by the 3GPP for mobile phone location services. One of the critical issues for mobile phone location, especially during an emergency call, is the so-called time-to-first-fix (**TTFF**) or the time until the first location fix can be calculated. In standard GNSS, this time is hugely impacted by the time required to download assistance data files (GNSS almanac and ephemerides) from the satellite link. This time is estimated up to 12.5 minutes for GPS [8, 9, 22].

The insufficiency of this TTFF for emergency calls leaded to the deployment, accelerated significantly by the FCC of the United States [1], of the Assisted-GNSS. AGNSS is able to dramatically improve the startup performance of GNSS satellite-based positioning and it is part of E911 and E112 regulations for emergency services. The TTFF is reduced by using available data from the network to avoid the need of downloading this data from the satellite link. This data comprehends the ephemerides, which contains orbital information allowing the receiver to calculate the position of each satellite, and the almanac, which contains status information about all satellites, their locations and the Coarse/Acquisition (PRN) code. There are two different operation modes in A-GNSS:

- **UE-Based**: in UE based or mobile based mode, the mobile network provide ephemerides and almanac data to the mobile phone, in order to decrease the time require to find and lock the satellites.
- **UE-Assisted**: in UE assisted mode, the GNSS receiver aboard the mobile phone captures the satellite data available and sends it to the mobile network. The position calculation is done by a positioning server on the network side. This approach reduces the computational requirements on the GNSS receiver in the mobile phone.

[1] `http://www.fcc.gov/`

Due to A-GNSS, the TTFF for mobile phone positioning can be reduced from several minutes to a few seconds.

2.2.3 Mathematical derivation

A satellite receiver measures the time between the transmission of a signal by the satellite and its reception. When multiplying this time by the speed of propagation of the signal, a measurement of the distance between the receiver and the satellite is obtained. This measurement is called a *pseudo-range*. The prefix *pseudo* is added to reflect that there are accuracy errors in the time measurement which affect the quality of the measurement [8,9]. A true range (without clock error) is defined as the distance between the transmitter and the receiver and, using Earth-centred Earth-fixed (**ECEF**) coordinates, it can be written as follows:

$$\rho_{true} = \overline{TxRx} = \sqrt{(x_{tx} - x_{rx})^2 + (y_{tx} - y_{rx})^2 + (z_{tx} - z_{rx})^2} \tag{2.13}$$

A pseudo-range will be a measurement of the true range contaminated by the clock biases from transmitter and receiver [6]:

$$\rho = \rho_{true} + c \cdot \tau_{rx} - c \cdot \tau_{tx} + \nu, \tag{2.14}$$

where τ_{tx} and τ_{rx} are the clock biases from transmitter and receiver, respectively and ν stands for the other errors associated with the measurement. ν is considered as Gaussian noise independent and identically distributed (**iid**) of mean $\langle \nu \rangle = 0$. The τ_{tx} as well as the transmitter coordinates (the satellite) can be derived from the assistance data available, i.e. the ephemerides and almanac data [6]. Most GNSS receivers are equipped with a quartz oscillator, which have a typical error bigger than one part per million. This error adds a bias to the measurement that would result in a completely wrong position estimation if it is not corrected. Thus, the variable τ_{rx} has to be considered along with the three location coordinates latitude, longitude and altitude if the coordinate system is World Geodetic System 84 (**WGS84**) or x, y and z in case of ECEF, giving a total of four variables to be calculated. Therefore, at least four satellites with a direct line-of-sight are required in order to estimate a position [6, 8].

Measuring the pseudo-ranges to n satellites results in a system of n equations with four unknowns, which is normally solved by Least Squares Estimation (**LSE**) [6].

A. Linearisation of a pseudo-range

The first step is to represent the pseudo-range as a Taylor series. A Taylor series is the representation of a function as an infinite sum of terms according to the following equation:

$$f(x) \approx \sum_{n=0}^{\infty} \frac{f^{(n)}(x=a)}{n!} \cdot (x-a)^n, \tag{2.15}$$

where $f^{(n)}(x = a)$ denotes the nth derivative of f evaluated at a point a. For a multivariate equation, this term represents the partial derivatives with respect to each of the variables.

Applying Eq. (2.15) to Eq. (2.14) around a point $P_0 = \{x_0, y_0, z_0, \tau_0\}$, neglecting second and higher order terms and simplifying the notation:

$$\begin{aligned}\rho(x,y,z,\tau) \approx \rho(x_0,y_0,z_0,\tau_0) + \nu + (x-x_0)\left.\frac{\partial\rho}{\partial x}\right|_{P=P_0} + (y-y_0)\left.\frac{\partial\rho}{\partial y}\right|_{P=P_0} + \dots \\ + (z-z_0)\left.\frac{\partial\rho}{\partial z}\right|_{P=P_0} + (\tau-\tau_0)\left.\frac{\partial\rho}{\partial \tau}\right|_{P=P_0} = \rho_0 + \nu + \dots \\ + \Delta x\left.\frac{\partial\rho}{\partial x}\right|_{P=P_0} + \Delta y\left.\frac{\partial\rho}{\partial y}\right|_{P=P_0} + \Delta z\left.\frac{\partial\rho}{\partial z}\right|_{P=P_0} + \Delta\tau\left.\frac{\partial\rho}{\partial \tau}\right|_{P=P_0}\end{aligned} \tag{2.16}$$

B. Equation system

Combining the equations from n satellites into a equation system and writing into matrix notation:

$$\begin{bmatrix}\rho^1\\ \rho^2\\ \vdots\\ \rho^n\end{bmatrix} = \begin{bmatrix}\rho_0^1\\ \rho_0^2\\ \vdots\\ \rho_0^n\end{bmatrix} + \begin{bmatrix}\left.\frac{\partial\rho^1}{\partial x}\right|_{P=P_0} & \left.\frac{\partial\rho^1}{\partial y}\right|_{P=P_0} & \left.\frac{\partial\rho^1}{\partial z}\right|_{P=P_0} & \left.\frac{\partial\rho^1}{\partial \tau}\right|_{P=P_0}\\ \left.\frac{\partial\rho^2}{\partial x}\right|_{P=P_0} & \left.\frac{\partial\rho^2}{\partial y}\right|_{P=P_0} & \left.\frac{\partial\rho^2}{\partial z}\right|_{P=P_0} & \left.\frac{\partial\rho^2}{\partial \tau}\right|_{P=P_0}\\ \vdots & \vdots & \vdots & \vdots\\ \left.\frac{\partial\rho^n}{\partial x}\right|_{P=P_0} & \left.\frac{\partial\rho^n}{\partial y}\right|_{P=P_0} & \left.\frac{\partial\rho^n}{\partial z}\right|_{P=P_0} & \left.\frac{\partial\rho^n}{\partial \tau}\right|_{P=P_0}\end{bmatrix} \cdot \begin{bmatrix}\Delta x\\ \Delta y\\ \Delta z\\ \Delta\tau\end{bmatrix} + \begin{bmatrix}\nu^1\\ \nu^2\\ \vdots\\ \nu^n\end{bmatrix} \tag{2.17}$$

The system in Eq. (2.17) can be solved iteratively starting from an initial guess of the location of the mobile device $P_0 = \{x_0, y_0, z_0, \tau_0\}$. For each iteration i, a new guess for the position of the mobile device $P_i = \{x_i, y_i, z_i, \tau_i\}$ will be calculated and used as input for the next iteration $i + 1$. The algorithm will continue iterating until $|\Delta P| = |P_i - P_{i-1}| < convergence\_limit$ [23].

Rewriting Eq. (2.17):

$$\begin{bmatrix} \rho_i^1 - \rho_{i-1}^1 \\ \rho_i^2 - \rho_{i-1}^2 \\ \vdots \\ \rho_i^n - \rho_{i-1}^n \end{bmatrix} = \begin{bmatrix} \frac{\partial \rho^1}{\partial x}\Big|_{P=P_0} & \frac{\partial \rho^1}{\partial y}\Big|_{P=P_0} & \frac{\partial \rho^1}{\partial z}\Big|_{P=P_0} & \frac{\partial \rho^1}{\partial \tau}\Big|_{P=P_0} \\ \frac{\partial \rho^2}{\partial x}\Big|_{P=P_0} & \frac{\partial \rho^2}{\partial y}\Big|_{P=P_0} & \frac{\partial \rho^2}{\partial z}\Big|_{P=P_0} & \frac{\partial \rho^2}{\partial \tau}\Big|_{P=P_0} \\ \vdots & \vdots & \vdots & \vdots \\ \frac{\partial \rho^n}{\partial x}\Big|_{P=P_0} & \frac{\partial \rho^n}{\partial y}\Big|_{P=P_0} & \frac{\partial \rho^n}{\partial z}\Big|_{P=P_0} & \frac{\partial \rho^n}{\partial \tau}\Big|_{P=P_0} \end{bmatrix} \cdot \begin{bmatrix} \Delta x \\ \Delta y \\ \Delta z \\ \Delta \tau \end{bmatrix} + \begin{bmatrix} \nu^1 \\ \nu^2 \\ \vdots \\ \nu^n \end{bmatrix} \tag{2.18}$$

$$\Delta\hat{\rho} = A \cdot \Delta\hat{X} + \hat{\nu}, \tag{2.19}$$

where

$$A = \begin{bmatrix} \frac{\partial \rho^1}{\partial x}\Big|_{P=P_0} & \frac{\partial \rho^1}{\partial y}\Big|_{P=P_0} & \frac{\partial \rho^1}{\partial z}\Big|_{P=P_0} & \frac{\partial \rho^1}{\partial \tau}\Big|_{P=P_0} \\ \frac{\partial \rho^2}{\partial x}\Big|_{P=P_0} & \frac{\partial \rho^2}{\partial y}\Big|_{P=P_0} & \frac{\partial \rho^2}{\partial z}\Big|_{P=P_0} & \frac{\partial \rho^2}{\partial \tau}\Big|_{P=P_0} \\ \vdots & \vdots & \vdots & \vdots \\ \frac{\partial \rho^n}{\partial x}\Big|_{P=P_0} & \frac{\partial \rho^n}{\partial y}\Big|_{P=P_0} & \frac{\partial \rho^n}{\partial z}\Big|_{P=P_0} & \frac{\partial \rho^n}{\partial \tau}\Big|_{P=P_0} \end{bmatrix} \tag{2.20}$$

is the system matrix or the *design matrix* [6]. The partial derivatives in A can be calculated as follows:

$$\frac{\partial \rho^j}{\partial x}\Big|_{P=P_0} = -\frac{1}{2} \cdot \frac{2 \cdot (x_{s_j} - x_0)}{\rho^j|_{P=P_0}} = \frac{(x_0 - x_{s_j})}{\rho^j(P_0)} \tag{2.21}$$

$$\frac{\partial \rho^j}{\partial y}\Big|_{P=P_0} = \frac{(y_0 - y_{s_j})}{\rho^j(P_0)} \tag{2.22}$$

$$\frac{\partial \rho^j}{\partial z}\Big|_{P=P_0} = \frac{(z_0 - z_{s_j})}{\rho^j(P_0)} \tag{2.23}$$

$$\frac{\partial \rho^j}{\partial \tau}\Big|_{P=P_0} = c, \tag{2.24}$$

where ρ^j represents the pseudo-range measurement j corresponding to satellite j and x_j, y_j and z_j stand for the coordinates in ECEF of the satellite j. Thus, the design matrix A in Eq. (2.20) at a time instant i can be rewritten as:

$$A = \begin{bmatrix} \frac{(x_{i-1} - x_{s_1})}{\rho^1(P_{i-1})} & \frac{(y_{i-1} - y_{s_1})}{\rho^1(P_{i-1})} & \frac{(z_{i-1} - z_{s_1})}{\rho^1(P_{i-1})} & c \\ \frac{(x_{i-1} - x_{s_2})}{\rho^2(P_{i-1})} & \frac{(y_{i-1} - y_{s_2})}{\rho^2(P_{i-1})} & \frac{(z_{i-1} - z_{s_2})}{\rho^2(P_{i-1})} & c \\ \vdots & \vdots & \vdots & \vdots \\ \frac{(x_{i-1} - x_{s_n})}{\rho^n(P_{i-1})} & \frac{(y_{i-1} - y_{s_n})}{\rho^n(P_{i-1})} & \frac{(z_{i-1} - z_{s_n})}{\rho^n(P_{i-1})} & c \end{bmatrix} \tag{2.25}$$

C. Least Squares Estimation

From Eq. (2.19), the error vector ν is isolated. This will be referred as the *estimated residuals vector* [6]:

$$\hat{\nu} = \Delta\hat{\rho} - A \cdot \Delta\hat{X}. \tag{2.26}$$

In order to find the least squares solution to Eq. (2.26), the following function should be minimized:

$$J(X) = \sum_{i=1}^{n} \nu_i^2 = \nu'\nu = (\rho - A \cdot X)' \cdot (\rho - A \cdot X). \tag{2.27}$$

Following the derivation in [6, 23], the solution to minimize Eq. (2.27) is:

$$\hat{X} = (A'A)^{-1} \cdot A' \cdot \Delta\hat{\rho} \tag{2.28}$$

D. Error Analysis

Analogously to Eq. (2.28), errors in the measurements $\hat{\nu}$ will affect the final position estimation linearly according to the expression:

$$\hat{\nu}_X = (A'A)^{-1} \cdot A' \cdot \hat{\nu}. \tag{2.29}$$

The *covariance matrix* of the measurement errors $\hat{\nu}$ is defined as $C = E(\nu\nu')$, with coefficients $C_{ij} = E(\nu_i\nu_j)$. Applying the definition of the error values as iid, it can be derived that $E(\nu_i\nu_j) = 0 \ \forall \ i \neq j$ and $E(\nu_i\nu_i) = E(\nu_i^2) = \sigma_i^2$ which is known as *variance*. The covariance matrix C can be written as:

$$C = \begin{bmatrix} \sigma_1^2 & 0 & \cdots & 0 \\ 0 & \sigma_2^2 & & \vdots \\ \vdots & & \ddots & 0 \\ 0 & \cdots & 0 & \sigma_n^2 \end{bmatrix} \tag{2.30}$$

The covariance matrix of the calculated position error can be calculated as $C_X = E(\hat{\nu}_X\hat{\nu}'_X)$. Replacing Eq. (2.29) into this formula, the following solution for C_X is found [6]:

$$C_X = C \cdot (A'A)^{-1}, \tag{2.31}$$

where $(A'A)^{-1}$ is called the *cofactor matrix*, Q. C is strictly dependant on the GNSS measurement errors, which are influenced by many sources and hence, very difficult to predict. However, the cofactor matrix Q is purely geometrical, and it depends only in the coordinates of the satellites and the receiver, and the clock bias. It can be defined as follows:

$$Q = (A'A)^{-1} = \begin{bmatrix} \sigma_x^2 & \sigma_{xy} & \sigma_{xz} & \sigma_{x\tau} \\ \sigma_{xy} & \sigma_y^2 & \sigma_{yz} & \sigma_{y\tau} \\ \sigma_{xz} & \sigma_{yz} & \sigma_z^2 & \sigma_{z\tau} \\ \sigma_{x\tau} & \sigma_{y\tau} & \sigma_{z\tau} & \sigma_\tau^2 \end{bmatrix}, \tag{2.32}$$

where it has been applied that $\sigma_{ij} = \sigma_{ji}$. This is the reason why A is called the design matrix, due to its influence in the cofactor matrix and the direct impact on the error of the position calculation. A can be used to *design* the satellite constellation to reduce the error due to bad geometry. It is important to notice the inversion of the matrix resulting from $(A'A)$. If this product is not resulting in a matrix of range (or column space) equal to the number of unknown variables, four, the matrix is not invertible and the system has no solution. That implies, for instance, that satellites which are in the same line-of-sight to the receiver will not constitute two independent equations or that if all satellites are in the same plane, a 3-D position cannot be computed.

A possibility if the matrix Q cannot be calculated, which means that a position cannot be found, is to drop the altitude coordinate z and calculate a 2-D position. This is a valid solution in ship navigation, as the ship is likely going to be at sea level.

2.2.4 Dilution of Precision

Dilution of Precision (**DOP**), also called as Geometrical Dilution of Precision (**GDOP**) is a term used in radio-localization systems to refer to the influence of the system geometry in the accuracy of the calculated position [6,8,9]. In terms of GNSS navigation, the DOP is directly related to the position of the satellites relative to the position of the receiver equipment.

In order to understand better the concept of DOP, Fig. 2.8 represents a system with two transmitters, A and B, and one receiver whose position is a priori unknown.

In the left part, the receiver measures the ToA of signals coming from both transmitters. These measurements are represented in color blue for transmitter A and in color red for transmitter B. The magenta and cyan lines represent the uncertainty in

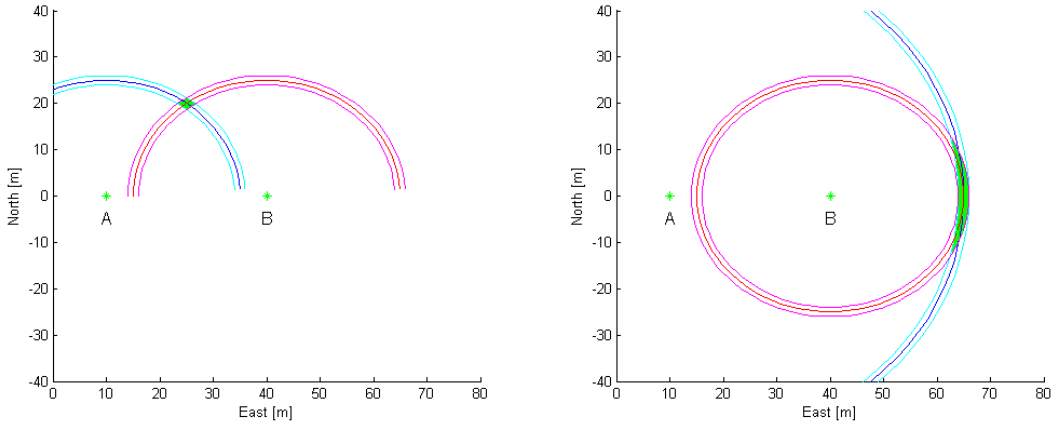

Figure 2.8: Dilution of Precision

the measurement, τ. Hence, the location of the receiver can be narrowed down to the relatively small green area in the figure. On the right side, the same transmitters constellation is depicted. However, the location of the receiver is now different, affecting the measurements. It can be seen that in this second scenario the green area is comparatively much bigger. The same measurement error, τ, has a much bigger impact on the second scenario than on the first. The system on the left has a low DOP value and it is what will be referred as a *good geometry*, while the system on the right has a high DOP value, being what is called a *bad geometry*.

The DOP is a very good estimator of the suitability of the constellation of visible/available satellites to calculate a certain receiver's position. A DOP value of 1 means that an error of 1 metre in the measurements translates to an average error of 1 metre in the calculations, while for a DOP value of 20, the same measurement error could result in around 20 metres error in the positioning.

The DOP is calculated from the trace of the cofactor matrix Q, depicted in Eq. (2.32). The DOP is calculated as follows:

$$DOP \equiv GDOP \equiv \sqrt{\sigma_x^2 + \sigma_y^2 + \sigma_z^2 + \sigma_\tau^2}. \tag{2.33}$$

Analogously to the definition of GDOP (Geometrical DOP), PDOP, HDOP, VDOP and TDOP can be defined, to represent *Position, Horizontal, Vertical* and *Time* DOP,

respectively.

$$PDOP \equiv \sqrt{\sigma_x^2 + \sigma_y^2 + \sigma_z^2} \tag{2.34}$$

$$HDOP \equiv \sqrt{\sigma_x^2 + \sigma_y^2} \tag{2.35}$$

$$VDOP \equiv \sigma_z \tag{2.36}$$

$$TDOP \equiv \sigma_\tau \tag{2.37}$$

The best possible value for the dilution of precision is generally DOP = 1. If a large number of satellites is available, this value could be smaller than one, but that is a very rare situation. Under 2, the DOP is optimal for the position calculation. Between 2 and 5 is considered good DOP value and above 5 it starts to be considered as a poor geometry for the localization. If the number of total measurements is smaller than the number of unknowns, the DOP value will diverge to infinity which symbolizes that a position cannot be calculated with that number of satellites.

2.2.5 Sources of error of GNSS

GNSS navigation is affected by several sources of error that cannot be easily predicted. In this section, these errors and their approximate impact in the calculated position will be discussed [24, 25]. All the values given here are the typical *variance* of the error for each error source.

- The satellite clock bias, noted as τ_{tx} in Eq. (2.14), is the error caused by the bias in the synchronization of the satellite. As satellites are normally equipped with an atomic clock to keep the timing, this error is smaller than the receiver clock bias. However, it is estimated it can add an error of $\sim \pm 2.1$m.
- The orbital errors comprehend the errors associated to the calculation of the satellite position at a certain time from the ephemerides data. They are caused mainly by approximations in the orbital models and non compensated gravitational forces. They can account for up to $\sim \pm 2.5$m of error in the pseudo-range measurement.
- Ionospheric effects: the ionosphere is a region of the atmosphere that goes from 80 to 600 kilometres above the earth surface. This layer can cause refractions and delays in the satellite signal proportional to the number of free electrons radiated

by the sun. The weekly ionized plasma or gas on the ionosphere changes rapidly and it is very difficult to model, although its effects are reduced during night time. It will affect more satellites with lower elevation angle, as the signal will cross the ionosphere in a longer trajectory. If they are not corrected, these effects are the largest source of error introducing up to $\sim \pm 4$m of uncertainty in the measurements. There are several models that can compensate a fraction of the ionospheric effects, but its study is beyond the scope of this Thesis.

- Tropospheric effects: the troposphere is the layer of the atmosphere in direct contact with the surface of the Earth, and it is where the meteorology phenomena occur: clouds, precipitation, wind, etc. Its impact in the GNSS positioning is mainly due to delays and refractions caused by varying temperature and humidity. It can be correct by basic models up to 90% of its error. It typically adds $\sim \pm 0.5$m of error.

- Receiver noise can cause jitter in the signal. $\sim \pm 0.4$m of error.

- Multipath errors due to reflections of the signal against terrestrial objects such as mountains or buildings. The reflected signals will have longer ToF (time of flight) which can induce errors in the time measurement and hence affect the pseudo-range. The multipath is more critical for satellites with low elevation angles. To understand better this phenomena, Fig. 2.9 depicts an example: the satellite is transmitting a signal with Right Hand Circular Polarization (**RHCP**) and a GPS receiver placed inside a car is receiving the signal. The direct signal coming from the line of sight direction reaches the receiver unaltered. However, there are also some building in the vicinity of the car. The signal from the satellite reflects against the buildings and reaches the receiver from a longer path. After one reflection, the signal polarization changes to Right Hand Circular Polarization (**LHCP**), which is easy to filter. Unfortunately, after a second reflection the signal has again a good RHCP, becoming hard to identify as a reflected signal by the receiver. The multipath effect can cause $\sim \pm 1.5$m of error.

2.2.6 A-GNSS accuracy measurements

There are some standards that allow the GNSS receiver to report an estimate of the accuracy of the position calculation. First of all, it it worth stating the difference between accuracy and precision:

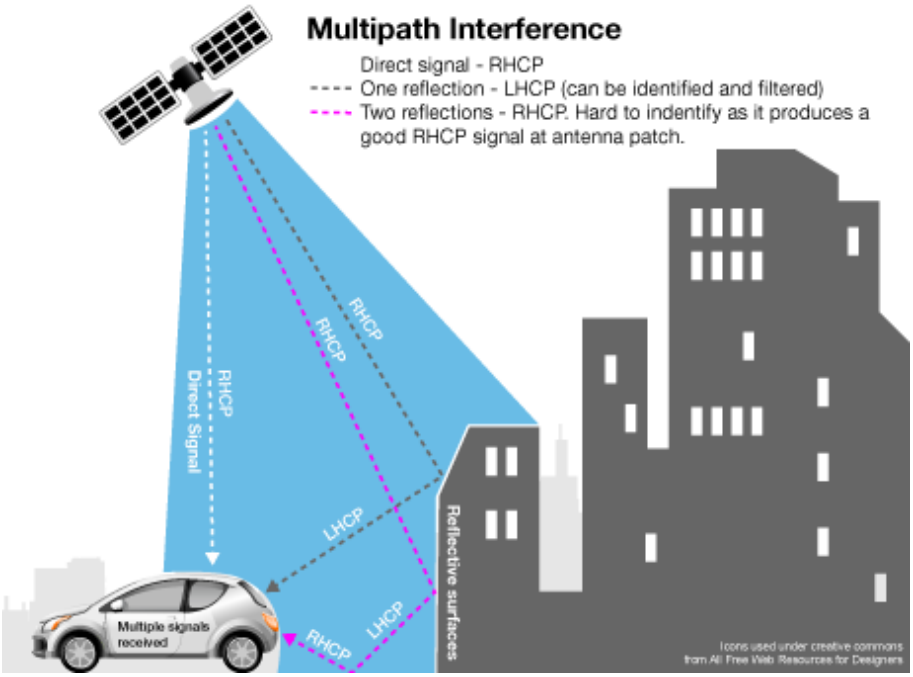

Figure 2.9: Multipath effect. Source: `www.stepglobal.com`

Accuracy: The accuracy of a measurement indicates the degree of proximity between the measurement and the real value.

Precision: The precision of a measurement is related to repeatability and reproducibility of the results. It is the degree of proximity between independent measurements performed under unchanged conditions.

In order to further clarify the difference, Fig. 2.10 gives a very good example of both terms.

There are several different parameters defined for representing GNSS accuracy, each of them associated to a different percentage of accuracy [9]:

- **CEP**: The Circular Error Probability gives the radius of a circle centred in the real position. 50% of the measurements of the GNSS receiver will be within this circle. Hence, if you have a certain measurement, the real position will be within a circle of *CEP* meters radius in half of the cases (50% confidence level). It is estimated with the following formula:

$$0.62 \cdot \sigma_y + 0.56 \cdot \sigma_x \tag{2.38}$$

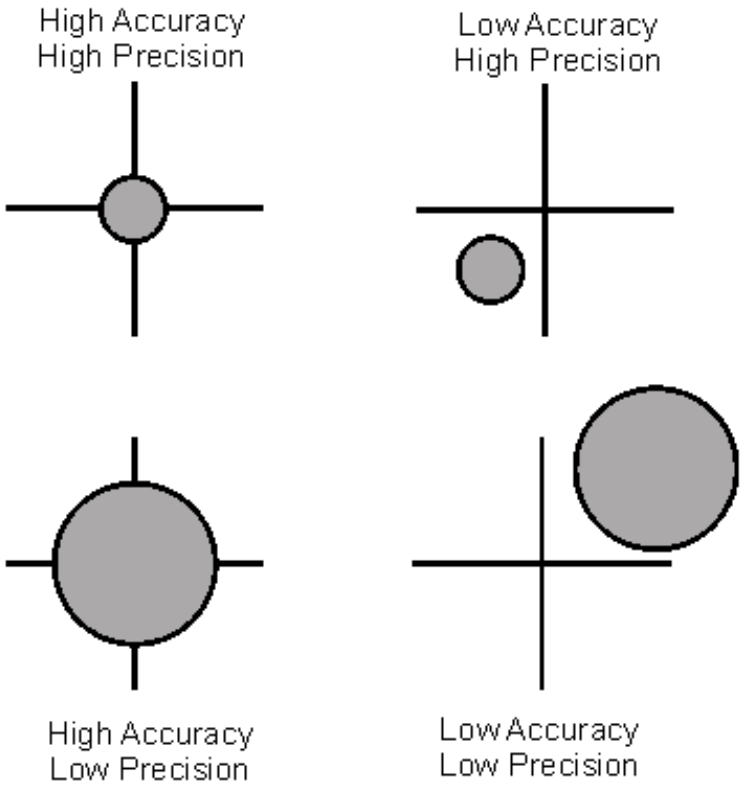

Figure 2.10: Definition of accuracy and precision. Source: `http://www.radio-electronics.com/info/satellite/gps/accuracy-errors-precision.php`

The standard deviations σ_x and σ_y can be predicted from the variances on the diagonal of the covariance matrix C (Eq. (2.30)).

- **SEP**: The Spherical Error Probability is the equivalent of CEP for 3-D. The real position will be within a sphere of *SEP* m radius with 50 percentile probability.

$$0.5 \cdot (\sigma_x + \sigma_y + \sigma_z) \tag{2.39}$$

- **DRMS**: The Deviation Root Mean Square is a frequently used measurement of the accuracy for estimators. For an unbiased estimator, it is defined as the square root of the variance, also known as the standard error. In GNSS, it is defined as follows:

$$DRMS = \sqrt{\sigma_x^2 + \sigma_y^2}. \tag{2.40}$$

The DRMS gives a confidence level of 63.2%.

- **2DRMS**: Twice the DRMS measurement. The confidence level is of 98.2%.

- **MSRE**: The extension of DRMS for the 3-D measurement. It is calculated as follows:
$$MSRE = \sqrt{\sigma_x^2 + \sigma_y^2 + \sigma_z^2}. \tag{2.41}$$
The value of the confidence level is 61%.

- **R95**: The Radius 95 is the measurement with 95% confidence level. Mathematically, it is defined as:
$$R \cdot (0.62 \cdot \sigma_y + 0.56 \cdot \sigma_x), \tag{2.42}$$
where R is a value dependent on the relation between σ_y and σ_x. If $\sigma_y = \sigma_x$, then R is 2.08.

- 90% Spherical Accuracy Standard: The measurement with 90% confidence level for 3-D.
$$0.833 \cdot (\sigma_x + \sigma_y + \sigma_z) \tag{2.43}$$

- 99% Spherical Accuracy Standard: The measurement with 99% confidence level for 3-D.
$$1.122 \cdot (\sigma_x + \sigma_y + \sigma_z) \tag{2.44}$$

All of these measurements have in common the dependency on the standard deviations along the coordinate axis. These dependency can be used to convert between different accuracy measurements. It can also be used to define a more generic measurement called the x-sigma, where x represent a positive number. Tab. 2.1 gives the equivalent between x (the number of sigmas) and the percentile of the confidence level for the 2-D positioning.

The 3GPP, in the TS 36.355 specification for the LTE Positioning Protocol (**LPP**) [7] defines the procedures, call flows and message contents for the LBS. The message with which the mobile device sends the GNSS measurements is called *ProvideLocationInformation* and it contains an element *GNSS-measurementList*. Within this element, one of the values that the mobile phone must report is the following:

codePhaseRMSError: *This field contains the pseudorange RMS error value. This parameter is specified according to a floating-point representation shown in the table floating-point representation in TS 36.355.*

Sigma	Percentile
1	0.394 (standard deviation)
1.18	0.5 (CEP)
1.25	0.544 (mean error)
1.414	0.632 (DRMS)
1.67	0.75
2	0.865
2.45	0.95 (R95)
2.818	0.982 (2DRMS)
3	0.989
3.03	0.99
4	0.9997
5	0.999997
6	0.999999985

Table 2.1: Equivalence between x-sigma and confidence level

The RMS calculation from the reported codePhaseRMSError is done following the formula defined in the Section F.3 of the TS36.171 [5]:

$$RMS_i = \frac{1}{2} \cdot \left(1 + \frac{X_i}{8}\right) \cdot 2^{Y_i}, \tag{2.45}$$

where X_i is a three bits mantissa and Y_i is a three bits exponent.

The RMS accuracy measurement can be used to improve the LSE algorithm by adding a weighting matrix that will give more importance to measurements with lower RMS.

2.2.7 Weighted Least Squares

The knowledge of the RMS accuracy estimated by the mobile phone for every pseudorange measurement allows the computation of a weighting matrix to influence the impact of each measurement in the calculated position. Measurements with higher RMS value have lower precision (the uncertainty ellipsoid or circle is bigger) and therefore they have potentially higher error. Given these measurements, a lower weight in the computation will improve the solution.

This enhancement of the LSE algorithm is called Weighted Least Squares (**WLS**) algorithm and it is the standard defined by the RAN# 4 of 3GPP for A-GNSS position

calculation. The steps of the algorithm are described in specification TS 36.171 from v9.0.0 (E-UTRA release 9) onwards [5].

The weighting matrix W for a equation system of n pseudo-range measurements is defined as follows:

$$W = \begin{bmatrix} w_1 & 0 & \cdots & 0 \\ 0 & w_2 & & 0 \\ \vdots & & \ddots & \vdots \\ 0 & 0 & \cdots & w_n \end{bmatrix}, \tag{2.46}$$

where w_i are the inverse of the RMS value for measurement i:

$$w_i = \frac{1}{RMS_i} \tag{2.47}$$

This matrix W can be input in Eq. (2.28) multiplying the system matrix A, according to the formula given in Section F.3 step 4.4.e of the TS 36.171:

$$\hat{X} = (A' \cdot W \cdot A)^{-1} \cdot A' \cdot W \cdot \Delta\hat{\rho}. \tag{2.48}$$

2.3 OTDOA

OTDOA stands for Observed Time Difference Of Arrival and it is a terrestrial or network-based positioning technology that tries to calculate the location of a mobile device by measuring the Time Difference Of Arrival between signals from different Evolved Node Bs (**eNBs**). The time difference of arrival between the two signals can be translated to a constant ratio of the distance between the mobile device and the two base stations. It is, therefore, a multilateration system as explained in Section 2.1.3. Although OTDOA is a recent topic, hyperbolic localization and navigation systems have been used for a long time.

2.3.1 Brief history of hyperbolic localization

Hyperbolic localization systems have been studied since last century. The first military applications were developed during the World War I, as an acoustic method to locate enemy artillery also called as *sound ranging*[2] [26]. The sound of the artillery firing was recorded by several microphones and the timing measurements were sent to a computing centre to calculate the position of the weapon.

During the World War II, the acoustic systems were replaced by the more advanced radio systems. New applications were found, not only to locate enemy equipment but also as a navigation method for ships and planes. The first hyperbolic navigation system was the one used by the Royal Air Force of the United Kingdom with code-name "Gee", which entered service in 1942 [27]. This system was followed by the Decca Navigator System used by the Royal Navy from 1944 on and the United States' LORAN system [28]. These two technologies were mainly used for ship navigation in coastal waters, being the accuracy of Decca superior to LORAN. Decca operated in the low frequency range (from 70 to 130 kHz) and it had a range of around 400 nautical miles, which is equivalent to 740 km. The accuracy was highly dependent of several factors like the angle of cut of the hyperbolic lines of position and also the time of the day. It could vary between a few meters on the best conditions up to a nautical mile.

After the war, hyperbolic navigation systems became popular also for non-military applications and they were used until they were replaced by GPS. Some of the most know systems included the evolution of LORAN, called LORAN-C, used by the US

[2]See `http://en.wikipedia.org/wiki/Sound_ranging`

Coast Guard services, the international Omega system or the Alpha and CHAYKA systems from the Soviet Union. LORAN-C was first introduced in 1957 as an evolution of the LORAN system, and its transmission was terminated in 2010[3] after the United States government decided it was no longer needed due to GPS. The accuracy of the first LORAN-C systems was a circle of <= 79 m in 50 % of the fixes and an area of 4.8 km under most operational conditions [29].

With the arrival of mobile phone communications, hyperbolic localization was revived as a method to locate a mobile device. Uplink Time Difference Of Arrival techniques were already applied in Global System for Mobile communications (**GSM**) and Global Packet Radio Service (**GPRS**) [30]. Nowadays, the tendency is to combine TDOA localization methods with GNSS to improve the accuracy of the estimated position and as a fall-back mechanism when GNSS is not available.

2.3.2 Description

OTDOA is a part of the E-UTRA Release 9 features defined by 3GPP. Below, the working principle is explained.

Each eNB of the network will transmit a particular signal, called Position Reference Symbol (**PRS**), embedded in the LTE frame. The PRS is defined by three parameters:

- PRS configuration index: it defines the periodicity of the transmission of PRS, that is, how often the PRS will be transmitted. It also indicates in which exact subframe is the PRS expected.
- PRS bandwidth: the frequency bandwidth used for the transmission of the PRS signal. It has to be smaller or equal to the BW of the cell and one of the valid LTE BW values: 1.4, 3, 5, 10, 15 or 20 MHz.
- Number of downlink frames: the number of consecutive frames in which the PRS signal will be transmitted. It can be 1, 2, 4 or 6 frames.

Given these three parameters, the mobile device knows when to expect a PRS signal. Each instant where a PRS signal can be received is called a PRS occasion. However, the eNB may not transmit the PRS at every single occasion. In order to

[3] See `http://www.navcen.uscg.gov/?pageName=loranMain`

spare some subframes, the 3GPP specifications have given the possibility to *mute* the PRS according to a pre-defined *muting sequence*. These muting sequence is a pattern of bits that repeats itself. At one particular PRS occasion, if the muting sequence has a value of 1, the PRS will be transmitted, while a value of 0 means the PRS will be muted.

The muting sequence must as well be communicated to the mobile device with two fields: the length in bits of the sequence and the sequence itself.

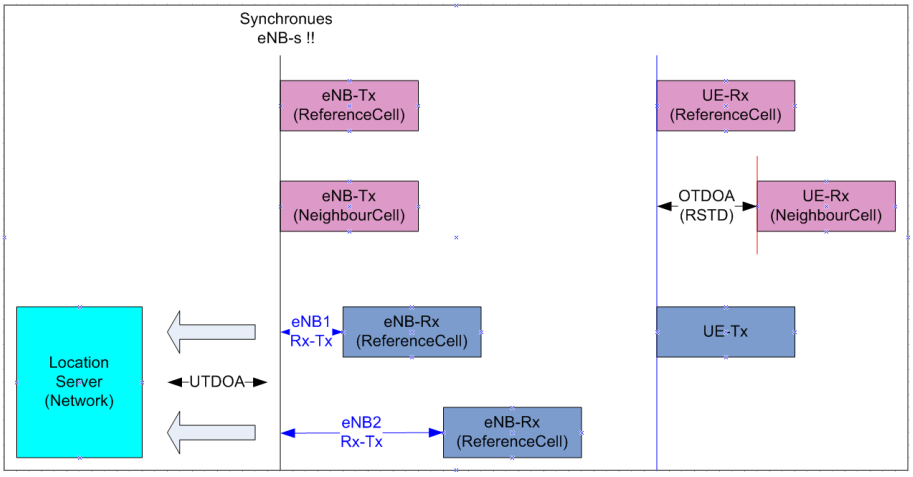

Figure 2.11: OTDOA RSTD measurement. Source: [2]

The mobile device should listen to the PRS symbols of multiple base stations and select one (typically the serving cell or the cell with better signal quality) as a *reference cell* (see the above half of Fig. 2.11). Then, it should compute the time difference between each of the other eNBs and the reference cell and report these values back. Each of these measurements is called Reference Symbol Time Delay (**RSTD**) and is defined as the time of arrival of the PRS of the neighbour cell minus the time of arrival of the PRS of the reference cell. The RSTD measurement is represented in a unit called T subframe or T_s, which is the basic unit of time in LTE.

This time unit is defined as:

$$T_s = \frac{1}{15000 \cdot 2048} seconds, \tag{2.49}$$

which is a bit more than 32 ns. The RSTD measurement for the neighbour eNB n calculated in T_s is given by the equation:

$$RSTD_n[T_s] = (PRS_n[s] - PRS_{ref}[s]) \cdot 15000 \cdot 2048 \tag{2.50}$$

$$= T_{PRS,subframeRxn} - T_{PRS,subframeRxref}, \tag{2.51}$$

where $T_{PRS,subframeRxn}$ is the *time when the mobile receives the start of the PRS subframe from cell n* [31]. The RSTD value is encoded according to Table 9.1.10.3-1 of 3GPP specification TS36.133 [32] and transmitted. The encoding is done by rounding the PRS and adding a constant value:

$$RSTD_n = \begin{cases} 0 & if \quad RSTD_n[T_s] < -15391 \\ \left\lfloor \frac{RSTD_n[T_s]+4096}{5} \right\rfloor + 2260 & if \quad -15391 \leq RSTD_n[T_s] < -4096 \\ \lfloor RSTD_n[T_s] \rfloor + 6356 & if \quad 4096 \leq RSTD_n[T_s] < 0 \\ \lceil RSTD_n[T_s] \rceil + 6355 & if \quad 0 \leq RSTD_n[T_s] \leq 4096 \\ \left\lceil \frac{RSTD_n[T_s]-4096}{5} \right\rceil + 10451 & if \quad 4096 < RSTD_n[T_s] \leq 15391 \\ 12711 & if \quad RSTD_n[T_s] > 15391 \end{cases} \tag{2.52}$$

The mobile device reports the RSTD measurements back to the serving cell, which forwards these values to the Location Server of the network to calculate the position by multilateration. During the position calculation, the coordinates of the eNBs used for the measurements are required. Up to now, the 3GPP specifications do not allow for any mechanism to send the base stations' coordinates to the network users. Hence, there is no possibility of *UE-Based* OTDOA. All position calculations must be done by the network.

2.3.3 Sources of error of OTDOA

A. Receiver and transmitter time errors

In OTDOA, as a time difference of arrival method, the receiver clock error τ_{rx} effect is minimized, as it will affect equally to the signals received from each eNB and then be cancelled out while calculating the time difference.

However, one of the drawbacks of OTDOA is that it requires a very good synchronization between base stations. The error in the synchronization of the base stations is translated directly to an error in the RSTD measurements and it can damage drastically the position calculation accuracy. To keep the synchronization as accurate as possible, base stations should have an atomic clock synchronized to GNSS.

B. Dilution of Precision

The DOP of the group of base stations used for the measurements (*base stations constellation*) is also an important contributor to the accuracy of OTDOA. An analysis of good DOP and bad DOP constellations and the influence on the position calculation will be presented as part of this work.

C. Transmitter antenna coordinates

The base station coordinates are used during the position calculation as focus points of the hyperboloids of location. Nevertheless, the base stations are not point sources. The coordinates used in the multilateration algorithm should be the coordinates of the transmitter antenna of the base station. In a real network, the base station coordinates could be calculated for a different point other than the antenna. If the antenna coordinates are not known accurately, this error will impact the algorithm and translate into an error in the calculated position.

D. Channel effects

The PRS signal is transmitted via air interface and can suffer reflections, diffractions and scattering caused by all kind of obstacles like buildings, mountain, trees, etc. Multipath and fading are major contributors to RSTD measurement errors.

Due to multipath, the mobile device will receive the PRS signal via different paths and with different time delays. The first arriving path should always be the direct line-of-sight path. However, if there is no direct line-of-sight or because of the channel conditions the signal from the direct line of sight is severely attenuated, the mobile device might select one of the other paths for the measurement. Selecting a path with an Excess Delay of $0.1\mu s$ results in 30 meters of ranging error.

E. RSTD measurement performance

The mobile device will be received signals from several eNBs simultaneously at it needs to decode all the signals and compute the RSTD measurements in a short period of time. The eNBs might be configured intra-frequency, inter-frequency or even in Carrier Aggregation mode and the PRS signal from each cell might have the same of different configuration parameters (bandwidth, configuration index, etc.). All these conditions depend of the network design of each network operator in each particular region or city and cannot be predicted before hand for all cases. They might cause interferences and other errors will can worse the accuracy of the OTDOA measurements. The performance of the mobile device processor also influences the result. The requirement from 3GPP is that the mobile device is able to calculate RSTD values with an accuracy of $\pm 5T_s$ ($\sim$50 m) under AWGN conditions. This error source will not be studied in more detail for this thesis.

The synchronization error between base stations, DOP, error in the antenna coordinates and propagation effects will be analysed during this thesis.

2.3.4 OTDOA measurement accuracy

As for A-GNSS, the message contents and procedures defined by 3GPP for OTDOA are part of TS 36.355 [7]. The *OTDOA-ProvideLocationInformation* required the mobile device to report a list of neighbour cell measurements which contain the physical cell ID of the neighbour cell, the RSTD value and some other parameters. Among then, there is an element called OTDOA-MeasQuality which should match the following structure:

OTDOA-MeasQuality ::= SEQUENCE error-Resolution BIT STRING (SIZE (2)), error-Value BIT STRING (SIZE (5)), error-NumSamples BIT STRING (SIZE (3)) OPTIONAL, ...

The parameter error resolution specifies the resolution used for the error value field. It can be 5, 10, 20 or 30 metres. The parameter error value specifies the mobile device's best estimate of the uncertainty of the OTDOA measurement. With these two values it is possible to calculate the uncertainty range as follows:

$$R \cdot V <= U <= R \cdot (V + 1) - 1\,\text{metres}, \tag{2.53}$$

where R is the error resolution, V is the error value and U is the uncertainty of the measurement. The specification does not mention to which confidence level corresponds this uncertainty measurement.

The parameter error NumSamples specifies how many samples have been considered to obtain the error value. If this parameter is ¨ 000¨ , the error value has been calculated from other measurement such as SNR or signal power.

This error value can be used in a similar way as the RMS reported for A-GNSS measurements to generate a weighting matrix to give more or less importance to different measurements based on their uncertainty. A definition for this matrix will be proposed as part of the algorithm developed for this Thesis.

2.4 ECID

Enhanced Cell ID is a network-based positioning method that calculates the distance between a mobile device and an eNB by measuring the Round Trip Time (**RTT**) of a signal. The RTT is the time between a signal is sent and the acknowledgement for the signal is received. ECID is a trilateration mechanism as seen in Section 2.1.2. This method was introduced by the 3GPP as a E-UTRA Rel. 9 feature. However, the RxTx measurement is only defined to the serving cell. Hence, ECID cannot be used as the only source for position calculation. It has to be combined with other methods to get more measurements. One approach is to combine it with distance calculated from power measurements (RSRP and/or RSRQ) to the neighbour cells to complete the measurements required for positioning. Nevertheless, the ranges obtained from power measurements are more inaccurate that the range from RxTx measurements and include those equations into the system will lower the precision of the calculated position.

2.4.1 Description

ECID is based on the acquisition of RxTx measurements. This measurement is defined in 3GPP specification TS 36.214 [31]. The process can be defined in three steps:

1. The eNB measures the RTT of a message transmitted by itself.

$$eNB\,Rx - Tx = T_{eNB,Rx} - T_{eNB,Tx}. \tag{2.54}$$

2. The eNB sends a Timing Advance (**TA**) command to the mobile device to correct its uplink timing.

3. The UE (User Equipment, here the mobile device) measures and reports its RTT.

$$UE\,Rx - Tx = T_{UE,Rx} - T_{UE,Tx}. \tag{2.55}$$

These three steps can be seen in Fig. 2.12.

The RxTx RTT measurement is encoded using Table 9.1.9.2-1 from 3GPP specification TS 36.133 [32].

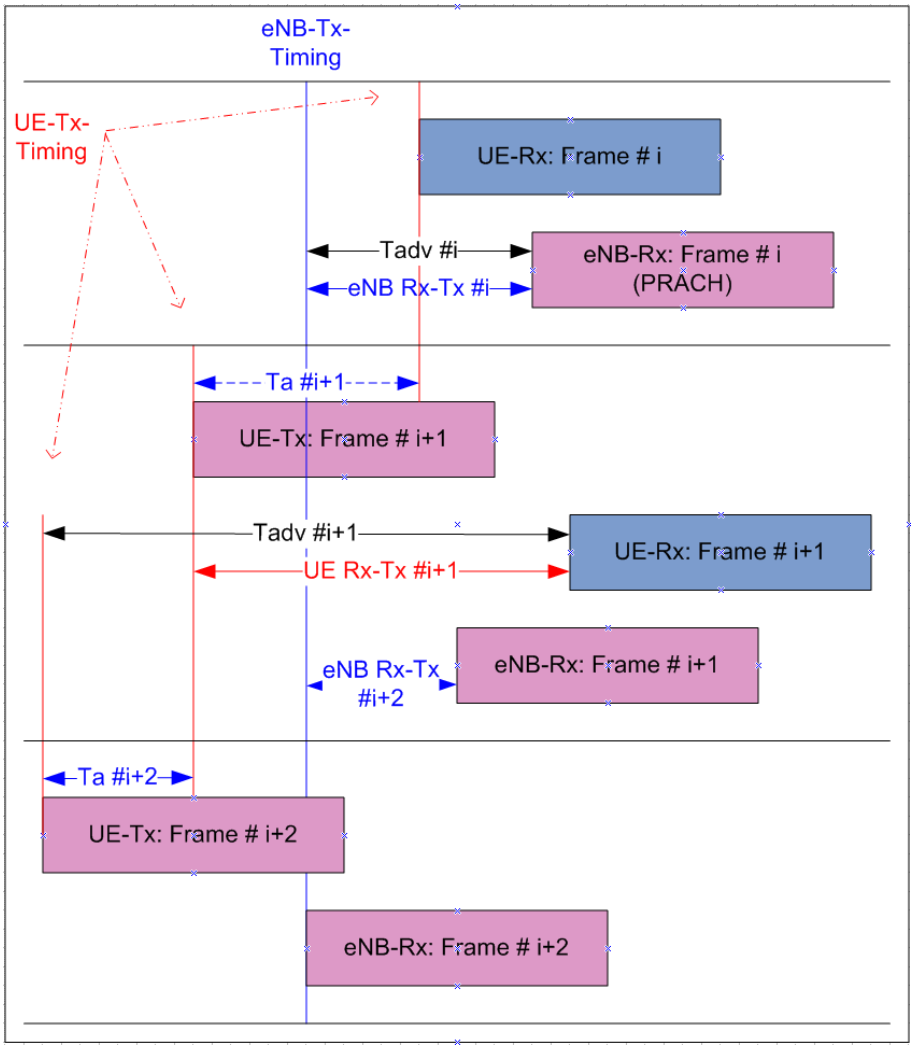

Figure 2.12: ECID RxTx measurement. Source: [2]

2.5 Comparison between terrestrial and satellite positioning systems

In this Chapter, three of the methods defined for mobile phone positioning in LTE have been explained. The three of them could be classified in satellite (A-GNSS) and terrestrial (OTDOA and ECID) methods. In this section some of the differences between the two types of systems will be detailed.

Satellite based	**Terrestrial based**
Low Bandwidth (∼1-2 MHz)	High Bandwidth (up to 20 MHz)
Weak received signal power	Stronger received signal power
The signals received from all satellites will have similar power levels	One signal can be stronger to the others, high interference situations
Very accurate synchronization of the satellites	Synchronization of base stations a priori not guaranteed
Signal known a priori due to low data rates	Only certain pilots of the signal known a priori to support high data rates
TTFF (Time To First Fix) of around 20 seconds in best case	TTFF of typically <3s
The position can be calculated by the mobile or by the network	Only the network can calculate the position
Not suitable for indoor positioning (satellite signals will not be received in most cases)	Suitable for indoor positioning as mobile network signals is (in most cases) also available indoor.
It can be used for 3-D positioning	Base stations might not have enough altitude diversity to calculate 3-D positions.

Table 2.2: Comparison between Satellite and Terrestrial-based location services

Chapter 3

Algorithm Derivation

3.1 OTDOA Positioning

As it has already been stated, OTDOA is a multilateration method. Hence, each OTDOA measurement can be used to form equations as Eq. (2.10), where P is the position on the mobile device, BS_2 is the neighbour cell, BS_1 is the reference cell and K is related to the RSTD measurement, defined by Eq. (2.12). Considering the definition of RSTD in seconds from Eq. (2.50) and adding the time errors at the transmitter and the receiver, τ_{tx} and τ_{rx}, respectively:

$$RSTD_n[s] = (t_{Rx,PRS_n}[s] - \tau_{Rx} - \tau_{Tx,n} - (t_{Rx,PRS_Ref}[s] - \tau_{Rx} - \tau_{Tx,ref})), \tag{3.1}$$

where t_{Rx,PRS_n} is the reception time for the PRS signal for the neighbour n. The time error of the receiver of the mobile device cancels out and the final equation can be rewritten as:

$$RSTD_n[s] = RSTD_{n,true} - \tau_{Tx,n} + \tau_{Tx,ref}, \tag{3.2}$$

where $RSTD_{n,true}$ represents the real RSTD value without timing errors. If the v_p equals the speed of light c, plugging Eq. (3.2) into Eq. (2.12) results into:

$$K = (RSTD_{n,true} - \tau_{Tx,n} + \tau_{Tx,ref}) \cdot v_p + e_{RSTD}, \tag{3.3}$$

and finally Eq. (2.10) is expressed as:

$$\sqrt{(x-x_n)^2+(y-y_n)^2+(z-z_n)^2}-\sqrt{(x-x_{ref})^2+(y-y_{ref})^2+(z-z_{ref})^2}$$
$$=(RSTD_{n,true}-\tau_{Tx,n}+\tau_{Tx,ref})\cdot c+e_{RSTD}. \tag{3.4}$$

Regrouping Eq. (3.4) to have notation similar to Eq. (2.14), an OTDOA range is defined by:

$$\rho_{otdoa}=RSTD_{n,true}\cdot c-\tau_{Tx,n}\cdot c+\tau_{Tx,ref}\cdot c+e_{RSTD}=RSTD_{n,true}\cdot c+\nu_{RSTD}=$$
$$=\sqrt{(x-x_n)^2+(y-y_n)^2+(z-z_n)^2}-\sqrt{(x-x_{ref})^2+(y-y_{ref})^2+(z-z_{ref})^2} \tag{3.5}$$

$$\sqrt{(x-x_n)^2+(y-y_n)^2+(z-z_n)^2}-\sqrt{(x-x_{ref})^2+(y-y_{ref})^2+(z-z_{ref})^2}-\dots$$
$$\cdots-RSTD_{n,true}\cdot c-\nu_{RSTD}=0, \tag{3.6}$$

where ν_{RSTD} represents all the errors associated to the RSTD measurement including clock errors from the base stations and is modelled as an i.i.d. Gaussian random process. These sources of error will be analysed more in detail later.

The first thing to notice is that the OTDOA measurement is not a pseudo-range as A-GNSS measurements: there is no unknown time variable to calculate. Hence, a 3-D position can be calculated with three equations (i.e. three RSTD measurements which means four eNBs). A LSE algorithm analogous to the one defined for A-GNSS positioning is proposed in the below sections.

A. Linearisation of the OTDOA measurement

The first step is to linearise Eq. (3.5) using a Taylor series representation (see Eq. (2.15)) around a point $P_0=\{x_0,y_0,z_0\}$. The variable ρ_{otdoa} will be denoted as ρ_T to simplify the notation.

$$\rho_T(x,y,z) \approx \rho_T(x_0,y_0,z_0) + \nu + (x-x_0)\left.\frac{\partial \rho_T}{\partial x}\right|_{P=P_0} + (y-y_0)\left.\frac{\partial \rho_T}{\partial y}\right|_{P=P_0} + \dots$$
$$+ (z-z_0)\left.\frac{\partial \rho_T}{\partial z}\right|_{P=P_0} = \rho_{T,0} + \nu + \Delta x \left.\frac{\partial \rho_T}{\partial x}\right|_{P_0} + \Delta y \left.\frac{\partial \rho_T}{\partial y}\right|_{P_0} + \Delta z \left.\frac{\partial \rho_T}{\partial z}\right|_{P_0}. \quad (3.7)$$

B. Equation system

Combining the equations from n neighbour cells into a equation system and writing into matrix notation:

$$\begin{bmatrix} \rho_T^1 \\ \rho_T^2 \\ \vdots \\ \rho_T^n \end{bmatrix} = \begin{bmatrix} \rho_{T,0}^1 \\ \rho_{T,0}^2 \\ \vdots \\ \rho_{T,0}^n \end{bmatrix} + \begin{bmatrix} \left.\frac{\partial \rho_T^1}{\partial x}\right|_{P=P_0} & \left.\frac{\partial \rho_T^1}{\partial y}\right|_{P=P_0} & \left.\frac{\partial \rho_T^1}{\partial z}\right|_{P=P_0} \\ \left.\frac{\partial \rho_T^2}{\partial x}\right|_{P=P_0} & \left.\frac{\partial \rho_T^2}{\partial y}\right|_{P=P_0} & \left.\frac{\partial \rho_T^2}{\partial z}\right|_{P=P_0} \\ \vdots & \vdots & \vdots \\ \left.\frac{\partial \rho_T^n}{\partial x}\right|_{P=P_0} & \left.\frac{\partial \rho_T^n}{\partial y}\right|_{P=P_0} & \left.\frac{\partial \rho_T^n}{\partial z}\right|_{P=P_0} \end{bmatrix} \cdot \begin{bmatrix} \Delta x \\ \Delta y \\ \Delta z \end{bmatrix} + \begin{bmatrix} \nu^1 \\ \nu^2 \\ \vdots \\ \nu^n \end{bmatrix} \quad (3.8)$$

As for the A-GNSS system, the OTDOA system in Eq. (3.8) can also be solved iteratively starting from an initial guess of the location of the mobile device $P_0 = \{x_0, y_0, z_0\}$. Each iteration i, a new guess for the position of the mobile device $P_i = \{x_i, y_i, z_i\}$ will be calculated and used as input for the next iteration i+1. The algorithm will continue iterating until $|\Delta P| = |P_i - P_{i-1}| < convergence\_limit$.

Rewriting Eq. (3.8):

$$\begin{bmatrix} \rho_{T,i}^1 - \rho_{T,i-1}^1 \\ \rho_{T,i}^2 - \rho_{T,i-1}^2 \\ \vdots \\ \rho_{T,i}^n - \rho_{T,i-1}^n \end{bmatrix} = \begin{bmatrix} \left.\frac{\partial \rho_T^1}{\partial x}\right|_{P=P_0} & \left.\frac{\partial \rho_T^1}{\partial y}\right|_{P=P_0} & \left.\frac{\partial \rho_T^1}{\partial z}\right|_{P=P_0} \\ \left.\frac{\partial \rho_T^2}{\partial x}\right|_{P=P_0} & \left.\frac{\partial \rho_T^2}{\partial y}\right|_{P=P_0} & \left.\frac{\partial \rho_T^2}{\partial z}\right|_{P=P_0} \\ \vdots & \vdots & \vdots \\ \left.\frac{\partial \rho_T^n}{\partial x}\right|_{P=P_0} & \left.\frac{\partial \rho_T^n}{\partial y}\right|_{P=P_0} & \left.\frac{\partial \rho_T^n}{\partial z}\right|_{P=P_0} \end{bmatrix} \cdot \begin{bmatrix} \Delta x \\ \Delta y \\ \Delta z \end{bmatrix} + \begin{bmatrix} \nu^1 \\ \nu^2 \\ \vdots \\ \nu^n \end{bmatrix} \quad (3.9)$$

$$\Delta\hat{\rho}_T = A_T \cdot \Delta\hat{X} + \hat{\nu}, \quad (3.10)$$

where

$$A_T = \begin{bmatrix} \left.\frac{\partial \rho_T^1}{\partial x}\right|_{P=P_0} & \left.\frac{\partial \rho_T^1}{\partial y}\right|_{P=P_0} & \left.\frac{\partial \rho_T^1}{\partial z}\right|_{P=P_0} \\ \left.\frac{\partial \rho_T^2}{\partial x}\right|_{P=P_0} & \left.\frac{\partial \rho_T^2}{\partial y}\right|_{P=P_0} & \left.\frac{\partial \rho_T^2}{\partial z}\right|_{P=P_0} \\ \vdots & \vdots & \vdots \\ \left.\frac{\partial \rho_T^n}{\partial x}\right|_{P=P_0} & \left.\frac{\partial \rho_T^n}{\partial y}\right|_{P=P_0} & \left.\frac{\partial \rho_T^n}{\partial z}\right|_{P=P_0} \end{bmatrix} \tag{3.11}$$

is the system matrix or the *design matrix* for OTDOA. The partial derivatives in A_T can be calculated as follows:

$$\left.\frac{\partial \rho_T^j}{\partial x}\right|_{P=P_0} = \frac{1}{2} \cdot \frac{2 \cdot (x_{ref} - x_0)}{d_{ref}|_{P=P_0}} - \frac{1}{2} \cdot \frac{2 \cdot (x_{bs_j} - x_0)}{d_{bs_j}|_{P=P_0}} = \\ = \frac{(x_{ref} - x_0)}{d_{ref}(P_0)} - \frac{(x_{bs_j} - x_0)}{d_{bs_j}(P_0)} \tag{3.12}$$

$$\left.\frac{\partial \rho_T^j}{\partial y}\right|_{P=P_0} = \frac{(y_{ref} - y_0)}{d_{ref}(P_0)} - \frac{(y_{bs_j} - y_0)}{d_{bs_j}(P_0)} \tag{3.13}$$

$$\left.\frac{\partial \rho_T^j}{\partial z}\right|_{P=P_0} = \frac{(z_{ref} - z_0)}{d_{ref}(P_0)} - \frac{(z_{bs_j} - z_0)}{d_{bs_j}(P_0)}, \tag{3.14}$$

where ρ_T^j represents the OTDOA measurement j corresponding to neighbour cell j, x_{bs_j}, y_{bs_j} and z_{bs_j} stand for the coordinates in ECEF of the neighbour cell j, x_{ref}, y_{ref} and z_{ref} stand for the coordinates in ECEF of the reference cell and d_{bs_j} and d_{ref} are the distances from the cell j and the reference cell to the mobile device P, evaluated at guess point P_0. Thus, the design matrix A_T in Eq. (3.11) at a time instant i can be rewritten as:

$$A_T = \begin{bmatrix} \frac{(x_{ref}-x_{i-1})}{d_{ref}(P_{i-1})} - \frac{(x_{bs_1}-x_{i-1})}{d_{bs_1}(P_{i-1})} & \frac{(y_{ref}-y_{i-1})}{d_{ref}(P_{i-1})} - \frac{(y_{bs_1}-y_{i-1})}{d_{bs_1}(P_{i-1})} & \frac{(z_{ref}-z_{i-1})}{d_{ref}(P_{i-1})} - \frac{(z_{bs_1}-z_{i-1})}{d_{bs_1}(P_{i-1})} \\ \frac{(x_{ref}-x_{i-1})}{d_{ref}(P_{i-1})} - \frac{(x_{bs_2}-x_{i-1})}{d_{bs_2}(P_{i-1})} & \frac{(y_{ref}-y_{i-1})}{d_{ref}(P_{i-1})} - \frac{(y_{bs_2}-y_{i-1})}{d_{bs_2}(P_{i-1})} & \frac{(z_{ref}-z_{i-1})}{d_{ref}(P_{i-1})} - \frac{(z_{bs_2}-z_{i-1})}{d_{bs_2}(P_{i-1})} \\ \vdots & \vdots & \vdots \\ \frac{(x_{ref}-x_{i-1})}{d_{ref}(P_{i-1})} - \frac{(x_{bs_n}-x_{i-1})}{d_{bs_n}(P_{i-1})} & \frac{(y_{ref}-y_{i-1})}{d_{ref}(P_{i-1})} - \frac{(y_{bs_n}-y_{i-1})}{d_{bs_n}(P_{i-1})} & \frac{(z_{ref}-z_{i-1})}{d_{ref}(P_{i-1})} - \frac{(z_{bs_n}-z_{i-1})}{d_{bs_n}(P_{i-1})} \end{bmatrix} \tag{3.15}$$

C. Least Squares Estimation

The derivation of the LSE algorithm for OTDOA can be done analogously to the LSE derivation for GNSS. Starting from Eq. (3.10), the estimated residuals vector ν is

isolated:

$$\hat{\nu} = \Delta\hat{\rho}_T - A_T \cdot \Delta\hat{X}. \tag{3.16}$$

In order to find the least squares solution to Eq. (3.16), the following function should be minimized:

$$J(x) = \sum_{i=1}^{n} \nu_i^2 = \nu'\nu = (\rho_T - A_T \cdot X)' \cdot (\rho_T - A_T \cdot X). \tag{3.17}$$

That means, the solution is to minimise the sum of the estimated vector residuals squared. The process is identical as for GNSS as described in [6, 23], and the solution is:

$$\hat{X} = (A_T' A_T)^{-1} \cdot A_T' \cdot \Delta\hat{\rho}_T \tag{3.18}$$

D. Error Analysis

For OTDOA the errors in the measurements $\hat{\nu}$ will affect the final position estimation linearly according to the expression:

$$\hat{\nu}_X = (A_T' A_T)^{-1} \cdot A_T' \cdot \hat{\nu}. \tag{3.19}$$

The *covariance matrix* of the measurement errors $\hat{\nu}$ is defined as $C = E(\nu\nu')$, with coefficients $C_{ij} = E(\nu_i\nu_j)$. Applying the definition of the error values as iid, it can be derived that $E(\nu_i\nu_j) = 0 \ \forall \ i \neq j$ and $E(\nu_i\nu_i) = E(\nu_i^2) = \sigma_i^2$ which is known as *variance*. The covariance matrix C can be written as:

$$C = \begin{bmatrix} \sigma_1^2 & 0 & \cdots & 0 \\ 0 & \sigma_2^2 & & \vdots \\ \vdots & & \ddots & 0 \\ 0 & \cdots & 0 & \sigma_n^2 \end{bmatrix} \tag{3.20}$$

The covariance matrix of the calculated position error can be calculated as $C_{T,X} = E(\hat{\nu}_X \hat{\nu}_X')$. Replacing Eq. (3.19) into this formula, the following solution for C_X is found [6]:

$$C_{T,X} = C \cdot (A_T' A_T)^{-1}, \tag{3.21}$$

where $(A_T' A_T)^{-1}$ is called the *cofactor matrix*, Q_T. As it was seen also for GNSS, C is strictly dependant on the OTDOA measurement errors, which are influenced by many sources and hence, very difficult to predict. However, the cofactor matrix Q_T is purely geometrical, and it depends only in the coordinates of the base stations and the mobile device. It can be defined as follows:

$$Q_T = (A_T' A_T)^{-1} = \begin{bmatrix} \sigma_x^2 & \sigma_{xy} & \sigma_{xz} \\ \sigma_{xy} & \sigma_y^2 & \sigma_{yz} \\ \sigma_{xz} & \sigma_{yz} & \sigma_z^2 \end{bmatrix}, \tag{3.22}$$

where it has been applied that $\sigma_{ij} = \sigma_{ji}$. In the OTDOA cofactor matrix there are no dependencies on the receiver clock bias, as it is cancelled out when calculating the time difference. A_T can be used to *design* the base station constellation to reduce the error due to bad geometry.

It is important to notice the inversion of the matrix resulting from $(A_T' A_T)$. If this product is not resulting in a matrix of range (or column space) equal to the number of unknown variables, 3, the matrix is not invertible and the system has no solution. This is critical for OTDOA if, for example, all the base stations are in the same (or similar) altitude plane. In this case a 3-D position cannot be computed.

A possibility if the matrix Q_T cannot be calculated, which means that a position cannot be found, is to drop the altitude coordinate z and calculate a 2-D position as a fall-back mechanism. In this case, it would be possible to use the surface of the earth as boundary condition assuming that the mobile device will be close to the surface. However, this solution will not be true in all cases.

3.1.1 Dilution of Precision

The concept of Dilution of Precision (**DOP**), introduced for A-GNSS in Section 2.2.4, can also be applied to OTDOA positioning. The DOP is calculated with the elements of the diagonal of the cofactor matrix, Q_T. For OTDOA, the DOP is related to the relative position between and the mobile device and each pair of base stations, one of them being always the reference base station.

The influence of the DOP for OTDOA positioning can be appreciated in Fig. 3.1, which represents a system with three base stations, BS1, BS2 and BS3, and one mobile receiver whose position is a priori unknown.

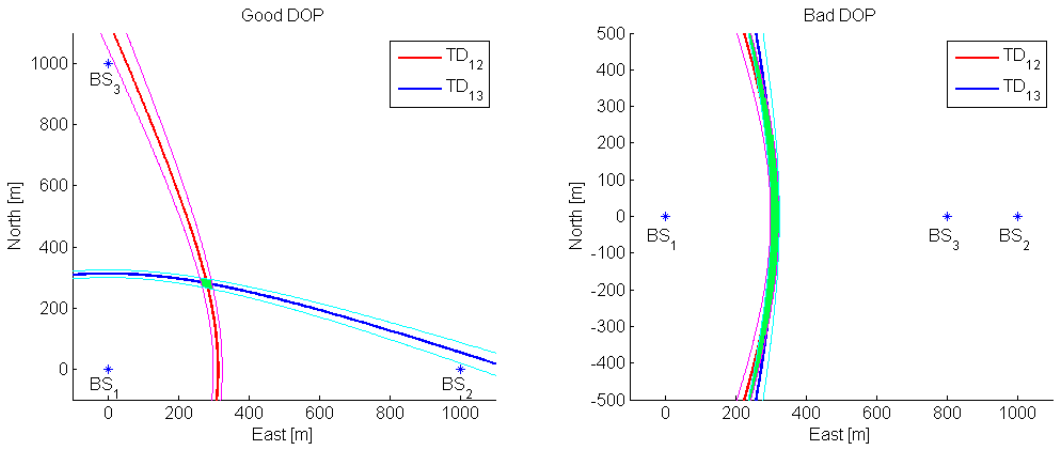

Figure 3.1: Dilution of Precision for OTDOA

In the left part, the receiver measures the TDoA of signals coming from BS2 and BS3 with respect to BS1, the reference base station. These measurements are represented in color red for BS2 and in color blue for transmitter BS3. The magenta and cyan lines represent the uncertainty in the measurement. Hence, the location of the mobile device can be narrowed down to the relatively small green area in the figure. In the right, the mobile device is in the same position, but now the visible base stations constellation has changed. BS3 is no longer north from the reference cell but east, in the same direction as BS2. It can be seen that in this second scenario the green area is comparatively much bigger. The same measurement uncertainty has a much bigger impact on the second scenario than on the first. The system on the left has a low DOP value and it is what will be referred as a *good geometry*, while the system on the right has a high DOP value, being what is called a *bad geometry*.

The DOP is calculated from the trace of the cofactor matrix Q_T, depicted in Eq. (3.22). The DOP for OTDOA is calculated as follows:

$$DOP \equiv GDOP \equiv \sqrt{\sigma_x^2 + \sigma_y^2 + \sigma_z^2}. \tag{3.23}$$

Analogously to the definition of GDOP (Geometrical DOP), PDOP, HDOP, VDOP and TDOP can be defined, to represent *Position, Horizontal, Vertical* and *Time* DOP, respectively. However, for OTDOA the TDOP is 0, as the clock bias of the receiver

is not affecting the measurement. Hence, the PDOP is identical to the GDOP. The equations for all different DOPs are as follows:

$$PDOP \equiv GDOP \equiv \sqrt{\sigma_x^2 + \sigma_y^2 + \sigma_z^2} \tag{3.24}$$

$$HDOP \equiv \sqrt{\sigma_x^2 + \sigma_y^2} \tag{3.25}$$

$$VDOP \equiv \sigma_z \tag{3.26}$$

$$TDOP \equiv 0 \tag{3.27}$$

As for A-GNSS, the best possible value for the dilution of precision is generally DOP = 1. If more than 3 base stations are available, and the mobile device is in an optimal relative location between them, the DOP can reach a value smaller than 1. Under 2, the DOP is optimal for the position calculation. Between 2 and 5 is considered good DOP value and above 5 it starts to be considered as a poor geometry for the localization. If the number of total measurements is smaller than the number of unknowns, the DOP value will diverge to infinity which symbolizes that a position cannot be calculated with that number of base stations.

A. GDOP and altitude diversity

A common real life scenario is that where all base stations are in similar altitudes. The GDOP calculation for such a constellation will throw a very high value, tending to infinity if all base stations are at exactly the same altitude. This scenario is not suitable for calculating a 3-D position, as the base station constellation does not have enough altitude diversity to allow the algorithm to estimate the altitude of the mobile device correctly.

In order to further explain this problem, the following scenario will be defined: four base stations placed at the corners of a square of 1000 metres side and the mobile device placed at coordinates $[480, 480]$. All base stations and the mobile device are at the same altitude 0 metres. GDOP calculation for such a scenario diverges to infinity, while HDOP has a value of 0.47. The hyperboloids resulting from the OTDOA measurement in this scenario are depicted in Fig. 3.2.

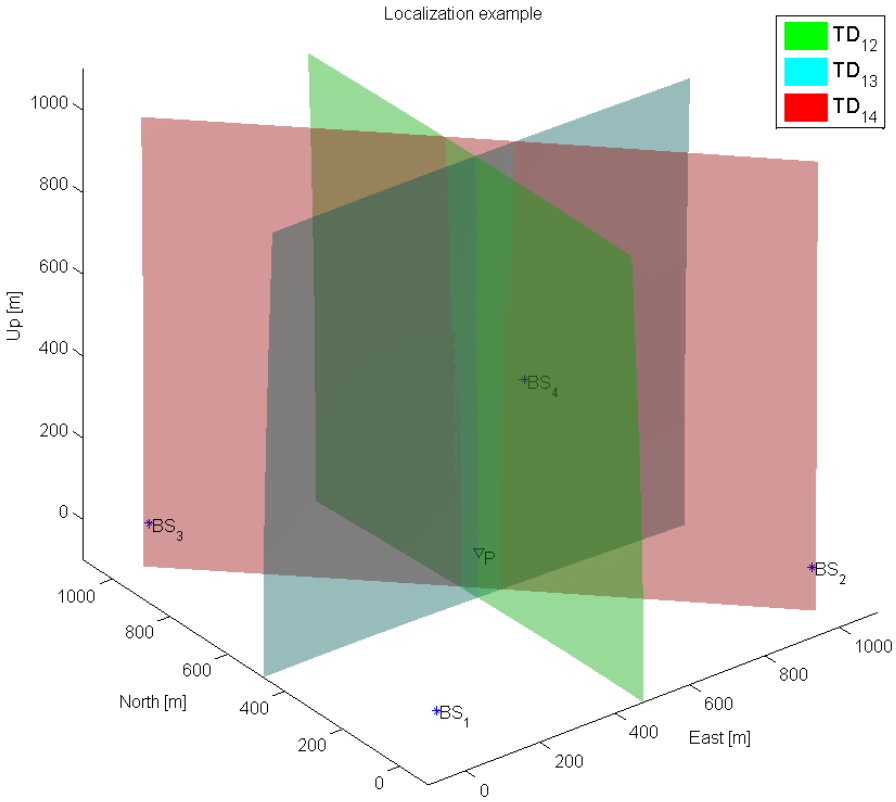

Figure 3.2: OTDOA 3D measurements in a high GDOP scenario.

Fig. 3.3 depicts the horizontal (left) and vertical (right) cuts of the 3D image. As it can be seen, the horizontal position can be calculated precisely from the measurements. However, in the vertical section, the three measurements do not converge to any point. The three lines in the image represent the intersections between each pair of measurements. The lines are almost parallel and do not cut.

Hence, 3D positioning with OTDOA is only possible if the base stations and the mobile device are placed at a different altitude. For this reason, in many real life scenarios OTDOA is seen as a 2D positioning method. The altitude information must be obtained from other technologies like A-GNSS or using a default value (e.g. using the Earth surface as a boundary condition).

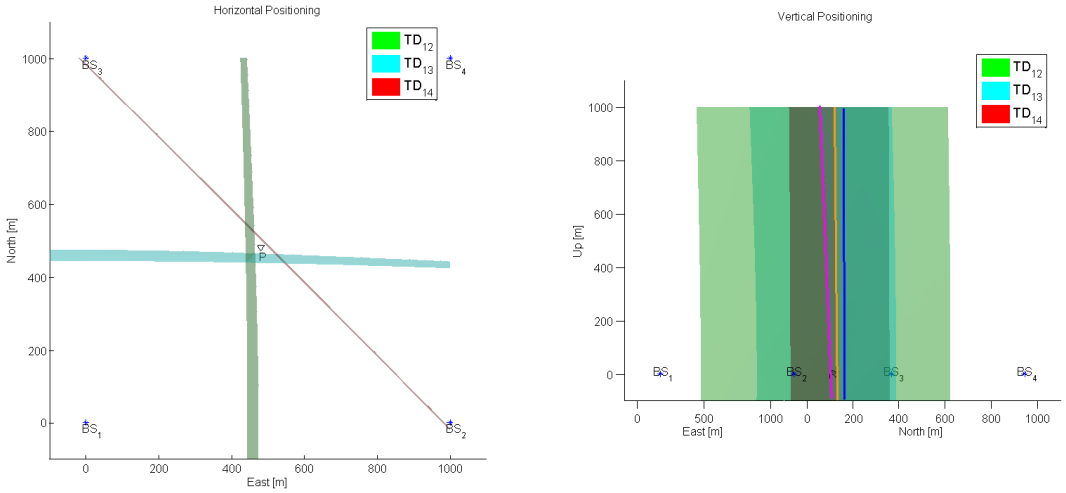

Figure 3.3: Horizontal and vertical sections of the OTDOA measurements in high GDOP scenario.

B. Analysis of HDOP for different base station constellations

The DOP is a parameter that depends only on the geometry of the base station constellation and the position of the mobile device. Therefore, it can be calculated a priori and compared for different base station constellations. Fig. 3.4 represents the DOP in all possible UE positions for six different base station constellations with between 3 and 6 base stations. The base station locations are represented as white circles.

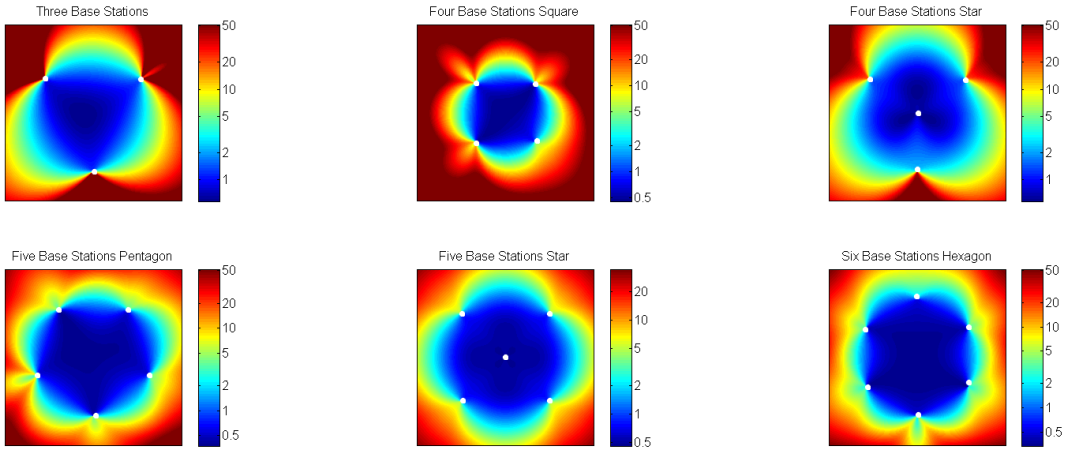

Figure 3.4: Comparison of the DOP values for different base station constellations

In general, all constellations present a low HDOP value when the mobile device is located somewhere close to the middle of the base stations and it increases if the mobile is outside the polygon formed by the eNBs. From all the different scenarios, the one

which obtains better HDOP is the constellation with five base stations disposed as a star, which the transmitter at the corners and centre of a square.

One extra configuration to analyse separately is a base station constellation formed by seven base stations distributed as a honeycomb: six base stations forming an hexagon and a base station in the center. This is the most typical way of representing LTE Cells and it seems hence a natural configuration to study for OTDOA networks. The HDOP results are painted in Fig. 3.5.

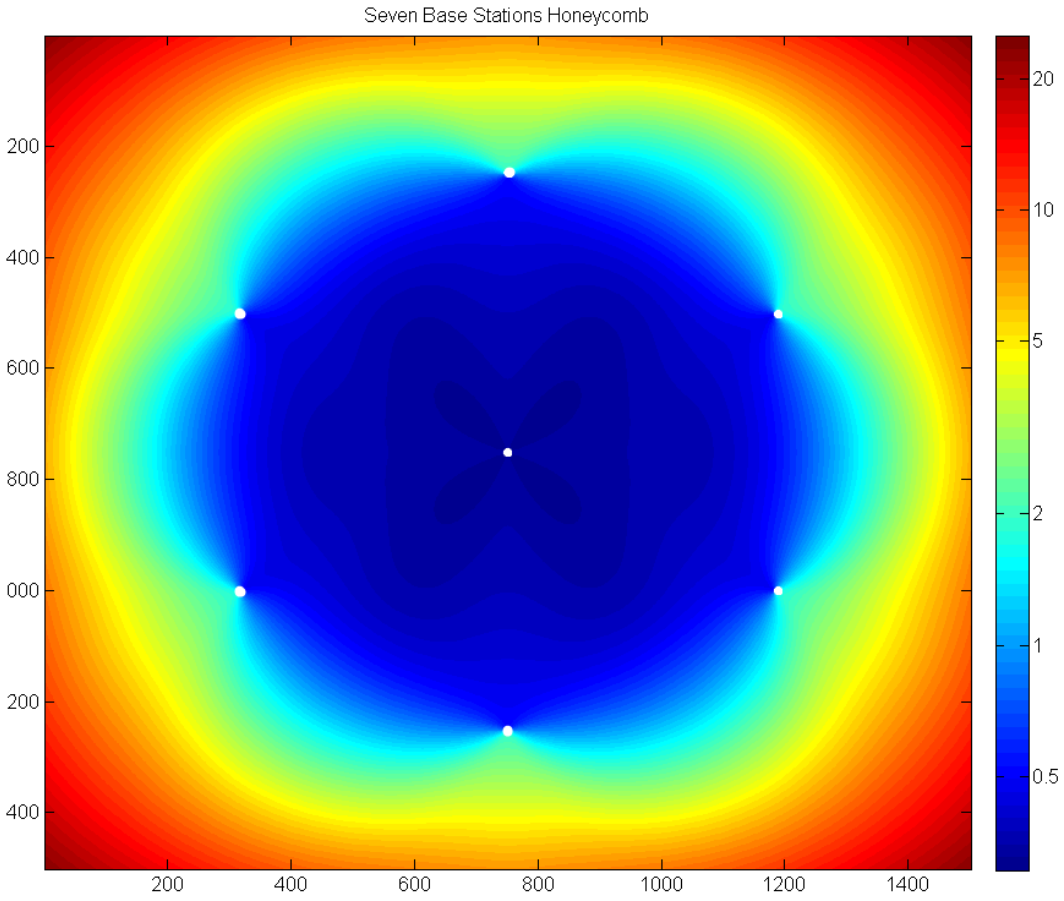

Figure 3.5: DOP values for the honeycomb distribution with seven base stations.

The DOP values obtained with this configurations are very good, as it is always below one in the area inside the hexagon. If the network is designed repeating such a pattern, the HDOP value would be smaller than 1 in almost every possible situation.

Such an analysis of HDOP can be used for network planning in order to develop a base station network that minimizes the HDOP value at all possible mobile device locations.

3.1.2 WLS algorithm for OTDOA

It is possible to defined a weighting matrix for OTDOA similar as the one defined by A-GNSS in Eq. (2.46). For a system with $n+1$ base stations and n measurements, this matrix can be defined as:

$$W_T = \begin{bmatrix} w_1 & 0 & \cdots & 0 \\ 0 & w_2 & & 0 \\ \vdots & & \ddots & \vdots \\ 0 & 0 & \cdots & w_n \end{bmatrix}, \tag{3.28}$$

where w_i is the weight associated to measurement i. Applying the same procedure defined by the 3GPP for A-GNSS, the solution of the LSE algorithm will be done by the formula:

$$\hat{X} = (A'_T \cdot W \cdot A_T)^{-1} \cdot A'_T \cdot W \cdot \Delta\hat{\rho}_T. \tag{3.29}$$

The only part left is to define the coefficients w_i of the weighting matrix. From Section 2.3.4, it has been seen that the mobile device reports a message OTDOA-MeasQuality along with each neighbour cell RSTD measurement. This message can be used to calculate an estimated error range according to Eq. (2.53). The coefficients of the weighting matrix should be of the form $w_i \propto \frac{1}{U}$, where U is the uncertainty of the measurement calculated in Eq. (2.53).

However, due to the lack of information in the TS36.355 specification regarding the equivalence between this error and a confidence level and the fact that the error value is defined as a range, there is no clear criteria which exact value should be given to the coefficients w_i. This thesis will propose an initial weighting value inversely proportional to the middle point of the error range. This value will be fine tuned during the simulations in later chapters. The initial weight will be calculated as:

$$w_H = \frac{2}{R_i \cdot (2V_i + 1) - 1} \tag{3.30}$$

3.1.3 Analysis of the error sources

A. Transmitter's synchronization error

As a time difference of arrival method, OTDOA does not require the receiver in the mobile device to be synchronized with the base stations. However, it requires a very accurate synchronization between eNBs. The most common solution to deploy OTDOA in a synchronous network consists on installing an atomic clock in each base station, synchronized to GPS time.

The synchronization between base stations needs to be met in the order of nanoseconds. In state of the art requirements from mobile phone manufacturers, they request the synchronization uncertainty to have a standard deviation σ_τ smaller than 50 nanoseconds [15]. However, the current uncertainty values in the networks which are already deploying OTDOA can go up to 200 ns.

Given two base stations BS_1 and BS_2 and a mobile device placed in an unknown position such that the time of flight of the signals coming from both base stations is the same (which means ideal RSTD is 0). Assuming that BS_1 has a timing error τ_{tx} and BS_2 is ideally synchronized, Eq. (3.3) can be rewritten, neglecting the other error sources associated to the RSTD measurement, as:

$$K = (RSTD_{n,true} + \tau_{Tx,ref}) \cdot v_p. \tag{3.31}$$

Fig. 3.6 represents the hyperbolas calculated from the ideal RSTD measurement with $\tau_{tx} = 0$ and the real RSTD measurements contaminated with the timing error $\tau_{tx} = 50ns$ and $\tau_{tx} = 200ns$.

Defining the error induced in the measurement by the base station timing error as $e_{m,\tau}$ equal to the distance in meters between the ideal RSTD and the real RSTD, it can be seen that this error is not constant: it varies depending on which point of the hyperbola the mobile device is placed. The error has a minimum if the mobile device is placed in the point where the distance between the hyperbolas is the smallest possible, in this example $North$: 0 m.

Calculating the minimum distance between the hyperbolas for Fig. 3.6, $Min(e_{m,\tau}) =$ 7.5 m for $\tau_{tx} = 50$ ns and $Min(e_{m,\tau}) = 30$ m for $\tau_{tx} = 200$ ns. This calculation is

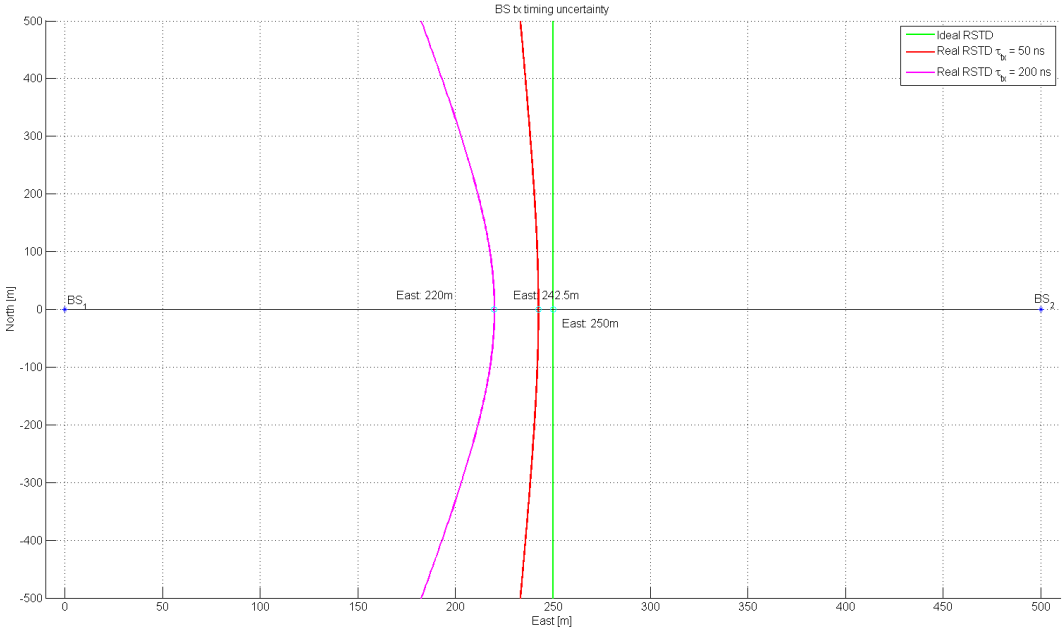

Figure 3.6: Analysis of the base station synchronization uncertainty for OTDOA

independent of the distance between base stations and of the ideal RSTD value. A lower bound for the measurement error induced by the base station timing uncertainty has been found. Hence, the measurement uncertainty created by the base station uncertainty also has a lower bound and it can be written as:

$$\sigma_{m,\tau} \geq \frac{1}{2} \cdot \sigma_{tau,tx} \cdot v_p. \tag{3.32}$$

This lower bound applies to the measurement involving the base station with a synchronization error. Therefore, it affects the quality of one measurement. However, due to the WLS algorithm, the rest of the measurements might compensate partially or totally the error and the final position may result more accurate than individual measurements.

The next scenario to be analysed is when all base stations are affected by synchronization errors. If BS_1 and BS_2 has both a positive timing error τ_{tx}, it can be seen from Eq. (3.3) that they will cancel out each other and the total timing error will be reduced:

$$K = (RSTD_{n,true} - \tau_{Tx,BS_2} + \tau_{Tx,BS_1}) \cdot v_p + e_{RSTD} \tag{3.33}$$

$$= (RSTD_{n,true} - (\tau_{Tx,BS_2} - \tau_{Tx,BS_1})) \cdot v_p + e_{RSTD}. \tag{3.34}$$

However, if the timing errors have opposite sign, they will add and the total timing error will increase.

Considering a base station constellation with three eNBs, BS_1, BS_2 and BS_3, in which the reference cell for the OTDOA measurement is BS_1, the worst possible scenario is that where each individual OTDOA measurement is affected by the biggest possible timing error. That occurs when the timing error of BS_1 has opposite sign to the timing errors from BS_2 and BS_3.

Considering $\tau_{tx,1} = 50$ ns and $\tau_{tx,1} = 200$ ns, as in the previous example, and $\tau_{tx,2} = \tau_{tx,3} = -\tau_{tx,1}$, and denoting the total timing error as τ_{tx}, the position error induced by the base station synchronization error is represented in Fig. 3.7. The mobile device is placed in P_{real}, while the positions calculated with $\tau_{tx,1} = 50$ and $\tau_{tx,1} = 200$ ns are P_1 and P_2, respectively. The position error for $P_1 = 29.82$ m and for $P_2 = 105.32$ m.

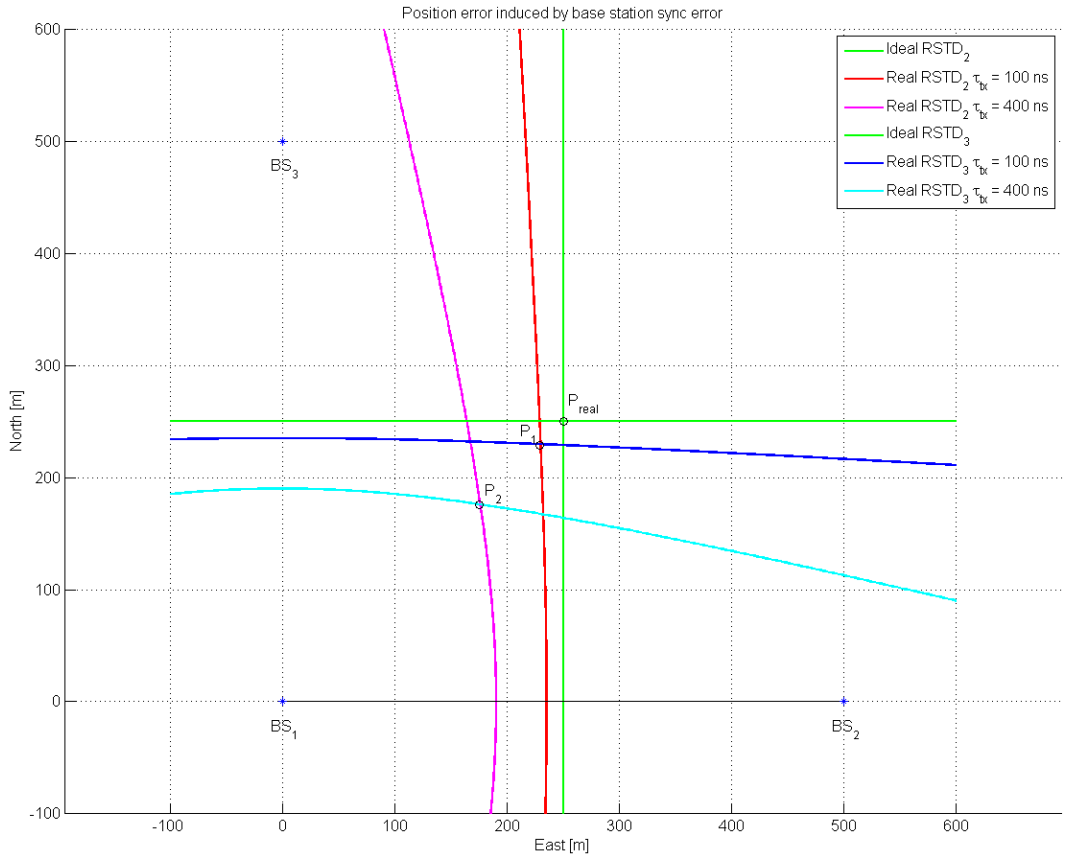

Figure 3.7: Position error induced by base station synchronization error for OTDOA

If the synchronization uncertainty of all the base stations in the network is the same, and considering the lower bound for the measurement uncertainty found in Eq. (3.32),

the individual measurement uncertainty if *both* base stations involved in the measurement have synchronization uncertainty is:

$$\sigma_{m,\tau} \geq \sigma_{tau,tx} \cdot v_p. \tag{3.35}$$

In Fig. 3.7 as the base stations are placed forming a right-angled triangle, the position error can be approached by the hypotenuse of the triangle whose other two sides are the measurement errors. Hence, the following equation is true for the right-angled base station constellation:

$$\sigma_{P,\tau} \approx \sqrt{(2)} \cdot \sigma_{m,\tau} \geq \sqrt{(2)} \cdot \sigma_{tau,tx} \cdot v_p. \tag{3.36}$$

If the base stations are not forming a right-angled triangle, Eq. (3.36) can be generalized applying the law of cosines:

$$\sigma_{P,\tau} \geq \sqrt{(2 - 2\cos\alpha)} \cdot \sigma_{tau,tx} \cdot v_p, \tag{3.37}$$

where α is the angle formed by the vectors $\overline{BS_1BS_3}$ and $\overline{BS_1BS_2}$.

The derivation above was considering that $\tau_{tx,1} > 0$ ns. If $\tau_{tx,1} < 0$ ns, keeping all other relations, the results are even worse, as it can be seen in Fig. 3.8. In this case, the position error for P_1 maintains as 29.82 m but for P_2 it increases until 223.78 m.

B. Transmitter's coordinates error

A key input to the WLS positioning algorithm are the coordinates of all base stations involved in the scenario. More precisely, the coordinates of the antennas transmitting the PRS signals. An error in the coordinates will directly translate into an error in the interpretation of the measurement by the location server and will impact the precision of the calculated position.

It is possible that when the base station was deployed, this requirement was still unknown/undefined and the antenna coordinates were not measured accurately.

In Fig. 3.9 the influence of antenna coordinate errors in the interpretation of the position server of a measurement is shown.

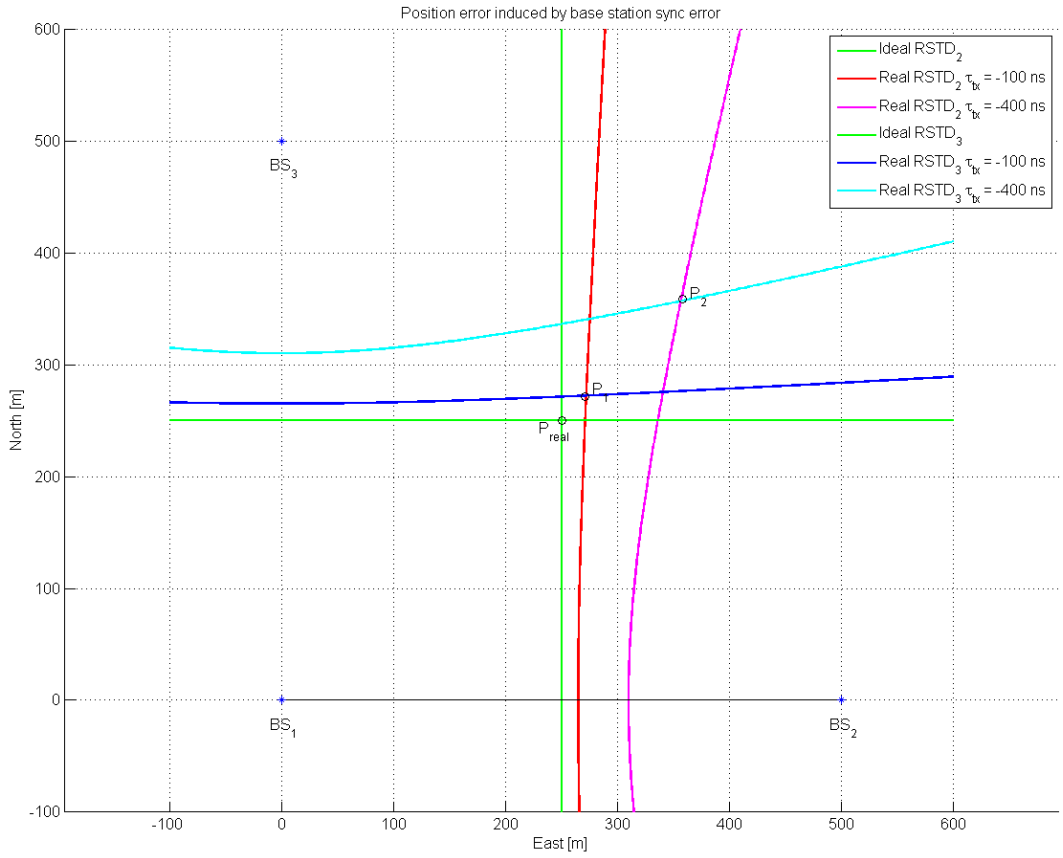

Figure 3.8: Position error induced by base station sync. error for OTDOA II

As it can be appreciated, the effect is highly dependant on the direction of the coordinate errors. If the error in the antenna position is towards the other base station involved in the measurement (the red line in the figure), the error is almost constant along the hyperbola with a standard deviation of approximately 25 meters ($\Delta E/2$). However, if the coordinate error is towards a different direction, the measurement error presents a high variance for each point of the hyperbola. Hence, the effect of lack of precision of the transmitter antenna coordinates on the positioning algorithm will vary for each individual situation and cannot be predicted a priori.

C. OTDOA measurement quantization error

The OTDOA measurement reported by the mobile device is an integer with the unit Ts, the basic unit of time in LTE, which is defined as $\frac{1}{15000 \cdot 2048}$ seconds. The real time difference is rounded to be multiple of this unit and this procedure results in a measurement quantization error which cannot be neglected.

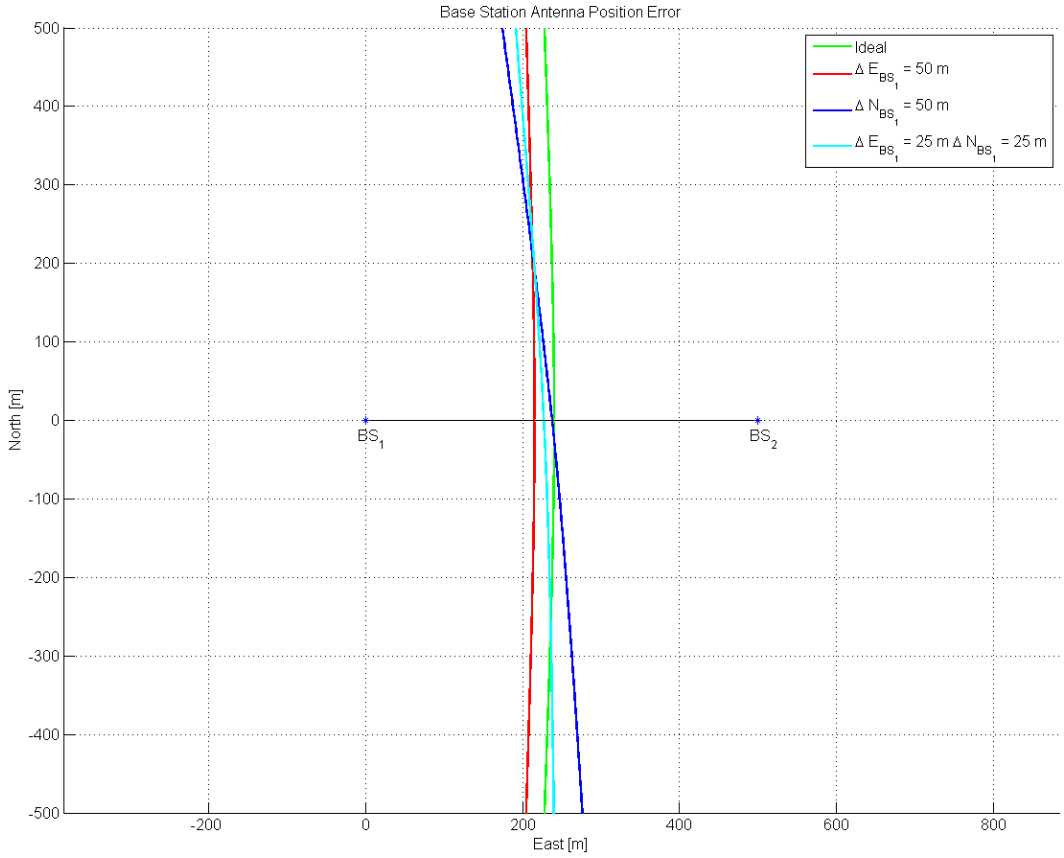

Figure 3.9: Measurement error induced by an error in the transmitter antenna coordinates.

The quantization is uniform, and the worse case scenario is when the real time difference value is exactly $n + 0.5$ Ts, where n represents any integer. In this case, the error cause by the quantization process is exactly 0.5 Ts, which equals:

$$0.5\,Ts = \frac{1}{2} \cdot \frac{1}{15000 \cdot 2048}\,s = 1.628 \cdot 10^{-8}\,s = 16,28\,ns, \tag{3.38}$$

which can be multiplied by the propagation speed, v_p, to find the maximum quantization error in meters:

$$1.628 \cdot 10^{-8}\,s \cdot 3 \cdot 10^{8}\,\frac{m}{s} = 4.88\,m. \tag{3.39}$$

3.2 ECID Positioning

ECID is a trilateration method based on measuring the round-trip timing of a signal. Thus, an ECID measurement can be represented as in Eq. (2.7), replacing m_T by the

transmission and reception times:

$$RTT = t_{Rx} + t_{Tx}, \tag{3.40}$$

and

$$K = RTT \cdot v_p + \nu_{RTT}, \tag{3.41}$$

where v_p represents the propagation speed and e_{RTT} is the error associated to the RTT measurement. The receiver and transmitter clock errors are compensated by taking a round-trip measurement instead of just Downlink or Uplink time measurement. Therefore, the ECID measurement is a range rather than a pseudo-range like GNSS. The equation of the ECID range is analogous to Eq. (2.13):

$$\rho_E = RTT \cdot v_p + \nu_{RTT} = \overline{BsUe} = \sqrt{(x_{bs} - x_{ue})^2 + (y_{bs} - y_{ue})^2 + (z_{bs} - z_{ue})^2} \tag{3.42}$$

As ECID is a spherical positioning system, the rest of the derivation is exactly identical as the derivation done in Section 2.2.3 for GNSS but with $\tau = 0$. To avoid repetition, just the relevant equations will be reproduced here. Before starting the derivation, it is worth remember that 3GPP in Release 9 has only defined ECID measurement to the serving cell. Hence, position calculation using ECID is not possible without additional methods. Power measurements (RSRP and RSRQ) of the neighbour cells and applying Friis transmission equation to estimate the distance to them. However, inferring the distance from the power measurements is much less accurate than ECID and will not be considered in this Thesis. The rest of this Section will presume that ECID measurements to the neighbour cells are already possible, as they will be defined in the LPP extension protocol (LPPe) for E-UTRA Release 11.

3.2.1 Mathematical Derivation

The linearisation of the ECID range by applying Taylor series results in:

$$\rho_E(x, y, z) \approx \rho_{E,0} + \nu + \Delta x \left.\frac{\partial \rho_E}{\partial x}\right|_{P=P_0} + \Delta y \left.\frac{\partial \rho_E}{\partial y}\right|_{P=P_0} + \Delta z \left.\frac{\partial \rho_E}{\partial z}\right|_{P=P_0}. \tag{3.43}$$

Hence, the equation system for ECID can be written as:

$$\begin{bmatrix} \rho^1_{E,i} - \rho^1_{E,i-1} \\ \rho^2_{E,i} - \rho^2_{E,i-1} \\ \vdots \\ \rho^n_{E,i} - \rho^n_{E,i-1} \end{bmatrix} = \begin{bmatrix} \frac{\partial \rho^1_E}{\partial x}\Big|_{P=P_0} & \frac{\partial \rho^1_E}{\partial y}\Big|_{P=P_0} & \frac{\partial \rho^1_E}{\partial z}\Big|_{P=P_0} \\ \frac{\partial \rho^2_E}{\partial x}\Big|_{P=P_0} & \frac{\partial \rho^2_E}{\partial y}\Big|_{P=P_0} & \frac{\partial \rho^2_E}{\partial z}\Big|_{P=P_0} \\ \vdots & \vdots & \vdots \\ \frac{\partial \rho^n_E}{\partial x}\Big|_{P=P_0} & \frac{\partial \rho^n_E}{\partial y}\Big|_{P=P_0} & \frac{\partial \rho^n_E}{\partial z}\Big|_{P=P_0} \end{bmatrix} \cdot \begin{bmatrix} \Delta x \\ \Delta y \\ \Delta z \end{bmatrix} + \begin{bmatrix} \nu^1 \\ \nu^2 \\ \vdots \\ \nu^n \end{bmatrix} \tag{3.44}$$

$$\Delta \hat{\rho}_E = A_E \cdot \Delta \hat{X} + \hat{\nu}, \tag{3.45}$$

where the system matrix for ECID A_E is:

$$A_E = \begin{bmatrix} \frac{(x_{i-1}-x_{s_1})}{\rho^1_E(P_{i-1})} & \frac{(y_{i-1}-y_{s_1})}{\rho^1_E(P_{i-1})} & \frac{(z_{i-1}-z_{s_1})}{\rho^1_E(P_{i-1})} \\ \frac{(x_{i-1}-x_{s_2})}{\rho^2_E(P_{i-1})} & \frac{(y_{i-1}-y_{s_2})}{\rho^2_E(P_{i-1})} & \frac{(z_{i-1}-z_{s_2})}{\rho^2_E(P_{i-1})} \\ \vdots & \vdots & \vdots \\ \frac{(x_{i-1}-x_{s_n})}{\rho^n_E(P_{i-1})} & \frac{(y_{i-1}-y_{s_n})}{\rho^n_E(P_{i-1})} & \frac{(z_{i-1}-z_{s_n})}{\rho^n_E(P_{i-1})} \end{bmatrix}. \tag{3.46}$$

The solution to the LSE algorithm is given by the formula:

$$\hat{X} = (A'_E A_E)^{-1} \cdot A'_E \cdot \Delta \hat{\rho}_E, \tag{3.47}$$

and the Covariance matrix C_E is identical to GNSS case:

$$C = \begin{bmatrix} \sigma_1^2 & 0 & \cdots & 0 \\ 0 & \sigma_2^2 & & \vdots \\ \vdots & & \ddots & 0 \\ 0 & \cdots & 0 & \sigma_n^2 \end{bmatrix}. \tag{3.48}$$

The cofactor matrix Q_E can be obtained from the system matrix:

$$Q_E = (A'_E A_E)^{-1} = \begin{bmatrix} \sigma_x^2 & \sigma_{xy} & \sigma_{xz} \\ \sigma_{xy} & \sigma_y^2 & \sigma_{yz} \\ \sigma_{xz} & \sigma_{yz} & \sigma_z^2 \end{bmatrix}. \tag{3.49}$$

3.2.2 Dilution of Precision

The Dilution of Precision is also a very important factor to analyse for ECID. Similar as for the other LBS technologies, the DOP for ECID is calculated from the elements in the diagonal of the cofactor matrix, Q_E. The graphical interpretation of the DOP can be done using the same figure as for GNSS, being both technologies based on spheres. See Fig. 2.8 for more details.

The values of the different DOPs are:

$$PDOP \equiv GDOP \equiv \sqrt{\sigma_x^2 + \sigma_y^2 + \sigma_z^2} \tag{3.50}$$

$$HDOP \equiv \sqrt{\sigma_x^2 + \sigma_y^2} \tag{3.51}$$

$$VDOP \equiv \sigma_z \tag{3.52}$$

$$TDOP \equiv 0 \tag{3.53}$$

It has been proven that $DOP_{ECID} = DOP_{OTDOA}$ [33]. This is a very important fact that implies that if a base station constellation is optimal for OTDOA positioning it will also be optimal for ECID positioning and vice-versa. It also means that the analysis done in Section 3.1.1 is applicable here.

3.2.3 WLS for ECID

The 3GPP in TS 36.355 [7] has not provided any mechanism for the mobile device to report or estimate the ECID measurement quality. Hence, the location server does not have any information regarding how accurate might the RTT measurement be.

This circumstance complicates the definition of the ECID weighting matrix. For ECID-only positioning, there will be no weighting matrix and the LSE algorithm will be used. However, for LBS Hybrid positioning, a weight is required in order to make ECID measurements comparable to A-GNSS and OTDOA measurements. One option is to use ECID weight factors inversely proportional to the total number of available measurements, N:

$$w_E \propto \frac{1}{N}. \tag{3.54}$$

The second option is to weight the ECID measurement with the mean value of the uncertainties of all other measurements:

$$w_E \propto \langle \sum_{i \neq E} \frac{1}{U_i} \rangle. \tag{3.55}$$

The decision on which of the weighting functions should be used for ECID will be taken after analysing the simulation results with both possibilities.

3.3 LBS Hybrid Positioning

A-GNSS, OTDOA and ECID standalone positioning methods have been described. The next step is to combine all three types of measurements in a hybrid algorithm. A priori, this hybrid algorithm should be able to handle ρ_G, ρ_T and ρ_E measurements, from Eq. (2.14), Eq. (3.5) and Eq. (3.42), respectively. The (pseudo)range measurements for hybrid will be generically denoted as ρ_H, which can get the form of any of the different technologies measurements. In order to keep this generality throughout the mathematical derivation, the variable τ will always be considered. In case of OTDOA and ECID, this variable will be equal to zero.

3.3.1 Hybrid Mathematical derivation

The Hybrid range linearised by Taylor expansion follows the formula:

$$\rho_H(x,y,z) \approx \rho_{H,0} + \nu + \Delta x \left.\frac{\partial \rho_H}{\partial x}\right|_{P=P_0} + \Delta y \left.\frac{\partial \rho_H}{\partial y}\right|_{P=P_0} + \Delta z \left.\frac{\partial \rho_H}{\partial z}\right|_{P=P_0} + \Delta \tau \left.\frac{\partial \rho_H}{\partial \tau}\right|_{P=P_0}, \tag{3.56}$$

resulting in a hybrid equation system:

$$\begin{bmatrix} \rho^1_{H,i} - \rho^1_{H,i-1} \\ \rho^2_{H,i} - \rho^2_{H,i-1} \\ \vdots \\ \rho^n_{H,i} - \rho^n_{H,i-1} \end{bmatrix} = \begin{bmatrix} \left.\frac{\partial \rho^1_H}{\partial x}\right|_{P=P_0} & \left.\frac{\partial \rho^1_H}{\partial y}\right|_{P=P_0} & \left.\frac{\partial \rho^1_H}{\partial z}\right|_{P=P_0} & \left.\frac{\partial \rho^1_H}{\partial \tau}\right|_{P=P_0} \\ \left.\frac{\partial \rho^2_H}{\partial x}\right|_{P=P_0} & \left.\frac{\partial \rho^2_H}{\partial y}\right|_{P=P_0} & \left.\frac{\partial \rho^2_H}{\partial z}\right|_{P=P_0} & \left.\frac{\partial \rho^2_H}{\partial \tau}\right|_{P=P_0} \\ \vdots & \vdots & \vdots & \vdots \\ \left.\frac{\partial \rho^n_H}{\partial x}\right|_{P=P_0} & \left.\frac{\partial \rho^n_H}{\partial y}\right|_{P=P_0} & \left.\frac{\partial \rho^n_H}{\partial z}\right|_{P=P_0} & \left.\frac{\partial \rho^n_H}{\partial \tau}\right|_{P=P_0} \end{bmatrix} \cdot \begin{bmatrix} \Delta x \\ \Delta y \\ \Delta z \\ \Delta \tau \end{bmatrix} + \begin{bmatrix} \nu^1 \\ \nu^2 \\ \vdots \\ \nu^n \end{bmatrix} \tag{3.57}$$

$$\Delta \hat{\rho}_H = A_H \cdot \Delta \hat{X} + \hat{\nu}, \tag{3.58}$$

where the system matrix A_H is:

$$A_H = \begin{bmatrix} \left.\frac{\partial \rho_H^1}{\partial x}\right|_{P=P_0} & \left.\frac{\partial \rho_H^1}{\partial y}\right|_{P=P_0} & \left.\frac{\partial \rho_H^1}{\partial z}\right|_{P=P_0} & \left.\frac{\partial \rho_H^1}{\partial \tau}\right|_{P=P_0} \\ \left.\frac{\partial \rho_H^2}{\partial x}\right|_{P=P_0} & \left.\frac{\partial \rho_H^2}{\partial y}\right|_{P=P_0} & \left.\frac{\partial \rho_H^2}{\partial z}\right|_{P=P_0} & \left.\frac{\partial \rho_H^2}{\partial \tau}\right|_{P=P_0} \\ \vdots & \vdots & \vdots & \vdots \\ \left.\frac{\partial \rho_H^n}{\partial x}\right|_{P=P_0} & \left.\frac{\partial \rho_H^n}{\partial y}\right|_{P=P_0} & \left.\frac{\partial \rho_H^n}{\partial z}\right|_{P=P_0} & \left.\frac{\partial \rho_H^n}{\partial \tau}\right|_{P=P_0} \end{bmatrix}. \tag{3.59}$$

The coefficients of the system matrix can take different forms depending on the technology of each measurement:

$$\left.\frac{\partial \rho_G^j}{\partial x}\right|_{P=P_0} = \frac{(x_0 - x_{s_j})}{\rho_G^j(P_0)} \tag{3.60}$$

$$\left.\frac{\partial \rho_G^j}{\partial y}\right|_{P=P_0} = \frac{(y_0 - y_{s_j})}{\rho_G^j(P_0)} \tag{3.61}$$

$$\left.\frac{\partial \rho_G^j}{\partial z}\right|_{P=P_0} = \frac{(z_0 - z_{s_j})}{\rho_G^j(P_0)} \tag{3.62}$$

$$\left.\frac{\partial \rho_G^j}{\partial \tau}\right|_{P=P_0} = c \tag{3.63}$$

$$\left.\frac{\partial \rho_T^j}{\partial x}\right|_{P=P_0} = \frac{(x_{ref} - x_0)}{d_{ref}(P_0)} - \frac{(x_{bs_j} - x_0)}{d_{bs_j}(P_0)} \tag{3.64}$$

$$\left.\frac{\partial \rho_T^j}{\partial y}\right|_{P=P_0} = \frac{(y_{ref} - y_0)}{d_{ref}(P_0)} - \frac{(y_{bs_j} - y_0)}{d_{bs_j}(P_0)} \tag{3.65}$$

$$\left.\frac{\partial \rho_T^j}{\partial z}\right|_{P=P_0} = \frac{(z_{ref} - z_0)}{d_{ref}(P_0)} - \frac{(z_{bs_j} - z_0)}{d_{bs_j}(P_0)} \tag{3.66}$$

$$\left.\frac{\partial \rho_T^j}{\partial \tau}\right|_{P=P_0} = 0 \tag{3.67}$$

$$\left.\frac{\partial \rho_E^j}{\partial x}\right|_{P=P_0} = \frac{(x_0 - x_{s_j})}{d_{bs_j}(P_0)} \tag{3.68}$$

$$\left.\frac{\partial \rho_E^j}{\partial y}\right|_{P=P_0} = \frac{(y_0 - y_{s_j})}{d_{bs_j}(P_0)} \tag{3.69}$$

$$\left.\frac{\partial \rho_E^j}{\partial z}\right|_{P=P_0} = \frac{(z_0 - z_{s_j})}{d_{bs_j}(P_0)} \tag{3.70}$$

$$\left.\frac{\partial \rho_E^j}{\partial \tau}\right|_{P=P_0} = 0 \tag{3.71}$$

After filling the system matrix with the proper coefficients, the solution to the LSE algorithm is given by the formula:

$$\hat{X} = (A'_H A_H)^{-1} \cdot A'_H \cdot \Delta\hat{\rho}_H, \tag{3.72}$$

and the Covariance matrix C_H is identical to all standalone technologies:

$$C = \begin{bmatrix} \sigma_1^2 & 0 & \cdots & 0 \\ 0 & \sigma_2^2 & & \vdots \\ \vdots & & \ddots & 0 \\ 0 & \cdots & 0 & \sigma_n^2 \end{bmatrix}. \tag{3.73}$$

The cofactor matrix Q_H can be obtained from the system matrix:

$$Q_H = (A'_H A_H)^{-1} = \begin{bmatrix} \sigma_x^2 & \sigma_{xy} & \sigma_{xz} & \sigma_{x\tau} \\ \sigma_{xy} & \sigma_y^2 & \sigma_{yz} & \sigma_{y\tau} \\ \sigma_{xz} & \sigma_{yz} & \sigma_z^2 & \sigma_{z\tau} \\ \sigma_{x\tau} & \sigma_{y\tau} & \sigma_{z\tau} & \sigma_\tau^2 \end{bmatrix}. \tag{3.74}$$

At this point, some assessments can be done. From the design matrix, it can be extracted that at least four measurements are required for computing a three dimensional location due to the GNSS receiver clock error. However, if no GNSS measurement is available, there is no need to calculate the τ variable, and three OTDOA and ECID measurement would suffice. As a direct consequence of this, if there is only one GNSS measurement, it will not add any value to the solution. At least two GNSS measurements are required, as one of them will be used for estimating the clock error. Summing up, that means three OTDOA and/or ECID measurement are required or four measurements with at least two GNSS *from the same GNSS technology.*

A. LBS Hybrid with multiple GNSS technologies

So far, GNSS has been treated as one unique system. However, there are multiple GNSS systems available and not all of them behave exactly the same way. Particularly, the two GNSS fully deployed as of today, GPS and GLONASS, have different independent system times [34]. This causes a time offset between both satellite system timescales and a bias between the GNSS measurements. The algorithm needs to cope with two different time offsets τ_1 and τ_2 in order to perform the position calculation. The same problem arises with BeiDou and Galileo [35]. In [36] the time system references for the different GNSS can be consulted.

In order to cope with this problem, the system matrix can be re-designed to compute multiple independent clock errors:

$$A_H = \begin{bmatrix} \frac{\partial \rho_H^1}{\partial x}\Big|_{P=P_0} & \frac{\partial \rho_H^1}{\partial y}\Big|_{P=P_0} & \frac{\partial \rho_H^1}{\partial z}\Big|_{P=P_0} & \frac{\partial \rho_H^1}{\partial \tau_1}\Big|_{P=P_0} & \frac{\partial \rho_H^1}{\partial \tau_2}\Big|_{P=P_0} \\ \frac{\partial \rho_H^2}{\partial x}\Big|_{P=P_0} & \frac{\partial \rho_H^2}{\partial y}\Big|_{P=P_0} & \frac{\partial \rho_H^2}{\partial z}\Big|_{P=P_0} & \frac{\partial \rho_H^2}{\partial \tau_1}\Big|_{P=P_0} & \frac{\partial \rho_H^2}{\partial \tau_2}\Big|_{P=P_0} \\ \vdots & \vdots & \vdots & \vdots & \vdots \\ \frac{\partial \rho_H^n}{\partial x}\Big|_{P=P_0} & \frac{\partial \rho_H^n}{\partial y}\Big|_{P=P_0} & \frac{\partial \rho_H^n}{\partial z}\Big|_{P=P_0} & \frac{\partial \rho_H^n}{\partial \tau_1}\Big|_{P=P_0} & \frac{\partial \rho_H^n}{\partial \tau_2}\Big|_{P=P_0} \end{bmatrix}, \tag{3.75}$$

where τ_1 and τ_2 are the clock errors for GNSS 1 and GNSS 2, respectively. The coefficient for τ_i for measurement j will be c if the measurement j is from GNSS i and 0 if the measurement is from a different GNSS system, OTDOA or ECID. The same concept could be applied to include τ_3, ..., τ_m. The cofactor matrix Q_H should also be re-defined.

$$Q_H = (A_H' A_H)^{-1} = \begin{bmatrix} \sigma_x^2 & \sigma_{xy} & \sigma_{xz} & \sigma_{x\tau_1} & \sigma_{x\tau_2} \\ \sigma_{xy} & \sigma_y^2 & \sigma_{yz} & \sigma_{y\tau_1} & \sigma_{y\tau_2} \\ \sigma_{xz} & \sigma_{yz} & \sigma_z^2 & \sigma_{z\tau_1} & \sigma_{z\tau_2} \\ \sigma_{x\tau_1} & \sigma_{y\tau_1} & \sigma_{z\tau_1} & \sigma_{\tau_1}^2 & \sigma_{\tau_1\tau_2} \\ \sigma_{x\tau_2} & \sigma_{y\tau_2} & \sigma_{z\tau_2} & \sigma_{\tau_1\tau_2} & \sigma_{\tau_2}^2 \end{bmatrix}. \tag{3.76}$$

The inconvenient this solution presents is that now at least five measurements are required to compute a three dimensional location, 2 for GNSS 1, 2 for GNSS 2 and 1 OTDOA or ECID.

An alternative solution is to treat the τ_2 for GNSS 2 as a constant offset to system GNSS 1. For some of the GNSS systems, this time offset can be pre-computed from the assistance data [35] and the algorithm can be solved with at least four measurements.

3.3.2 WLS algorithm for hybrid

The weighted version of the least squares algorithm for hybrid follows the same formula as the WLS for OTDOA and GNSS.

$$\hat{X} = (A'_H \cdot W_H \cdot A_H)^{-1} \cdot A'_H \cdot W_H \cdot \Delta\hat{\rho}_H. \tag{3.77}$$

The system matrix and the range measurements have already been defined. The only thing left to define is the weighting matrix, W_H. The weighting matrix will be a diagonal matrix with coefficients w_i in the main diagonal:

$$\begin{bmatrix} w_1 & 0 & \cdots & 0 \\ 0 & w_2 & & \vdots \\ \vdots & & \ddots & 0 \\ 0 & \cdots & 0 & w_n \end{bmatrix}, \tag{3.78}$$

where $w_i = w_H$ and w_H equals w_G, w_T or w_E according to Eq. (2.47), Eq. (3.30) or Eq. (3.54), depending on the type of the measurement i.

However, that definition of the weighting matrix require the weights assigned for different technologies to be comparable in order of magnitude and meaning. For GNSS, the weight was the inverse of the RMS estimated by the mobile device for the GNSS measurement. For OTDOA, the weight is representing some error range in meters, but the specifications do not clarify what is the meaning of that error range. For ECID, the specification is not providing any mechanism to report the measurement quality. Thus, some scaling factor might need to be introduced in order to adjust the magnitude of the weights and make them comparable across technologies.

3.3.3 Hybrid DOP

The Dilution of Precision for LBS Hybrid is defined identically as the DOP for each of the three standalone technologies. It can be calculated with main diagonal elements of the hybrid cofactor matrix in Eq. (3.74) and it can be separated into five different components:

$$DOP \equiv GDOP \equiv \sqrt{\sigma_x^2 + \sigma_y^2 + \sigma_z^2 + \sigma_\tau^2} \tag{3.79}$$

$$PDOP \equiv \sqrt{\sigma_x^2 + \sigma_y^2 + \sigma_z^2} \tag{3.80}$$

$$HDOP \equiv \sqrt{\sigma_x^2 + \sigma_y^2} \tag{3.81}$$

$$VDOP \equiv \sigma_z \tag{3.82}$$

$$TDOP \equiv \sigma_\tau \tag{3.83}$$

The system matrix A_H which has been used to calculate the cofactor matrix Q_H contains equations for all the satellites and all the base stations than are involved in the positioning. These set of satellites and base stations will be denoted as transmitters constellation. It is possible for a base station to be part of OTDOA and ECID measurements. Hence, the same base station might appear in the system matrix twice (even multiple times if it is the reference cell for OTDOA) as part of a TDoA and of a ToA equations.

A. DOP with multiple GNSS technologies

If the transmitter constellation contains satellites from multiple GNSS technologies and the algorithm implements a solution which calculated more than one clock error τ_2, following Eq. (3.75) and Eq. (3.76), the GDOP and TDOP parameters need to be redefined to match the new elements in the main diagonal of the cofactor matrix:

$$GDOP \equiv \sqrt{\sigma_x^2 + \sigma_y^2 + \sigma_z^2 + \sigma_{\tau_1}^2 + \sigma_{\tau_2}^2} \tag{3.84}$$

$$TDOP \equiv \sqrt{\sigma_{\tau_1}^2 + \sigma_{\tau_2}^2} \tag{3.85}$$

3.3.4 The Earth surface as equation

If the system matrix A_H is not rank 4, a three dimensional position calculation can not be done. In a such a case, the vertical coordinate, z, will not be calculated.

The algorithm uses an extra *measurement*, the Earth surface. The Earth can be seen as an spherical measurement with a *transmitter* being in the centre of the Earth at the range measurement ρ being equal to the Earth radius. That will allow the algorithm to converge to a three dimensional position. The algorithm will then discard the altitude coordinate and send the two dimensional position $[x, y]$ as solution.

3.3.5 RAIM enhancements for Hybrid

Letting aside indoor scenarios, it will be often be the case in Hybrid positioning that the number of measurements from all three technologies exceeds the number of unknowns to calculate. The WLS algorithm tries to find the solution which fits better *all* the equations, minimising the so-called *residuals*. Nevertheless, not all measurements will have the same accuracy. Trying to fit non-accurate measurements will probably reduce the quality of the solution. This problem is partially mitigated by using the weighting matrix directly proportional to the reported measurement quality. However, it has also been that the same error does not affect equally different measurements. The geometry of the transmitter (satellite or base station) relative to the mobile device influences how critical is a certain error for that particular transmitter. For instance, one meter measurement error for one transmitter might cause a two meters error in the position calculation, while for a different transmitter it might cause just half a meter position error.

This asymmetric sensitivity to measurement errors will also affect the positioning algorithm, making it more sensitive to errors in some measurements than in others. Hence, it makes the algorithm suitable for a Receiver Autonomous Integrity Monitoring (**RAIM**) implementation, which helps detecting faulty measurements and improves the overall stability of the positioning.

RAIM methods are commonly used by GNSS applications since the 90s, especially for military and SoL (safety of life) applications [37–39]. There are several different algorithms, but they can be grouped in two main families: the Measurement Rejection Approach (**MRA**) and the Error Characterization Approach (**ECA**). The algorithm

proposed in this thesis will implement a MRA variant called Maximum Solution Separation [37].

The Measurement Rejection Approach's core feature is the t (**Fault Detection and Exclusion**)echniques, which is based of detecting the faulty measurements and exclude them from the positioning calculation in order to improve the solution. The Maximum Solution Separation method consists on comparing the separation between the position estimate using all available measurements and the position estimate on a series of subsets of the measurements, generated by a certain *subset filter*.

The proposed RAIM algorithm for LBS Hybrid is the following:

1. Try to calculate a position estimate using the full set of measurements.
2. IF the position estimate converges below a certain threshold, THEN return the calculated position and finish the algorithm.
3. ELSE IF the position estimate does not converge or the convergence is not better than the threshold THEN perform RAIM.
4. Compute a position estimate for each subset of measurements. The subsets are created by using all but one of the measurements. For n measurements, there will n subsets.
5. Compare the different estimates obtained in step 4. Return the one that has converged with the best convergence.
6. IF none of the subset estimates have converged, the position calculation has failed.

The algorithm has converged at iteration k if the difference between the position calculated at that iteration and the position calculated at iteration $k-1$ is below a certain threshold value. The convergence fails if the algorithm has not converged after a limit number of iterations or if the difference between the position calculated at iteration k and the position calculated at iteration $k-1$ exceeds a certain limit (the calculation diverges).

A possibility when the Maximum Solution Separation algorithm has not given a position estimate is to continue one step forward and implement a Multiple Hypothesis

Solution Separation (**MHSS**). The MHSS allows to include multiple faulty measurements. After creating the sub-sets excluding one measurement, it will continue creating all the subsets excluding two measurements, then three, etc. until it reaches a solution or there are not enough measurements left in the subsets to try a position calculation. However, the number of subsets to calculate greatly increases with the number of measurements to exclude. In a system with N total measurements and m measurements to exclude, the total number of combinations is $\binom{N}{m} = \frac{N!}{m!(N-m)!}$.

3.3.6 LBS Hybrid and Indoor scenarios

One of the main requirements for a Hybrid positioning solution is to have an accurate way of locate a mobile device in Indoor locations. Typically, in indoor scenarios the number of satellites with direct LoS will not suffice to calculate a position. If the user is close to a window, the mobile device might get some satellites in LoS. However, these satellites will come from the same region of the sky, having a bad DOP, as in Fig. 3.10.

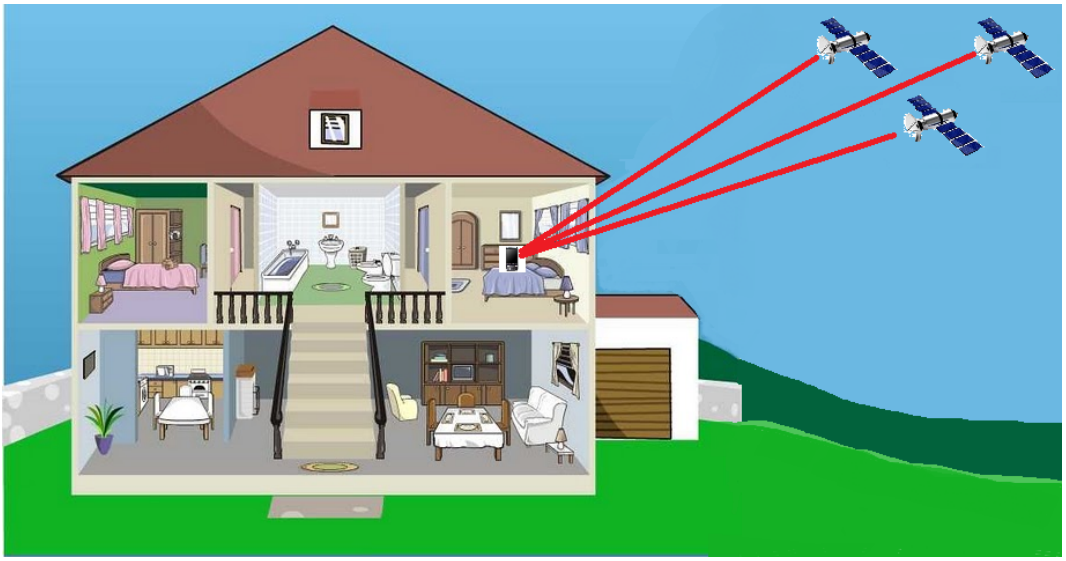

Figure 3.10: Indoor Scenario with three satellites from the same sky region

The constellation of satellites in Fig. 3.10 is not suitable for a position calculation, as the satellites have a very bad DOP and the calculated position will have high uncertainty. However, complementing these three satellites with OTDOA and/or ECID measurements from the surrounding base stations, the DOP of the complete system will improve, being able to calculate an indoor location.

Thus, LBS Hybrid offers a solution for the indoor location problem when there are few satellites available. Nevertheless, another possible is scenario is when no satellite is visible. How will the positioning algorithm behave in such scenario?

As it has been discussed in Section 3.1.1.A., base station constellations will often not present variation in altitude between transmitters sufficient to estimate a three dimensional position. If the mobile device is within a building with multiple floors, OTDOA and ECID technologies might not offer a robust solution to determine in which floor the device is. The 2-D position can be found accurately, but without the altitude information accurate position indoors cannot be delivered.

This situation is depicted in Fig. 3.11, where a building with multiple floors is depicted. For simplicity, there are only three base stations in this example and the measurements are ToA. A similar situation occurs with more base stations and TDoA measurements. It can be seen that the 2D position can be calculated quite accurately, but it is not possible to decide whether the mobile device is in floor 3, 4 or 5.

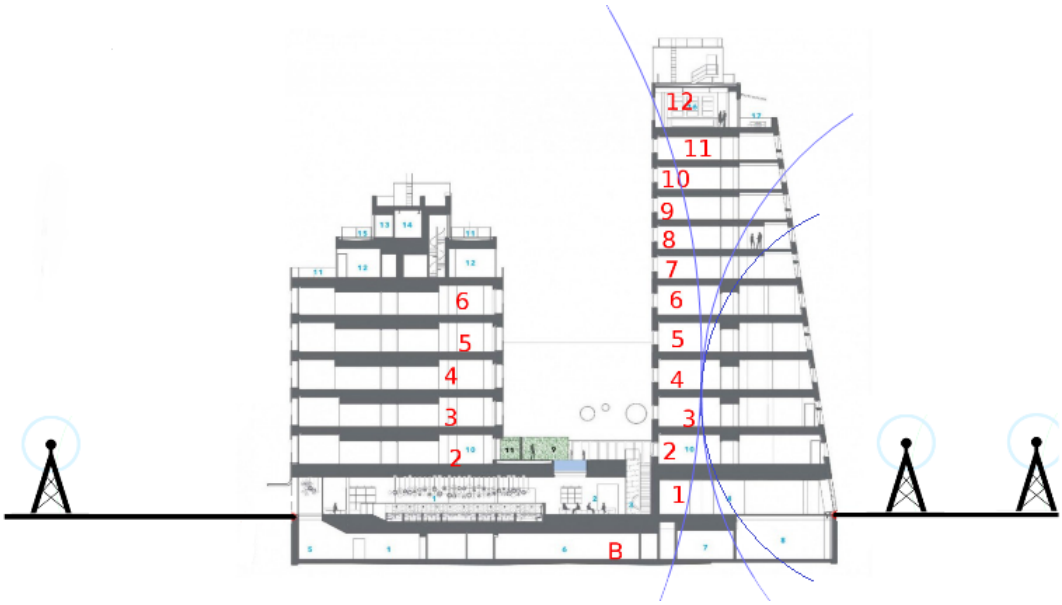

Figure 3.11: Terrestrial location in building with multiple floors: no altitude diversity

In Fig. 3.12, the same scenario is depicted but adjusting the altitude of the base stations for obtaining a significant difference between them. It can be seen that the position can now be precisely calculated to floor 5.

Unfortunately, the altitude of the base stations cannot be adjusted to obtain the required altitude diversity in all possible scenarios. Most base stations are already deployed and its location depends on the geography of the city and its surroundings.

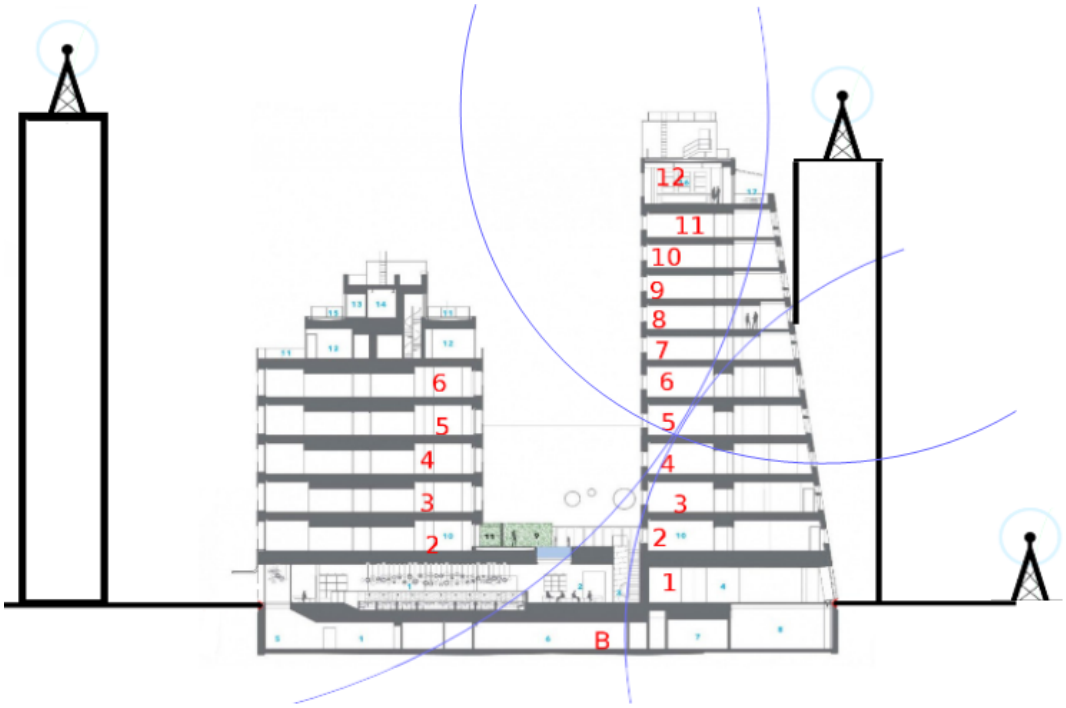

Figure 3.12: Terrestrial location in building with multiple floors: altitude diversity between eNBs

Additional solutions are required in order to achieve the necessary vertical accuracy for indoor location. Some of them are the following:

A. Pico- and femto-cell deployments

Picocells and femtocells are the names given to small cellular base stations used to increase network coverage in small areas Their typical ranges are 200 metres or less for a picocell and 10 meters or less for a femtocell. These small cells are often used to improve in-building signal availability where outdoor signals do not reach well or to increase the network capacity in places with dense network usage such as shopping centres, train stations, stadiums, etc.

Deploying these cells in a number of floors of the building will add the required altitude diversity to calculate a three dimensional location. In Fig. 3.13, the same scenario as in the previous section is shown. However, two pico-cells have been deployed in floors 6 and 11. The algorithm is now able to calculate the mobile device position accurately, even though the two LTE macro-cells are placed at the same altitude.

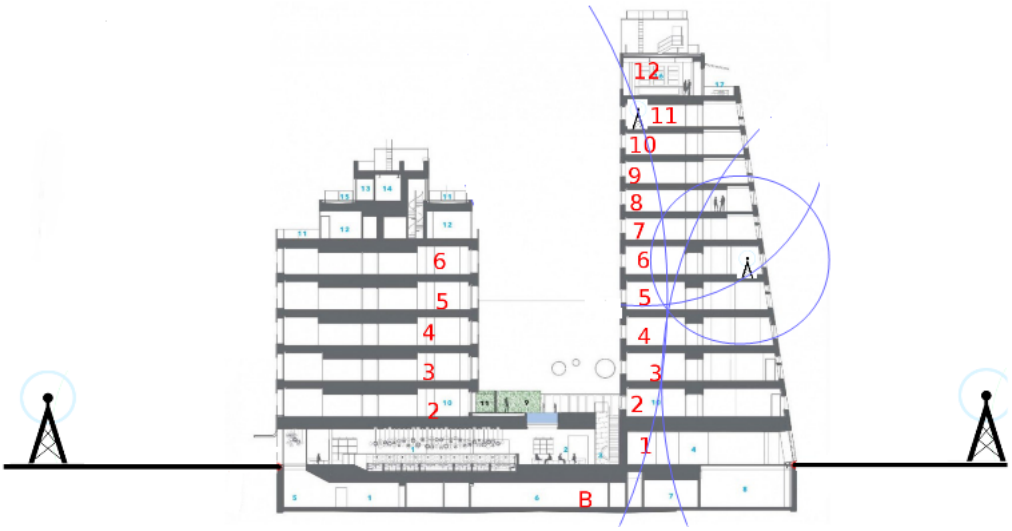

Figure 3.13: Terrestrial location in building with multiple floors: pico-cells

One of the main drawbacks of this approach is the synchronization requirements (in the order of tens of nanoseconds) for the LTE cells in order to perform OTDOA positioning. Initially, the pico- and femto-cells were planned to be a cost effective solution to increase network capacity in certain specific places. The synchronization of the cells to the require level of nanoseconds is a technical challenge that will increase significantly the cost of the deployment. Another drawback is the need of knowing the exact WGS-84 coordinates where the transmitter antenna of the small cell is located. Otherwise the localization algorithm cannot make use of these extra cells.

Nevertheless, LTE small cells are promising for the future of indoor location and efforts are being towards finding an efficient solution to synchronize these cells within the LTE network [40, 41]. These solutions go from using the LTE Backhaul network to use the GNSS time in combination with collaborative techniques. Apart from synchronization, the deployment of small cells in the so-called heterogeneous network presents other challenges like interference cancellation, which will be addressed in E-UTRAN Release 11 and 12 with Enhanced Inter Cell Interference Cancellation (**eICIC**) and further enhanced ICIC (**feICIC**).

B. LTE Cells in the unlicensed spectrum

A current topic for increasing network capacity is to exploit the open spectrum or unlicensed spectrum (the part of the frequency spectrum that is available for use by everyone) to transmit LTE signals [42]. The use of the so called LTE-U aims to meet

the increasing capacity demands allowing mobile carriers to add extra MHz to their blocks of licensed spectrum.

The LTE-U is planned to work with small unlicensed cells. The process to use these unlicensed cells for LBS is the same as using licensed pico- or femto-cells. However, the open spectrum brings more technological challenges as the LTE signal needs to co-exist with WiFi and other emissions in the non-licensed frequencies.

C. WLAN access points

Instead of deploying and maintaining a network of small LTE cells, an alternative that is winning strength is to use the widely available WiFi access points to perform range measurements that can be added to the LBS Hybrid set of measurements.

The first type of WLAN measurements which can be considered for LBS Hybrid positioning are Received Signal Strength Indicator (**RSSI**). RSSI measurement are power measurements: the mobile device measures the received signal power and it estimates the distance to the transmitter by using the transmission power and Friis formula [43]. However, in indoor locations the signal will be typically distorted with reflections, diffractions and refractions, and the Line Of Sight path will most likely not be the strongest one due to the effect of walls. Thus, the RSSI measurements will not meet the accuracy levels of OTDOA and ECID. A more accurate alternative is to use RSSI in combination with fingerprinting or RF pattern matching methods. These methods try to estimate the position by matching the characteristics of the received signal to a precomputed radio map of the indoor area [44]. This offers a more accurate solution than calculating the distance from the path loss and the received power, but it is not compatible with the other distance measurements from GNSS, ECID and OTDOA. Therefore, it cannot be added to this algorithm.

The second type of measurements that can be used are WLAN Round Trip Time measurements. The RTT measurements can be based on either ToA or TDoA between signals. Hence, they can be treated similar to ECID or OTDOA measurements, respectively [45]. The main advantage of this method with respect to the RSSI measurement is that, while the power of the signal will be drastically reduced by going through walls and obstacles, the time of arrival will be less affected. The propagation in a solid medium is slower than in free space, but this difference is less significant than the power loss. However, the strong multipath conditions caused by the multiple

reflections typical in indoor environments will remain as a problem as well for RTT measurements.

An extra requirement of the RTT measurements with respect to RSSI, is the time synchronization. For ToA measurements, both receiver and transmitter need to be very well synchronized. In case of TDoA measurements, the synchronization of the receiver is not required, but the network of access points need to be strongly synchronized to each other. Typical WLAN synchronization is of 1 μs, which equals 300 meters at the propagation speed. This is not sufficient for the E911 indoor positioning accuracy requirements.

The addition of WLAN to LBS is one of the most promising candidates to solve the indoor positioning challenge. Hence, research is focusing on solving the remaining open issues, as is the WLAN network synchronization and multipath mitigation. The 3GPP is already working on standardization towards integrating WLAN as an additional feature for Location Based Services.

D. Bluetooth or other technologies

Analogously to WLAN, Bluetooth devices or any other device transmitting an RF signal is susceptible of being included as an additional measurement to improve the algorithm. However, the technical challenges are even greater than those of WLAN, and its inclusion as a Location Based Service is at best only remotely possible. Hence, they will not be further studied in this Thesis.

Chapter 4

Simulation Results

4.1 OTDOA Positioning

In this section, the performance of the OTDOA positioning algorithm proposed in Chapter 3 will be analysed, studying the results in different scenarios and under different error conditions in a simulation environment created with MATLAB.

4.1.1 Base station constellations

The results will be reproduced in several base stations constellation with different geometries in order to produce good and bad values for the HDOP and the GDOP. Every constellation contains four base stations, giving three OTDOA measurements. Therefore, all the scenarios meet the requirement of number of equation in order to calculate a 3D position. Unless otherwise stated, the mobile device position simulated will be the one defined in this section for each base station scenario.

A. Constellation 1

The first proposed constellation is meant to have ideal conditions for calculating three dimensional locations. The base stations have enough altitude diversity to present an acceptable GDOP. The coordinates and real time delays of the base stations and the mobile device are specified in Tab. 4.1.

	East [m]	North [m]	Up [m]	Time Delay [ns]	RSTD
BS1 (Ref)	0	0	300	-	-
BS2	0	1000	100	886	6383
BS3	1000	0	150	1328	6396
BS4	1000	1000	500	2352	6428
mobile	200	300	0	-	-

Table 4.1: Base Stations constellation 1

These geometry presents an HDOP value of 0.87 and a GDOP value of 3.31. The GDOP is not optimal, but to obtain a lower value would require even more altitude diversity in the base station coordinates, which would not be possible in normal real life conditions. In this example, altitude 0 is considered to be the surface of the Earth.

B. Constellation 2

The second scenario under consideration presents a more realistic distribution of the base station altitudes. The good HDOP value is still maintained, but the GDOP is drastically worse. The coordinates and real time delays of the base stations and the mobile device are specified in Tab. 4.2.

	East [m]	North [m]	Up [m]	Time Delay [ns]	RSTD
BS1 (Ref)	0	0	100	-	-
BS2	0	1000	110	1207	6393
BS3	1000	0	90	1616	6405
BS4	1000	1000	95	2310	6426
mobile	200	300	0	-	-

Table 4.2: Base Stations constellation 2

This constellation has $HDOP = 0.87$ and $GDOP = 69.25$.

C. Constellation 3

The third scenario is formed by the same base stations of Scenario 2. However, the mobile device is placed on different coordinates so the HDOP value is worse. The updated coordinates of the mobile device and the new time delays are detailed in Tab. 4.3.

	East [m]	North [m]	Up [m]	Time Delay [ns]	RSTD
BS1 (Ref)	0	0	100	-	-
BS2	0	1000	110	3210	6454
BS3	1000	0	90	3210	6454
BS4	1000	1000	95	4714	6500
mobile	-100	-100	100	-	-

Table 4.3: Base Stations constellation 3

This constellation has $HDOP = 3.24$ and $GDOP > 1000$. The GDOP value is so high that the algorithm will not converge to a three dimensional position.

D. Constellation 4

The last geometry that will be considered in this section is formed by four base stations on the same plane of altitude and placed forming a straight line. Such a scenario will have very poor HDOP values. The scenario is described in Tab. 4.4.

	East [m]	North [m]	Up [m]	Time Delay [ns]	RSTD
BS1 (Ref)	0	0	0	-	-
BS2	0	-250	0	196	6362
BS3	0	250	0	196	6362
BS4	0	-500	0	690	6377
mobile	500	0	0	-	-

Table 4.4: Base Stations constellation 4

In this case, $HDOP = 4.31$ and $GDOP \to \infty$, which means the system matrix is singular for the three dimensional case and a solution cannot be calculated.

4.1.2 Proof of concept under ideal conditions

The first simulation will serve to proof the validity of the OTDOA positioning algorithm. For that purpose, a position will be calculated for all scenarios in Section 4.1.1 if the mobile phone reports the perfect RSTD measurements under ideal conditions, i.e. without any source of error. The entry point for the algorithm will be generated from the Reference Cell coordinates with G $(Guess) = [Ref_{East} + 10, Ref_{North} + 10, 0]$.

In order to give a step by step example of the performance of the algorithm, this process is detailed in Fig. 4.1. The real point is depicted with a blue star. The base station locations are represented as green circles. The red circles represent the positioning guesses for each iteration of the algorithm, each iteration getting closer to the real position. Finally, the algorithm converges after 5 iterations to $G = [199.33, 294.90, -1.52]$, with an error of 5.37 meters to the real location. This error can be explained due to the loss of accuracy in the conversion to RSTD measurements (the RSTD is represented in multiples of T_s and $1 \cdot T_s = 9.7656$ meters).

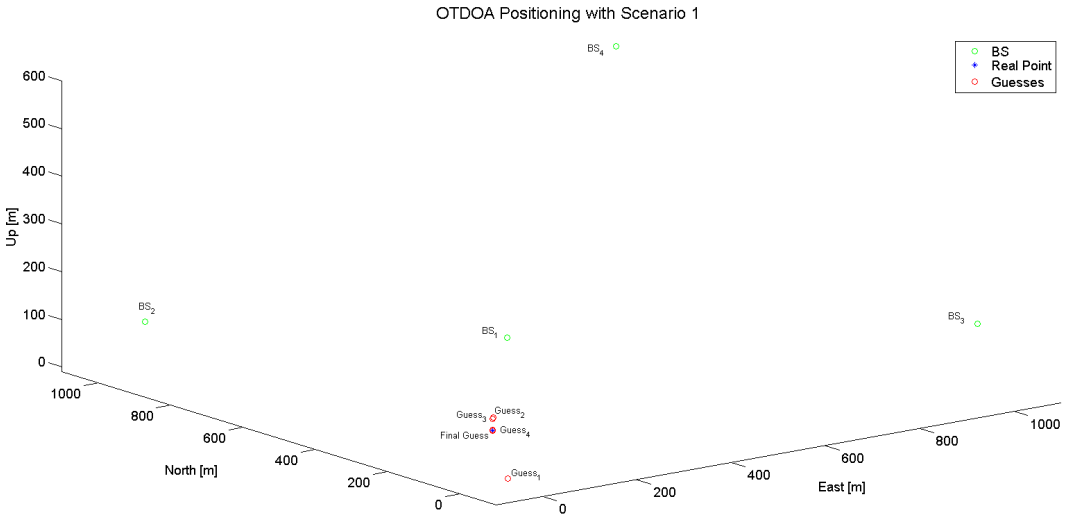

Figure 4.1: OTDOA Positioning example with OTDOA Scenario 1

Doing the same calculation for all the four scenarios, the results are written in Tab. 4.5, where N_{It} is the number of iterations required for the algorithm to converge.

Scn	Real Position	Calculated Position	3D Err.[m]	2D Err.[m]	N_{It}
1	[200, 300, 0]	[199.33, 294.90, -1.52]	5.37	5.15	5
2	[200, 300, 0]	[199.44, 291.08, 226.01]	226.18	8.93	6
2[1]	[200, 300, 0]	[198.95, 299.14]	-	1.36	4
3	[-100, -100, 100]	-	-	-	-
3[1]	[-100, -100, 100]	[-90.90, -90.90]	-	12.87	3
4	[500, 0, 0]	[454.10, -4.83, 0]	46.15	46.15	5
4[1]	[500, 0, 0]	[454.10, -4.83]	-	46.15	5
[1]: Using a 2D algorithm and neglecting Up coordinate					

Table 4.5: OTDOA Positioning: Proof of concept under ideal conditions

It can be seen that scenario 2 gives a much better 2D position if the altitude coordinate is completely neglected. The altitude can only be calculated accurately for

the Scenario 1, all other scenarios are not giving correct altitude values. Scenario 3 has not converged for a 3-D location. That matches the expectancies as the GDOP for this scenario was > 1000. Finally, although scenario 4 has converged to a three dimensional position with correct altitude, this is purely circumstantial. The initial guess was set to altitude 0, which matches the altitude of the mobile device for scenario 4. Therefore, the algorithm was able to find a solution. Trying to calculate the same 3-D starting from any other guess with altitude different than 0 has thrown errors of over 300 meters in the final result.

4.1.3 Algorithm performance under non-ideal RSTD measurements

In this section the RSTD measurements will no longer be ideal. It will be assumed that due to external influences (noise, multipath, interferences with other cells, mobile device performance, etc) the RSTD measurement is contaminated with measurement error of $\sigma^2 \approx 5T_s$. Under such conditions, a thousand independent samples will be taken for each scenario, and a position calculation will be triggered for each sample.

Tab. 4.6 contains the results of the simulation for the four scenarios. The convergence is considered achieved if the algorithm has been able to find a solution in less than 2000 iterations and this solution is less than 10000 meters apart from the real position.

Scn	**Errors 3D [m]**			**Errors 2D [m]**			**Convergences[%]**	
	E_{min}	E_{max}	$\langle E \rangle$	E_{min}	E_{max}	$\langle E \rangle$	Conv. 3D	Conv. 2D
1	5.37	316.93	84.34	1.73	98.12	35.00	100	100
2	55.69	8024.00[1]	860.20[1]	1.04	63.65	27.72	41.8	100
3	52.29	392.42[1]	129.68[1]	1.66	442.59	93.01	29.9	63.7
4	353.56	1970.40	446.84	4.61	1161.60	194.29	99.9	99.9
4[2]	NA	NA	NA	1.15	1795.4	187.79	NA	100
[1]: All position calculations with more than 10 kilometres error have been considered non-convergent and neglected for calculating the Max and Mean errors.								
[2]: Using a 2D algorithm and neglecting Up coordinate								

Table 4.6: OTDOA Positioning: Algorithm performance with $\sigma^2 \approx 5T_s$ measurement errors.

A. Analysis of results for Scenario 1

In Scenario 1, the algorithm has been able to find a 3D solution in 100 % of the occasions with an average error of 84.34 metres in 3D and 35.00 metres in the horizontal location fix. Fig. 4.2 represents the relation between the total RSTD error, calculated as the sum of the absolute values of the error for the RSTD measurement from each neighbour, and the average position error in metres.

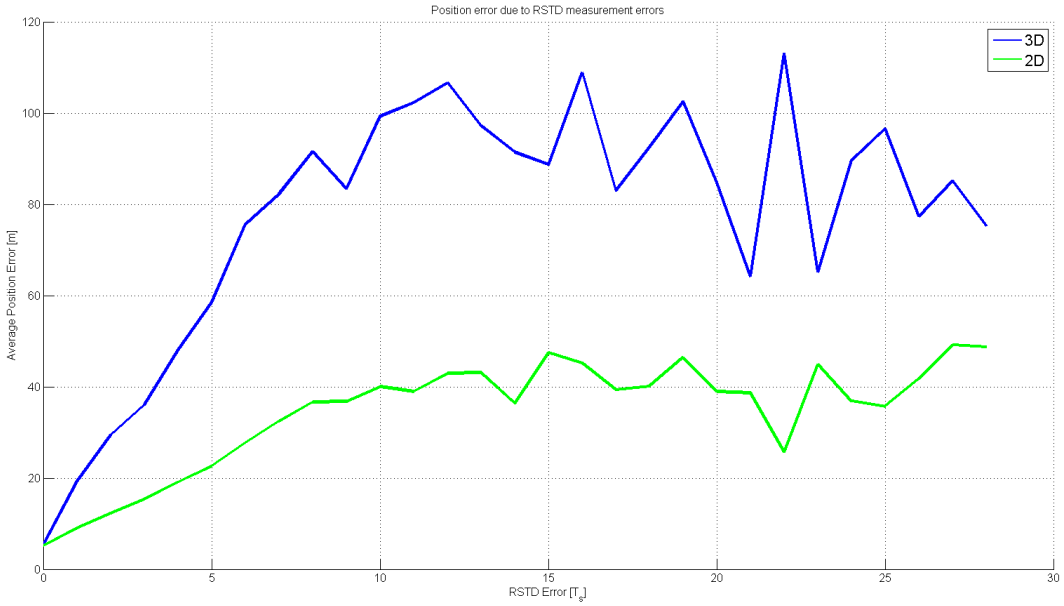

Figure 4.2: Evolution of the calculated position error with respect to the total RSTD error for Scn 1.

As expected, the calculated position is more accurate the more accurate are the RSTD measurements, especially with measurement errors close to 0. If the measurements differ from the real RSTD values in more than 10 T_s units in total, the graphic stops the monotonous growing and starts oscillating. However, this graph is taking the absolute value of the error in the RSTD measurements without considering the direction. If the measurement errors from different base stations are opposite in sign, the uncertainty increases, but the errors will partially compensate each other, having less impact in the position calculation. This explains the oscillations seen in the graph.

B. Analysis of results for Scenario 2

In Scenario 2, the 3D algorithm has been less successful, not converging to a position in 58.2% of the cases. The three dimensional position error had a minimum value of

more than 55 meters and an average of over 860 meters. The maximum position error goes to more than 8 Km. All these results are aligned with the theory: the poor GDOP value of scenario 2 makes this base station geometry bad to calculate 3D positions. On the other hand, the HDOP value was optimal for the calculation of horizontal fixes, and the algorithm has converged in every of the runs. The average 2D error was 27.72 metres, with a minimum value of 1.04 m. Fig. 4.3 represents the relation between the total RSTD error and the average position error for this base station geometry.

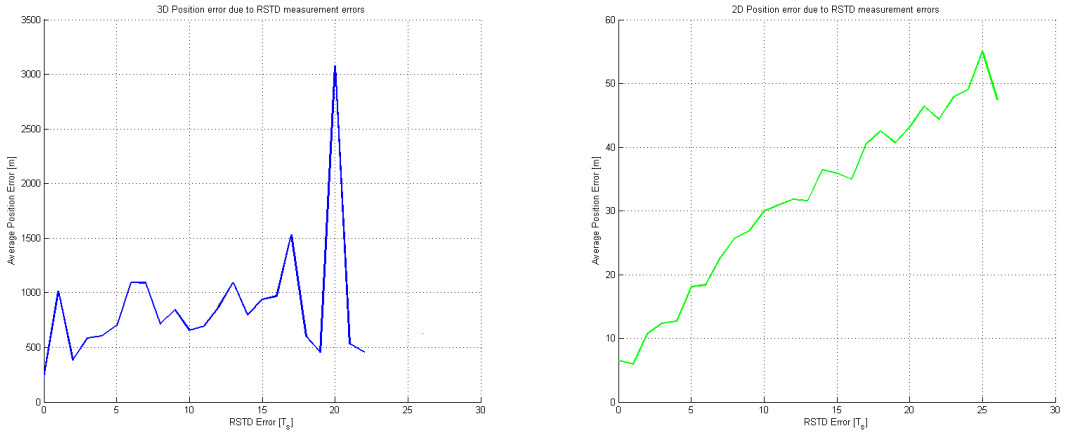

Figure 4.3: Evolution of the calculated position error with respect to the total RSTD error for Scn 2.

In the three dimensional calculation, the error is always large and there does not seem to be much of a correlation between measurement error and calculated position error. However, the 2D algorithm shows a pronounced proportional relation between the RSTD error and the final position calculated.

C. Analysis of results for Scenario 3

Base station constellation 3 was designed with slightly bad HDOP value and really high GDOP. It converges to a 3D fix only in 29.9 % of the simulations and even then the average position error is above 129 metres. The conversion rate improves to 63.7 % for 2D computation, but the mean value of the error is still of 93 metres. However, it has returned acceptable positions (under 30 meters error) if the RSTD measurements were within a range of $\pm 2T_s$ of the real RSTD (see Fig. 4.4).

From these results it can be seen that in sub-optimal geometries a position can still be calculated if the other sources of error are below a certain limit. In other words,

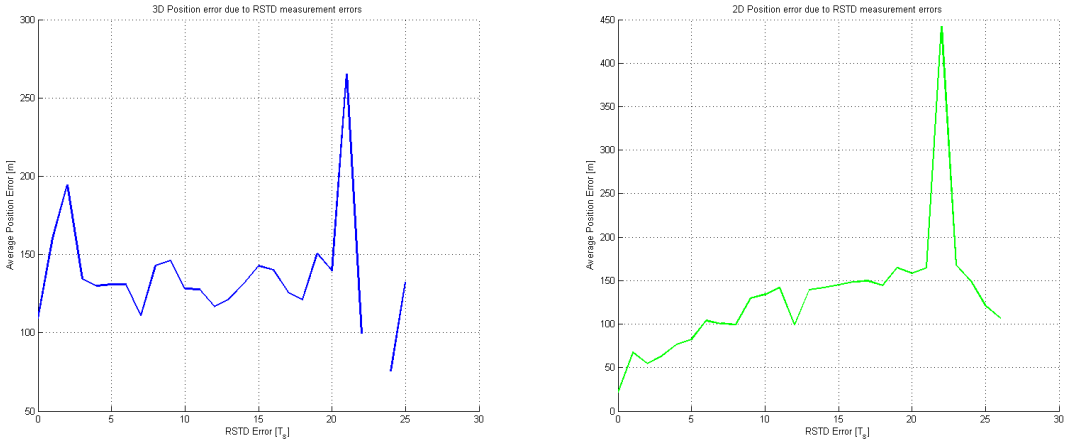

Figure 4.4: Evolution of the calculated position error with respect to the total RSTD error for Scn 3.

base station constellations with bad DOP values are more sensitive to noise, multipath, interferences and other sources of error.

D. Analysis of results for Scenario 4

The last of the scenarios under test has converge to a solution 99.9 % of the times, which might give the false impression that the performance is better than scenario 2 or 3. Nevertheless, it must be noticed that the errors in both 3D and 2D computed positions are really large. This scenario is useless for meeting the position accuracy requirements of the FCC. Completely neglecting the altitude coordinate and using the 2D algorithm has rendered a few good results in some of the simulations but the average error is still over 187 meters.

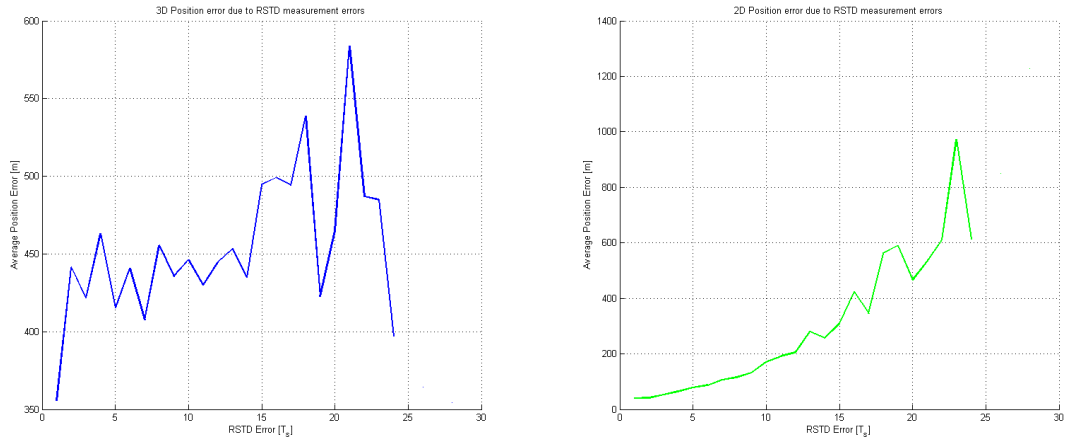

Figure 4.5: Evolution of the calculated position error with respect to the total RSTD error for Scn 4.

4.1.4 Relation between the calculated position error and the RSTD uncertainty

The previous section has assumed an RSTD measurement uncertainty of $\sigma^2 = 5T_s$, as the one assumed by some important players in the mobile communications' sector [15]. This section will show the influence of this uncertainty on the position calculation. For that, new simulations will be executed, changing the RSTD variance from 0 T_s to 10 T_s and calculating 2D positions in Base Stations' constellation 2 and 3D positions in Base Stations' constellation 1. In each of the steps, 1000 independent samples will be generated.

The average positioning error against the RSTD measurement uncertainty is depicted in Fig. 4.6 and Fig. 4.7, for 2D and 3D locations, respectively.

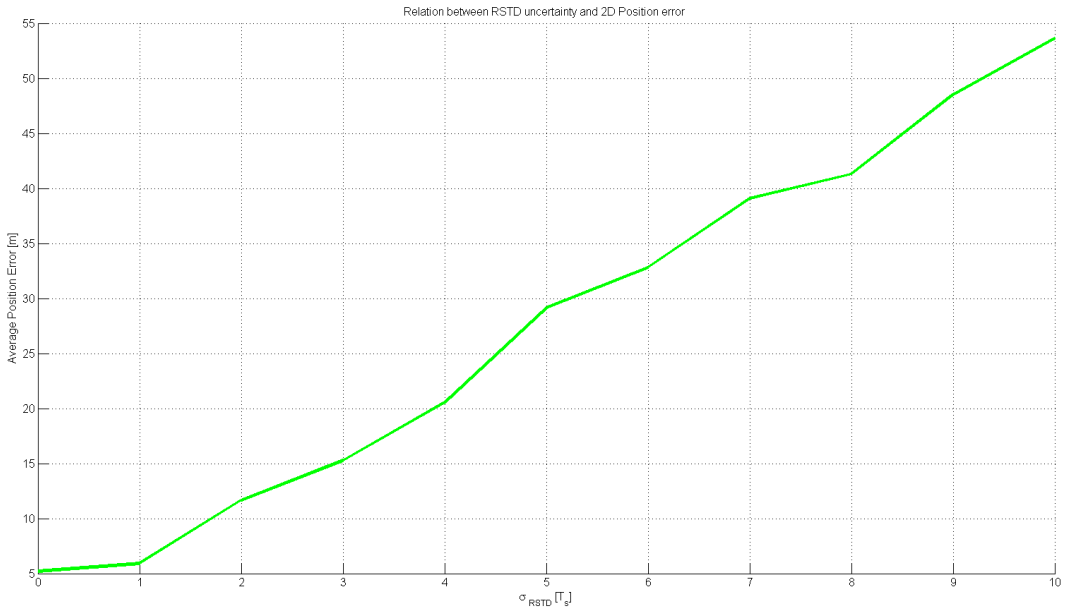

Figure 4.6: 2D Positioning error against RSTD measurement variance.

It can be appreciated that the relation between the RSTD measurement uncertainty and the position error is quite linear and directly proportional. Keeping the RSTD measurements under a certain uncertainty will play an important role in reaching the FCC's position accuracy requirements.

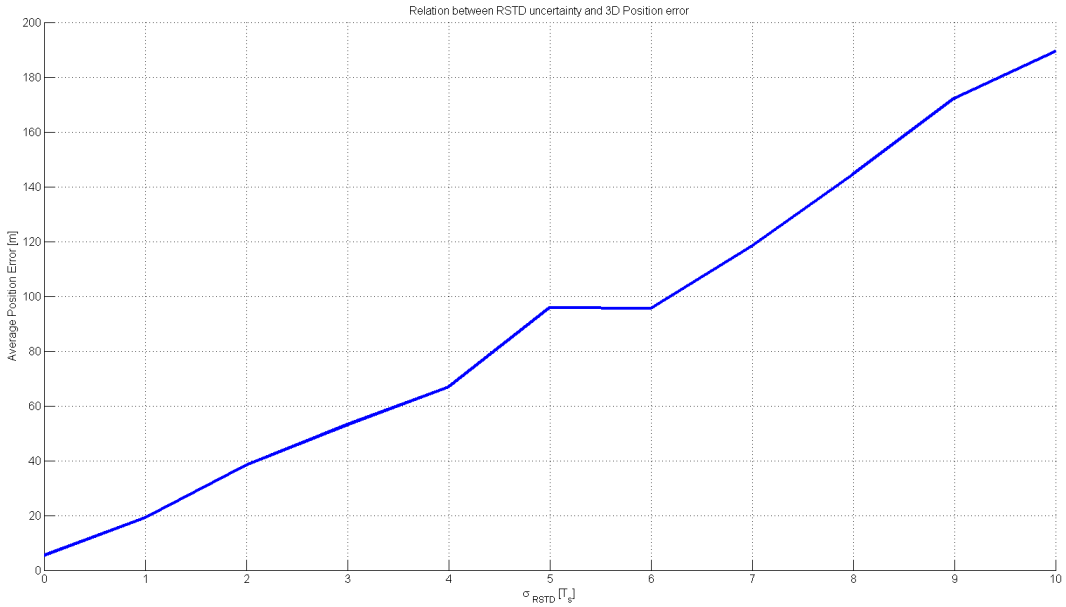

Figure 4.7: 3D Positioning error against RSTD measurement variance.

4.1.5 Analysis of base station's asynchronism

In the next, a detailed analysis of the effects of synchronization errors in the base station transmitters will be performed. Base stations constellation 1 will be used for the 3D measurements and Base stations constellation 2 will be used for the 2D measurements.

A. One base station is out of sync

For this simulation, one of the base stations will have a synchronization problem. The error will be simulated with the values (in nanoseconds): [-200, -100, -50, -25, 0, 25, 50, 100, 200]. For each of the asynchrony values, the scenario under test will be executed with RSTD uncertainty of [0, 3, 5, 10] T_s. A thousand independent measurements will be performed for each configuration.

The results for the three dimensional scenario are shown in Fig. 4.8. The average three dimensional positioning error is kept under 100 meters if the base station synchronization error is ≤ 100 ns and the RSTD variance is $\leq 5T_s$.

Fig. 4.9 shows the results for the 2D algorithm. If the synchronization of the base station is better than 100 ns and the RSTD uncertainty is $\leq 5T_s$, the average positioning error in this scenario is kept below 35 metres. Reaching a better synchronization

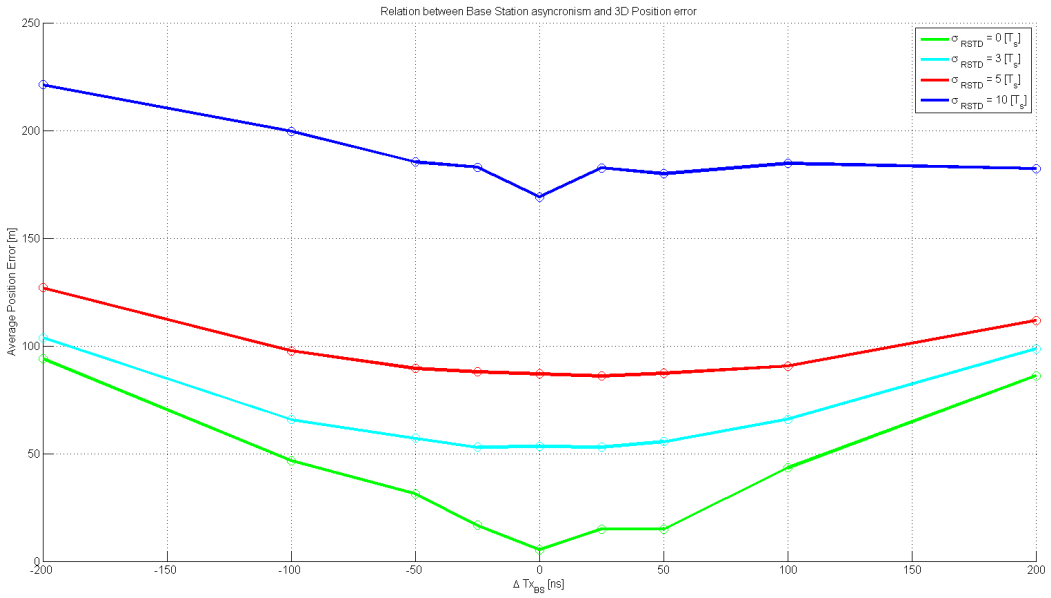

Figure 4.8: 3D Positioning error against base station synchronization error.

(±50 ns) reduces the impact of the base station asynchronism in the final result, as the average errors remain quite stable in all the interval [-50, 50] ns.

B. All base stations are out of sync

In the previous section, only one of the base stations was out of sync. However, a more realistic scenario is that where all base stations are slightly out of sync. Carrying out such a simulation trying to consider all possible scenarios would result in a huge number of different combinations and it will not much valuable information. Instead of that, this section will depict the worst case scenario, where the reference base station has a synchronization error of opposite sign to all neighbour cells. Under such conditions, the synchronization error of all base stations will add: a sync error of 50 ns will contribute to an error in the RSTD measurement of 100 ns.

The results of the simulation are depicted in Fig. 4.10 and Fig. 4.11, for 3D and 2D scenarios, respectively. Although the results will vary depending on each specific scenario and UE location, a general criteria that can be extracted from these simulations is that the base station synchronization should be kept within $\pm 50ns$ in order to obtain accurate OTDOA positioning.

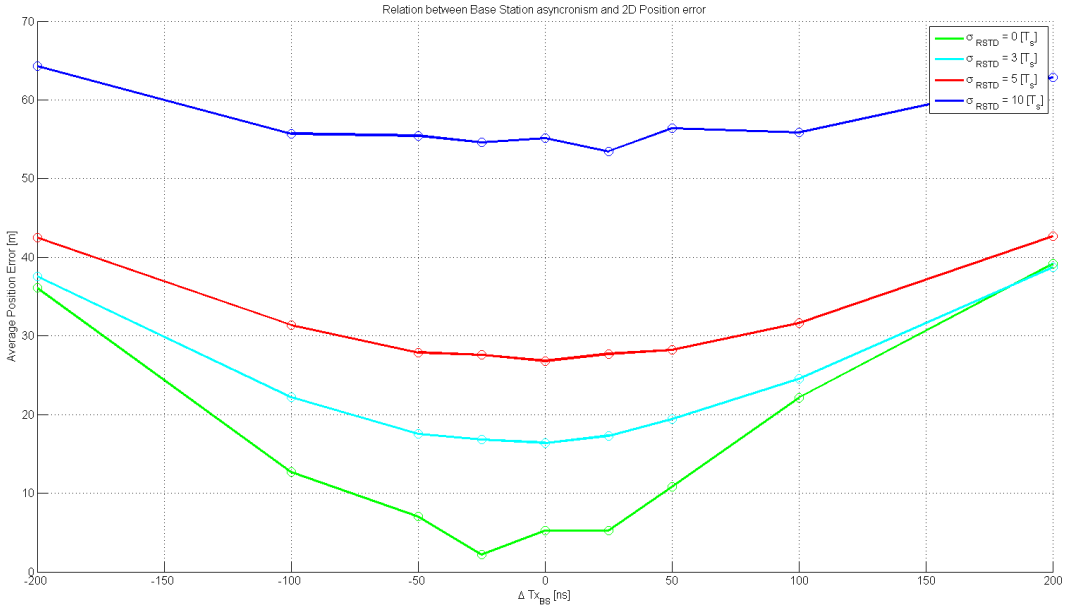

Figure 4.9: 2D Positioning error against base station synchronization error.

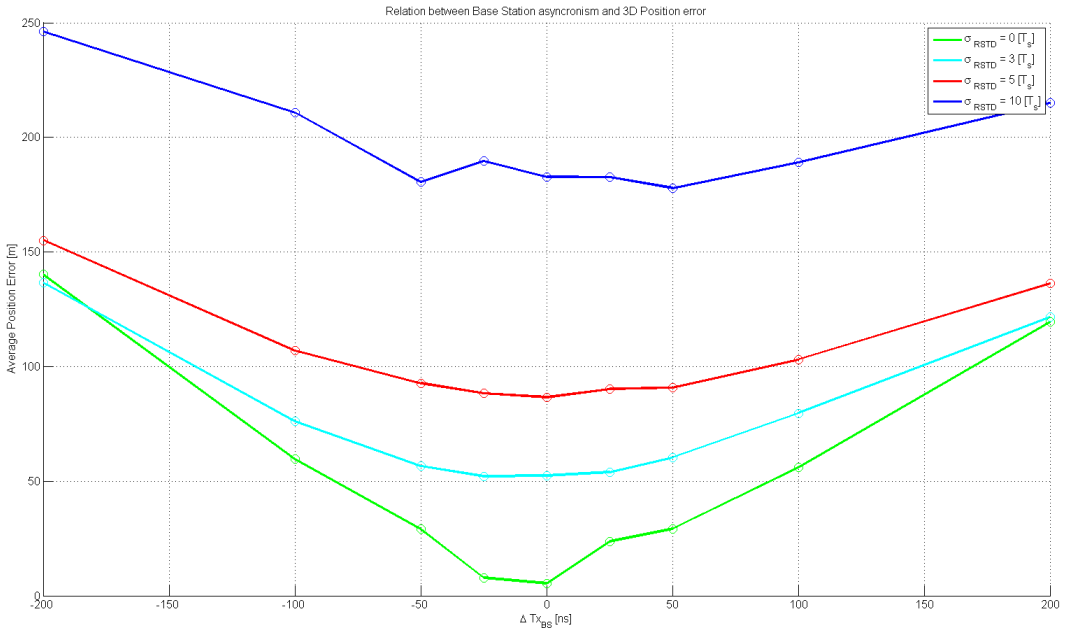

Figure 4.10: 3D Positioning error against base stations' synchronization error.

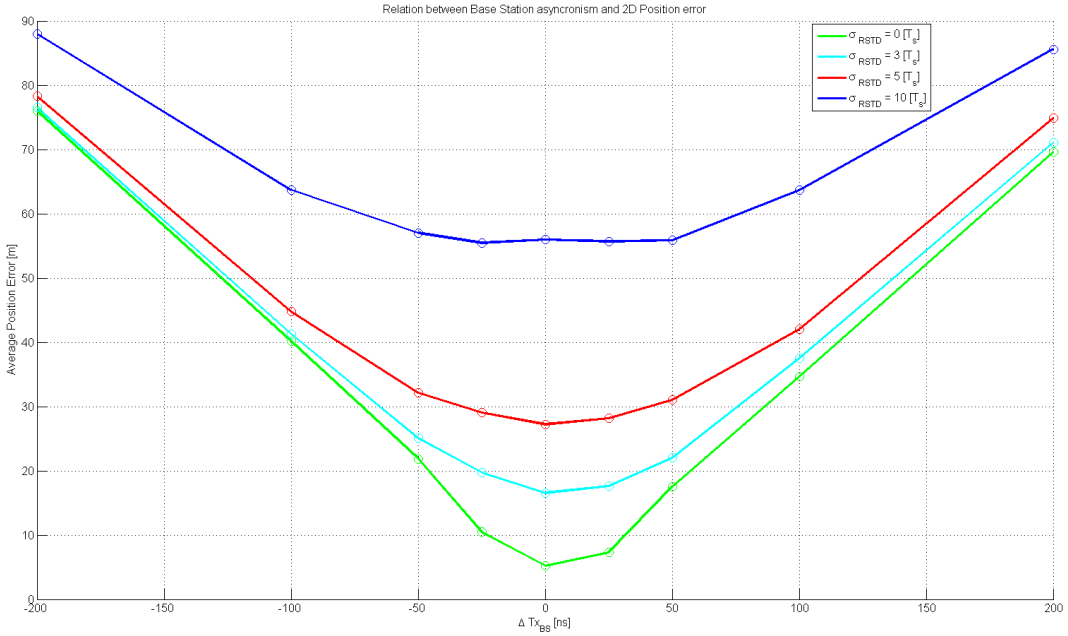

Figure 4.11: 2D Positioning error against base stations' synchronization error.

4.1.6 Analysis of Base Stations coordinates error

Another source of error for OTDOA positioning are the errors in the base station coordinates. As it has been mentioned in Section 3.1.3.B., the coordinates of the transmitter antennas are a key element of the localization algorithm and they need to be accurately known in order to calculate the mobile device's position.

However, in real-life cases the coordinates of the base station antenna are unknown or not accurate. The coordinates of the base stations are normally known, but they might be calculate on the Earth surface and not on the transmitter antenna. Furthermore, it is possible that a base station has more than one transmitter antenna and the algorithm does not know which one of them has transmitted the signal received by the mobile device.

In this section, the effect of an error in the antenna coordinates is analysed. In order to perform the simulation, the position calculation is performed applying an error of [-20, -10, -5, -2.5, 0, 2.5, 5, 10, 20] metres in East, North and Up coordinates for each of the four base stations of the Constellation 1 in turns. For each of the errors, 1000 measurements are simulated with RSTD variances of [0, 3, 5, 10] T_s. The results are depicted in Fig. 4.12 to Fig. 4.15.

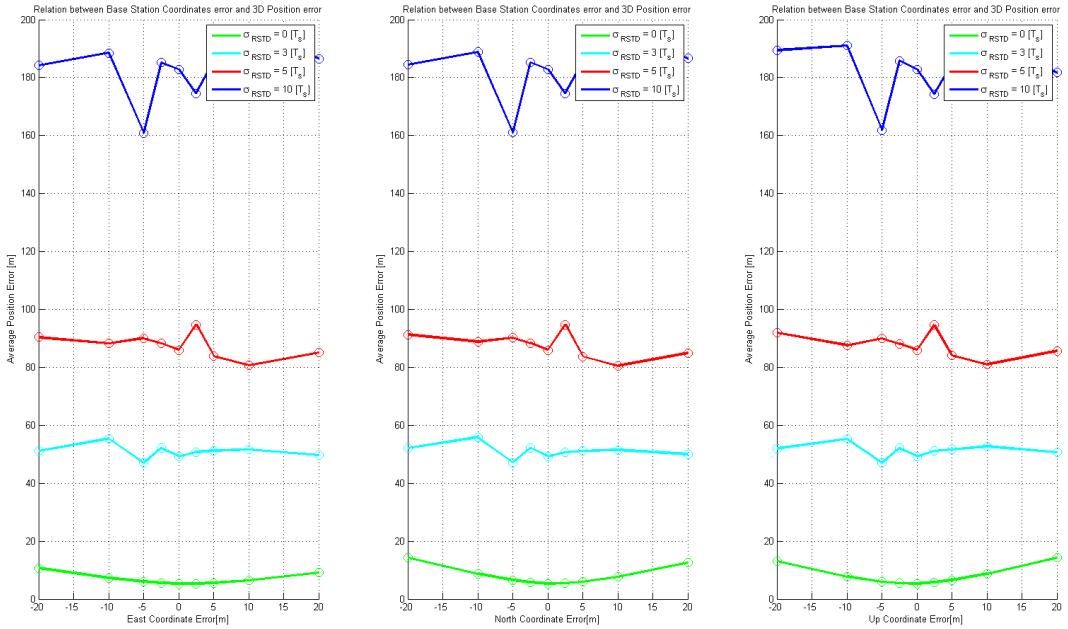

Figure 4.12: 3D Positioning error against base stations' antenna coordinates error for BS1.

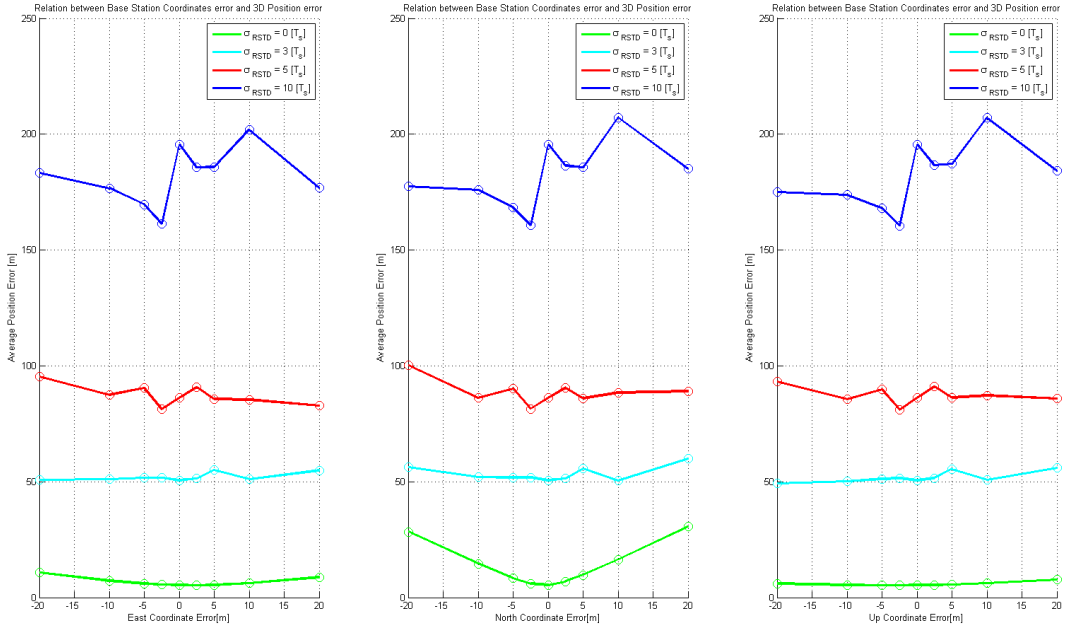

Figure 4.13: 3D Positioning error against base stations' antenna coordinates error for BS2.

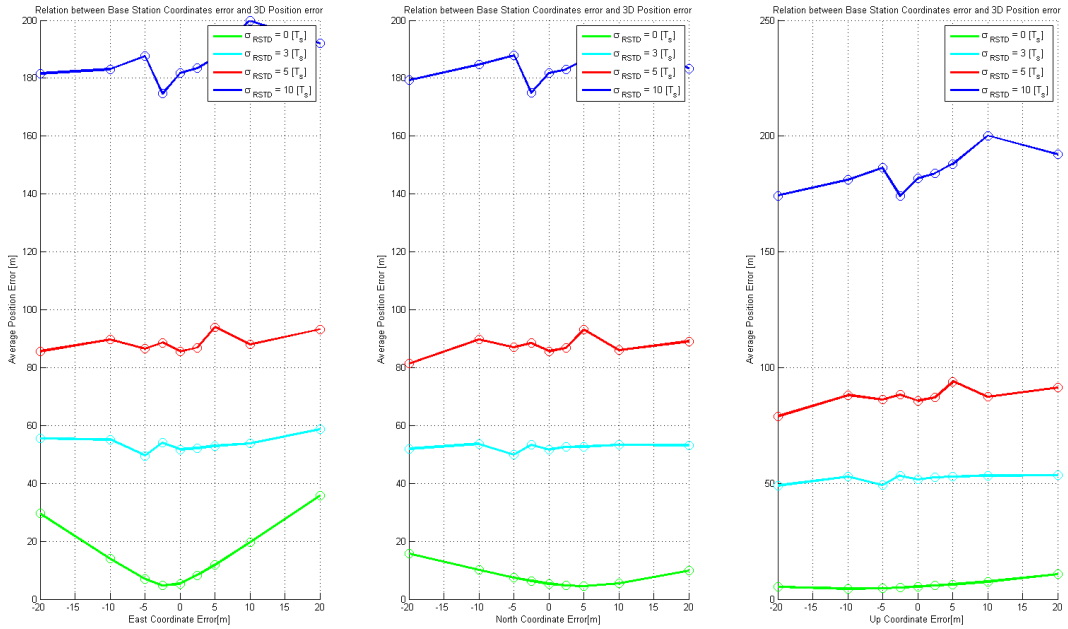

Figure 4.14: 3D Positioning error against base stations' antenna coordinates error for BS3.

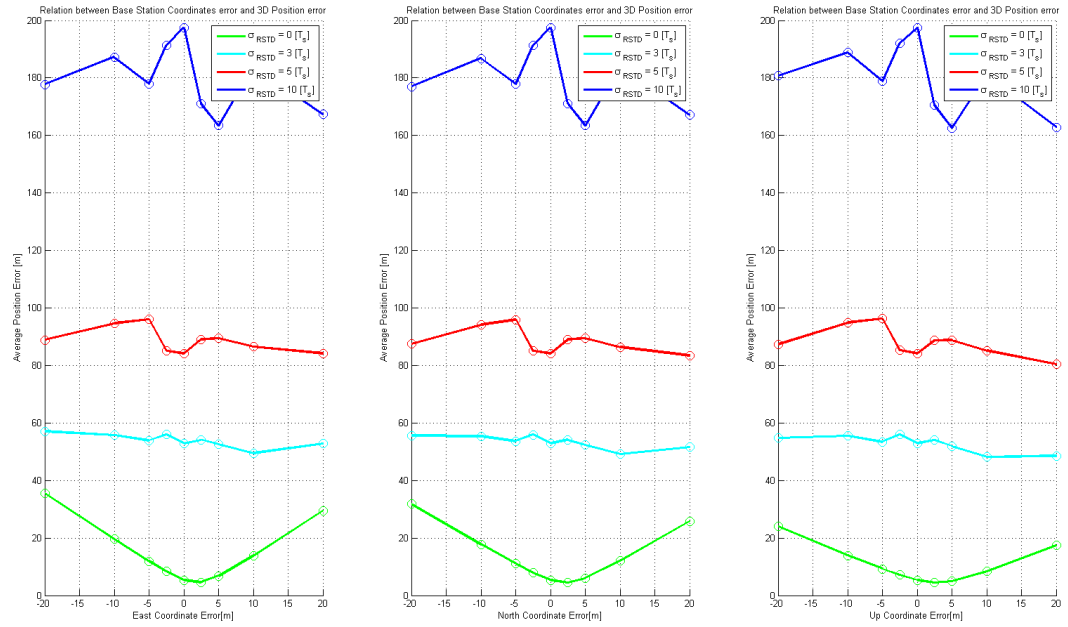

Figure 4.15: 3D Positioning error against base stations' antenna coordinates error for BS4.

As it can be seen from the results, there is no clear pattern on how the antenna coordinate errors will affect the final calculated position. It depends on a number of factors: the mobile device position; the base station affected; the relative position

between the base station affected, the reference cell and the mobile device, etc. The effect is more critical with more accurate RSTD measurements. If the base station transmitter whose location is not accurately is the reference cell, the error partially cancels out. Nevertheless, the number of unknown factors make impossible to predict how will an error in the antenna coordinates affect in a real-life scenario. However, it is safe to assume from the results that if the antenna location is known to an accuracy of $\pm$ 5 metres, the error in the calculated position induced by the error in the coordinates will still fulfil the FCC accuracy requirements.

4.1.7 Performance of OTDOA positioning with random mobile device locations

Throughout the previous sections, some of the error sources that might affect OTDOA positioning for LBS have been analysed individually. For that analysis, the mobile device has always been kept at a fixed location in order to make the results comparable and reproducible. After that analysis, a range of acceptable values for each error source has been proposed.

This section will apply the conclusions found so far to study the performance of the position calculation algorithm if the mobile device is at a random location. A thousand different random locations have been generated with the following assumptions:

- The mobile device can be at any point within the area formed by the base stations. If the mobile device was outside the area formed by the base stations, it would more likely measure other base stations closer in distance which would form a new constellation.
- The East and North coordinates of the mobile device position are samples from the uniform distribution between 0 and 1000 $\sim U[0, 1000]$.
- The Up coordinate is formed by samples taken from the normal distribution of mean 0 and standard deviation 5 metres $\sim \mathcal{N}(0, 5)$.

A. Results for the 3D scenario

The three dimensional position have been calculated with the base stations of Scenario 1. The results are depicted in Fig. 4.16. The image on the left shows the average position error for 1000 random mobile locations against the base station synchronization error and for different variances of the error in the RSTD measurement. The image of the right shows a closer zoom to the most interesting area.

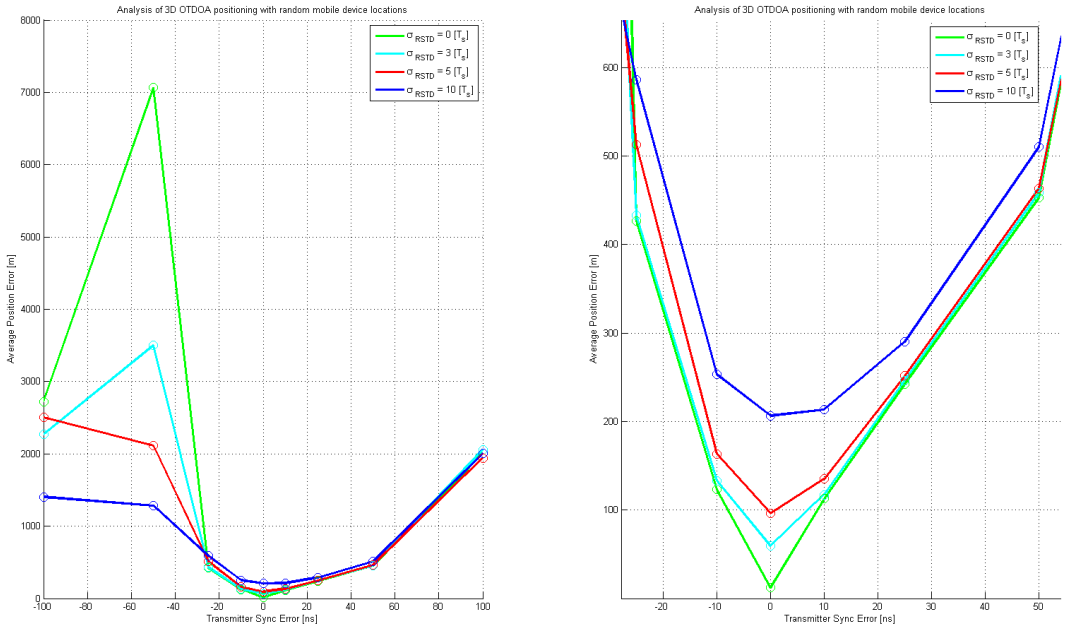

Figure 4.16: Performance of the 3D OTDOA positioning algorithm with random mobile locations.

In order to obtain an average position accuracy below 100 metres in all possible locations within the area formed by the base stations' constellation, the transmitter synchronization needs to be better than 10 nanoseconds and the RSTD measurements better than $\pm 5T_s$. Detailed information of the results for each step are written in Tab. 4.7 to Tab. 4.10. The cases where the algorithm has not been able to find a position after 2000 iterations have been discarded to calculate the maximum, minimum and average errors. However, they have been taken into account for the success % calculations.

$\mathbf{E}_{Sync}[ns]$	$\Delta E_{RSTD} = 0[T_s]$					
	Errors [m]			[%] Positions under		
	E_{avr}	E_{max}	E_{min}	$<$ 100 m Error	$<$ 300 m Error	$<$ 500 m Error
-100	2719.6	16556.4	845.4	0	0	0
-50	7063.4	99186.6	267.9	0	2.3	15.5
-25	426.5	2719.1	115.6	0	33.7	55.9
-10	123.3	461.5	39.2	38.8	93.5	94.0
0	12.4	74.9	1.1	99.8	99.8	99.8
10	112.6	208.6	46.9	41.5	99.9	99.9
25	242.3	417.3	112.3	0	77.7	100
50	452.9	792.9	220.2	0	14.8	64.0
100	2004.8	40551.2	756.7	0	0	0

Table 4.7: OTDOA Positioning 3D: Algorithm performance with random mobile locations 1.

$\mathbf{E}_{Sync}[ns]$	$\Delta E_{RSTD} = 3[T_s]$					
	Errors [m]			[%] Positions under		
	E_{avr}	E_{max}	E_{min}	$<$ 100 m Error	$<$ 300 m Error	$<$ 500 m Error
-100	2268.3	16979.4	695.4	0	0	0
-50	3502.3	83958.6	198.0	0	4.0	16.2
-25	432.8	2284.6	87.7	1.3	35.1	55.0
-10	133.3	527.4	9.0	42.5	88.6	93.1
0	59.5	266.6	2.4	85.0	97.8	97.8
10	117.3	286.8	14.6	45.5	99.6	99.6
25	246.6	494.4	86.7	1.7	72.4	100
50	458.3	953.9	197.9	0	14.7	61.3
100	2052.2	41207.2	431.2	0	0	0.2

Table 4.8: OTDOA Positioning 3D: Algorithm performance with random mobile locations 2.

$\mathbf{E}_{Sync}[ns]$	$\Delta E_{RSTD} = 5[T_s]$					
	Errors [m]			[%] Positions under		
	E_{avr}	E_{max}	E_{min}	$<$ 100 m Error	$<$ 300 m Error	$<$ 500 m Error
-100	2505.9	14078.8	500.1	0	0	0
-50	2111.5	28402.6	162.7	0	4.7	14.3
-25	512.5	16405.5	65.1	3.5	36.0	53.4
-10	163.5	1465.8	5.5	37.0	82.3	89.8
0	96.4	854.8	3.7	59.3	95.3	96.1
10	134.9	369.6	12.2	36.3	97.1	99.0
25	251.5	561.5	61.6	2.3	69.6	98.9
50	463.6	1274.4	174.9	0	16.3	60.9
100	1943.5	50458.1	411.2	0	0	0.5

Table 4.9: OTDOA Positioning 3D: Algorithm performance with random mobile locations 3

$\mathbf{E}_{Sync}[ns]$	$\Delta E_{RSTD} = 10[T_s]$					
	Errors [m]			[%] Positions under		
	E_{avr}	E_{max}	E_{min}	$<$ 100 m Error	$<$ 300 m Error	$<$ 500 m Error
-100	1404.3	10073.1	0396.1	0	0	0.5
-50	1284.1	25835.4	118.7	0	9.6	17.8
-25	586.4	12511.5	7.9	6.6	39.7	52.7
-10	253.5	5332.3	10.5	19.5	69.6	80.1
0	206.6	1416.5	12.2	22.3	75.3	86.6
10	213.5	1828.50	20.0	19.2	74.8	93.2
25	290.1	973.5	8.9	5.6	57.7	88.6
50	510.4	1742.6	127.8	0	16.4	55.4
100	2005.6	39509.1	353.5	0	0	3.9

Table 4.10: OTDOA Positioning 3D: Algorithm performance with random mobile locations 4

Some very valuable information can be extracted from these tables. First of all, if the network and the mobile device performances are taken from the OTDOA error budget proposed in [15] (i.e. base station synchronization error of $\pm 50ns$ and mobile device RSTD measurement error of $\pm 5T_s$), the 3D positioning calculation will converge to 100 metres or better in **0 %** of the occasions. That is far from the FCC requirement of a position with an accuracy of 50 metres in 80 % of the emergency calls. Secondly, even improving the network and the mobile to reach 10 ns base station synchronization and 3 T_s RSTD error, the calculated position will be within a 100 metres radius of the real position $\sim$ 45% of the times. A position of 50 metres accuracy in those conditions is reached with only around 10 % probability. Hence, it has been proven that OTDOA standalone **cannot** fulfil the FCC requirements, at least for three dimensional positioning.

B. Results for the 2D scenario

After concluding that 3D OTDOA positioning is not reliable enough to achieve the FCC goals, the next step is to verify if at least 2D OTDOA positioning can be used to obtain accurate horizontal positions for the E911 calls. The same simulation has been performed, but calculating 2-Dimensional locations and with the base stations of Scenario 2. The average error against the base station synchronization error is shown in Fig. 4.17.

The results are detailed in Tab. 4.11 to Tab. 4.14.

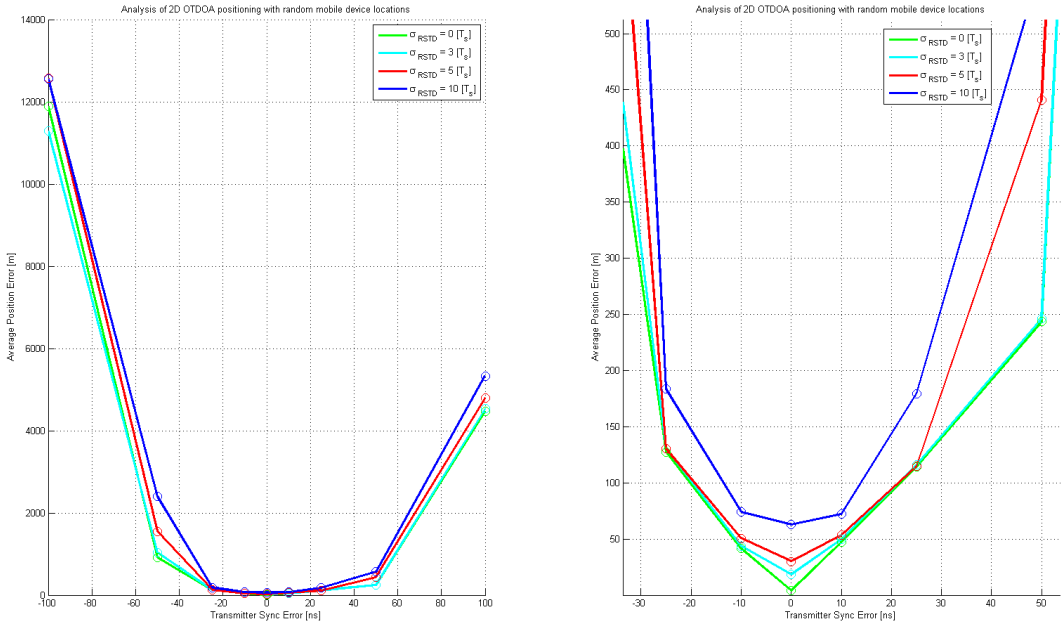

Figure 4.17: Performance of the 2D OTDOA positioning algorithm with random mobile locations.

$\mathbf{E}_{Sync}[ns]$	$\Delta E_{RSTD} = 0[T_s]$					
	Errors [m]			[%] Positions under		
	E_{avr}	E_{max}	E_{min}	$<$ 50 m Error	$<$ 100 m Error	$<$ 500 m Error
-100	11884.5	99438.2	339.6	0	0	44.8
-50	912.2	80283.5	165.8	0	0	85.6
-25	127.7	850.5	81.6	0	33.7	95.8
-10	41.6	223.7	28.9	88.6	99.1	99.5
0	4.1	8.9	0.5	99.8	99.8	99.8
10	47.2	82.2	35.2	73.2	99.8	99.8
25	114.2	453.1	86.9	0	14.9	99.5
50	243.6	1789.8	170.5	0	0	95.3
100	4469.8	99564.3	349.8	0	0	65.9

Table 4.11: OTDOA Positioning 2D: Algorithm performance with random mobile locations 1.

$\mathbf{E}_{Sync}[ns]$	$\Delta E_{RSTD} = 3[T_s]$					
	Errors [m]			[%] Positions under		
	E_{avr}	E_{max}	E_{min}	$<$ 50 m Error	$<$ 100 m Error	$<$ 500 m Error
-100	11285.7	97843.2	332.5	0	0	44.6
-50	1027.2	88240.1	147.9	0	0	85.8
-25	130.6	1019.6	62.6	0	38.0	95.7
-10	43.7	252.3	4.0	68.8	98.6	99.5
0	18.3	118.3	0.9	99.6	99.6	99.8
10	49.6	102.6	11.6	52.5	99.7	99.8
25	116.1	846.7	66.6	0	26.7	99.3
50	246.5	2361.4	152.1	0	0	95.3
100	4532.1	94363.1	323.4	0	0	67.0

Table 4.12: OTDOA Positioning 2D: Algorithm performance with random mobile locations 2.

$\mathbf{E}_{Sync}[ns]$	$\Delta E_{RSTD} = 5[T_s]$					
	Errors [m]			[%] Positions under		
	E_{avr}	E_{max}	E_{min}	$<$ 50 m Error	$<$ 100 m Error	$<$ 500 m Error
-100	12568.1	98920.5	309.6	0	0	44.5
-50	1554.3	86491.2	129.3	0	0	84.3
-25	130.3	1606.5	42.0	0.4	38.5	95.7
-10	50.7	590.2	0.8	54.4	96.2	99.5
0	29.9	103.6	1.7	91.3	99.5	99.6
10	53.3	335.6	3.2	47.3	95.9	99.7
25	114.9	427.2	51.3	0	32.7	99.4
50	441.1	93722.7	137.3	0	0	95.1
100	4795.3	98558.7	323.3	0	0	64.1

Table 4.13: OTDOA Positioning 2D: Algorithm performance with random mobile locations 3.

$\mathbf{E}_{Sync}[ns]$	$\Delta E_{RSTD} = 10[T_s]$					
	Errors [m]			[%] Positions under		
	E_{avr}	E_{max}	E_{min}	$<$ 50 m Error	$<$ 100 m Error	$<$ 500 m Error
-100	12551.1	99937.5	291.3	0	0	44.7
-50	2398.5	97095.7	91.0	0	0.6	83.9
-25	183.7	12442.1	5.7	7.4	36.7	94.7
-10	74.3	714.5	2.7	31.4	78.9	98.7
0	63.2	558.1	2.6	37.7	88.9	98.8
10	72.2	1032.4	1.3	33.2	78.8	99.4
25	179.6	47567.7	6.8	5.1	36.7	98.7
50	564.5	74117.8	82.9	0	0.3	95.4
100	5332.8	98189.7	285.2	0	0	59.7

Table 4.14: OTDOA Positioning 2D: Algorithm performance with random mobile locations 4.

The performance of the positioning algorithm has significantly improved with respect to the 3D case. However, with the values proposed in [15], the algorithm will still not reach the accuracy of 50 metres in any occasion. In fact, calculated positions with accuracy 50 metres or better can only be achieved with base station synchronization of 10 nanoseconds or better. Under such conditions, the algorithm will calculate locations with $<$ 50 m error in $\sim$ 50 % of the occasions if $\Delta E_{RSTD} = 5T_s$ and $\sim$ 60-65 % of the occasions if $\Delta E_{RSTD} = 3T_s$. These values still do not meet the 80 % requirement of the FCC. However, they meet the initial 50 % transitory requirement [3, 4]. Hence, OTDOA can be used to temporarily achieve the FCC E911 accuracy until a better system like LBS-Hybrid can be deployed.

The reason why OTDOA does not meet the requirements in this simulation is that the mobile is randomly placed at any point within the area formed by the base station's constellation. OTDOA performs optimally when the HDOP value is $<$ 1. However, the base station constellation used for this example has a HDOP value that goes from $\sim$ 0.5 to $\sim$ 2, as it has been shown in Fig. 3.4. This example used the *Four Base Stations Square* constellation.

4.1.8 Performance of the algorithm for different base stations' geometries

In this section the same 1000 random mobile device positions will be tested in different constellations deploying all the different geometries seen in Fig. 3.4, reproduced here again for convenience. The results will be compared to verify if the network planning can be adapted to enhance OTDOA performance.

A. Three base stations

Three base stations forming an equilateral triangle. The HDOP values in the area under analysis variate from $\sim$ 0.5 to $\sim$ 3. The average error is shown in Fig. 4.19 and the simulation results are summarized in Tab. 4.15.

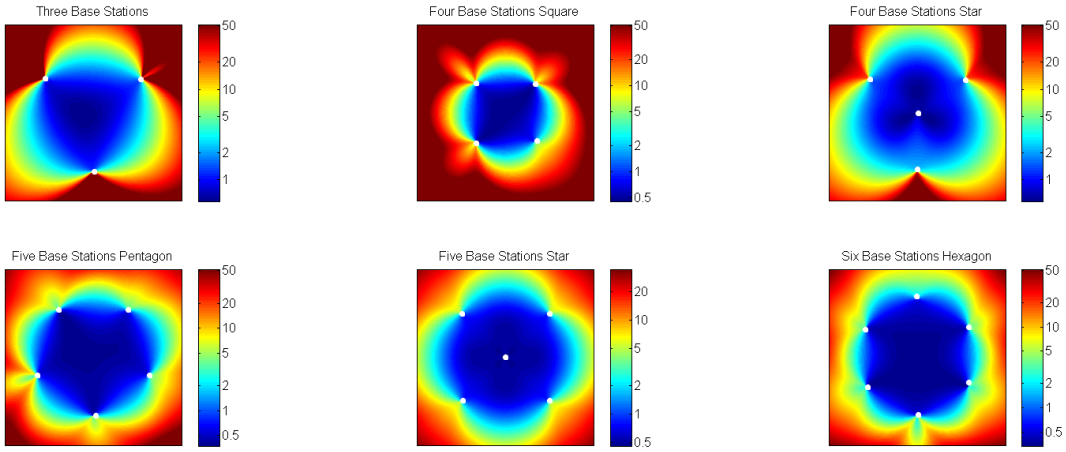

Figure 4.18: Comparison of the DOP values for different base station constellations

$\Delta E_{RSTD}[T_s]$	[%]$\mathbf{E}_P <$	$\mathbf{E}_{Sync}[ns]$								
		-100	**-50**	**-25**	**-10**	**0**	**10**	**25**	**50**	**100**
0	**< 50 m**	0	0	0	53.3	93.9	31.1	0	0	0
	< 100 m	0	0	16.2	85.0	94.4	85.3	10.5	0	0
	< 300 m	0	59.0	81.6	93.1	94.4	94.0	89.3	53.6	0
	< 500 m	28.0	68.4	87.6	93.1	94.8	94.4	91.2	78.4	29.2
3	**< 50 m**	0	0	0	44.1	84.6	32.9	0	0	0
	< 100 m	0	0	17.4	83.2	92.2	80.5	14.8	0	0
	< 300 m	0	57.9	80.9	92.5	93.0	92.8	88.4	53.8	0
	< 500 m	28.1	67.9	88.2	92.6	93.0	93.3	90.4	78.1	29.2
5	**< 50 m**	0	0	0.6	40.8	65.1	29.7	0	0	0
	< 100 m	0	0	23.8	78.3	87.1	73.5	19.3	0	0
	< 300 m	0	56.0	81.2	91.1	91.3	91.6	85.3	53.1	0
	< 500 m	27.7	68.3	85.5	92.0	91.6	92.0	89.1	78.5	29.0
10	**< 50 m**	0	0	6.4	21.3	22.3	18.7	3.6	0	0
	< 100 m	0	0.2	26.7	56.9	62.8	54.0	22.8	0.4	0
	< 300 m	0.4	53.4	78.4	87.9	89.6	88.8	78.7	51.5	0.5
	< 500 m	27.8	67.5	84.0	89.6	90.2	90.3	86.6	73.3	29.7

Table 4.15: OTDOA Positioning 2D: Algorithm performance with three base stations.

As it can be seen, the average errors are much higher here. The % of occasions where the position has been calculated with a certain accuracy is as well lower as for the previous example with four base stations. These results are expected: the number of base stations has been decreased, which means there is one measurement less available, and the base station constellation shows worse HDOP interval in the area under consideration, reaching to ~ 3 in some points. This constellation is not a good choice for a high performance OTDOA network.

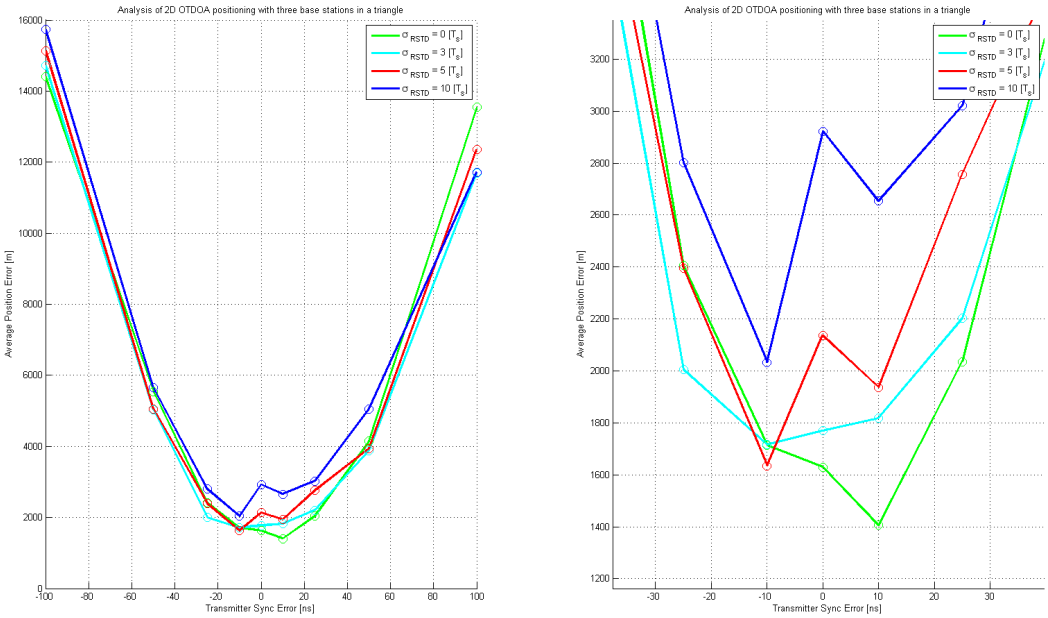

Figure 4.19: Performance of the 2D OTDOA positioning algorithm for three base stations.

B. Four Base Stations in a square

This has been the constellation used in the previous example, whose results are already detailed in Tab. 4.11 to Tab. 4.11.

C. Four Base Stations in a star

Another possibility to deploy four base stations is to form an equilateral triangle with a base station in the centre, what will resemble a star-shape. The HDOP values for this constellation oscillate from ~ 0.5 to ~ 2.5. The average error is shown in Fig. 4.20 and the simulation results are summarized in Tab. 4.16.

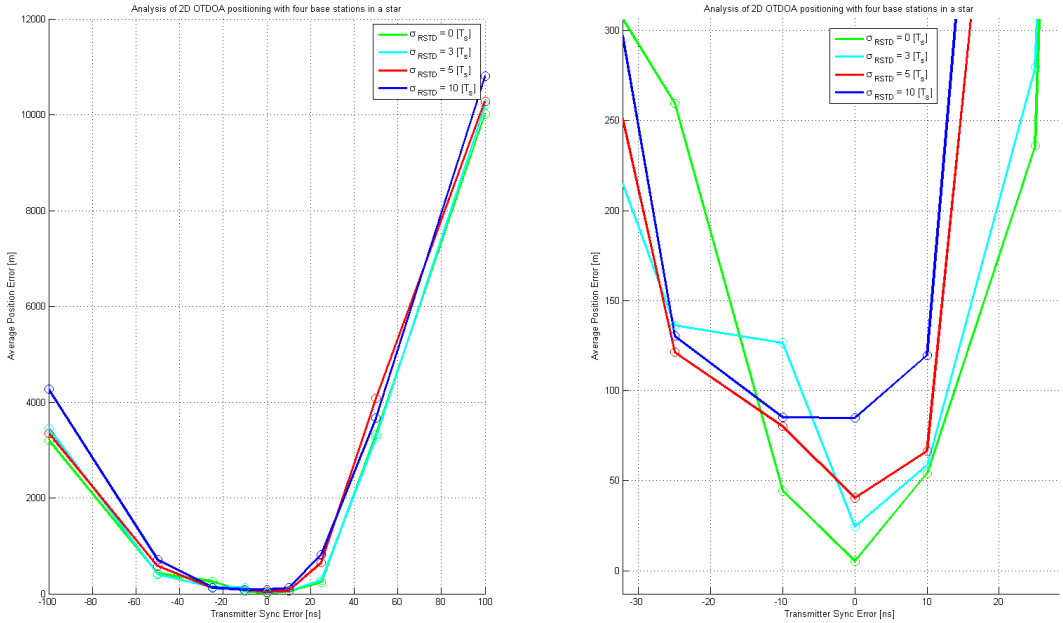

Figure 4.20: Performance of the 2D OTDOA positioning algorithm for four base stations forming a star.

$\Delta E_{RSTD}[T_s]$	[%]$\mathbf{E}_P <$	$\mathbf{E}_{Sync}[ns]$								
		-100	**-50**	**-25**	**-10**	**0**	**10**	**25**	**50**	**100**
0	**< 50 m**	0	0	0	74.7	99.9	48.3	0	0	0
	< 100 m	0	0	30.2	99.5	99.9	96.7	19.8	0	0
	< 300 m	0	82.2	99.4	99.5	99.9	99.5	93.0	68.7	0
	< 500 m	52.7	97.0	99.4	99.5	99.9	99.5	97.4	80.0	42.6
3	**< 50 m**	0	0	0	58.7	94.4	44.0	0	0	0
	< 100 m	0	0	31.0	96.6	99.7	92.2	21.2	0	0
	< 300 m	0	79.4	98.9	99.4	99.9	99.2	93.6	68.3	0
	< 500 m	51.4	96.1	98.9	99.4	99.9	99.3	96.6	80.3	42.7
5	**< 50 m**	0	0	1.5	45.1	74.5	38.0	0	0	0
	< 100 m	0	0	32.1	91.7	96.5	85.9	26.9	0	0
	< 300 m	0.1	80.3	98.7	99.6	99.8	99.2	92.0	66.4	0
	< 500 m	52.1	96.4	98.7	99.6	99.8	99.4	94.7	80.6	42.5
10	**< 50 m**	0	0	8.6	25.9	26.7	21.9	5.9	0	0
	< 100 m	0	0.5	34.7	66.9	72.3	60.4	28.5	0.5	0
	< 300 m	1.8	75.7	97.7	99.3	97.8	96.6	87.4	63.2	0.8
	< 500 m	51.2	93.0	98.9	99.6	98.3	98.3	93.5	78.9	39.3

Table 4.16: OTDOA Positioning 2D: Algorithm performance with four base stations forming a star.

This constellation offers better results than the one with three base stations, both in average error and in percentage of calculated positions under a certain threshold limit. However, the performance is around 10 % worse than the performance of the

four base stations forming a square. This can be explained by looking at the HDOP distribution in Fig. 4.18. This constellation presents very good HDOP values in some areas around the centre of the triangle. However, the overall HDOP in the area under consideration is slightly higher than for the square-shaped scenario.

D. Five base stations forming a pentagon

The next proposed scenario contains five base stations distributed along a regular pentagon. The HDOP values for this constellation oscillate from $\sim$ 0.5 to $\sim$ 1.8. The average error is shown in Fig. 4.21 and the simulation results are summarized in Tab. 4.17.

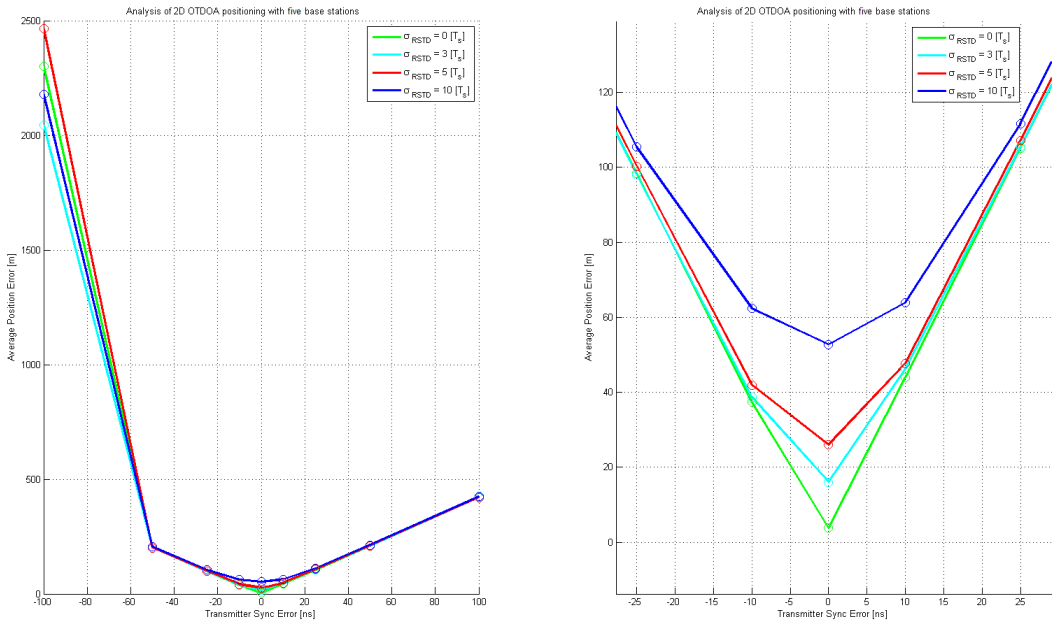

Figure 4.21: Performance of the 2D OTDOA positioning algorithm for five base stations forming a pentagon.

$\Delta E_{RSTD}[T_s]$	[%]$\mathbf{E}_P <$	$\mathbf{E}_{Sync}[ns]$								
		-100	**-50**	**-25**	**-10**	**0**	**10**	**25**	**50**	**100**
0	**< 50 m**	0	0	0	100	99.9	99.3	0	0	0
	< 100 m	0	0	67.8	100	99.9	99.9	17.8	0	0
	< 300 m	0	99.8	99.7	100	99.9	99.9	99.9	99.6	0
	< 500 m	88.2	99.8	99.7	100	99.9	99.9	99.9	99.6	92.5
3	**< 50 m**	0	0	0	80.3	99.8	59.0	0	0	0
	< 100 m	0	0	56.4	99.7	99.8	99.8	36.3	0	0
	< 300 m	0	99.7	99.7	99.7	99.8	99.8	99.6	99.7	0
	< 500 m	88.3	99.7	99.7	99.7	99.8	99.8	99.6	99.8	92.6
5	**< 50 m**	0	0	0.4	65.5	96.1	55.1	0	0	0
	< 100 m	0	0	51.9	99.8	99.7	99.5	39.1	0	0
	< 300 m	0	99.8	99.9	99.9	99.7	99.7	99.8	99.1	0
	< 500 m	87.1	99.9	99.9	99.9	99.7	99.7	99.8	99.5	92.5
10	**< 50 m**	0	0	9.5	39.9	47.3	37.2	6.4	0	0
	< 100 m	0	0.2	46.8	85.8	96.0	83.7	41.4	0.1	0
	< 300 m	0.3	97.2	99.8	99.8	99.2	99.6	99.3	97.1	0.3
	< 500 m	83.9	99.8	99.8	99.8	99.2	99.6	99.3	99.6	87.2

Table 4.17: OTDOA Positioning 2D: Algorithm performance with five base stations forming a pentagon.

This new proposal outstrips all other options seen so far, due to the extra base station which is improving the HDOP value of the constellation and giving an additional measurement to the algorithm. With a base station synchronization error of $\pm 10ns$, around 60% of the calculations will result in a position accuracy of 50 metres of better with $\pm 5T_s$ of measurement error and around 70% for $\pm 3T_s$ of measurement error. Nevertheless, the synchronization error of the base stations cannot still be bigger than 10 ns in order to obtain acceptable results. Up to $\pm 25ns$ of synchronization error, the algorithm can return a position with an accuracy of 100 metres half of the times. A position within half a kilometre radius is achieved in almost every situation.

E. Five Base Stations forming a star

Five base stations can also be distributed forming a square with one extra base station in the centre, resulting in a star-shape. The HDOP values for this constellation oscillate from ~ 0.5 to ~ 1.8. The average error is shown in Fig. 4.22 and the simulation results are summarized in Tab. 4.18.

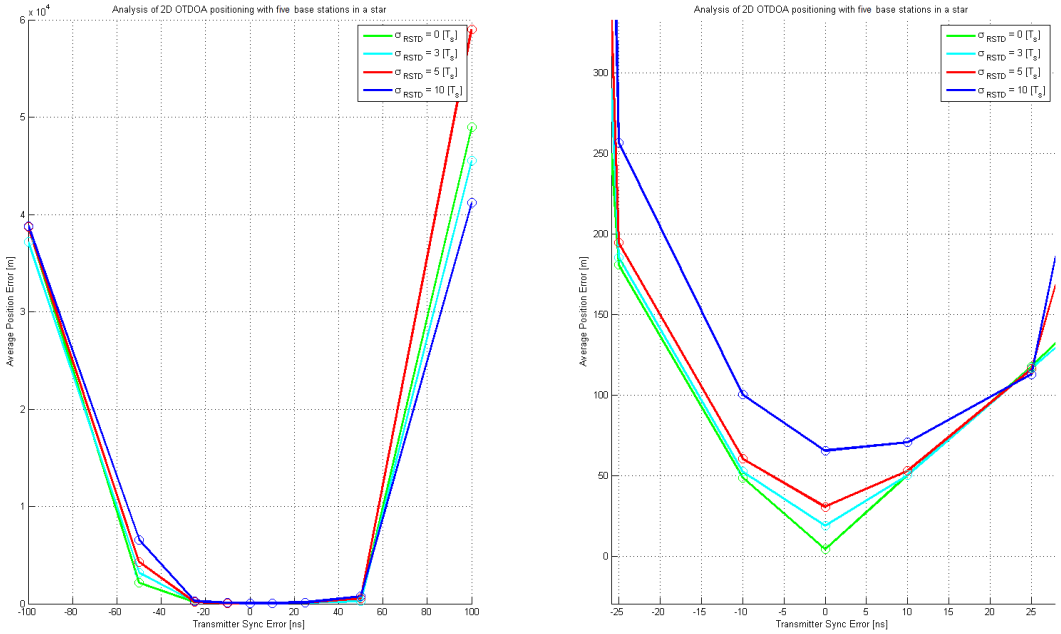

Figure 4.22: Performance of the 2D OTDOA positioning algorithm for five base stations forming a star.

$\Delta E_{RSTD}[T_s]$	[%]$\mathbf{E}_P <$	$\mathbf{E}_{Sync}[ns]$								
		-100	**-50**	**-25**	**-10**	**0**	**10**	**25**	**50**	**100**
0	**< 50 m**	0	0	0	70.0	99.1	56.9	0	0	0
	< 100 m	0	0	12.9	96.7	99.1	95.7	0.6	0	0
	< 300 m	0	36.4	89.7	98.4	99.2	95.7	83.6	12.8	0
	< 500 m	2.3	58.9	90.4	98.4	99.2	95.7	83.6	12.8	1.4
3	**< 50 m**	0	0	0	57.8	99.2	48.6	0	0	0
	< 100 m	0	0	19.4	95.1	99.4	95.4	16.2	0	0
	< 300 m	0	36.2	89.7	98.1	99.4	95.4	83.1	15.0	0
	< 500 m	3.0	59.0	91.0	98.5	99.4	95.4	83.1	15.0	1.5
5	**< 50 m**	0	0	0.2	46.7	89.5	43.2	0.1	0	0
	< 100 m	0	0	23.1	90.1	99.0	92.3	25.8	0	0
	< 300 m	0	35.2	88.4	98.2	99.2	95.6	82.1	17.1	0
	< 500 m	2.2	57.4	91.3	98.9	99.2	95.6	82.1	17.1	1.3
10	**< 50 m**	0	0	7.1	31.1	38.0	32.8	6.7	0	0
	< 100 m	0	0.1	28.3	72.4	84.9	75.6	32.5	0	0
	< 300 m	0	34.9	85.4	96.9	96.8	94.3	77.8	16.5	0
	< 500 m	3.8	58.8	89.1	97.8	97.0	94.4	77.8	18.5	1.6

Table 4.18: OTDOA Positioning 2D: Algorithm performance with five base stations forming a star.

This constellation gives worse results than the regular pentagon. Once again, even though there are some areas close to the centre of the constellation where the HDOP is better and the results are really accurate, the overall HDOP is slightly higher, so

the locations close to the limits of the square formed by the outer four base stations contribute to decrease the average accuracy.

F. Six Base Stations forming a hexagon

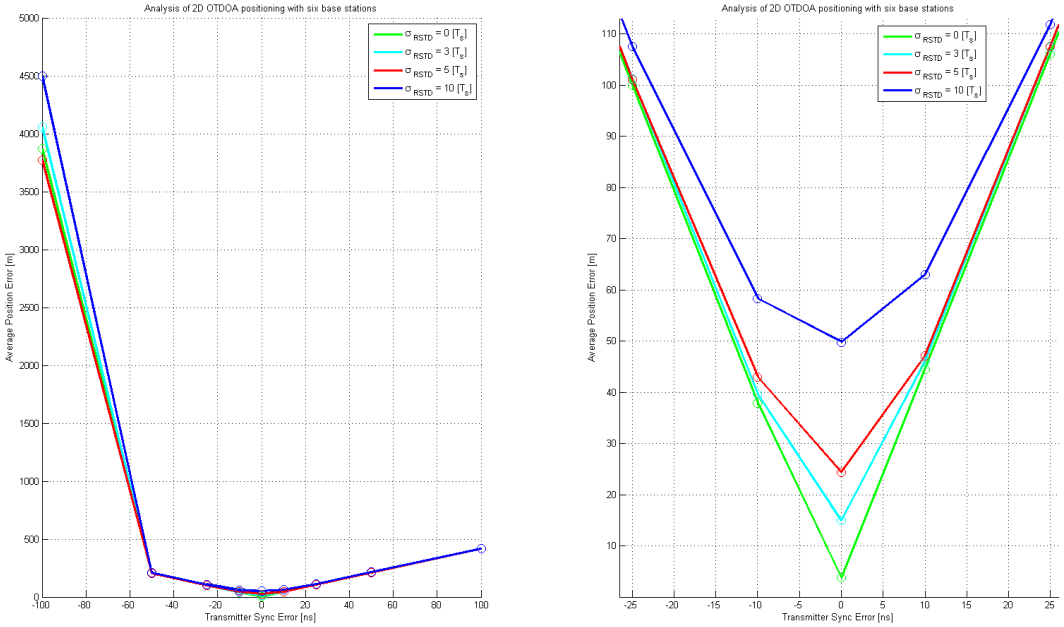

Figure 4.23: Performance of the 2D OTDOA positioning algorithm for six base stations forming a hexagon.

$\Delta E_{RSTD}[T_s]$	[%]$\mathbf{E}_P <$	$\mathbf{E}_{Sync}[ns]$								
		-100	**-50**	**-25**	**-10**	**0**	**10**	**25**	**50**	**100**
0	**< 50 m**	0	0	0	99.9	99.7	96.0	0	0	0
	< 100 m	0	0	61.7	99.9	99.7	99.8	12.2	0	0
	< 300 m	0	97.9	99.2	99.9	99.7	99.8	99.8	99.8	0
	< 500 m	75.4	98.5	99.2	99.9	99.7	99.8	99.8	99.8	99.2
3	**< 50 m**	0	0	0	75.8	99.3	60.6	0	0	0
	< 100 m	0	0	49.9	99.6	99.3	99.8	33.3	0	0
	< 300 m	0	97.6	98.7	99.6	99.3	99.8	99.9	99.5	0
	< 500 m	75.9	98.1	98.7	99.6	99.3	99.8	99.9	99.5	99.0
5	**< 50 m**	0	0	0.2	62.9	98.2	55.6	0	0	0
	< 100 m	0	0	49.5	99.5	99.5	99.7	40.1	0	0
	< 300 m	0	96.9	99.5	99.5	99.5	99.8	99.8	99.8	0
	< 500 m	76.1	98.3	99.5	99.5	99.5	99.8	99.8	99.8	98.3
10	**< 50 m**	0	0	9.1	44.9	51.3	39.5	5.9	0	0
	< 100 m	0	0.2	43.9	87.3	97.4	84.0	41.2	0	0
	< 300 m	0.5	93.4	99.0	98.9	99.2	99.4	99.7	98.1	0.2
	< 500 m	74.2	97.9	99.0	98.9	99.2	99.4	99.7	99.9	93.8

Table 4.19: OTDOA Positioning 2D: Algorithm performance with six base stations forming a hexagon.

This scenario equals the results of the five base stations distributed as a pentagon, reaching similar percentages of convergences under 50 meters error.

G. Seven Base Stations forming a honeycomb

The last scenario that will be showed in this section is formed by seven base stations distributed forming a regular hexagon with one base station in the middle. LTE Cells are often represented as a honeycomb. Hence, this configuration seems natural for OTDOA over LTE.

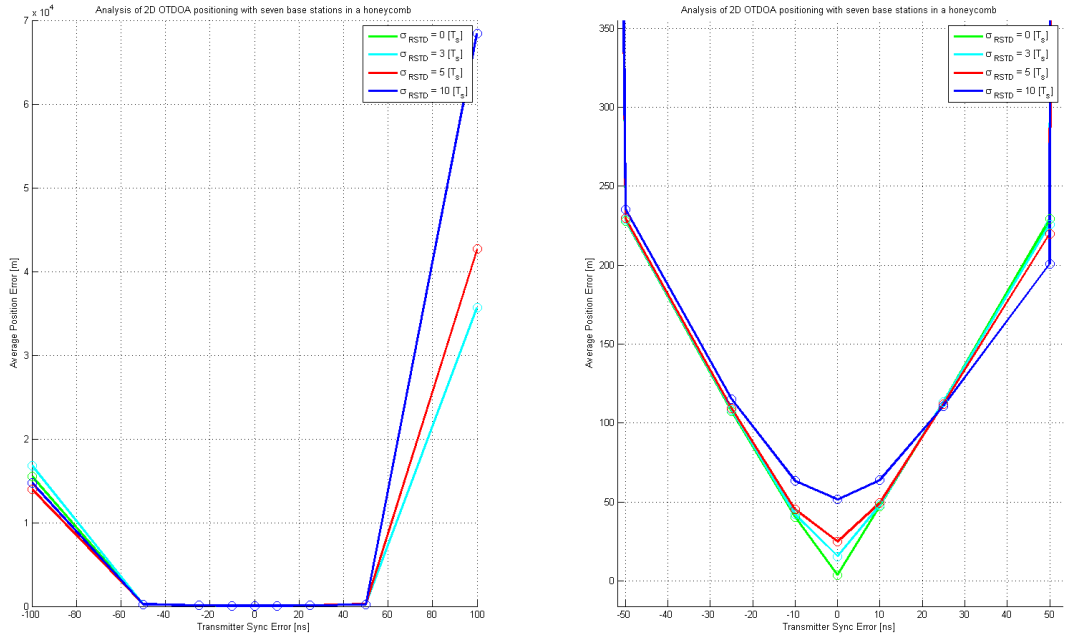

Figure 4.24: Performance of the 2D OTDOA positioning algorithm for seven base stations forming a honeycomb.

$\Delta E_{RSTD}[T_s]$	[%]$\mathbf{E}_P <$	$\mathbf{E}_{Sync}[ns]$								
		-100	**-50**	**-25**	**-10**	**0**	**10**	**25**	**50**	**100**
0	**< 50 m**	0.0	0.0	0.0	99.3	99.5	83.8	0.0	0.0	0.0
	< 100 m	0.0	0.0	10.0	99.4	99.5	96.2	0.0	0.0	0.0
	< 300 m	0.0	89.8	98.4	99.4	99.5	96.2	84.1	32.6	0.0
	< 500 m	32.4	93.5	98.4	99.4	99.5	96.2	84.1	32.6	0.0
3	**< 50 m**	0.0	0.0	0.0	71.5	99.4	59.2	0.0	0.0	0.0
	< 100 m	0.0	0.0	31.7	99.0	99.4	95.6	16.4	0.0	0.0
	< 300 m	0.0	87.6	97.3	99.0	99.4	95.6	84.3	32.5	0.0
	< 500 m	33.5	91.7	97.3	99.0	99.4	95.6	84.3	32.5	0.0
5	**< 50 m**	0.0	0.0	0.0	63.4	95.9	54.7	0.0	0.0	0.0
	< 100 m	0.0	0.0	36.7	98.9	99.3	96.2	29.4	0.0	0.0
	< 300 m	0.0	85.7	96.9	99.3	99.3	96.8	83.4	33.3	0.0
	< 500 m	32.0	90.2	96.9	99.3	99.3	96.8	83.4	33.4	0.0
10	**< 50 m**	0.0	0.0	8.2	39.6	47.4	37.6	6.5	0.0	0.0
	< 100 m	0.0	0.1	40.0	83.4	93.9	78.3	34.5	0.0	0.0
	< 300 m	0.0	79.2	96.7	98.5	96.7	94.1	80.5	32.7	0.0
	< 500 m	32.7	89.7	96.7	98.5	96.7	94.1	80.5	33.5	0.0

Table 4.20: OTDOA Positioning 2D: Algorithm performance with seven base stations forming a honeycomb.

This last configuration shows results similar to the pentagon and hexagon constellations. The convergence percentages from under 50 metres are very similar. However, the convergences under 100, 300 and 500 metres are slightly worse with higher base station sync errors.

4.1.9 Summary of the OTDOA simulation results

Throughout this section, the OTDOA positioning algorithm has been deeply analysed, as well as some of the errors sources that could affect its performance. It has been seen that the 3D algorithm performance is not sufficient to achieve the accuracy and availability requirements of the FCC. However, the 2D algorithm looks promising, if not as a final solution, at least as a transitory solution until LBS Hybrid is completely developed.

During the analysis of the error sources, some maximum error values have been found, in order to achieve the desired performance: the base station synchronization should be guaranteed to $\pm 10ns$ and the RSTD reports from the mobile phone need to have a maximum standard deviation of $5T_s$ with respect to the real RSTD value.

With respect to the base station geometry, it seems that geometries with all base stations distributed in the vertices of a polygon perform better than geometries where a base station is in the middle. Nevertheless, the number of possible geometries is infinite. This section has only proposed a few geometries with regular shapes and under the premise that all base stations have the same range. The reality is much more colourful, especially with macro, micro, pico and femto cell scheme proposed for LTE. An intelligent geometry analysis for DOP should be a core step before deploying any OTDOA network.

In conclusion, the OTDOA 2D algorithm looks as a good proposal for two dimensional positioning after analysis the results in a simulation environment. The percentages and figures obtained here can only been used as reference, because of the limitations of the simulation. For instance, the RSTD error has been simulated as a completely independent process for each RSTD measurement, while measurement errors can have a common component which affects all measurements equally. Hence, these results will be verified in the next chapter using real mobile devices and a Test System from the TS8980 family of Rohde & Schwarz.

4.2 OTDOA and ECID Hybrid Positioning

ECID-only positioning is discarded until the development of the 3GPP LPPe protocol, where RTT measurements are also defined for the neighbour cells and not just for the serving cell. Meanwhile, ECID will only be considered as a complimentary method to provide one extra measurement. This section will incorporate one ECID measurement to all the different scenarios proposed in the OTDOA Positioning simulations in order to check if this additional ECID measurement improves the overall performance of the algorithm.

The RxTx measurements that the mobile device reports for ECID can be affected by measurement errors. For simplicity, this section will assume the same standard deviation for the RSTD and the RxTx measurement errors in T_s. Due to its nature of round-trip time measurement, the RxTx will not be affected by the base station synchronization error.

The seven different constellations used in the previous section will be enhanced with an ECID measurement. The base stations will still be the same, but the DOP

value will change, as the system matrix A_H includes now one more measurement. The new DOP distributions are depicted in Fig. 4.25 for the constellation with 3 to 6 base stations and Fig. 4.26 for the seven base stations distributed in a honeycomb.

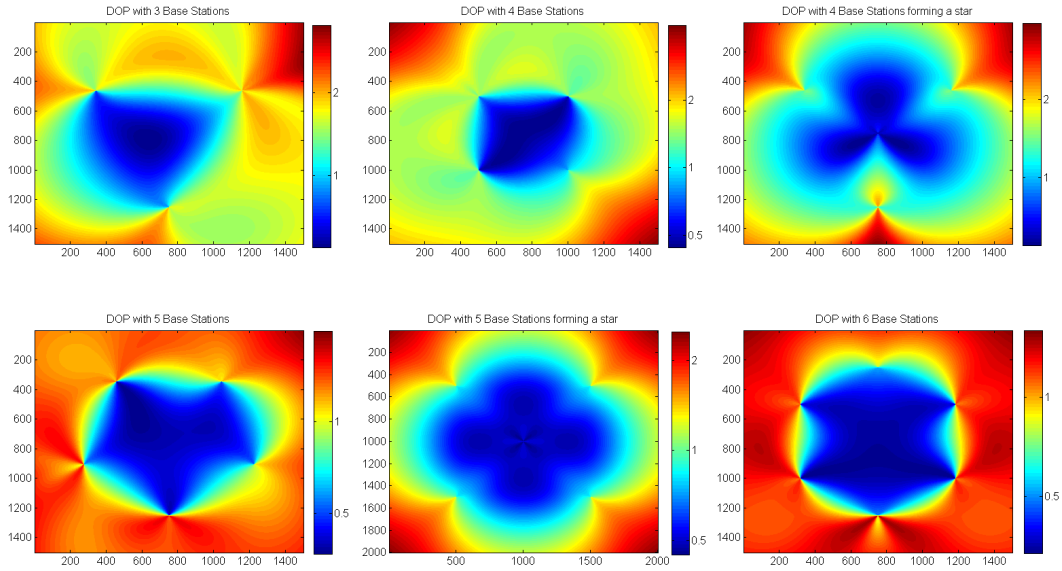

Figure 4.25: DOP of different base station constellations for Hybrid OTDOA + ECID.

The DOP values have improved substantially for all the constellations, being smaller than one in all the positions inside the area formed by the eNBs and lower than 2 in the surroundings. These DOP values should translate in more accurate position results, as this section will try to prove. For that, the same 1000 random mobile device locations will be analysed under the same conditions as in Section 4.1.8.

4.2.1 Performance of the algorithm for different base stations' geometries

New simulations will be run for the seven base station constellations of Section 4.1.8. An ECID measurement will be generated for the serving base station, which is the same as the reference cell for OTDOA. The RxTx will be contaminated for an error in T_s with the same standard deviation as the RSTD error in each loop.

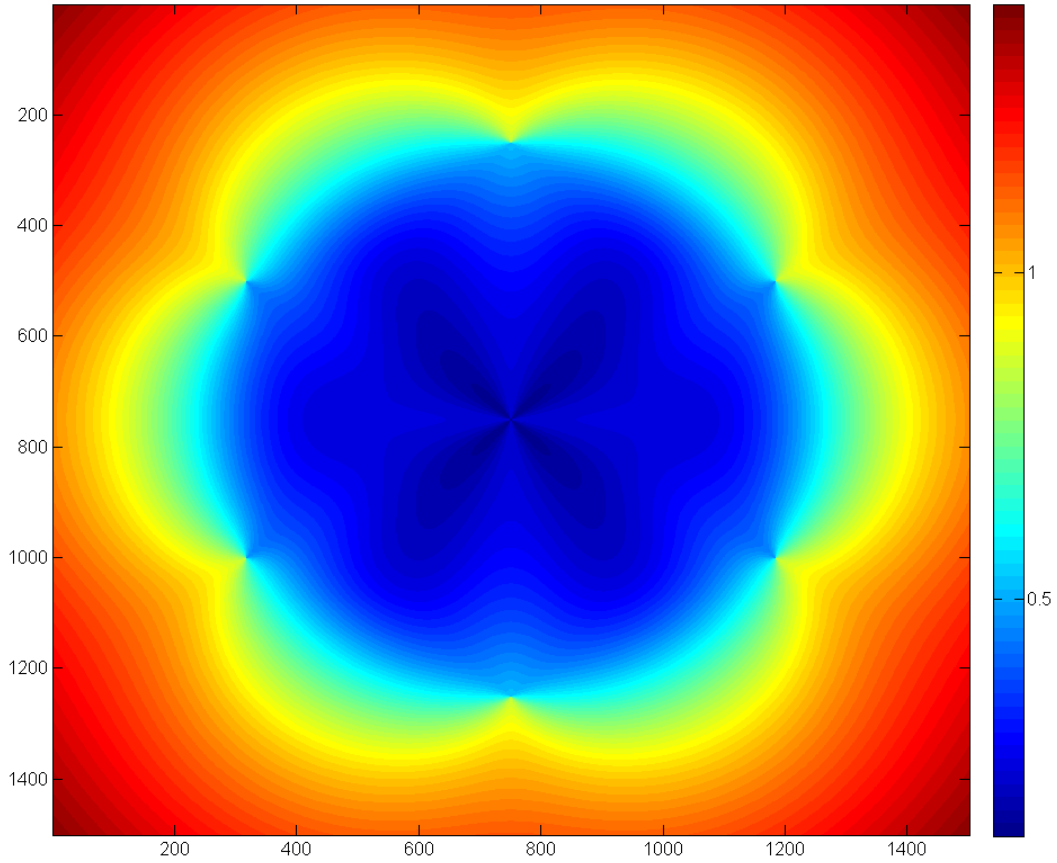

Figure 4.26: DOP of a 7-base stations honeycomb constellation for Hybrid OTDOA + ECID.

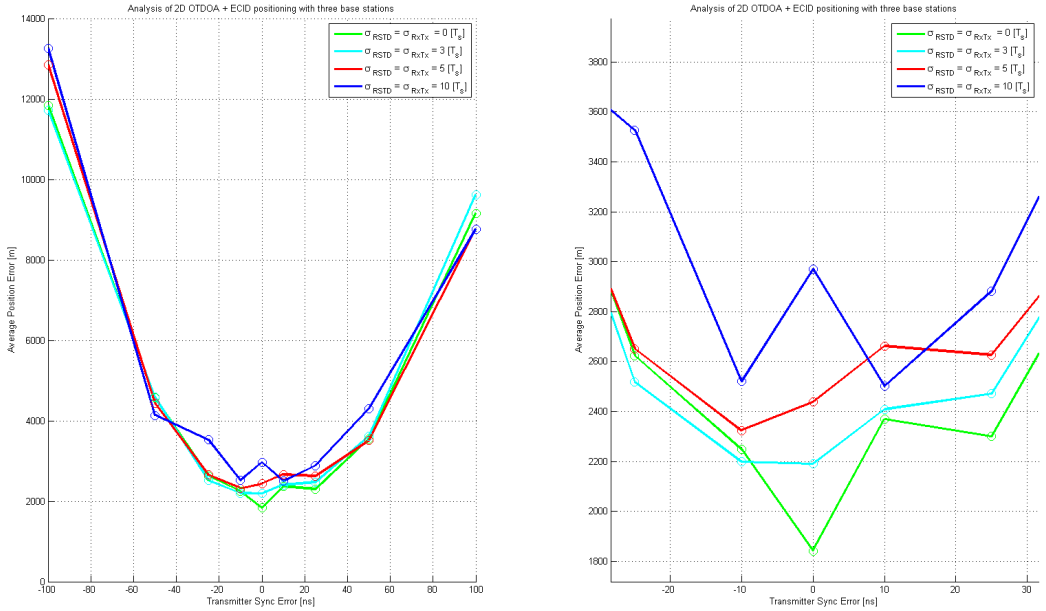

Figure 4.27: Performance of the 2D Hybrid (OTDOA + ECID) positioning algorithm for 3 base stations

A. Three base stations

$\Delta E_{RSTD}[T_s]$	[%]$\mathbf{E}_P <$	$\mathbf{E}_{Sync}[ns]$								
		-100	**-50**	**-25**	**-10**	**0**	**10**	**25**	**50**	**100**
0	**< 50 m**	0.0	0.0	0.0	54.4	91.5	34.4	0.0	0.0	0.0
	< 100 m	0.0	0.0	13.8	84.1	92.4	83.4	9.8	0.0	0.0
	< 300 m	0.0	59.2	82.6	90.7	92.4	91.2	87.9	58.6	0.0
	< 500 m	26.9	69.7	87.9	90.7	92.4	92.0	89.8	79.9	39.0
3	**< 50 m**	0.0	0.0	0.0	50.7	89.7	33.3	0.0	0.0	0.0
	< 100 m	0.0	0.0	16.2	83.1	91.0	82.5	11.0	0.0	0.0
	< 300 m	0.0	59.3	81.9	90.2	91.4	91.1	87.9	58.4	0.0
	< 500 m	27.3	69.8	87.6	90.3	91.4	91.6	89.7	79.9	38.7
5	**< 50 m**	0.0	0.0	0.0	46.0	85.7	35.9	0.0	0.0	0.0
	< 100 m	0.0	0.0	16.1	81.1	90.0	81.2	13.7	0.0	0.0
	< 300 m	0.0	58.5	81.9	89.4	90.8	89.5	87.9	57.7	0.0
	< 500 m	27.3	70.2	87.7	89.5	91.0	90.2	89.1	80.6	39.9
10	**< 50 m**	0.0	0.0	0.4	34.6	64.0	33.7	0.1	0.0	0.0
	< 100 m	0.0	0.0	20.5	76.0	84.9	72.5	18.7	0.0	0.0
	< 300 m	0.0	57.6	81.0	89.2	89.4	88.5	85.7	57.4	0.0
	< 500 m	28.1	70.2	85.2	89.5	89.6	89.2	88.2	79.7	38.1

Table 4.21: Performance of the 2D Hybrid (OTDOA + ECID) positioning algorithm for 3 base stations

The results are shown in Fig. 4.27 and Tab. 4.21. The addition of ECID improves slightly the average position error and the % of convergences. Positions within 50 metres accuracy are obtained with around 5-6 % more probability than with OTDOA only.

B. Four base stations

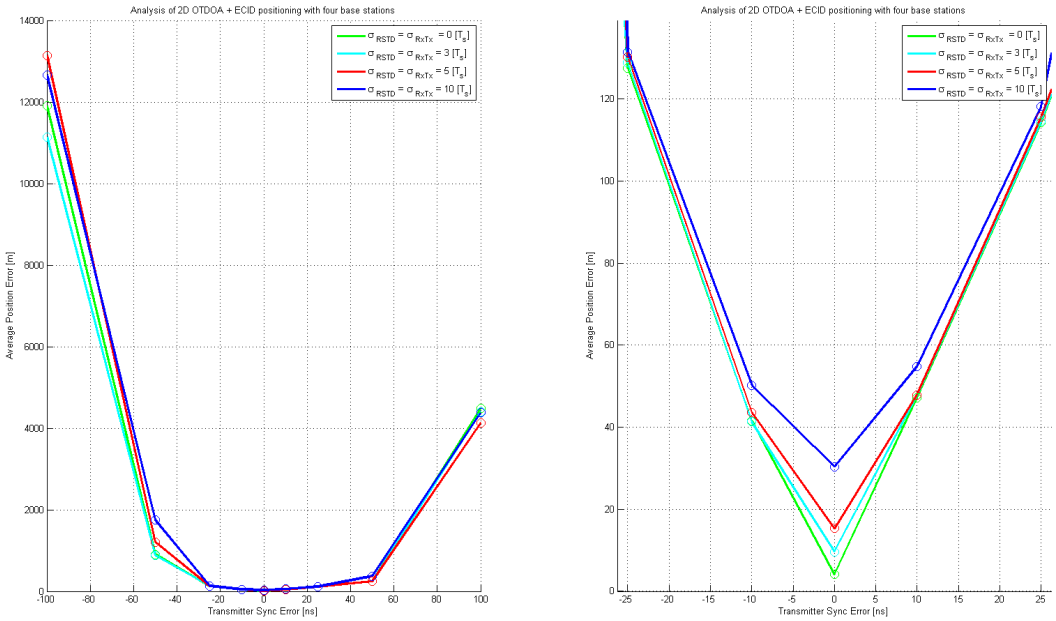

Figure 4.28: Performance of the 2D Hybrid (OTDOA + ECID) positioning algorithm for 4 base stations

$\Delta E_{RSTD}[T_s]$	[%]$\mathbf{E}_P <$	$\mathbf{E}_{Sync}[ns]$								
		-100	**-50**	**-25**	**-10**	**0**	**10**	**25**	**50**	**100**
0	**< 50 m**	0.0	0.0	0.0	92.7	99.7	83.2	0.0	0.0	0.0
	< 100 m	0.0	0.0	40.8	99.3	99.7	99.8	14.9	0.0	0.0
	< 300 m	0.0	74.8	95.3	99.6	99.7	99.8	98.8	93.5	0.0
	< 500 m	44.8	85.6	95.6	99.6	99.7	99.8	99.4	95.4	65.9
3	**< 50 m**	0.0	0.0	0.0	82.2	99.9	61.3	0.0	0.0	0.0
	< 100 m	0.0	0.0	38.9	99.2	99.9	99.8	20.6	0.0	0.0
	< 300 m	0.0	74.4	95.5	99.6	99.9	99.8	99.0	93.5	0.0
	< 500 m	44.7	85.7	95.9	99.6	99.9	99.8	99.5	95.5	66.5
5	**< 50 m**	0.0	0.0	0.0	71.1	99.9	57.8	0.0	0.0	0.0
	< 100 m	0.0	0.0	37.2	98.9	100.0	99.6	24.4	0.0	0.0
	< 300 m	0.0	74.4	95.2	99.7	100.0	99.8	98.8	92.9	0.0
	< 500 m	44.8	85.4	95.5	99.7	100.0	99.8	99.1	95.2	66.1
10	**< 50 m**	0.0	0.0	0.3	55.5	91.3	45.1	0.0	0.0	0.0
	< 100 m	0.0	0.0	37.8	95.2	99.8	96.2	33.3	0.0	0.0
	< 300 m	0.1	73.7	95.4	98.9	100.0	99.6	98.9	91.0	0.0
	< 500 m	44.2	85.0	96.1	99.2	100.0	99.7	99.2	94.6	64.1

Table 4.22: Performance of the 2D Hybrid (OTDOA + ECID) positioning algorithm for 4 base stations

The results are shown in Fig. 4.28 and Tab. 4.22. Here, the improvement is more pronounced: between 10 and 15 % more convergences with respect to OTDOA only and an average of around 70% or 65% with RSTD/RxTx standard deviations of 3 and 5 T_s, respectively, always if the base stations are synced to 10 nanoseconds.

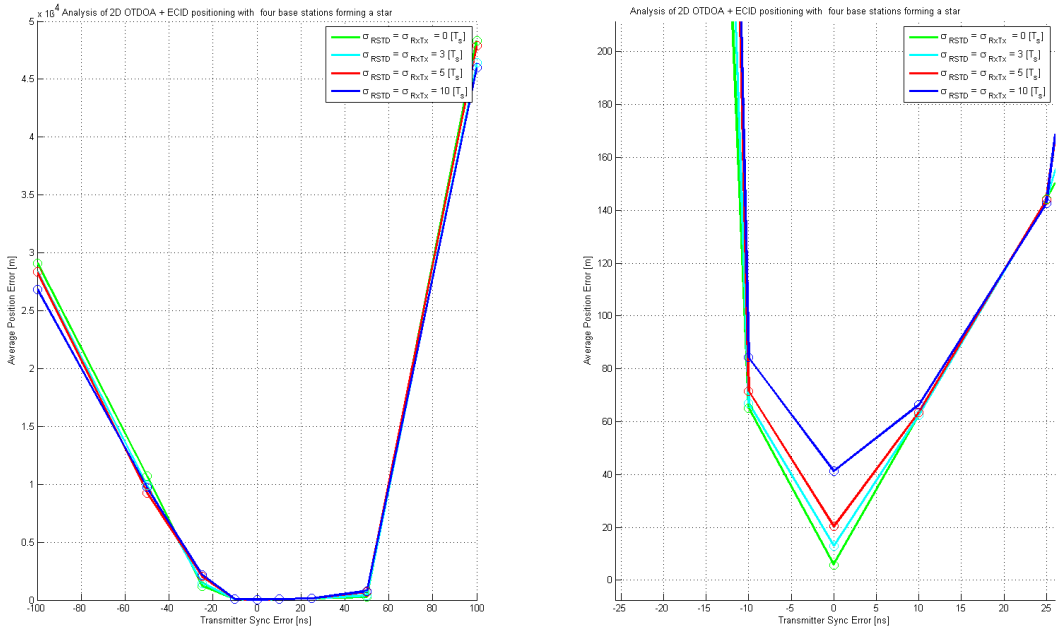

Figure 4.29: Performance of the 2D Hybrid (OTDOA + ECID) positioning algorithm for 4 base stations forming a star.

C. Four base stations forming a star

$\Delta E_{RSTD}[T_s]$	[%]$\mathbf{E}_P <$	$\mathbf{E}_{Sync}[ns]$								
		-100	**-50**	**-25**	**-10**	**0**	**10**	**25**	**50**	**100**
0	**< 50 m**	0.0	0.0	0.0	68.9	99.8	59.9	0.0	0.0	0.0
	< 100 m	0.0	0.0	10.1	85.1	99.8	86.8	9.4	0.0	0.0
	< 300 m	0.0	24.3	77.3	99.5	99.8	96.5	75.4	10.1	0.0
	< 500 m	4.2	51.9	87.4	99.5	99.8	96.5	75.8	16.7	0.0
3	**< 50 m**	0.0	0.0	0.0	46.8	99.8	39.4	0.0	0.0	0.0
	< 100 m	0.0	0.0	10.2	85.4	99.9	86.4	9.9	0.0	0.0
	< 300 m	0.0	25.7	76.6	99.3	99.9	96.4	74.8	9.6	0.0
	< 500 m	4.9	52.3	87.5	99.4	99.9	96.4	75.3	16.7	0.0
5	**< 50 m**	0.0	0.0	0.0	42.0	96.2	34.7	0.0	0.0	0.0
	< 100 m	0.0	0.0	11.6	84.3	99.5	85.8	12.5	0.0	0.0
	< 300 m	0.0	25.2	76.4	98.9	99.5	96.3	74.8	10.4	0.0
	< 500 m	5.1	52.6	87.2	99.0	99.5	96.3	75.6	17.4	0.0
10	**< 50 m**	0.0	0.0	0.3	38.2	73.3	34.2	0.1	0.0	0.0
	< 100 m	0.0	0.0	15.3	79.0	95.4	79.0	18.0	0.0	0.0
	< 300 m	0.0	26.3	77.4	97.6	98.7	93.8	75.0	13.5	0.0
	< 500 m	5.5	51.8	86.8	98.8	98.8	93.8	76.9	20.4	0.0

Table 4.23: Performance of the 2D Hybrid (OTDOA + ECID) positioning algorithm for 4 base stations forming a star

The results are shown in Fig. 4.29 and Tab. 4.23.This configuration is not improving the results of the algorithm without OTDOA and also not better than the previous configuration with four base stations forming a square.

D. Five base stations

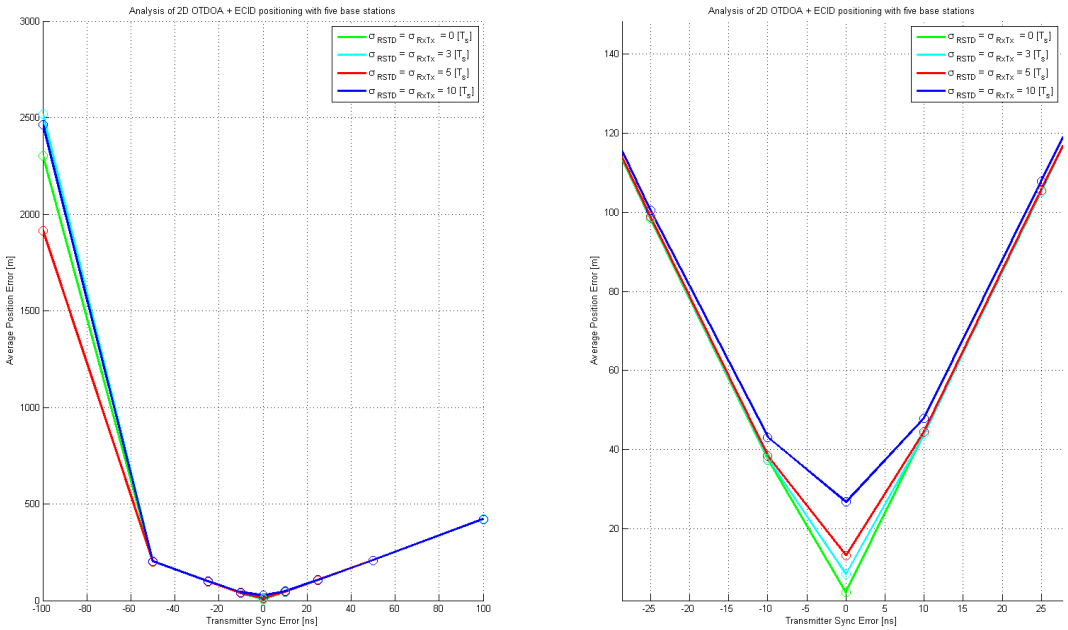

Figure 4.30: Performance of the 2D Hybrid (OTDOA + ECID) positioning algorithm for 5 base stations

$\Delta E_{RSTD}[T_s]$	[%]$\mathbf{E}_P <$	$\mathbf{E}_{Sync}[ns]$								
		-100	**-50**	**-25**	**-10**	**0**	**10**	**25**	**50**	**100**
0	**< 50 m**	0.0	0.0	0.0	100.0	99.9	99.3	0.0	0.0	0.0
	< 100 m	0.0	0.0	67.8	100.0	99.9	99.9	17.8	0.0	0.0
	< 300 m	0.0	99.8	99.7	100.0	99.9	99.9	99.9	99.6	0.0
	< 500 m	88.2	99.8	99.7	100.0	99.9	99.9	99.9	99.6	92.5
3	**< 50 m**	0.0	0.0	0.0	97.0	99.6	79.2	0.0	0.0	0.0
	< 100 m	0.0	0.0	56.9	100.0	99.6	99.7	29.0	0.0	0.0
	< 300 m	0.0	99.8	100.0	100.0	99.6	99.7	99.9	99.6	0.0
	< 500 m	88.6	99.8	100.0	100.0	99.6	99.7	99.9	99.6	93.0
5	**< 50 m**	0.0	0.0	0.0	83.3	99.6	65.6	0.0	0.0	0.0
	< 100 m	0.0	0.0	53.4	100.0	99.6	99.8	35.4	0.0	0.0
	< 300 m	0.0	99.7	99.7	100.0	99.6	99.8	99.9	99.5	0.0
	< 500 m	87.9	99.7	99.7	100.0	99.6	99.8	99.9	99.6	92.2
10	**< 50 m**	0.0	0.0	0.4	62.7	95.2	52.8	0.1	0.0	0.0
	< 100 m	0.0	0.0	48.7	99.7	99.5	98.9	36.6	0.0	0.0
	< 300 m	0.0	99.3	99.8	99.7	99.5	99.1	100.0	99.7	0.0
	< 500 m	87.0	99.6	99.8	99.7	99.5	99.1	100.0	99.9	93.2

Table 4.24: Performance of the 2D Hybrid (OTDOA + ECID) positioning algorithm for 5 base stations

The results are shown in Fig. 4.30 and Tab. 4.24. The five base stations distributed as a pentagon was one of the best scenarios for OTDOA only and the results for OTDOA+ECID are even better: it is the first configuration of all the simulations that meets the FCC requirement of 80% of the 2D-locations calculated with less than 50 metres error, if the base station synchronization is $\leq 10ns$ and the measurement errors $\leq 3T_s$. For measurement errors $\leq 5T_s$, the algorithm comes very close to the requirement, with around 75% of convergences.

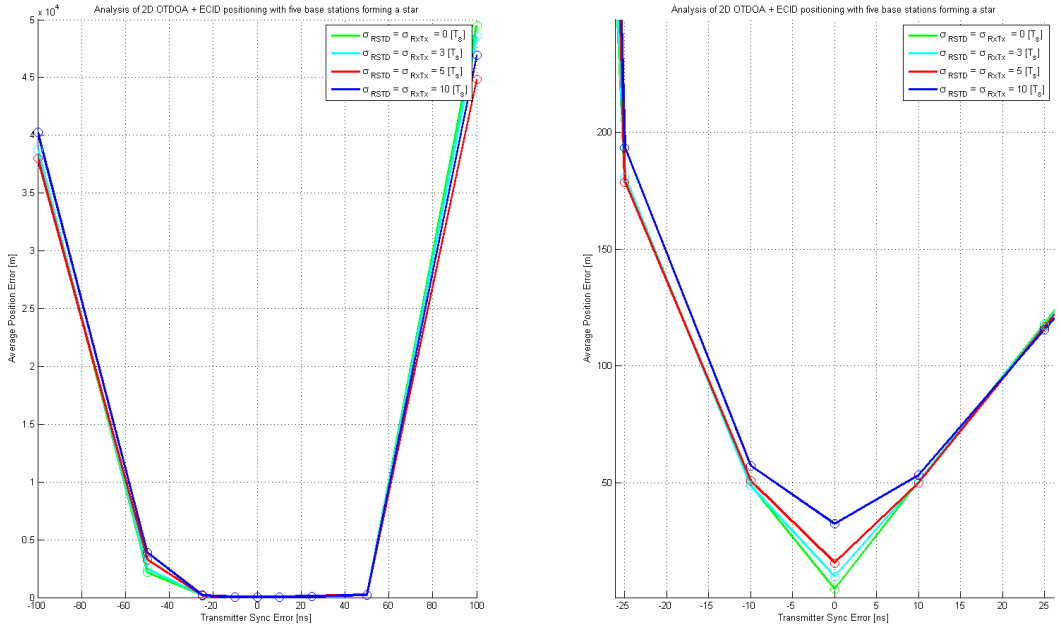

Figure 4.31: Performance of the 2D Hybrid (OTDOA + ECID) positioning algorithm for 4 base stations forming a star.

E. Five base stations forming a star

$\Delta E_{RSTD}[T_s]$	[%]$\mathbf{E}_P <$	$\mathbf{E}_{Sync}[ns]$								
		-100	**-50**	**-25**	**-10**	**0**	**10**	**25**	**50**	**100**
0	**< 50 m**	0.0	0.0	0.0	70.0	99.1	56.9	0.0	0.0	0.0
	< 100 m	0.0	0.0	12.9	96.7	99.1	95.7	0.6	0.0	0.0
	< 300 m	0.0	36.4	89.7	98.4	99.2	95.7	83.6	12.8	0.0
	< 500 m	2.3	58.9	90.4	98.4	99.2	95.7	83.6	12.8	0.0
3	**< 50 m**	0.0	0.0	0.0	68.1	99.6	52.4	0.0	0.0	0.0
	< 100 m	0.0	0.0	15.5	96.6	99.6	95.6	6.9	0.0	0.0
	< 300 m	0.0	36.2	89.9	98.4	99.6	95.6	82.3	14.3	0.0
	< 500 m	2.0	58.1	90.9	98.4	99.6	95.6	82.3	14.3	0.0
5	**< 50 m**	0.0	0.0	0.0	59.1	99.4	50.6	0.0	0.0	0.0
	< 100 m	0.0	0.0	15.9	96.2	99.4	96.1	13.1	0.0	0.0
	< 300 m	0.0	34.9	88.8	98.8	99.5	96.2	83.3	16.8	0.0
	< 500 m	2.3	56.7	90.0	99.2	99.5	96.2	83.3	16.8	0.0
10	**< 50 m**	0.0	0.0	0.1	49.5	83.9	46.3	0.0	0.0	0.0
	< 100 m	0.0	0.0	24.2	90.5	98.5	92.7	24.1	0.0	0.0
	< 300 m	0.0	35.7	89.1	97.8	98.7	95.5	82.0	18.5	0.0
	< 500 m	2.9	57.3	92.4	98.5	98.7	95.5	82.0	18.5	0.0

Table 4.25: Performance of the 2D Hybrid (OTDOA + ECID) positioning algorithm for 5 base stations forming a star

The results are shown in Fig. 4.31 and Tab. 4.25. The addition of an ECID measurement to this constellation improves the results, but they are still worse than with the pentagon-shaped distribution.

F. Six base stations forming a hexagon

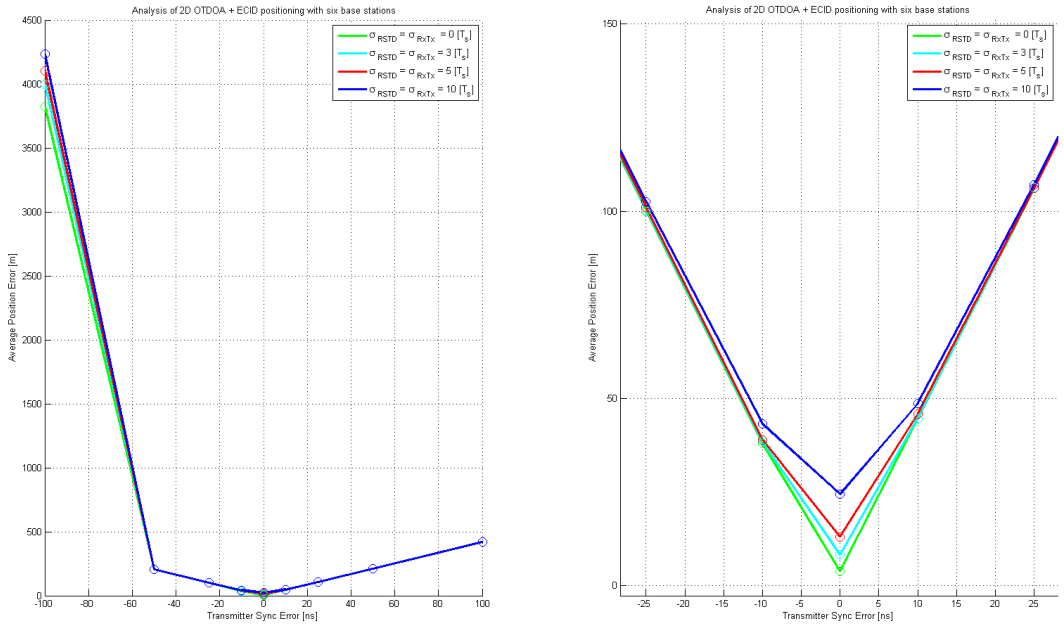

Figure 4.32: Performance of the 2D Hybrid (OTDOA + ECID) positioning algorithm for 6 base stations.

$\Delta E_{RSTD}[T_s]$	[%]$\mathbf{E}_P <$	$\mathbf{E}_{Sync}[ns]$								
		-100	**-50**	**-25**	**-10**	**0**	**10**	**25**	**50**	**100**
0	**< 50 m**	0.0	0.0	0.0	99.9	99.8	95.8	0.0	0.0	0.0
	< 100 m	0.0	0.0	61.7	99.9	99.8	99.7	12.2	0.0	0.0
	< 300 m	0.0	97.9	98.9	99.9	99.8	99.7	99.9	99.9	0.0
	< 500 m	77.1	98.5	98.9	99.9	99.8	99.7	99.9	99.9	99.0
3	**< 50 m**	0.0	0.0	0.0	95.1	99.3	77.8	0.0	0.0	0.0
	< 100 m	0.0	0.0	52.8	100.0	99.3	100.0	24.4	0.0	0.0
	< 300 m	0.0	97.8	99.9	100.0	99.3	100.0	99.9	99.7	0.0
	< 500 m	76.4	98.5	99.9	100.0	99.3	100.0	99.9	99.7	99.3
5	**< 50 m**	0.0	0.0	0.0	84.2	99.1	62.3	0.0	0.0	0.0
	< 100 m	0.0	0.0	49.0	99.7	99.1	100.0	31.7	0.0	0.0
	< 300 m	0.0	97.4	99.5	99.7	99.1	100.0	99.9	99.9	0.0
	< 500 m	76.6	97.9	99.5	99.7	99.1	100.0	99.9	99.9	98.6
10	**< 50 m**	0.0	0.0	0.2	61.0	97.1	53.3	0.1	0.0	0.0
	< 100 m	0.0	0.0	48.1	98.8	98.9	99.3	40.5	0.0	0.0
	< 300 m	0.0	97.2	99.6	99.0	98.9	99.5	99.7	99.7	0.0
	< 500 m	75.6	98.2	99.6	99.0	98.9	99.5	99.7	99.7	98.1

Table 4.26: Performance of the 2D Hybrid (OTDOA + ECID) positioning algorithm for 6 base stations.

The results are shown in Fig. 4.32 and Tab. 4.26. The success percentages are very similar to the pentagon-shaped constellation.

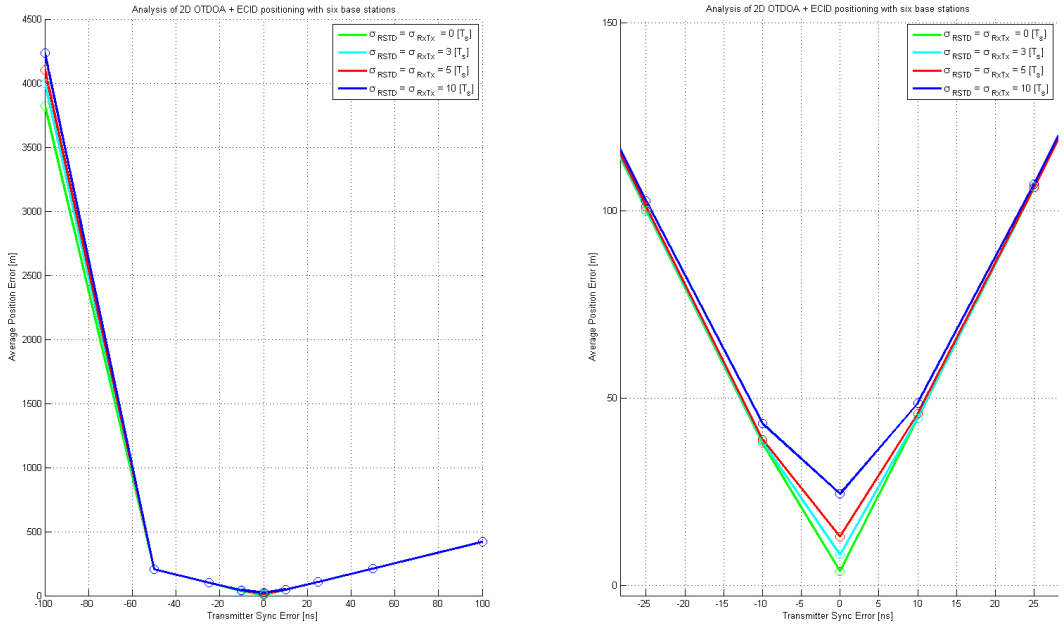

Figure 4.33: Performance of the 2D Hybrid (OTDOA + ECID) positioning algorithm for 7 base stations.

G. Seven base stations forming a honeycomb

$\Delta E_{RSTD}[T_s]$	[%]$\mathbf{E}_P <$	$\mathbf{E}_{Sync}[ns]$								
		-100	**-50**	**-25**	**-10**	**0**	**10**	**25**	**50**	**100**
0	**< 50 m**	0.0	0.0	0.0	99.3	99.5	83.8	0.0	0.0	0.0
	< 100 m	0.0	0.0	10.0	99.4	99.5	96.2	0.0	0.0	0.0
	< 300 m	0.0	89.8	98.4	99.4	99.5	96.2	84.1	32.6	0.0
	< 500 m	32.4	93.5	98.4	99.4	99.5	96.2	84.1	32.6	31.2
3	**< 50 m**	0.0	0.0	0.0	87.8	99.2	59.0	0.0	0.0	0.0
	< 100 m	0.0	0.0	23.3	99.4	99.2	95.9	3.9	0.0	0.0
	< 300 m	0.0	88.3	97.7	99.4	99.2	95.9	84.4	32.7	0.0
	< 500 m	32.3	91.5	97.7	99.4	99.2	95.9	84.4	32.7	29.7
5	**< 50 m**	0.0	0.0	0.0	75.1	99.7	53.6	0.0	0.0	0.0
	< 100 m	0.0	0.0	31.7	99.4	99.7	96.8	10.4	0.0	0.0
	< 300 m	0.0	86.8	97.3	99.4	99.7	96.8	83.6	32.3	0.0
	< 500 m	35.2	90.4	97.3	99.4	99.7	96.8	83.6	32.3	33.0
10	**< 50 m**	0.0	0.0	0.2	59.7	96.9	50.4	0.0	0.0	0.0
	< 100 m	0.0	0.0	36.0	99.0	99.7	95.4	25.9	0.0	0.0
	< 300 m	0.0	86.4	97.9	99.3	99.7	95.8	82.9	33.2	0.0
	< 500 m	32.1	91.0	97.9	99.3	99.7	95.8	82.9	33.2	27.9

Table 4.27: Performance of the 2D Hybrid (OTDOA + ECID) positioning algorithm for 7 base stations

The results are shown in Fig. 4.33 and Tab. 4.27. The success percentages are very similar to the pentagon-shaped and the hexagon-shaped constellations, being the three of them good candidates for LTE OTDOA network deployments.

4.2.2 Summary of the results for Hybrid OTDOA + ECID positioning

This section has studied the effect of adding one ECID measurement to OTDOA positioning scenarios presented in Section 4.1.8. It has been proven that the additional ECID measurement increases the performance of the algorithm and the accuracy of the results, reaching the FCC requirements for 2D positions with three of the proposed constellations: 5 base stations in a pentagon, six base stations and seven base stations. The lack of accurate altitude calculation can be solved in some of the situations by assuming that the mobile device will be on the surface of the Earth. When this assumption is not possible, additional methods like GNSS or WLAN need to be incorporated to the algorithm to calculate 3D locations.

These simulations results are encouraging, and they will be verified in the next chapter against a real mobile device and a LTE test system.

4.3 OTDOA and ECID positioning in indoor locations with small cell deployment.

One of the key issues for the E911 calls is the possibility to estimate accurately indoor locations, where they might be no LoS to any GNSS satellite. This Thesis has proposed a solution based on OTDOA and ECID with pico and femto cell deployment in large buildings. The positioning algorithm should be able to determine not only the 2D location, but also the altitude, as it is important to determine in which floor is the person calling the emergency services.

In order to simulate such a situation and verify if the proposed solution is a suitable candidate, the following scenario is presented: a building of six floors each of them having the dimensions East = 500 metres and North = 200 metres. The distance between two floors is 20 metres. The macro cell which serves the building is located

at East: 0 and North: 0 and the antenna is placed at an altitude of 200 metres on top of a hill. There are two other macro-cells nearby, which are placed atop two buildings at [1000,0,120] and [0,1000,100]. The corner of the building closest to the antenna is situated at [250,100,0]. As the building is usually frequented by a lot of users of LTE mobile phones, there are several pico-cells installed on the ground floor, the second floor, the third floor and the fifth floor. The locations of these cells are: [720,120,0], [270,120,40], [650,280,60] and [400,200,100].

The distribution of the HDOP in the building is shown in Fig. 4.34. The HDOP varies around a value of 0.5, from 0.32 to 0.88, and it is never bigger than 1 in the full building. The GDOP value oscillates between 1.00 and 10.12, which is not optimal but should still allow the calculation of 3D locations.

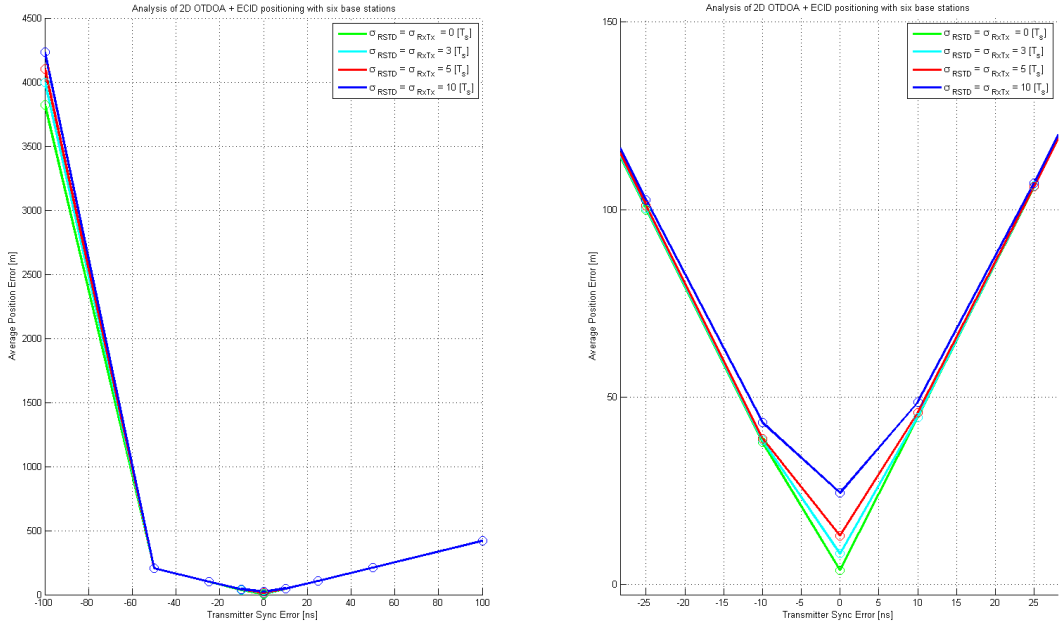

Figure 4.34: HDOP map for the indoor building.

Using this scenario, a thousand random locations inside the building are calculated, with East and North sampling integers from the uniform distributions U[250, 750] and U[100,300] and Up coordinate taking values from the discrete group 1,21,41,61,81,101, which are the altitudes of each of the floors of the building.

The simulation has been done with two different configurations. The first simulation was done without the pico-cells, so only using the three macro-cells close to the building. The algorithm *has not converged* to a position with 500 metres accuracy in any occasion.

The second simulation has been done including the pico-cells. The average error of the position calculated against the base stations synchronization error is shown in Fig. 4.35. The detailed results are written in Tab. 4.28, where a new row has been incorporated to show the % of occasions where the algorithm has converged to the correct floor.

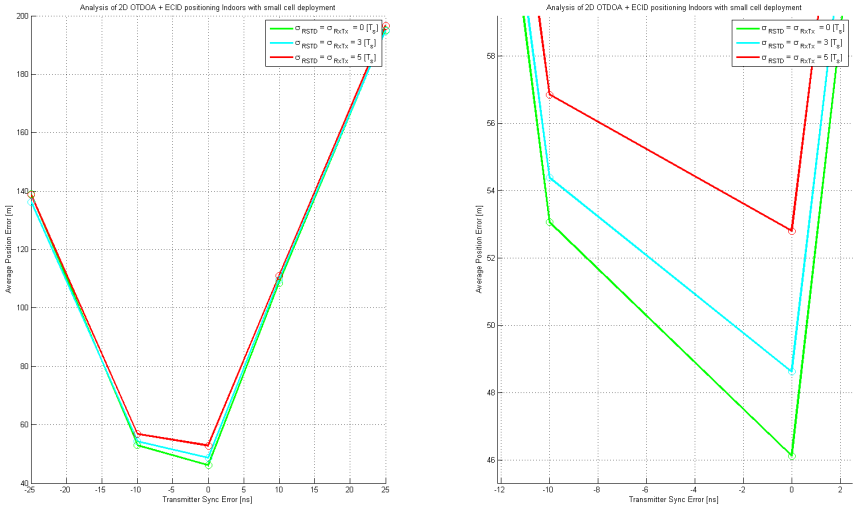

Figure 4.35: Performance of the 3D Hybrid (OTDOA + ECID) positioning algorithm for indoors with pico-cells.

$\Delta E_{RSTD}[T_s]$	**[%]E**$_P$ $<$	**E**$_{Sync}[ns]$				
		-25	**-10**	**0**	**10**	**25**
0	$<$ **50 m**	0.0	37.0	59.6	0.3	0.0
	$<$ **100 m**	3.3	61.3	97.3	45.9	0.0
	$<$ **300 m**	17.0	66.2	99.9	96.9	95.3
	$<$ **500 m**	17.0	66.2	99.9	96.9	95.6
	% Correct Floor	1.9	20.6	29.9	5.5	1.8
3	$<$ **50 m**	0.0	33.3	56.5	1.7	0.0
	$<$ **100 m**	3.6	58.4	91.8	44.8	0.1
	$<$ **300 m**	17.0	63.4	97.8	97.4	95.6
	$<$ **500 m**	17.0	63.4	97.8	97.4	95.9
	% Correct Floor	1.9	18.2	29.4	6.1	2.4
5	$<$ **50 m**	0.0	31.3	53.0	3.1	0.0
	$<$ **100 m**	3.5	55.9	86.9	42.3	0.0
	$<$ **300 m**	17.1	62.5	95.0	96.8	93.3
	$<$ **500 m**	17.1	62.5	95.0	96.8	95.0
	% Correct Floor	2.0	17.6	25.9	7.5	1.6

Table 4.28: Performance of the 3D Hybrid (OTDOA + ECID) positioning algorithm for indoors with pico-cells.

As it can be seen from the results, the algorithm is able to converge to a position with less than 50 metres error with more than 50 % probability only if the base stations, including pico-cells, are perfectly in sync. This is a big drawback that increases the cost of the pico-cell deployment.

Even in those ideal conditions, the algorithm does not meet the final 80% requirement of the FCC for indoors, although it fulfils the intermediate 50% requirement, so it can be used in the transitory period of 3 years before the final requirement is enforced. For a final solution, OTDOA and ECID positioning can be combined with WLAN, bluetooth and dispatchable locations to improve the indoor results.

The percentage of occasions where the algorithm is able to converge to the correct floor is below 30%, being the altitude calculation the biggest challenge for OTDOA + ECID indoor positioning.

4.4 LBS Hybrid Positioning

The final step is to include the satellites in the algorithm. In order to simulate LBS GNSS and LBS Hybrid positioning, information about real satellites is required. In this Thesis, the satellite coordinates and other relevant information will be extracted from the 3GPP predefined GNSS Scenario 1, Section 6.2.1.2.1 of the TS 37571-5 [46]. This scenario provides the assistance data and almanac files for GNSS GPS and GLONASS satellites as visible in Tokyo, Japan on January 1^{st}, 2012 at 00:31:00 GPS time at the exact WGS84 location: 35° 44′ 39.432″ North, 139° 40′ 48.633″ East and 300 m altitude. This location will be used as reference position and as the location of the serving base station.

The mobile device is supposed to be in a circle of 1000 metres radius around the reference location. For simplicity defining the base station constellations, the mobile device location will be simulated with positive East and North coordinates. One thousand random mobile device positions will be computed and the same positions will be used throughout this section.

4.4.1 LBS GNSS and hybrid positioning with good DOP conditions

This first section will analyse the performance of the localization algorithm if there are enough satellites visible with a direct line of sight and the DOP of the satellite's constellation is optimal. The purpose of this simulation is to understand if including OTDOA measurements is of benefit even when GNSS standalone would be sufficient for the position calculation.

The satellite constellation is formed by the following GPS satellites: [G04, G17, G19, G20 and G28]. The DOP values of this constellation at the reference point of GNSS Scenario 1 are: HDOP = 2.06 and GDOP = 2.68. These values remain almost constant in all the surface around the reference point which will be used for the simulation.

Each GNSS pseudo-range measurement is the ideal distance between the satellite and the mobile device contaminated by a random error component which takes values from the Uniform distribution U[-15,15] metres. These limit values are taken from the GNSS error budget discussed in Section 2.2.5 of this Thesis, as the error in the worst case scenario.

The base station constellation is formed by four base stations distributed in a square of 1000 metres radius, with the first base station used as reference and serving cell and placed at the reference point. The hybrid DOP values of base stations plus satellites are: HDOP = 1.70 and GDOP = 1.93. The variance of the GDOP in the East-North area around the reference point where the mobile device locations are simulated are shown in Fig. 4.36, for Up coordinate equal to 0. It changes between 1.34 and 1.98, improving the GDOP of the satellites-only constellation.

Including one ECID measurement to the reference cell and recalculating the DOPs gives a value of 1.48 for HDOP and 1.70 for the GDOP at the reference location and a GDOP distribution shown in Fig. 4.37, varying between 1.34 and 1.87.

The ECID and OTDOA measurements are simulated with an additive noise of 5 T_s standard deviation. The base stations' synchronization error used is 0, 10, 25 and 50 ns.

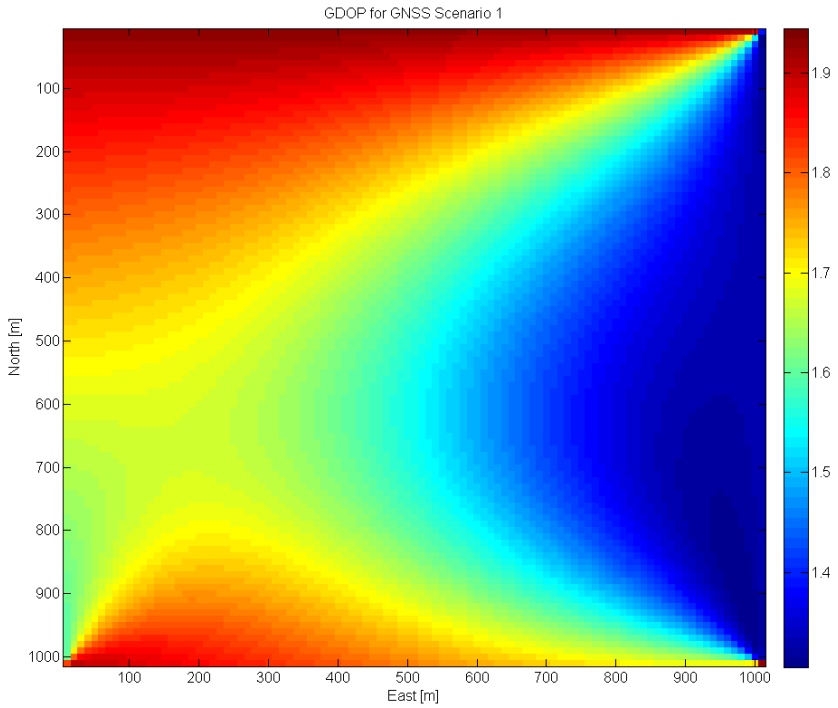

Figure 4.36: GDOP of the Base Stations plus satellites constellation for Up = 0

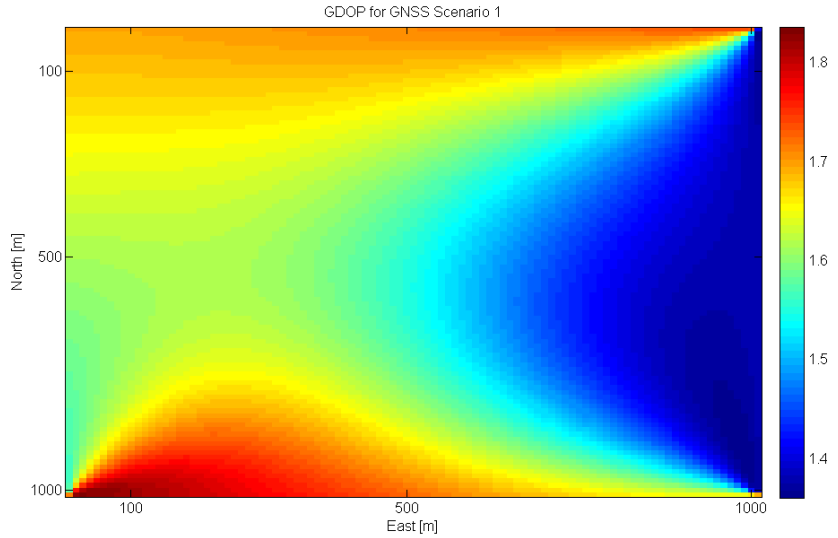

Figure 4.37: GDOP of the Base Stations plus satellites constellation for Up = 0 with one ECID

Different combinations of LBS technologies have been used to calculate the position of the mobile device under the above conditions. The results are detailed in Tab. 4.29.

LBS type	**BS$_{sync}$ [ns]**	**Errors [m]**			**[%]E$_P$ <**		
		$\langle E \rangle$	Max$_E$	Min$_E$	< 50 m	< 100 m	< 500 m
GNSS	-	15.34	39.06	0.58	100	100	100
GNSS + OTDOA	0	12.53	34.02	0.94	100	100	100
	10	33.48	67.77	10.79	95.5	100	100
	25	85.81	117.37	60.93	0	91.7	100
	50	174.25	208.08	143.57	0	0	100
GNSS + ECID	0	14.57	40.76	0.98	100	100	100
	10	14.36	44.19	1.22	100	100	100
	25	14.93	42.03	0.92	100	100	100
	50	14.60	41.86	1.58	100	100	100
Hybrid	0	11.98	30.39	1.48	100	100	100
	10	27.84	64.78	11.71	98.7	100	100
	25	75.82	103.23	47.56	7.5	97.7	100
	50	172.25	271.69	135.85	0	0	96.9

Table 4.29: Performance of the LBS GNSS and Hybrid algorithm with optimal satellite constellation

A few conclusions can be drawn from these results: LBS-GNSS positioning fulfils the FCC requirements for three dimensional positioning if enough satellites are available and the satellite geometry is adequate. Adding one ECID measurement to the reference base station improves slightly the algorithm in all of the situations studied, independently of base station synchronization errors. The addition of OTDOA measurements can improve the algorithm **only** if the base stations are perfectly synchronized. Including OTDOA measurements to base stations with synchronization errors decreases the performance of the algorithm, rendering worse results than LBS-GNSS standalone. According to this, in an open environment with good satellite reception, OTDOA should only be included to the location algorithm if the accuracy of the base station's synchronization can be guaranteed to be almost perfect.

4.4.2 LBS GNSS and hybrid positioning with bad satellite DOP

The previous scenario used a good satellite constellation, which was able of meeting the FCC requirements on its own. However, what happens if the visible satellites are not so optimal for location? This section will select a group of satellites with bad DOP values and repeat the simulations from the previous section, with all other parameters remaining untouched.

The chosen satellites are G04, G19, G20 and G28, which form a constellation with HDOP = 37.53 and GDOP = 51.55. Including OTDOA, the GDOP varies between 1.41 and 2.14, a critical improvement with respect to GNSS only. Furthermore, including ECID, the range of variation is between 1.40 and 2.09, as represented in Fig. 4.38.

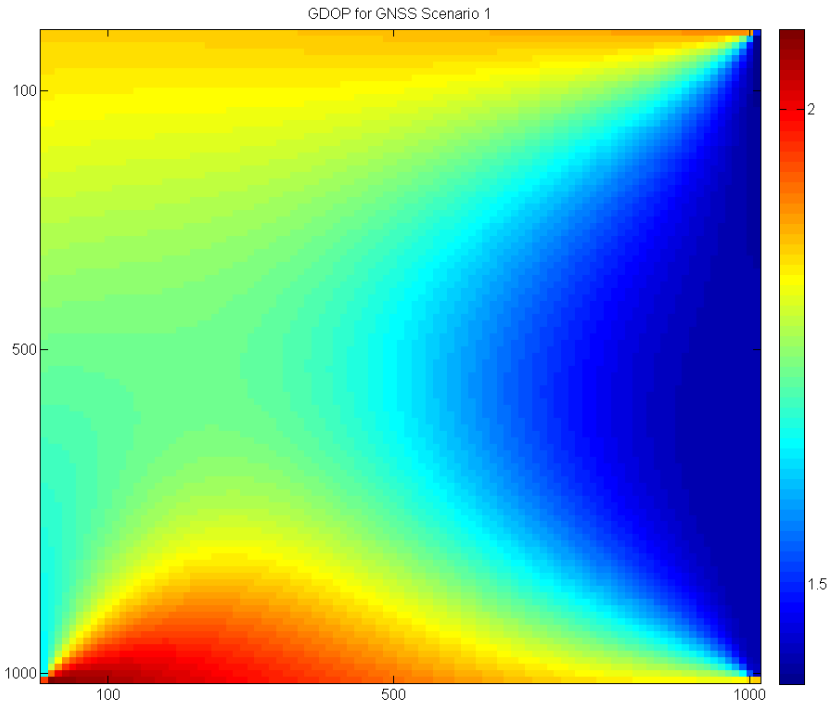

Figure 4.38: GDOP of the Base Stations plus satellites constellation for Up = 0 with bad satellite geometry

The results of the simulations are shown in Tab. 4.30.

The performance of the A-GNSS based localization is worse, as the geometry of the satellites is not suitable for positioning. The average error has increased, and the percentage of convergences with 50 metres position accuracy has fallen until 61 %. In such conditions, the addition of an ECID measurement is very beneficial, reaching percentages of around 99 % of iterations which successfully calculate a position within a 50 metres radius of the real location of the mobile device, independently of the base station synchronization. Including OTDOA measurements is a bit more controversial: if the base station synchronism is of 10 nanoseconds or better, the OTDOA improves the overall algorithm performance to between 95 and 100 % of success, depending on the value of the sync error. If the error is bigger than 10 nanoseconds, the addition of OTDOA does not render any benefit, greatly decreasing the convergence rates. The synchronization of the base stations has again proven itself as a key factor towards accomplishing the FCC requirements in positioning.

LBS type	BS_{sync} [ns]	Errors [m]			[%]E_P <		
		$\langle E \rangle$	Max_E	Min_E	< 50 m	< 100 m	< 500 m
GNSS	-	49.93	128.87	2.65	61.0	89.6	100
GNSS + OTDOA	0	13.71	39.63	0.44	100	100	100
	10	36.02	69.57	10.45	91.1	100	100
	25	89.59	126.35	60.61	0	80.2	100
	50	181.57	217.07	146.89	0	0	100
GNSS + ECID	0	19.51	61.08	0.74	98.5	100	100
	10	19.89	60.56	0.66	99.2	100	100
	25	19.56	69.99	1.97	98.9	100	100
	50	19.45	65.41	0.94	99.3	100	100
Hybrid	0	13.16	33.95	0.70	100	100	100
	10	33.06	68.71	8.42	95.0	100	100
	25	80.91	129.95	56.18	0	95.5	100
	50	161.31	208.80	130.86	0	0	100

Table 4.30: Performance of the LBS GNSS and Hybrid algorithm with bad satellite constellation

4.4.3 LBS Hybrid positioning with few satellites

During the previous section, LBS OTDOA + ECID has been almost completely discarded for three dimensional positioning, due to the difficulties to calculate the altitude, as the base stations do not provide enough altitude diversity. LBS GNSS and LBS Hybrid overcome this problem, and throughout this section all the calculated positions were 3D. The next step is to prove if the 3D algorithm for LBS Hybrid can also achieve a good performance when not enough satellites are visible with direct line of sight. In order to simulate that scenario, two satellites from the same region of the sky at the date and time of GNSS scenario 1 will be selected, with SVIDs G11 and G17. The calculation of DOP is not possible, as the number of satellites is insufficient.

Maintaining the same base stations as from previous examples, the combined DOP values are 3.35 for the HDOP and 3.51 for the GDOP using only OTDOA and GNSS, and 2.19 for the HDOP and 2.36 for the GDOP if an ECID measurement is added. In this last scenario, the total GDOP varies from 1.63 to 3.24, with a distribution shown in Fig. 4.39 with respect to East and North coordinates.

The results are shown in Tab. 4.31. In this scenario, the calculation of a position using GNSS only is not possible, as only two measurements are available and at least four are needed to compute the ENU coordinates plus the clock error of the receiver. For the same reason, GNSS + ECID is as well not possible, as it has only three measurements. For the GNSS + OTDOA, the target 80 % of iterations under 50

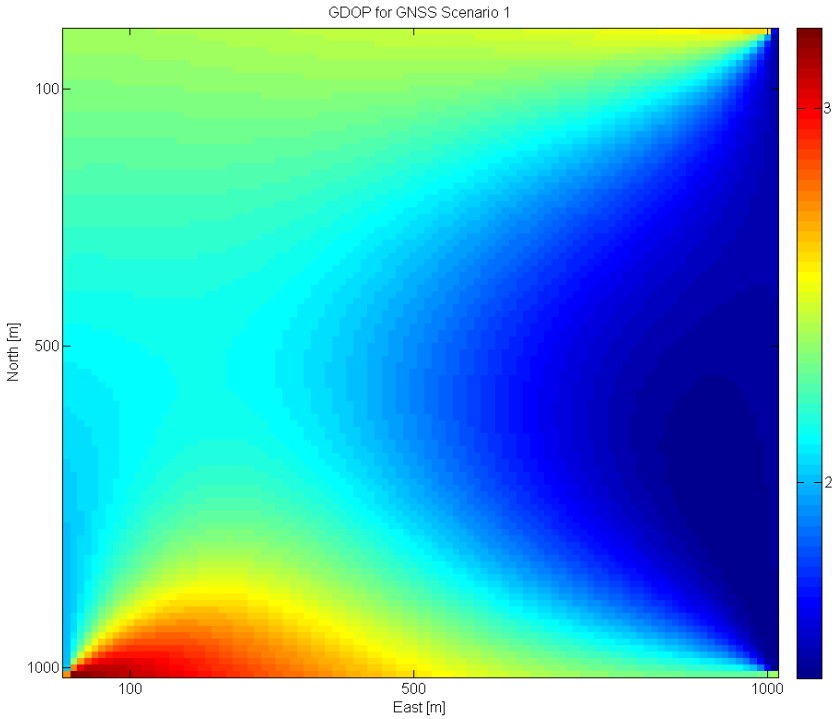

Figure 4.39: GDOP of the Base Stations plus satellite constellation with only 2 satellites.

metres position accuracy is reached only if the base stations are perfectly synchronized. If the synchronization error is 10 ns, the percentage of success falls short by 10.5 %. However, a position is still always calculated within 100 metres accuracy. For the pure Hybrid algorithm, the goal is achieved with base station synchronization errors up to 10 nanoseconds.

LBS type	**BS$_{sync}$ [ns]**	**Errors [m]**			**[%]E$_P$ <**		
		$\langle E \rangle$	Max$_E$	Min$_E$	< 50 m	< 100 m	< 500 m
GNSS	-	∞	∞	∞	0.0	0.0	0.0
GNSS + OTDOA	0	17.74	60.05	0.81	99.6	100	100
	10	43.04	91.42	10.95	69.5	100	100
	25	106.83	149.81	70.67	0	33.4	100
	50	216.34	263.72	171.77	0	0	100
GNSS + ECID	-	∞	∞	∞	0.0	0.0	0.0
Hybrid	0	16.83	64.43	0.81	99.8	100	100
	10	39.01	81.29	11.12	80.1	100	100
	25	93.37	143.45	59.72	0	69.8	100
	50	179.72	237.55	139.31	0	0	100

Table 4.31: Performance of LBS algorithms with only two visible satellites.

4.4.4 LBS Hybrid positioning indoor with pico cell deployment

One of the main challenges of LBS is the calculation of indoor positions. Indoor positioning with LBS OTDOA + ECID has already been studied in this Thesis and the results, although promising, did not meet the accuracy requirements pursued. The main obstacle for indoor positioning is the lack of LoS to a sufficient number of satellites. However, under certain conditions there might be LoS to a few satellites, even though the DOP of the satellite constellation will likely be bad, due to the satellite signals coming from similar directions.

Maintaining the 2 satellites selected for the previous section, G11 and G17, and the scenario with pico cells deployed for Section 4.3, this section will simulate the same indoor scenario under the assumption that two satellites are visible.

The scenario presents a GDOP value oscillating between 1.5 and 2.5 in the area of the building. The results are presented in Tab. 4.32. Again, LBS GNSS and GNSS + ECID algorithms cannot be used due to the low number of measurements. For GNSS + OTDOA and Hybrid, the percentage of occasions where the algorithm was able to calculate correctly the floor is bigger than 80 %, with $\approx$ 98 % of calculated positions within 50 metres accuracy if the base stations and the pico cells are perfectly synchronized.

LBS type	**BS$_{sync}$ [ns]**	**Errors [m]**			**[%]E$_P$ <**		**% Correct Floor**
		$\langle E \rangle$	Max$_E$	Min$_E$	< 50 m	< 100 m	
GNSS	-	∞	∞	∞	0.0	0.0	0.0
GNSS + OTDOA	0	19.53*	73.49*	2.65	98.8	99.7	82.3
	10	53.36*	119.57*	12.87	47.0	96.6	31.0
	25	125.63*	202.12*	77.01	0.0	12.7	0.6
GNSS + ECID	-	∞	∞	∞	0.0	0.0	0.0
Hybrid	0	20.02*	73.62*	1.74	98.6	99.7	80.8
	10	51.95*	107.67*	15.66	44.5	93.7	31.3
	25	124.87*	194.51*	76.42	0.0	9.8	0.0
* Discarding the non-converging measurements.							

Table 4.32: Performance of LBS Indoor with two visible satellites and small cells.

4.4.5 Summary of the results for LBS Hybrid positioning

This section has focused on the analysis of LBS Hybrid scenarios combining GNSS, ECID and OTDOA. It has been seen that GNSS standalone fulfils the FCC require-

ments in outdoors scenarios, if the number of visible satellites is four or more, and the geometry of the satellites gives an acceptable DOP. In such conditions, the addition of an ECID measurement slightly improves the results. The addition of OTDOA is beneficial only if the synchronization between base stations is better than 10 nanoseconds, decreasing the accuracy of the calculated position otherwise.

When the number of GNSS measurements is not sufficient, or the satellite geometry is bad for positioning, the hybrid algorithm is still able to achieve the desired performance, always constrained to the base stations' synchronization being better than 10 nanoseconds.

For indoor scenarios, having two visible satellites has greatly raised the accuracy of the solution, being able to accomplish the goals set by FCC if the small cells and the base stations are synchronized.

Nevertheless, one major obstacle remains: the synchronization of all the LTE cells present in the scenario is a critical requirement for OTDOA positioning. If a minimum synchronization accuracy of 10 nanoseconds is not achieved, the accuracy of the algorithm is poor.

4.5 LTE Positioning Protocol extensions

The biggest drawback of the proposed algorithm is the demanding requirement for base station synchronization. Having all cells synchronized within 10 nanoseconds greatly increases both the cost of the deployment of LTE cells and the technical complexity. However, this requirement only affects OTDOA. ECID, being a method based on Round Trip Time measures, does not rely on neither the synchronization of the base stations nor the mobile device receiver. The problem is that UE RxTx measurements have only been defined to the serving cell, and the power measurements (RSRP and RSRQ) used to estimate distances to the neighbour cells are much more inaccurate. This problem is solved as part of the LPPe protocol which will be introduced in the near future for LTE.

This protocol provides the support to perform RxTx measurements to neighbour cells, making ECID a very promising solution for indoor positioning. This section will try to determine whether this feature combined with GNSS and OTDOA will

accomplish the performance requirements for the emergency services or not. The focus will be on indoor scenarios, where the lack of GNSS measurements forces the algorithm to rely more on terrestrial based positioning.

4.5.1 Indoor positioning with small cells without GNSS

The base station constellation and all other parameters of the scenario are the same used for Section 4.3. The same 1000 mobile locations are used to study the performance of the algorithm, now having ECID UE RxTx measurements to all the cells of the scenario. The simulations are performed without OTDOA, with OTDOA to the macro and micro cells only and with OTDOA to all cells in the scenario, including pico and femto cells. The results are detailed in Tab. 4.33.

LBS type	**BS$_{sync}$ [ns]**	**Errors [m]**			**[%]E$_P$ <**		**% Correct Floor**
		$\langle E \rangle$	Max$_E$	Min$_E$	< 50 m	< 100 m	
ECID	-	27.51	96.74	2.93	89.5	97.6	50.6
ECID +	0	26.97*	109.01*	3.65	90.5	98.7	52.4
OTDOA Big	10	37.25*	91.55*	3.46	78.4	92.4	39.3
Cells	25	72.55*	128.38*	44.19	1.3	73.5	22.6
ECID +	0	24.65*	103.24*	1.57	92.0	99.2	60.1
OTDOA All	10	40.04*	86.94*	10.78	63.9	80.5	36.9
Cells	25	84.54*	125.97*	58.78	0.0	44.9	9.5
* Discarding the non-converging measurements.							

Table 4.33: Performance of OTDOA + ECID Indoor with RxTx measurements to neighbour cells.

Comparing these results with Section 4.3, the gain is obvious. The accuracy requirements of the FCC for indoor positioning are met with ECID only, as well as including OTDOA, if the base stations are synchronized to 10 ns or better. Furthermore, the possibility to include OTDOA only for the macro and micro cells of the LTE network and not for the small cells simplifies and reduces the cost of the deployment of such small cells inside buildings. Nevertheless, improvements can still be done in order to obtain a better % of convergences to the correct floor.

4.5.2 Indoor positioning with small cells with two satellites

The last simulation to be performed is the same indoor scenario with ECID measurements possible to all cells and with 2 visible satellites, G11 and G17, from the same region of the sky. The results are shown in Tab. 4.34.

LBS type	**BS$_{sync}$ [ns]**	**Errors [m]**			**[%]E$_P$ <**		**% Correct Floor**
		$\langle E \rangle$	Max$_E$	Min$_E$	< 50 m	< 100 m	
ECID + GNSS	-	17.02*	55.41*	0.71	99.4	99.6	86.4
Hybrid	0	15.27*	45.89*	1.91	99.8	99.8	92.1
(OTDOA	10	30.68	69.26	2.57	95.4	100	59.4
Big Cells)	25	67.87*	118.94*	33.50	7.4	97.4	20.1
Hybrid	0	16.10	69.29	0.92	99.7	100	89.0
(OTDOA	10	37.42*	90.62*	9.51	80.7	94.8	48.9
All Cells)	25	81.65*	125.89*	53.51	0.0	68.1	12.2
* Discarding the non-converging measurements.							

Table 4.34: Performance of LBS Indoor with RxTx measurements to neighbour cells and two satellites.

Analysing the results, it can be seen that GNSS + ECID can provide a position within 50 metres of the real location of the mobile device in almost all occasions. The percentage of iterations were the algorithm was able to estimate the correct floor is also high. If the network of macro and micro cells is well synchronized, with base station synchronism errors of less than 10 nanoseconds, including OTDOA measurements improves the performance of the LBS hybrid location algorithm. Adding OTDOA measurements to femto and pico cells does not bring any benefit, as the cost of synchronizing the small cells to the network is too big and the improvement on the results is minimal. Furthermore, small synchronization errors will severely damage the accuracy of the calculated positions. Hence, the small cells should only be used for RTT ECID measurements.

Chapter 5

Test System Results

In the previous Chapter, the algorithm proposed in this Thesis has been verified in a simulation environment recreated with Matlab. This Chapter will try to reproduce a real life environment in the lab, using test system equipment to generate LTE and Satellite signals and real mobile phones to collect the measurements.

5.1 Description of the testing environment

5.1.1 Test System

In order to reproduce a LTE network and GNSS signals, a test system TS-Extended of the TS8980 RF Test System Family from Rohde & Schwarz will be used. This family of test system is certified as Test Platform for certification and validation of 3GPP conformance and performance tests for mobile phones, according to the Device Certification Criteria of the Global Certification Forum.

The TS-Extended system is depicted in Fig. 5.1. It consists of two CMW500 devices, each of them able to simulate two real LTE Cells and one SMBV100A, capable of simulating up to 24 satellite signals from GPS or GLONASS. Additional devices in the system include a TS-CONN for combining and routing the signals from the CMW500 to the antenna ports of the mobile device, a system controller PC and a NGMO to automate the mobile device.

Figure 5.1: R& S TS-Extended Test System

5.1.2 Mobile Devices

Throughout these chapter, three different mobile devices will be used. Each of the tests will be performed in at least two of them.

- Samsung SGH-T399, also known as Samsung Galaxy Light. This is a commercial device which supports GPS, GLONASS and OTDOA.
- Prototype Device 1 from a mobile chipset manufacturer, which supports OTDOA. The name of the manufacturer and the device cannot be disclosed.
- Prototype Device 2 from a second mobile chipset manufacturer. It supports OTDOA and GPS.

All of these devices are equipped with two downlink LTE antenna ports (for the main and diversity LTE signals), one uplink LTE antenna port and one downlink GNSS port.

5.1.3 Test Procedure

All tests executed in this chapter follow a similar procedure. The main steps are the following:

1. Configure the Hardware Equipment involved in the test.

2. Set up the LTE serving cell and bring it to registration power (-85 dBm).
3. Power on the mobile device and wait for a connection request.
4. Complete attach procedure in LTE.
5. Set up the remaining LTE cells and configure the SMBV100A to generate the satellite signals (if required).
6. Send an ETC ResetLocationInformation message: this forces the mobile to delete all previous stored positioning information.
7. Start the LPP session with the mobile device and provide the required information (assistance data).
8. Request LPP position information.
9. Call the positioning algorithm to compute a position.
10. Evaluate the calculated position and count a PASS or FAIL iteration as appropriate.
11. Repeat steps 6-10 for 100 iterations.

A PASS iteration is considered if the difference between the real and the calculated position is smaller than 51.3 metres (50 metres from the FCC requirement plus 1.3 metres of test system uncertainty).

5.2 OTDOA Positioning

The OTDOA positioning test cases have been tested against the SG Light and Prototype Device 1. For each of the tests, the test system has been used to generate four LTE cells.

5.2.1 Configuration

The cells are configured according to the minimum requirements defined by 3GPP in TS 36.133 Clause 8.1.2.5.1 [32]. The PRS configuration index (12), bandwidth (10

MHz) and number of consecutive downlink frames (6) have been chosen to provide enough PRS occasions. The cell powers meet the minimum requirement of $\hat{E}_s/Iot$ for the PRS signal (signal power over total noise):

$$PRS(\hat{E}_s/Iot)_{ref\,cell} \geq -6dB \tag{5.1}$$

$$PRS(\hat{E}_s/Iot)_{neighbours} \geq -13dB \tag{5.2}$$

The cell power settings for the reference cell are shown in Fig. 5.2. For the neighbour cells are shown in Fig. 5.3. The PRS RA has been chosen to be always 0 dB, which means that the PRP (power of the PRS signal) coincides with the RSRP of the cell.

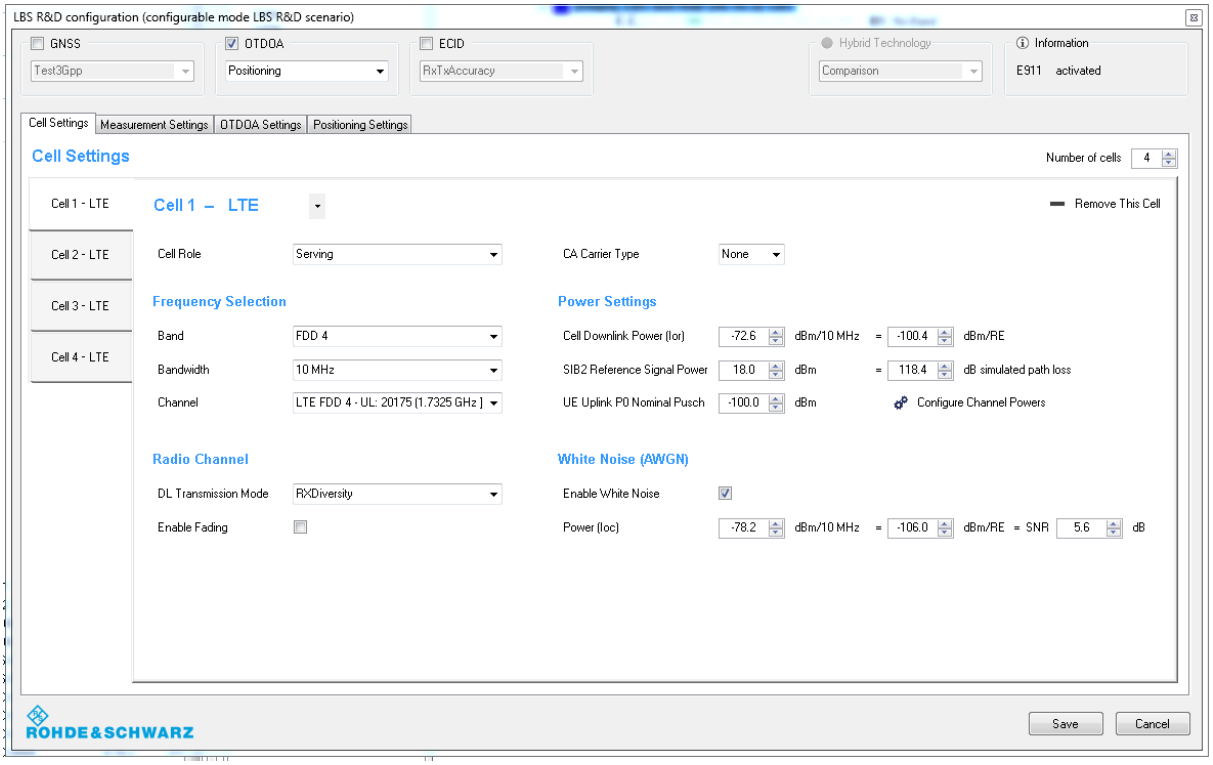

Figure 5.2: Reference cell power settings.

The base station constellation and the mobile device position have been chosen to generate two different scenarios: one with good HDOP and one with bad HDOP. The configuration leading to the good HDOP value is depicted in Fig. 5.4.

The configuration for bad DOP contains the same set of base stations, but the mobile device is placed in ENU = [-700, 500, 0], giving HDOP of 5,9.

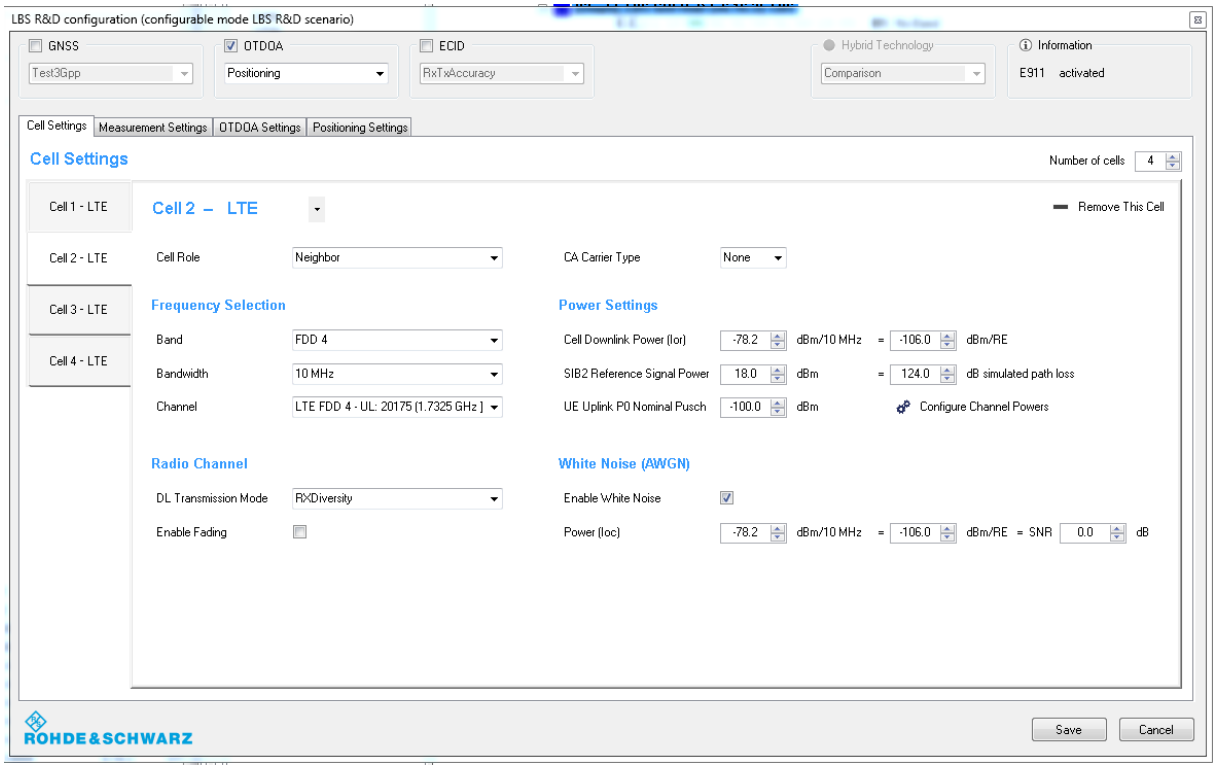

Figure 5.3: Neighbour cells power settings.

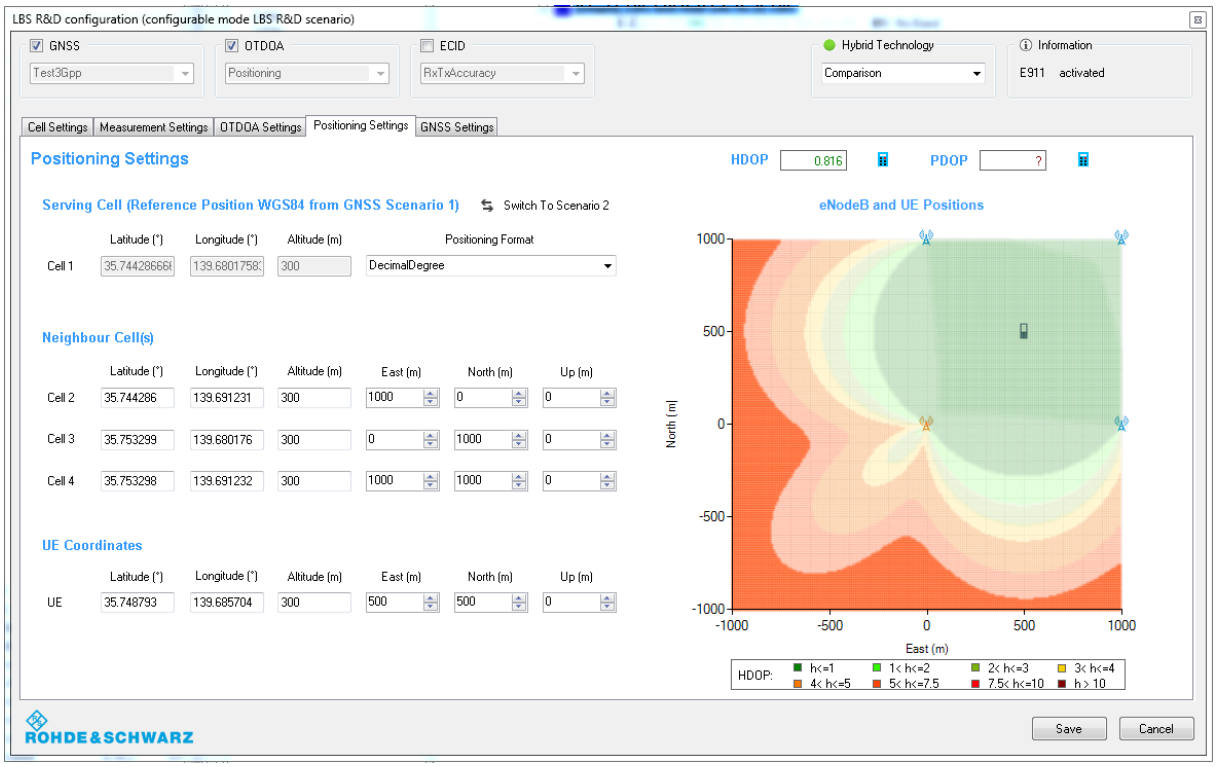

Figure 5.4: Base station constellation and mobile device position.

5.2.2 Results with ideal base station synchronization

Considering the LTE base stations as perfectly synchronized, the test case has been run for both mobile devices, under good and bad HDOP conditions. In Fig. 5.5, one sample iteration is shown, including the hyperbolas resulting from the RSTD measurements, the position of the base stations and the real and calculated position of the mobile device.

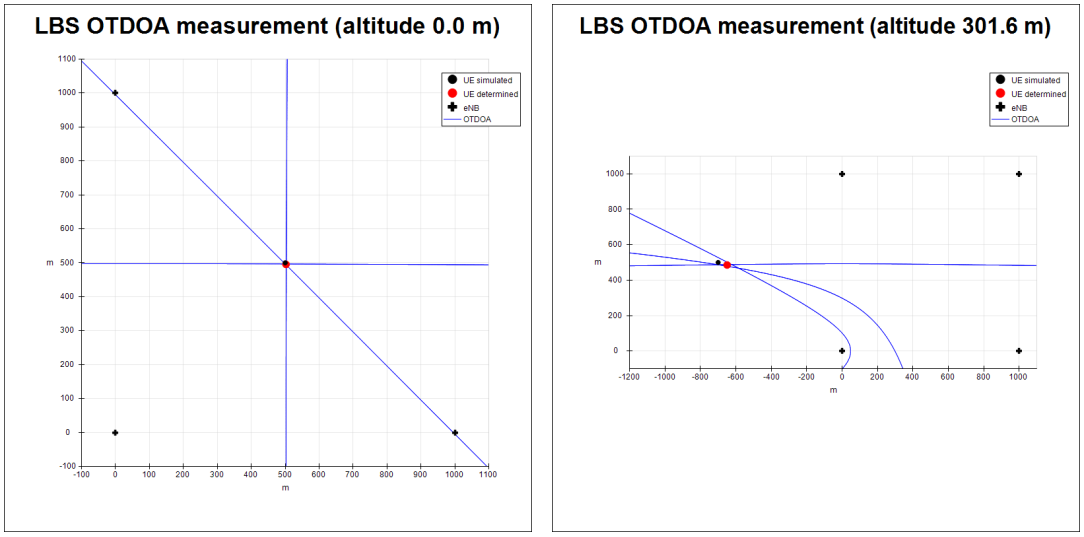

(a) Good DOP (b) Bad DOP

Figure 5.5: Example of one iteration calculation with hyperbolas.

Fig. 5.6 shows an error polar diagram. The difference between the real and calculated positions is shown relative to East and North coordinates. Errors which are bigger than 1.5 times the accuracy requirement are outside the bounds of the graph.

In general, the results from the prototype present less scattering than the results from the commercial device, being both more accurate and more precise. Several iterations have given exactly the same measurements. Thus, the number of points in the graph is much smaller than one hundred. The results in bad DOP conditions are far worse than the results with good DOP. The number of iterations passed for each case is detailed in Tab. 5.1. The prototype device has successfully met the FCC requirements in both good and bad DOP conditions, although the average error is higher in bad DOP. The Samsung Galaxy Light has not met the 80 % requirement for bad DOP conditions, reaching only 58 %.

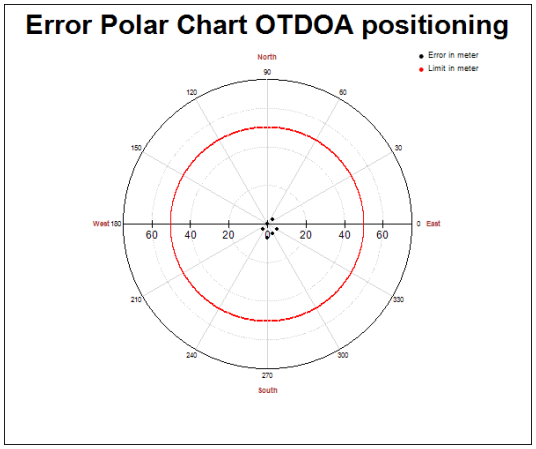

(a) Proto 1, Good DOP

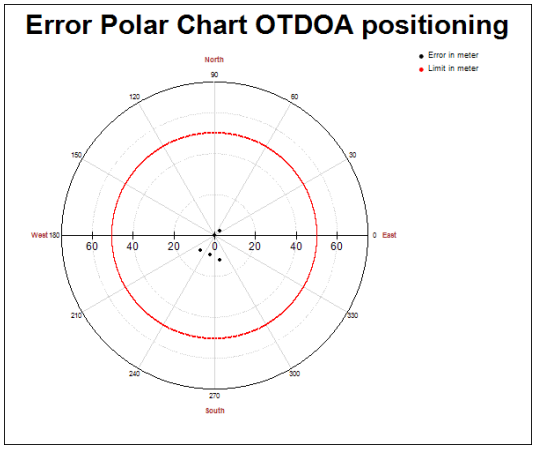

(b) SG Light, Good DOP

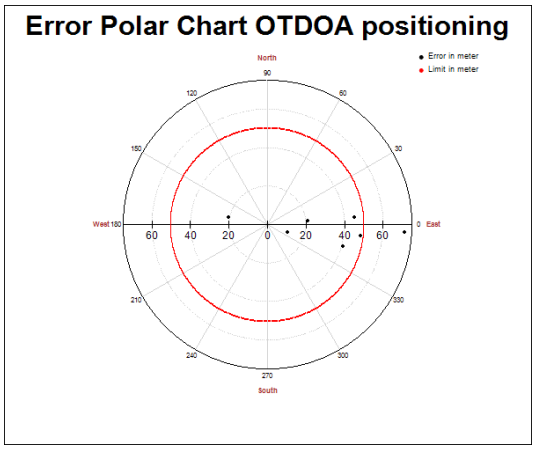

(c) Proto 1, Bad DOP

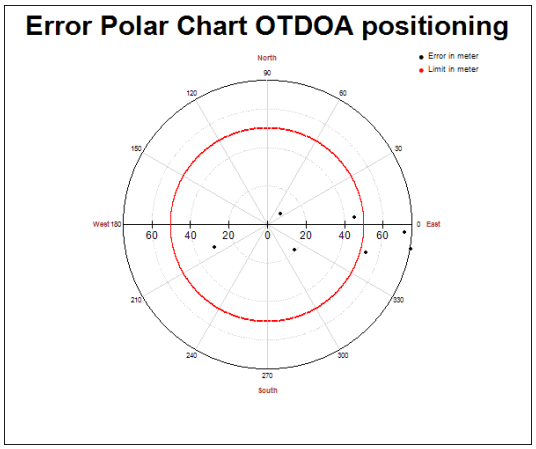

(d) SG Light, Bad DOP

Figure 5.6: OTDOA positioning results with no base station sync error.

Device	Good DOP	Bad DOP
Proto 1	100%	90%
SG Light	100%	58%

Table 5.1: Percentage of passed iterations for OTDOA positioning.

5.2.3 Results with base station synchronization errors

During the Matlab simulations, it had been observed that the base station synchronization errors were critical for OTDOA positioning. In order to reproduce that situation, an additional delay can be added to each of the LTE base stations. This delay is not reflected in the assistance data provided to the mobile and it is not taken into account in the algorithm for calculating the position.

The tests have been performed for synchronization errors of 10, 25, 50 and 100 nanoseconds, representing the error polar charts in Fig. 5.7 to Fig. 5.10. The percentage of passed iterations for each test has been summarized in Tab. 5.2.

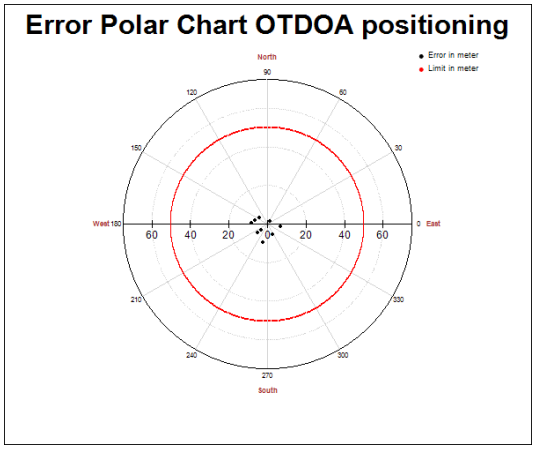

(a) Proto 1, Good DOP

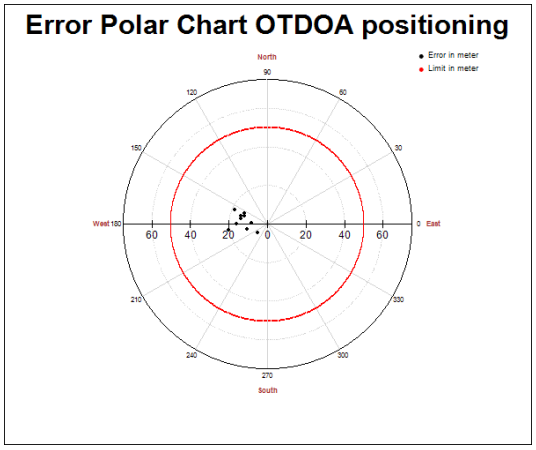

(b) SG Light, Good DOP

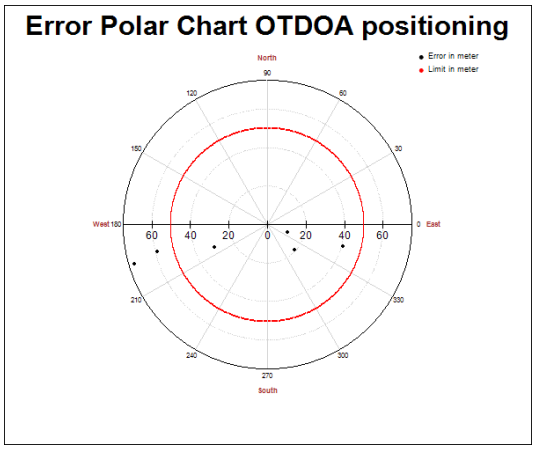

(c) Proto 1, Bad DOP

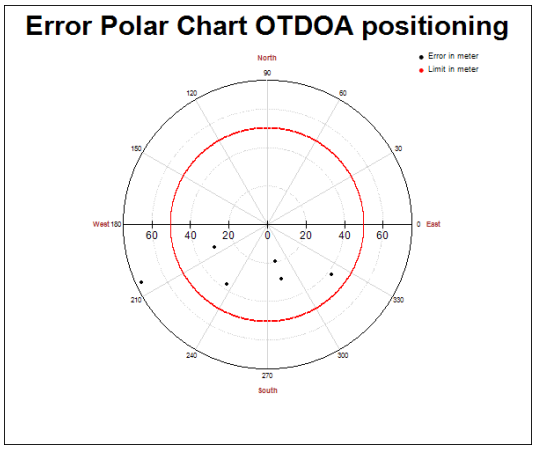

(d) SG Light, Bad DOP

Figure 5.7: OTDOA positioning results with 10 ns of base station sync error.

Analysing the results, it can be seen how both devices are still meeting the FCC requirements even with the highest base station synchronization error, in the case where the DOP is good. On the other, for bad DOP, the prototype is able to accomplish the

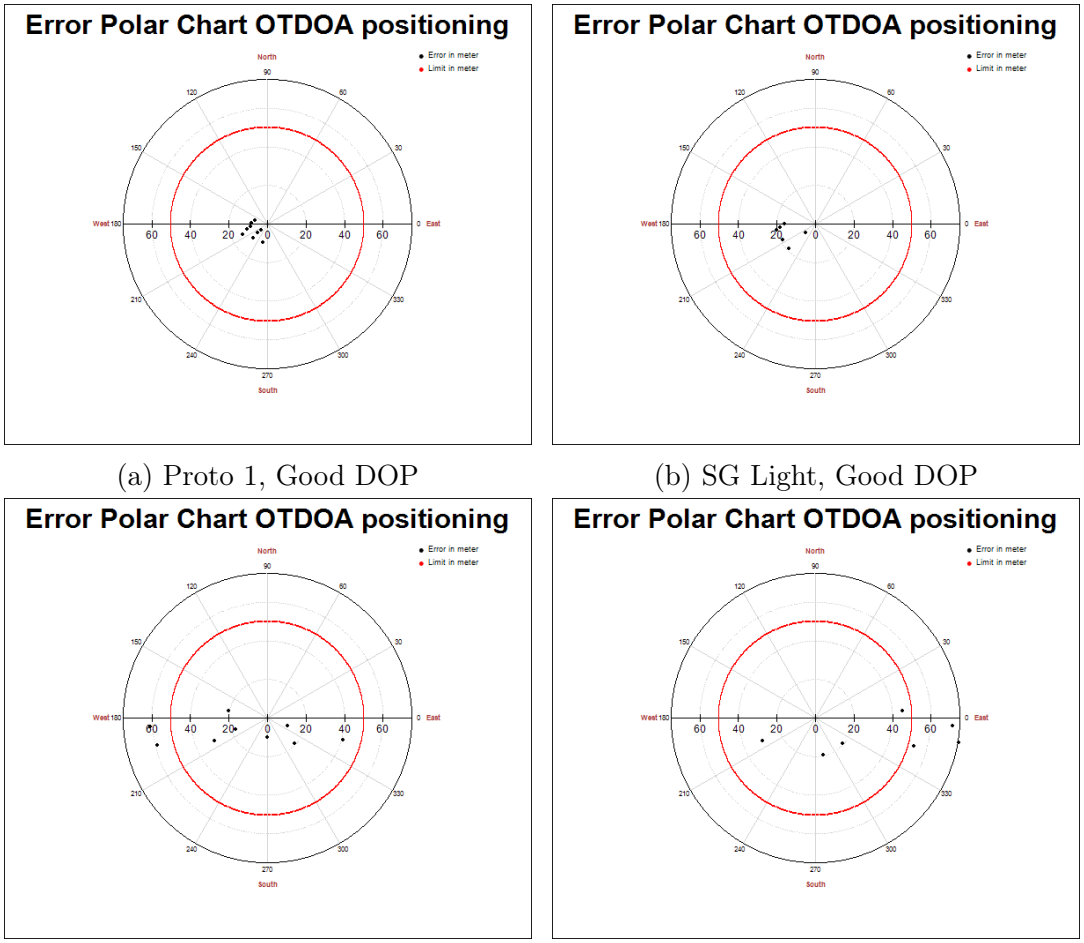

(a) Proto 1, Good DOP (b) SG Light, Good DOP

(c) Proto 1, Bad DOP (d) SG Light, Bad DOP

Figure 5.8: OTDOA positioning results with 25 ns of base station sync error.

desired results for 10 nanoseconds base station sync error. In any other case, both devices fail to meet the target percentage of passed iterations.

The results for good DOP conditions seem to contradict the results obtained during matlab simulations, where it had been concluded that a base station synchronization error bigger than 10 nanoseconds led to performances worse than the FCC demands. However, there are a few reasons to explain this. First of all, in the matlab simulation, the mobile device location was randomly generated at any point of the area formed by the base station constellation, which is not possible here due to test system limitations. For this test, the device is either placed exactly in the middle, having a very good DOP, or far aside, where the DOP is bad. This impacts directly the results: the base station synchronization errors have a higher impact if the DOP is bad, i.e. in locations which are not close to the geometrical centre of the base station constellation. Secondly, the measurement errors added to the Matlab simulation were i.i.d. samples from a random

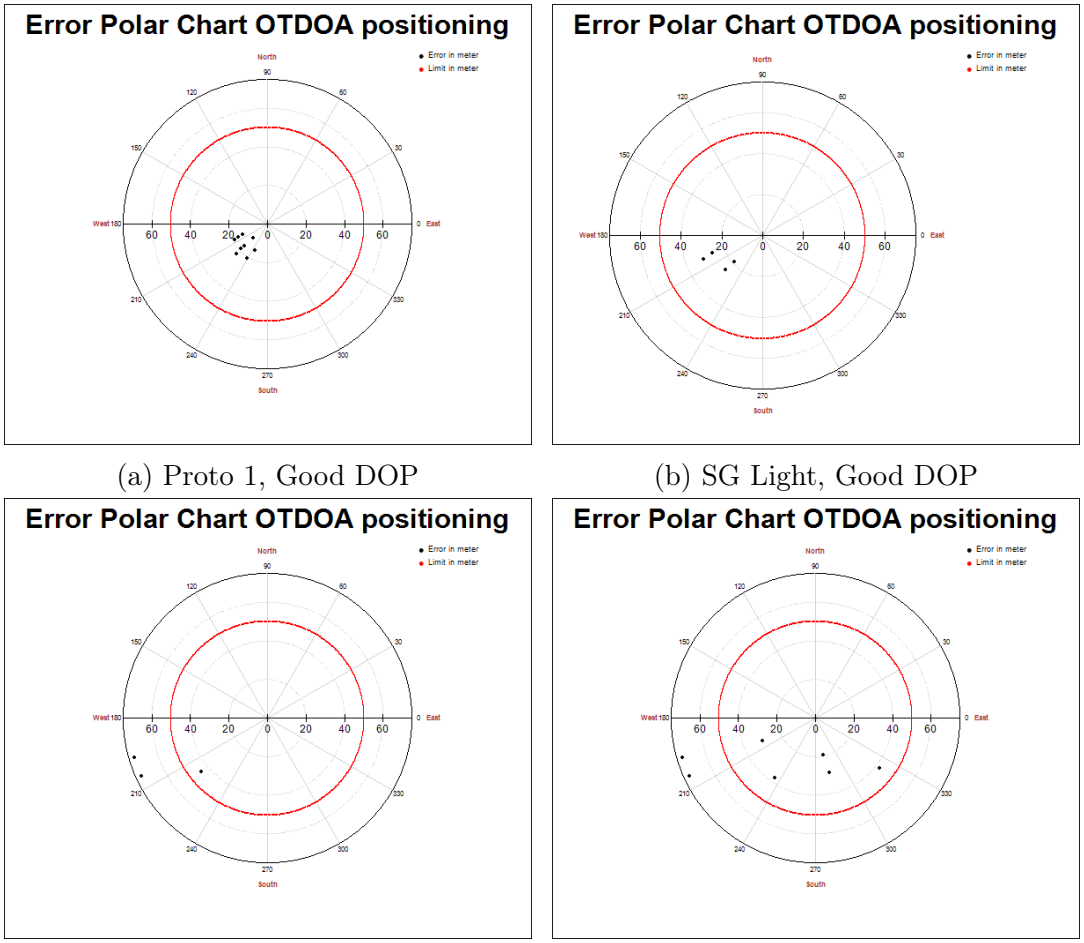

(a) Proto 1, Good DOP

(b) SG Light, Good DOP

(c) Proto 1, Bad DOP

(d) SG Light, Bad DOP

Figure 5.9: OTDOA positioning results with 50 ns of base station sync error.

distribution. Here, the measurements are taken from the mobile devices. The errors are not independent and identically distributed, there is a correlation over time. Thirdly, the expected RSTD value for each of the neighbour cells is transmitted to the mobile phones as part of the LPP assistance data. This expected RSTD is the ideal value, without the time delay added by base stations sync errors. It has been noticed that some mobile devices tend to apply a correction factor to the measurements to approach this expected value.

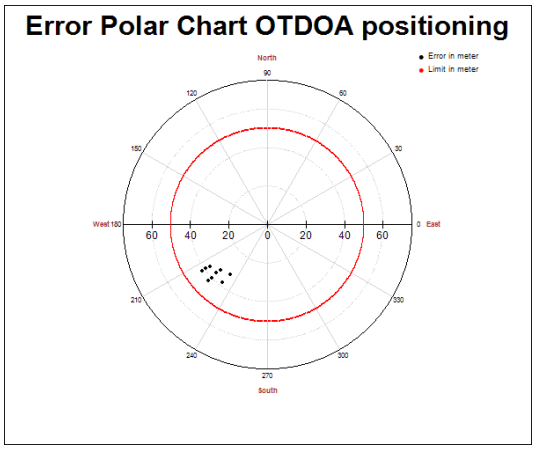

(a) Proto 1, Good DOP

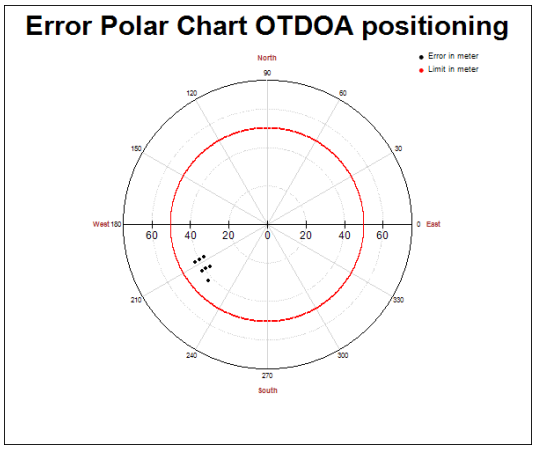

(b) SG Light, Good DOP

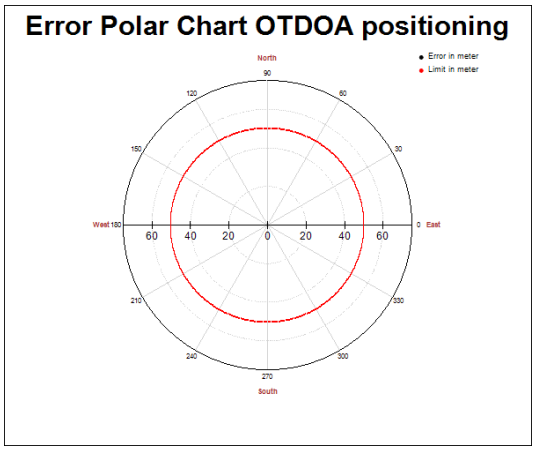

(c) Proto 1, Bad DOP

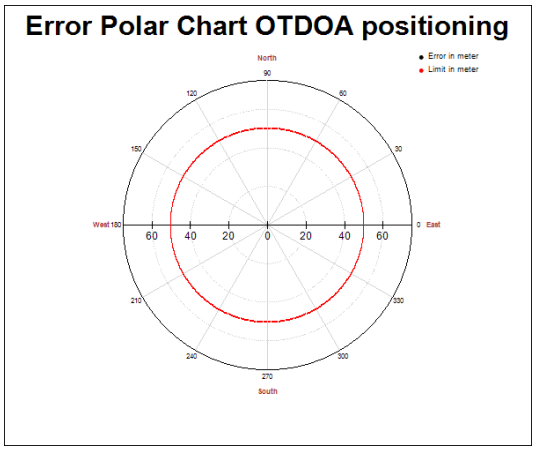

(d) SG Light, Bad DOP

Figure 5.10: OTDOA positioning results with 100 ns of base station sync error.

BS$_{sync}$ [ns]	**Proto 1**		**SG Light**	
	Good DOP	Bad DOP	Good DOP	Bad DOP
10	100	96	100	68
25	100	49	100	37
50	100	11	100	17
100	100	0	98	0

Table 5.2: Percentage of passed iterations for OTDOA positioning with BS sync errors.

5.3 Hybrid Positioning

The LBS Hybrid positioning test cases have been tested against the SG Light and the Prototype Device 2. These tests combine OTDOA and GNSS (GPS). ECID could not be included due to lack of mobile devices supporting simultaneously the three technologies. The test system has been used to simulate between 2 and 4 satellites and 3 or 4 cells in each test.

5.3.1 Comparison between Hybrid and pure GNSS with bad satellite DOP

The first test is to compare the performance of the hybrid algorithm against a pure GNSS algorithm in the situation where the DOP of the visible satellite constellation is poor. In order to replicate that scenario, the same satellites as in Section 4.4.2 have been used. These satellites were G04, G19, G20 and G28 from GNSS Scenario 1 defined in Section 6.2.1.2.1 of the TS 37571-5 [46]. All the satellites are simulated with a received signal power of -128 dBm at the mobile device GNSS antenna port. The test has been run with and without OTDOA. The configuration for OTDOA base stations in the same as in the previous Section for OTDOA positioning, four cells forming a square of 1000 metres radius. The cell powers remain as in the previous section.

The results are shown in Fig. 5.11 and the percentage of passed iterations in Tab. 5.3. It can be seen that the results with GNSS only are not meeting the FCC requirements, as only 64 % and 51 % of the iterations have passed, for the prototype and the commercial device, respectively. The Hybrid algorithm reaches an accurate solution for all iterations with both devices. The prototype performs slightly better than the commercial device, especially in GNSS.

Device	GNSS	Hybrid
Proto 2	64%	100%
SG Light	51%	100%

Table 5.3: Percentage of passed iterations for GNSS and Hybrid.

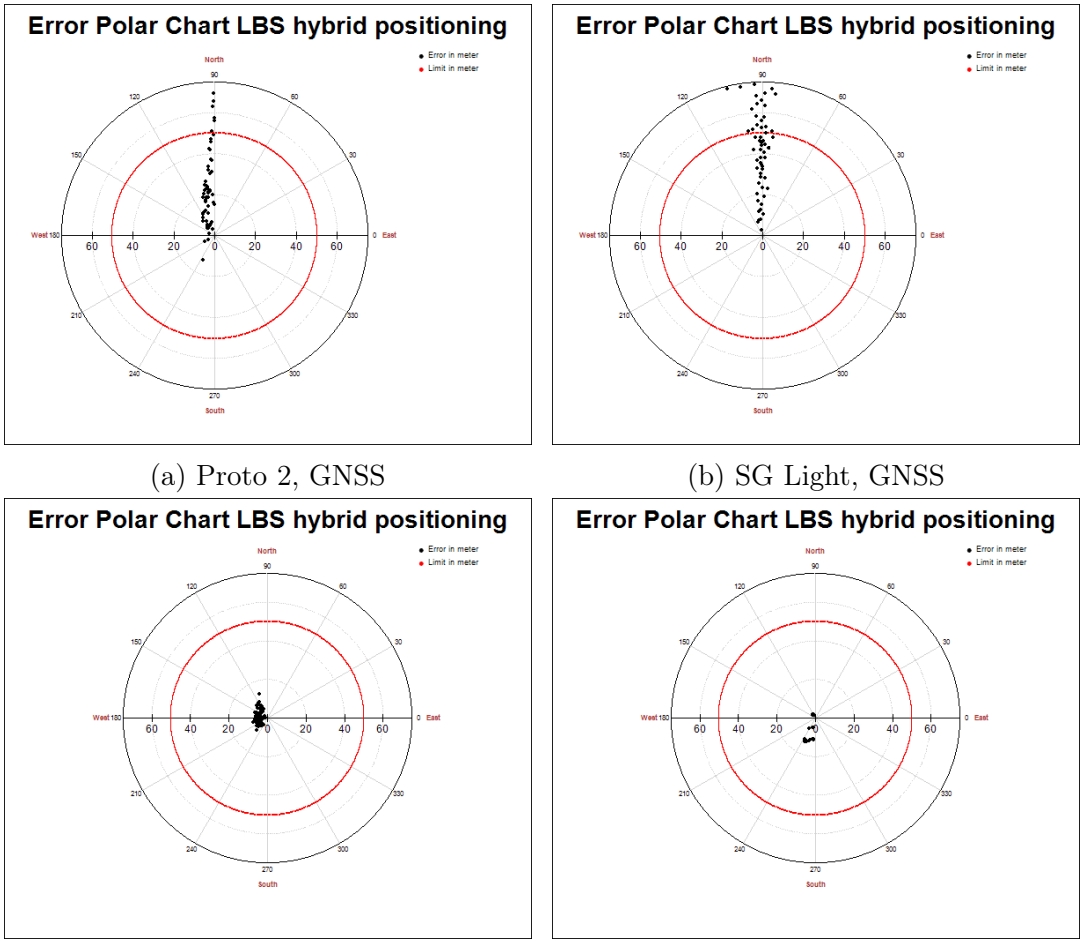

(a) Proto 2, GNSS

(b) SG Light, GNSS

(c) Proto 2, Hybrid

(d) SG Light, Hybrid

Figure 5.11: Comparison between pure GNSS and Hybrid for bad satellite DOP.

5.3.2 LBS Hybrid against base station sync error

Maintaining the same satellite and base station constellation as in the previous example, the base station sync error is increased to 10, 25, 50 and 100 nanoseconds, in order to study how critical is the impact of this error in the LBS hybrid algorithm. The results are depicted in Fig. 5.12 and Fig. 5.13 and the percentage of passed iterations are shown in Tab. 5.4. The base station synchronization error are affecting the results, increasing the error and the algorithm obtains some failed iterations with 100 ns of sync error. However, the results are much better than for OTDOA only. The prototype device is able to met the target pass percentage for all situations and the commercial device up to 50 nanoseconds base station synchronization error.

Another observation which can be done from these results is that the synchronization error affects principally the accuracy of the calculated position, and it has a much

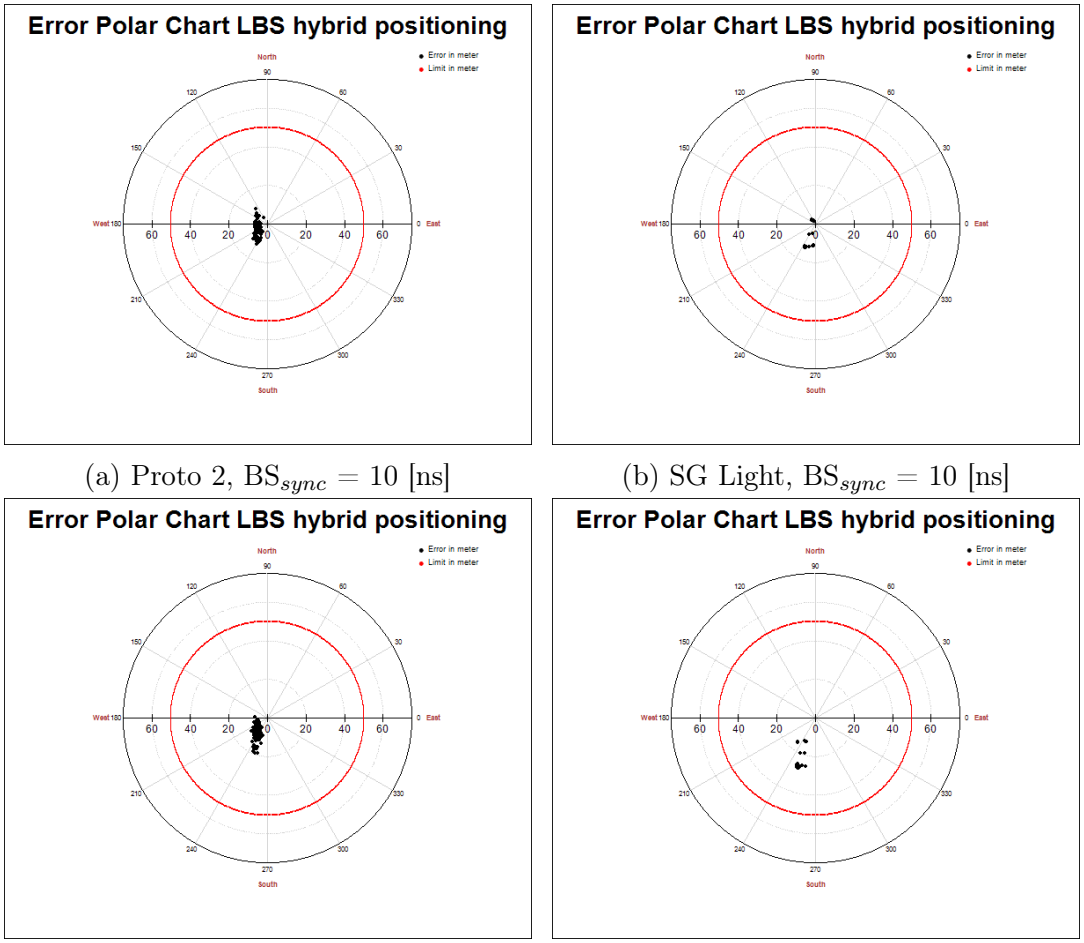

(a) Proto 2, $BS_{sync} = 10$ [ns]

(b) SG Light, $BS_{sync} = 10$ [ns]

(c) Proto 2, $BS_{sync} = 25$ [ns]

(d) SG Light, $BS_{sync} = 25$ [ns]

Figure 5.12: Impact of base station sync error in Hybrid positioning 1.

lower impact in the precision of the measurements: independent measurements under the same conditions obtain similar results.

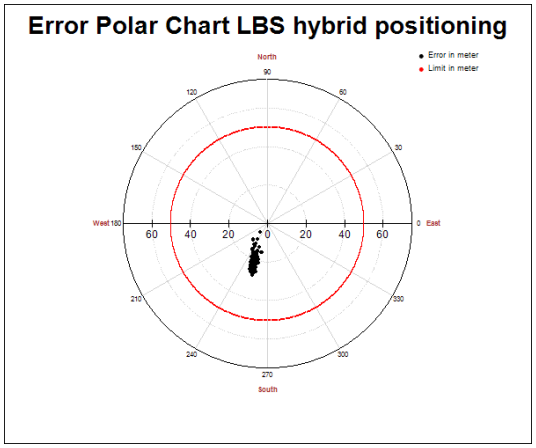

(a) Proto 2, $BS_{sync} = 50$ [ns]

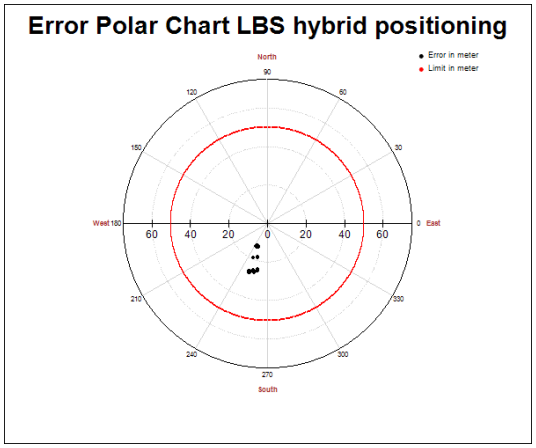

(b) SG Light, $BS_{sync} = 50$ [ns]

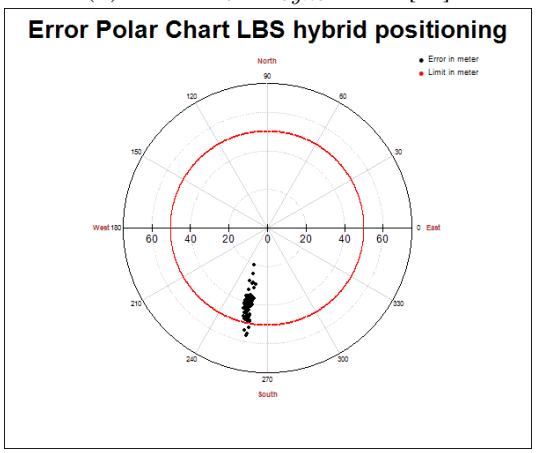

(c) Proto 2, $BS_{sync} = 100$ [ns]

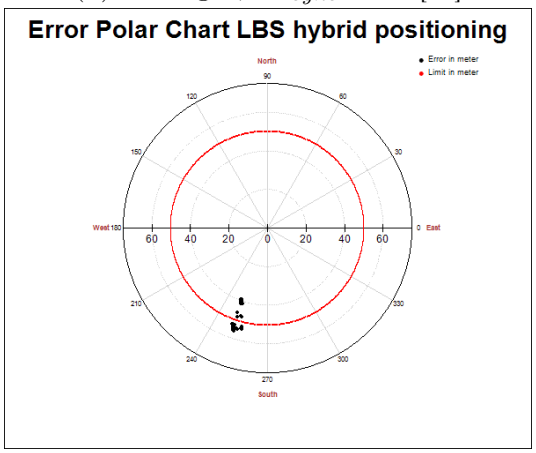

(d) SG Light, $BS_{sync} = 100$ [ns]

Figure 5.13: Impact of base station sync error in Hybrid positioning 2.

BS_{sync} [ns]	Proto 2	SG Light
10	100	100
25	100	100
50	100	100
100	95	56

Table 5.4: Percentage of passed iterations for Hybrid positioning with BS sync errors.

5.3.3 LBS Hybrid with just two satellites

The good performance of the algorithm has been proven in case enough satellites are available, even if the satellite DOP is bad. In this section, the performance of the algorithm will be tested with the minimum possible number of satellites, two. The satellite IDs are G11 and G17, as in Section 4.4.3. The test has been performed with no base station sync error, 25 and 50 nanoseconds of error. The results are displayed in Fig. 5.14 and Tab. 5.5.

BS_{sync} [ns]	**Proto 2**	**SG Light**
0	100	100
25	100	92
50	100	77

Table 5.5: Percentage of passed iterations for LBS Hybrid positioning with 2 satellites.

In this test, the difference in performance between the two devices is clear. The prototype device has obtained worse results than with four satellites, but it is still reaching a valid solution in all iterations, even with 50 nanoseconds base station synchronization error. The commercial mobile phone measurements are significantly worse, and with 50 nanoseconds of sync error it does not meet the FCC performance requirements. The precision of the results is as well much better with the prototype, being the positions calculated from the commercial device measurements much more scattered.

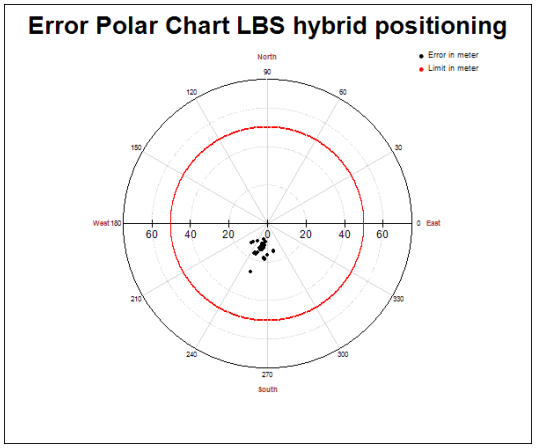

(a) Proto 2, $BS_{sync} = 0$ [ns]

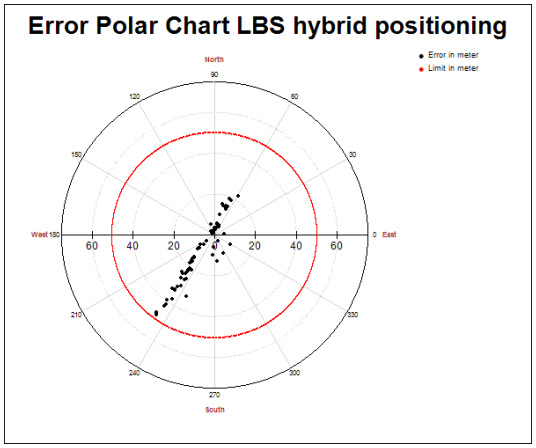

(b) SG Light, $BS_{sync} = 0$ [ns]

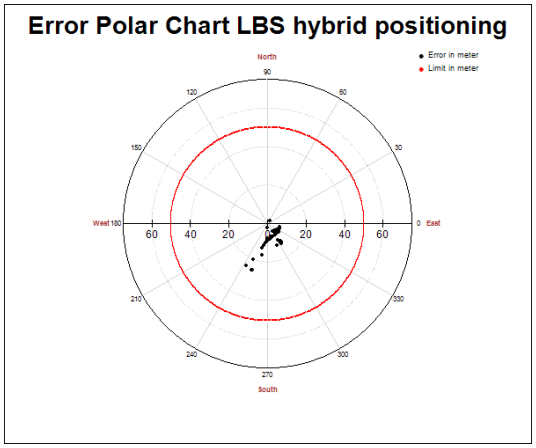

(c) Proto 2, $BS_{sync} = 25$ [ns]

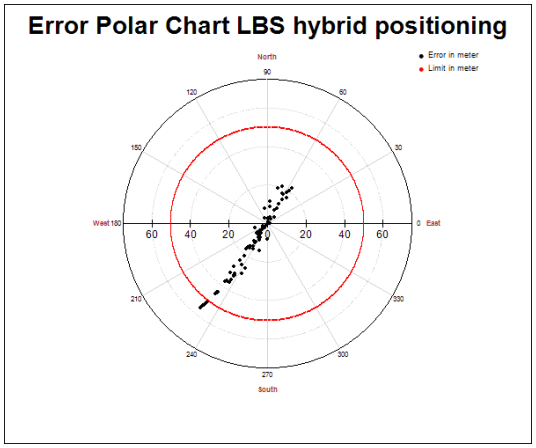

(d) SG Light, $BS_{sync} = 25$ [ns]

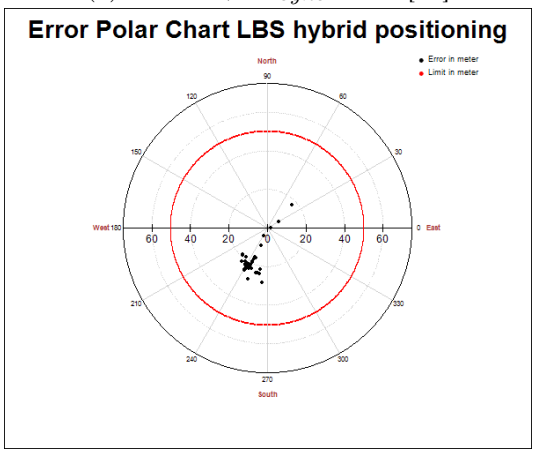

(e) Proto 2, $BS_{sync} = 50$ [ns]

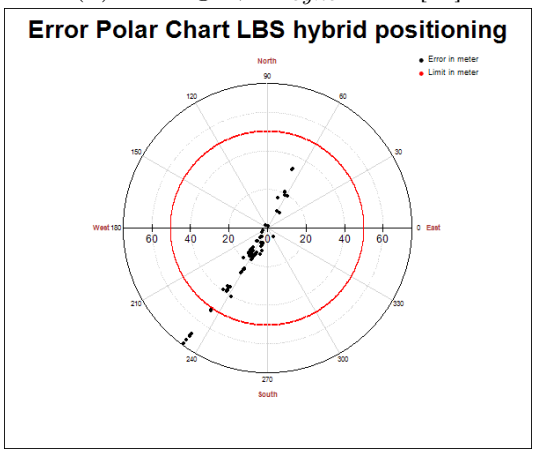

(f) SG Light, $BS_{sync} = 50$ [ns]

Figure 5.14: LBS Hybrid positioning with 2 satellites.

5.3.4 LBS Hybrid algorithm with fading

The last test of this Chapter and hence the last test of the Thesis, will analyse the performance of the proposed algorithm against fading conditions. Due to limitations of the test system, only three LTE Cells will be generated for this test. The LTE cells will be affected by a fading profile ETU30. ETU stands for Extended Typical Urban, and it is a profile defined by the 3GPP in specification TS 36.101 [**?**]. The 30 stands for the maximum Doppler frequency of the profile, 30 Hz. This is a typical high dense urban profile, which has been modelled from channel measurements performed in cities such as Tokyo and New York. It presents a series of Excess tap delays, each of them with a relative power difference in dB to the power of the signal. These tap delays are presented in Tab. 5.6.

Excess tap delay [ns]	**Relative Power [dB]**
0	-1
50	-1
120	-1
200	0
230	0
500	0
1600	-3
2300	-3
5000	-3

Table 5.6: ETU delay profile

As it can be seen from the table, it is a critical profile for OTDOA, as the taps with lower delays as well as the direct line of sight path have a lower power than other taps with higher delays. The taps at 200, 230 and 500 nanoseconds have the maximum power. If the mobile device chooses one of these taps to perform the measurement, the position calculations will be really inaccurate.

For the satellite signal, each of the three satellites present one multipath component with a delay of 300 nanoseconds and a relative power of -7 dB with respect to the direct LoS signal.

The test has been performed with no base station sync error, 10, 25 and 50 nanoseconds of error. The results are displayed in Fig. 5.15, Fig. 5.16 and Tab. 5.7.

The performance of the prototype device is quite good even under fading conditions. The scattering of the results is small, and the algorithm finds a position within 50

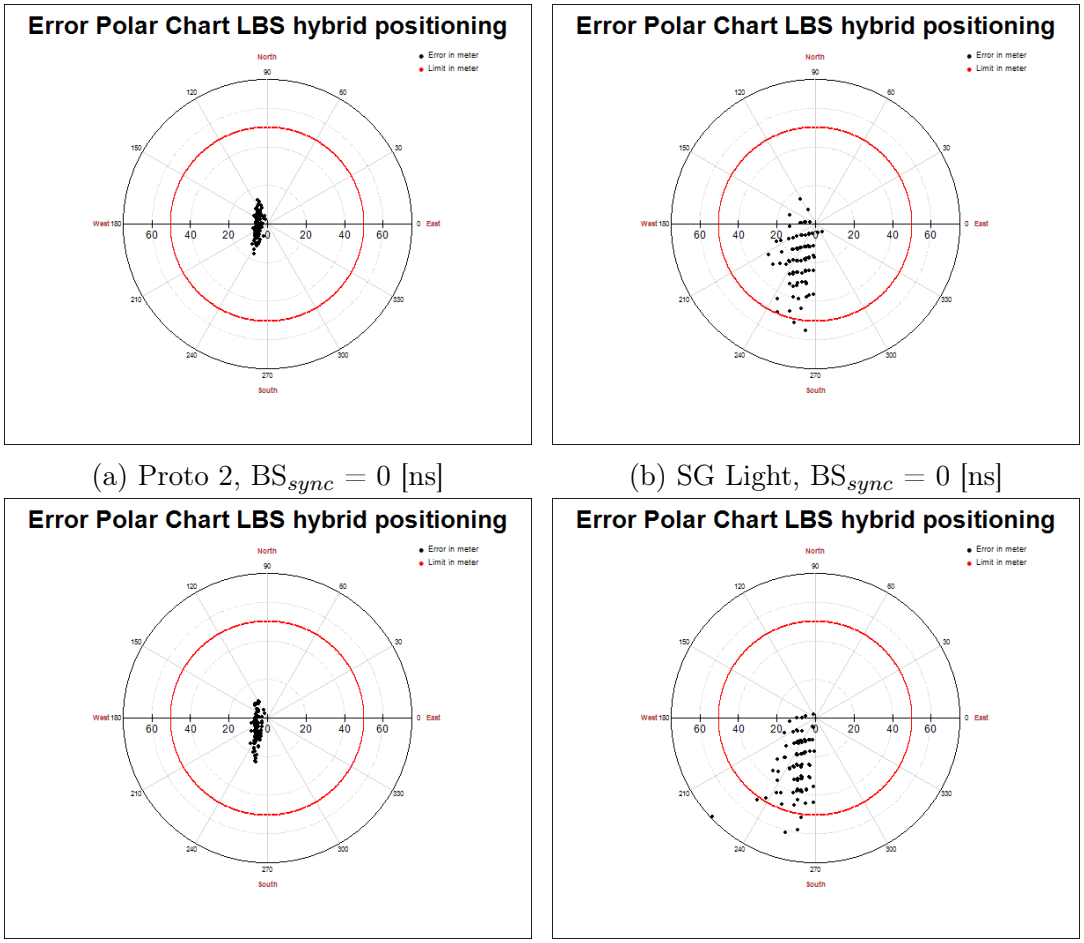

(a) Proto 2, $BS_{sync} = 0$ [ns]

(b) SG Light, $BS_{sync} = 0$ [ns]

(c) Proto 2, $BS_{sync} = 10$ [ns]

(d) SG Light, $BS_{sync} = 10$ [ns]

Figure 5.15: Hybrid algorithm with fading 1.

metres accuracy in all simulations. The results obtained with the commercial device are far worse in both accuracy and precision. The scattering of the calculated positions is quite significant. For 25 nanoseconds, the device falls close to the FCC limit, with just 81 % of passed iterations. For 50 nanoseconds the device does not accomplish the FCC requirements.

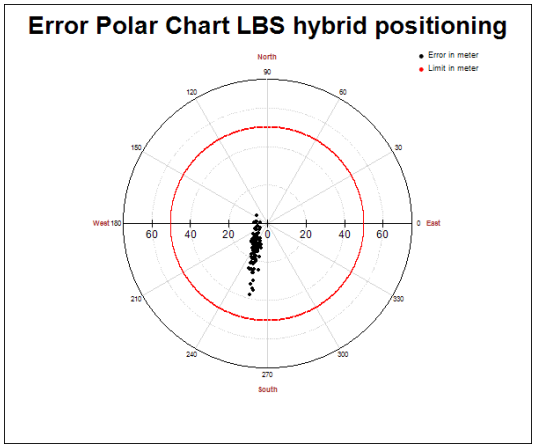

(a) Proto 2, $BS_{sync} = 25$ [ns]

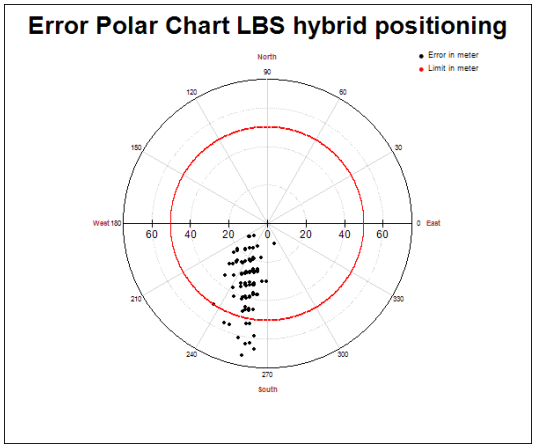

(b) SG Light, $BS_{sync} = 25$ [ns]

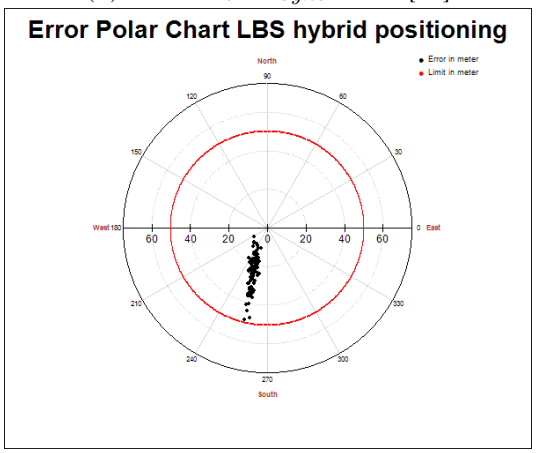

(c) Proto 2, $BS_{sync} = 50$ [ns]

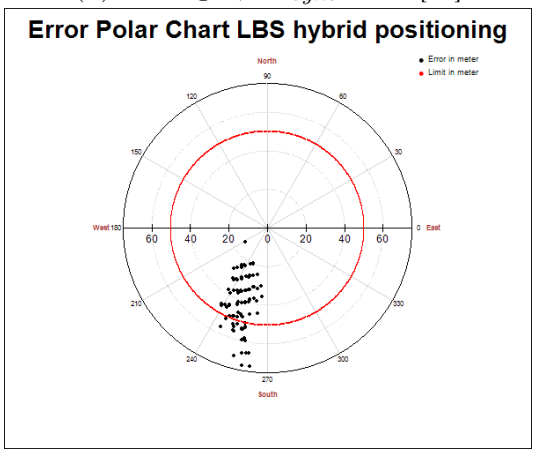

(d) SG Light, $BS_{sync} = 50$ [ns]

Figure 5.16: Hybrid algorithm with fading 2.

BS_{sync} [ns]	Proto 2	SG Light
0	100	97
10	100	90
25	100	81
50	100	67

Table 5.7: Percentage of passed iterations for LBS Hybrid algorithm with fading.

Chapter 6

Conclusions

6.1 Conclusions

In this Thesis, a mobile device localization algorithm combining GNSS, OTDOA and ECID measurements for LTE has been presented. Its performance has been analysed in a simulation environment as well as against real mobile devices with a certificated LTE test system for both indoors and outdoors scenarios. The main target of the algorithm is to meet the accuracy requirements proposed by network operators and emergency services authorities as part of the E911 regulations. Additionally, key concepts like the Dilution Of Precision (DOP) and its influence over the accuracy of the calculated position have been introduced. Moreover, possible error sources for OTDOA and ECID have been studied in detail. From all this work, a few conclusions can be drawn:

- If enough satellites are available (four or more) and the DOP of the satellites is good, GNSS standalone is able to calculate accurate positions which meet the requirements of the FCC.
- If less than four satellites are available, or the DOP of the visible satellites is bad, GNSS can be combined with OTDOA and/or ECID measurements in order to achieve the desired accuracy.
- OTDOA and ECID without GNSS are suitable for calculating only two-dimensional positions. The altitude coordinate is difficult to calculate due to the base stations being all in similar altitudes, which gives a bad GDOP.

- In some scenarios, the altitude coordinate can be inferred. For instance, it can be supposed that the mobile device is on the surface of the Earth.
- The Dilution Of Precision for TDoA systems and ToA systems in the same.
- The analysis of the DOP of the base station's constellation should be part of the network planning in order to develop a network suitable for OTDOA and ECID positioning. Different base station geometries have been proposed in this Thesis.
- The base station synchronism is critical for OTDOA. The synchronization error should be kept at least under 50 nanoseconds in order to maintain an acceptable accuracy. In case of standalone OTDOA, the base stations should be within 10 nanoseconds sync for optimal performance.
- ECID is a better option if the synchronization of the eNBs cannot be guaranteed. ECID measurements will be possible to all neighbour cells as part of E-UTRA Release 11.
- Indoors, the combination of OTDOA, ECID and GNSS (if any satellite is visible) does not suffice. Additional mechanisms must be used. Deploying femto and pico cells inside buildings is an option that will help meeting the FCC requirements for indoor positioning. These cells should be very good synchronized or used for ECID measurements only.

In summary, the algorithm derived in this Thesis will achieve the desired accuracy in most of the scenarios, if the restrictions regarding base station synchronization and geometry are met by the network. However, a few particular cases need to be analysed further:

In very dense urban environments, tunnels or other places where no satellites are available, OTDOA and ECID measurements can be used to render 2D locations. The Earth surface can be used as a boundary condition to calculate the altitude.

In indoor scenarios there will typically be no satellite or very few satellites in Line Of Sight conditions. If small cells are not deployed, the proposed location algorithm might not meet the accuracy requirements of the FCC. Indoor scenarios must be studied in more detail and additional solutions are required for indoor locations where pico cells are not an option due to deployment and maintenance costs.

6.2 Future works

There are some topics not fully covered by the work of this Thesis and which are worthy of further study.

6.2.1 Deep analysis of the OTDOA channel

This Thesis has used a fading propagation model defined by the 3GPP, the ETU30 profile. This model has been designed from real channel measurements in dense urban areas in cities such as New York and Tokyo. However, as a model, it does some simplifications and assumptions. Furthermore, this model is valid for a particular set of dense urban scenarios, but it is not suitable for other areas like sub-urban or open field. OTDOA is greatly affected by an incorrect measurement of the timing of the signal. Hence, a detailed characterisation of the OTDOA channel will be beneficial to better understand its limitations and sources of error. In order to do that, field measurements should be taken in a set of representative locations. These measurements should be analysed and a new set of propagation profiles should be proposed for each different scenario.

6.2.2 WLAN, bluetooth and other technologies

This Thesis has proposed a model based on deploying small LTE cells for achieving the required performance for the indoor scenario. In order to reduce the deployment costs, already existing equipment could be used. The LPP extensions (LPPe) define the protocol for measurements to other devices like WLAN spots or bluetooth transmitters.

The next steps to enhance and improve the proposed algorithm are related to study and include these technologies:

- Analyse the accuracy of RSSI (Received Signal Strength Indication) measurements and whether including them to the algorithm will improve the results or not.
- Implement an extension of the algorithm capable of including WLAN RTT (Round Trip Time) measurements in the position calculation. These measurements fol-

low the same concept as ECID. Therefore, the success of ECID can be taken as a proof of concept that WLAN RTT measurements will be useful for indoor positioning.

- Study further possibilities like Bluetooth.

Bibliography

[1] Eurostat, "The european union and the african union - a statistical portrait - 2014 edition," tech. rep., European Commission, 2014.

[2] Rohde and Schwarz, "Lte location based services technology introduction," 2013. Checked on the 5th of February, 2015.

[3] APCO, NENA, and Carriers, "Wireless e9-1-1 location accuracy requirements, ps docket no. 07-114," tech. rep., Federal Communications Commission, Association of Public-Safety Communications Officials International, National Emergency Number Association of the US and the Carriers AT&T, Sprint, TMobile USA and Verizon, November 2014.

[4] FCC, "Wireless e911 location accuracy requirements," tech. rep., Federal Communications Commission, Washington D.C., December 2014.

[5] "Ts36.171: Evolved universal terrestrial radio access E-UTRA; requirements for support of assisted global navigation satellite system A-GNSS.," Tech. Rep. V12.1.0, 3GPP, January 2015.

[6] G. Blewitt, "Basics of the gps technique," *Geodetic applications of GPS*, 1997.

[7] "Ts36.355: Evolved universal terrestrial radio access E-UTRA; LPP LTE postioning protocol," tech. rep., 3GPP, January 2015. RP67 V12.4.0.

[8] J. J. Spilker Jr., P. Axelrad, B. W. Parkinson, and P. Enge, *Global Positioning System : Theory and Applications Volume I.* American Institute of Aeronautics and Astronautics, 1996.

[9] B. Dr. Hofmann-Wellenhof and H. Dr Lichtenegger, *GNSS Global Navigation Satellite Systems.* Springer Wien New York, 2008.

[10] FCC, "Wireless e911 location accuracy requirements fourth report and order," Tech. Rep. 07-114, Federal Communications Comission, Washington D.C., February 2015.

[11] T. M. King, G. J. Geier, R. P. Landers, M. J. Slade, and P. DeClerck, "Time determination in satellite positioning system receivers and methods therefore," 2005.

[12] C. Mensing, S. Sand, and A. Dammann, "Hybrid data fusion and tracking for positioning with gnss and 3gpp-lte," *International Journal of Navigation and Observation*, 2010.

[13] RAN#42, "Rp-080995: Positioning support for lte," tech. rep., 3GPP TSG, Athens, Greece, December 2008.

[14] QualComm, "Extending benefits of lte advanced to unlicensed spectrum." https://www.qualcomm.com/invention/technologies/lte/unlicensed. Checked on the 8$^{\text{th}}$ of February, 2015.

[15] S. Fischer, "Observed time difference of arrival positioning in 3gpp lte," *QualComm*, June 2014.

[16] E. G. Bakhoum, "Closed-form solution of hyperbolic geolocation equations," *IEEE TRANSACTIONS ON AEROSPACE AND ELECTRONIC SYSTEMS*, 2006.

[17] M. S. Grewal, L. R. Weill, and A. P. Andrews, *Global Positioning Systems, Inertial Navigation and Integration*. John Wiley & Sons, 2 ed., 2007.

[18] K. Rantaaho, "Performance of 3gpp rel-9 lte positioning methods," tech. rep., 2 Invitational Workshop on Opportunistic RF Localization for Next Generation Wireless Devices, 2010.

[19] E. Commission, *EGNOS and Galileo: The EU satellite navigation programmes explained*. No. NB-01-14-211-EN-C, 2014. ISBN: 978-92-79-36329-0.

[20] C. Hegarty and E. Chatre, "Evolution of the global navigation satellitesystem (gnss)," *Proceedings of the IEEE*, 2008.

[21] C. Alexandrow, "The story of gps," *DARPA: 50 years of bridging the gap*, 2008.

[22] "Systems engineering & integration interface specification is-gps-200," tech. rep., Global Positioning Systems Directorate, 2012.

[23] W. H. Foy, "Position location solutions by taylor series estimation," IEEE *Transactions on Aerospace and Electronic Systems*, 1976.

[24] Y.-W. Ahn, "GPS error sources and mitigation."

[25] P. D. Groves, *Principles* GNSS*, Intertial and Multisensor Integrated Navigation Systems*, ch. 8 GNSS: Fundamentals, Signals and Satellites. No. ISBN-13: 978-1-60807-005-3, GNSS technology and application series, 2 ed., 2013.

[26] W. Van der Kloot, "Lawrence bragg's role in the development of sound-ranging in world war i," *The Royal Society Publishing*, 2005.

[27] D. R. Society. http://www.duxfordradiosociety.org/restoration/restoredequip/r1355/r1355.html

[28] W. Blanchard, *The Journal of Navigation.* Royal Institute of Navigation, 1991. Chapter 4.

[29] B. Wieder, "Precise time and frequency dissemination via the loran-c system," *Proceeding of the IEEE*, 1972.

[30] GERAN1, "Tr 45.811: Uplink - time difference of arrival (u-tdoa) in gsm and gprs," tech. rep., 3GPP, 2002.

[31] "Ts36.214: Evolved universal terrestrial radio access E-UTRA; physical layer measurements," tech. rep., 3GPP, January 2015.

[32] "Ts36.133: E-utra; requirements for support of radio resource management," tech. rep., 3GPP, January 2015.

[33] D. H. Shin and T. K. Sung, "Comparison of error characteristics between TOA and TDOA positioning," *IEEE Transactions on Aerospace and Electronic Systems*, vol. 38, no. 1, pp. 307–311, 2002.

[34] Y. G. Changsheng Cai, "Estimation of GPS-GLONASS system time difference with application to PPP," in *Proceedings of the 21st International Technical Meeting of the Satellite Division of the Institute of Navigation*, 2008.

[35] I. Vanschoenbeek, B. Bonhoure, M. Boschetti, and J. Legenne, "GNSS time offset: Effects on GPS-Galileo interoperability performance," *CNES, Le Centre National D'Etudies Spatiales*, 2007.

[36] J. Sanz Subirana, J. Juan Zornoza, and M. Hernandez Pajares, "Time references in GNSS," *Technical University of Cataluña*, 2011.

[37] R. G. Brown and P. W. McBurney, "Self-container GPS integrity check using maximum solution separation," *Journal of the Institute of Navigation*, vol. 35, no. 1, 1988.

[38] R. G. Brown, "Solution of the two-failure GPS RAIM problem under worst-case bias conditions: parity space approach," *Journal of the Institute of Navigation*, vol. 44, no. 4, pp. 425–431, 1998.

[39] R. G. Brown and G. Chin, "GPS RAIM: Calculation of the threshold and protection radius using chi-square methods: A geometric approach," *Global Positioning System: The Institute of Navigation*, vol. 5, 1997.

[40] "Synchronization for LTE small cells.," tech. rep., Small Cells Forum, 2013.

[41] D. Serant, F. Jambou, A. Garcia Peña, and L. Ries, "Collaborative LTE femtocell synchronization and receiver location for improved capacity and indoor positioning.," in *The Institute of Navigation GNSS+*, 2015.

[42] QualComm, "Extending benefits of LTE advanced to unlicensed spectrum," tech. rep., QualComm Technologies, 2014.

[43] C. Zou, A. S. Kim, J. G. Hwang, and J. G. Park, "Enhanced positioning method using WLAN RSSI measurements considering dilution of precision of access point configuration," in *ICSNC 2012: The Seventh International Conference on Systems and Networks Communications*, 2012.

[44] E. Navarro, B. Peuker, and Q. M., "Wi-fi localization using RSSI fingerprinting," 2010.

[45] A. Ramirez, *Time-of-flight in Wireless Networks as Information Source for Positioning*. PhD thesis, Technische Universitaet Muenchen, 2011.

[46] "Ts37.51-5: UTRA and E-UTRA and EPC; user equipment conformance specification for UE positioning; part 5: Test scenarios and assistance data," Tech. Rep. V12.1.0, 3GPP, 03 2015. Rel.12.

[47] G. Wuebbena, "Gnss network-RTK today and in the future concepts and RTCM standards," in *International Symposium on* GNSS*, Space-based and Ground-based Augmentation Systems and Applications*, 2008.